

TRANSCRIPTOME-BASED IDENTIFICATION OF
CIRCULAR RNA (circRNA) AND ITS FUNCTIONAL
ROLE IN OSIMERTINIB-RESISTANT NON-SMALL CELL
LUNG CANCER (NSCLC) CELLS

NALINI DEVI VERUSINGAM

DOCTOR OF PHILOSOPHY (MEDICAL SCIENCE)

M.KANDIAH FACULTY OF MEDICINE
AND HEALTH SCIENCES
UNIVERSITI TUNKU ABDUL RAHMAN
SEPTEMBER 2024

**TRANSCRIPTOME-BASED IDENTIFICATION OF CIRCULAR RNA
(circRNA) AND ITS FUNCTIONAL ROLE IN OSIMERTINIB-
RESISTANT NON-SMALL CELL LUNG CANCER (NSCLC) CELLS**

By

NALINI DEVI VERUSINGAM

A thesis submitted to the Department of Pre-Clinical Sciences,
M.Kandiah Faculty of Medicine and Health Sciences,
Universiti Tunku Abdul Rahman,
in partial fulfillment of the requirements for the degree of
Doctor of Philosophy (Medical Science)
SEPTEMBER 2024

© 2024 Nalini Devi Verusingam. All rights reserved.

This thesis is submitted in partial fulfilment of the requirements for the Doctor of Philosophy (Medical Science) at Universiti Tunku Abdul Rahman (UTAR).

This thesis represents the work of the author, except where due acknowledgment has been made in the text. No part of this thesis may be reproduced, stored, or transmitted in any form or by any means, whether electronic, mechanical, photocopying, recording, or otherwise, without the prior written permission of the author or UTAR, in accordance with UTAR's Intellectual Property Policy.

ABSTRACT

TRANSCRIPTOME-BASED IDENTIFICATION OF CIRCULAR RNA (circRNA) AND ITS FUNCTIONAL ROLE IN OSIMERTINIB-RESISTANT NON-SMALL CELL LUNG CANCER (NSCLC) CELLS

Nalini Devi Verusingam

Recent GLOBOCAN 2022 report identifies lung cancer as the leading cause of cancer mortality worldwide, with 85% of cases being non-small cell lung cancer (NSCLC). Patients with classical EGFR mutations (E19 Delins/L858R) respond to first- and second-generation EGFR-TKIs, while those with the secondary EGFR-T790M mutation initially benefit from Osimertinib (AZD9291). However, unceasing resistance in these patients, poses ongoing challenges in NSCLC treatment. Recent advancements in RNA biomarkers have shown that circular RNAs (circRNAs) significantly contribute to NSCLC progression. Remarkable stability in blood plasma makes circRNAs promising cancer biomarkers, though their roles in Osimertinib-resistant (OR) remain unclear. In this study, we aimed to identify a putative circRNA biomolecule that regulates OR and elucidate its functional and mechanism involvements to reveal potential therapeutic targets for OR lung adenocarcinoma. Transcriptome-wide profiling via circRNA sequencing identified circSPINT2 (hsa_circ_0050818) as significantly downregulated in OR cell lines against parental H1975 cell line (fold change [FC] ≥ 2.0 ; $P < 0.05$). Characterization and validation of

circSPINT2 were performed using qRT-PCR, Sanger sequencing (Back Splicing Junction: TATGAAGAGAATGC), ddPCR, actinomycin D, and RNase R assays (n=3, P<0.0001). Overexpression of circSPINT2 increased sensitivity to Osimertinib, reducing tumoursphere formation, colony formation, and migration, while knockdown induced resistance and enhanced tumorigenicity in the targeted cells. Biotinylated-RNA probe pull-down, miRNA sequencing, and in-silico analysis identified hsa-miR-1296-3p as a target of circSPINT2, regulating RBP1 expression. *In-vivo* validation using an Osimertinib induced resistant H1975 xenograft tumour model confirmed these findings. This study concludes that circSPINT2 has a tumour-suppressive effect and enhances Osimertinib sensitivity in OR cells by sponging oncogenic miR-1296-3p, leading to increased expression of tumour-suppressive RBP1. These findings may have a substantial influence on detection and treatment of Osimertinib resistance, potentially leading to tailored treatment options for patients with NSCLC.

Keywords: biomarkers; drug resistant; epithelial growth factor receptor; lung cancer; RNA therapeutics; transcriptomic profiling

Subject Area: Subclass RM Therapeutics. Pharmacology; RC254-282

Neoplasms. Tumours. Oncology including cancer and carcinogens

ACKNOWLEDGEMENT

I would like to convey my profound thanks and gratitude to my supervisors, Professor Dr. Alan Ong Han Kiat and Academician Emeritus Professor Dr. Cheong Soon Keng, for providing unwavering guidance, support, and encouragement during the entire course of my research and thesis writing. Without their timely wisdom and counsel, my research work would have been a frustrating and overwhelming pursuit. It would be an oversight not to express my sincere appreciation to my supervisors from National Yang Ming Chiao Tung University, Professor Dr. Chiou Shih-Hwa and Dr. Lotus Wang Mong-Lien for their valuable advice, research fundings, research facilities, expertise, and encouragement. Indeed, their expertise and insightful feedback have been instrumental in shaping this work. This work was supported by UTAR Research Fund (IPSR/RMC/UTARRF/2018-C1/A01), Malaysia, Ministry of Science and Technology in Taiwan (MOST 110-2320-B-075-006-MY3) and GHUST Joint Research Program VGHUST112-G1-5-1, the SPROUT Project Center For Intelligent Drug Systems and Smart Bio-devices (IDS2B) from the Ministry of Education, Taiwan.

I express my sincere gratitude to Dr. Tsai Ping-Hsing for his diligent efforts in bioinformatic analysis, constructive criticisms, and valuable suggestions, all of which significantly contributed to the improvement of the quality of the study. I extend my appreciation to my fellow seniors in SCII laboratory, Taipei Veteran General Hospital (Ms. Chen Yi-Chen, Ms. Futting Tsai, Mr. Tsai Ming-Long, Mr. Wang Yu-yang) for providing guidance, necessary resources and research facilities that facilitated the completion of this project.

Special thanks to my lovely friends (Dr. Nguyen Nhi Nguyen Phan, Dr. Henkie Lai, Dr. Lin Yi-Ying, Mr. Viet Quoc Nguyen, Dr. Afeez Adekunle Ishola, Dr. Choong Pei Feng, Dr. Teoh Hoon Koon, Ms. Tai Lihui, Dr. Lim Sheng Jye, Dr. Chiew Men Yee,) who have offered encouragement, shared their expertise, and provided a supportive academic community during my PhD journey in both Taiwan and Malaysia.

Finally, I want to express my heartfelt thanks and I am truly grateful to both my parents and brothers for their unwavering love, encouragement, and understanding during the ups and downs of this academic journey. This thesis would not have been possible without the support and encouragement of these wonderful family members of mine.

APPROVAL SHEET

This thesis entitled “**TRANSCRIPTOME-BASED IDENTIFICATION OF CIRCULAR RNA (circRNA) AND ITS FUNCTIONAL ROLE IN OSIMERTINIB-RESISTANT NON-SMALL CELL LUNG CANCER (NSCLC) CELLS**” was prepared by NALINI DEVI A/P VERUSINGAM and submitted as partial fulfillment of the requirements for the degree of Doctor of Philosophy (Medical Science) at Universiti Tunku Abdul Rahman.

Approved by:

(Prof. Dr. Alan Ong Han Kiat)
Date:4/9/2024
Professor/Supervisor
Department of Pre-clinical Sciences
M. Kandiah Faculty of Medicine and Health Sciences
Universiti Tunku Abdul Rahman

(Academician Emeritus Prof. Dr. Cheong Soon Keng)
Date: 4/9/2024
Emeritus Professor/Co-supervisor
Department of Medicine
M. Kandiah Faculty of Medicine and Health Sciences
Universiti Tunku Abdul Rahman

M.KANDIAH FACULTY OF MEDICINE AND HEALTH SCIENCE

UNIVERSITI TUNKU ABDUL RAHMAN

Date: 4th SEPTEMBER 2024

SUBMISSION OF THESIS

It is hereby certified that **NALINI DEVI A/P VERUSNGAM** (ID No: **18UMD00999**) has completed this thesis entitled “TRANSCRIPTOME-BASED IDENTIFICATION OF CIRCULAR RNA (circRNA) AND ITS FUNCTIONAL ROLE IN OSIMERTINIB-RESISTANT NON-SMALL CELL LUNG CANCER (NSCLC) CELLS” under the supervision of Prof. Dr. Alan Ong Han Kiat (Supervisor) from the Department of Pre-Clinical Sciences, M.Kandiah Faculty of Medicine and Health Sciences, and Academician Emeritus Prof. Dr. Cheong Soon Keng (Co-Supervisor) from the Department of Medicine, M.Kandiah Faculty of Medicine and Health Sciences.

I understand that University will upload softcopy of my thesis in pdf format into UTAR Institutional Repository, which may be made accessible to UTAR community and public.

Yours truly,

(Nalini Devi Verusingam)

DECLARATION

I NALINI DEVI A/P VERUSINGAM hereby declare that the dissertation is based on my original work except for quotations and citations which have been duly acknowledged. I also declare that it has not been previously or concurrently submitted for any other degree at UTAR or other institutions.

Name: NALINI DEVI VERUSINGAM

Date: 4th SEPTEMBER 2024

TABLE OF CONTENTS

	Page
ABSTRACT	ii
ACKNOWLEDGEMENT	iv
APPROVAL SHEET	vi
SUBMISSION SHEET	vii
DECLARATION	viii
TABLE OF CONTENTS	ix
LIST OF TABLES	xvi
LIST OF FIGURES	xviii
LIST OF ABBREVIATIONS	xxi
CHAPTERS	
1.0 INTRODUCTION	1
2.0 LITERATURE REVIEW	6
2.1 Lung Cancer: Statistics	6
2.1.1 Lung Cancer: Risk Factors	7
2.1.2 Lung Cancer: Histological Subtypes	8
2.2 Non-Small Cell Lung Cancer (NSCLC)	9
2.2.1 Adenocarcinoma (AD)	10
2.2.2 Squamous Cell Carcinoma (SCC)	10
2.2.3 Large Cell Carcinoma (LCC)	11
2.3 NSCLC-Lung Adenocarcinoma (LUAD): Overview	11
2.4 NSCLC-LUAD: Treatment Algorithm	13
2.5 Predominant Driver Mutation in NSCLC-LUAD	16

2.6	Epidermal Growth Factor Receptor (EGFR)	16
2.7	Tyrosine Kinase Domain (TKD) of EGFR	17
2.8	EGFR Mutations in NSCLC-LUAD	19
2.8.1	EGFR Exon 18	19
2.8.2	EGFR Exon 19 Deletion-Insertion (E19 delins)	20
2.8.3	EGFR Exon 20	20
2.8.4	EGFR Exon 21 L858R Substitution	22
2.9	EGFR Tyrosine Kinase Inhibitors (EGFR-TKIs)	22
2.10	Trajectory of EGFR-TKIs Development	23
2.10.1	First Generation EGFR-TKIs	26
2.10.2	Second Generation EGFR-TKIs	28
2.10.3	Third Generation EGFR-TKIs	29
2.10.4	Fourth Generation EGFR-TKI – EAI045	311
2.11	Mechanism of Resistance in NSCLC-LUAD	322
2.11.1	Intrinsic Resistance	33
2.11.2	Acquired Resistance	33
2.11.2.1	Ligand-independent EGFR Signalling	34
2.11.2.2	Histological Transformation	36
2.11.2.3	Activation of Additional Oncogenic Mutations	38
2.11.2.4	Brain Metastases	38
2.12	Unceasing EGFR-TKI Resistance and the Anticipated Corrective Strategy	39
2.13	Biomarkers in NSCLC-LUAD Progression	42
2.14	RNA Biomarkers	43
2.14.1	Messenger RNA (mRNA)	45

2.14.2	Micro RNA (miRNA)	46
2.14.3	Long Non-Coding RNA (lncRNA)	47
2.14.4	Circular RNA (circRNA)	47
2.15	Latest Breakthrough: Circular RNAs (circRNAs)	48
2.15.1	Biogenesis of circRNAs	49
2.15.2	Characteristics of circRNAs	51
2.15.3	Biological Function of circRNAs	52
	2.15.3.1 Regulation of Splicing and Transcription	53
	2.15.3.2 miRNA Sponge	54
	2.15.3.3 Protein Decoy/Sponge	54
	2.15.3.4 CircRNA Facilitates Protein Translation	55
2.16	CircRNA Detection and Analysis Methods	57
2.16.1	CircRNA Sequencing (circRNA-seq)	58
	2.16.1.1 CircRNA Enrichment	59
	2.16.1.2 CircRNA Library Preparation	60
	2.16.1.3 CircRNA Computational Analysis	61
2.16.2	Fluorescence In-Situ Hybridization (FISH) Assay	62
2.16.3	CircRNA Affinity Pull Down Assay	63
2.16.4	Northern Blot	64
2.16.5	CircRNA Overexpression System	65
2.16.6	CircRNA Knockdown System	67
2.17	CircRNA Implication in Cancer Hallmark	69
2.17.1	Sustaining Proliferative Signalling	69
2.17.2	Resistance to Cell Death	71
2.17.3	Sustained Angiogenesis	72
2.17.4	Insensitivity to Antigrowth Signals	74

2.17.5	Acquired Limitless Cell Division Potential	75
2.17.6	Activation of Tissue Invasion and Metastasis Cascade	77
2.18	CircRNA in Lung Cancer (NSCLC)	79
2.18.1	CircRNA in EGFR-TKI Resistance Lung Cancer (NSCLC)	81
2.19	Understanding the role of circRNA in Mechanism of Resistance to Osimertinib	82
2.20	Future Application of CircRNA as Diagnostic, Prognosis, Predictive And Monitoring Biomarker in Osimertinib Resistance	86
2.21	Future Application of CircRNA as Therapeutic Target in Osimertinib Resistance	87
3.0	MATERIALS AND METHODOLOGY	90
3.1	Overview of Methods	90
3.2	Cell Culture and Maintenance of Cell lines	93
3.2.1	Maintenance of H1975 Cell Line in Active Cell Culture	93
3.2.2	Maintenance of Osimertinib-Resistant Cell Lines in Active Cell Culture	94
3.2.3	Maintenance of circRNA Overexpressed and Knockdown Cell Lines	95
3.3	Generation of Osimertinib-Resistant Cell Lines	96
3.3.1	Step-wise Dose Escalation Method	96
3.4	Transcriptomic Profiling of circRNA – Next Generation Sequencing (NGS)	97
3.4.1	Total RNA Extraction	97
3.4.2	Circular RNA Next Gene Sequencing (circRNA-seq)	98
3.5	Characterization of Osimertinib Resistance Properties	1011
3.5.1	Drug Sensitivity Assay (AlamarBlue)	101
3.5.2	Colony Formation Assay (CFA)	102
3.5.3	Migration Assay	103

3.5.4	Tumour Formation Assay	103
3.5.5	Western Blot	104
	3.5.5.1 Protein Lysis	104
	3.5.5.2 Protein Quantification	105
	3.5.5.3 SDS-Polyacrylamide Gel (PAGE) Electrophoresis	106
3.6	Validation of Apoptosis Activity	109
	3.6.1 TUNEL Assay (BrdU and 7-AAD Staining)	109
3.7	Characterisation of circRNAs	111
	3.7.1 Gene Expression Study	111
	3.7.1.1 CDNA Synthesis from Total RNA	111
	3.7.1.2 Quantitative Real-Time Reverse Transcription PCR (qRT-PCR)	112
	3.7.1.3 Calculation and Analysis	114
	3.7.2 Ribonuclease R (RNase R) Treatment	114
	3.7.3 Actinomycin D Assay	115
	3.7.4 Droplet Digital PCR (ddPCR)	116
3.8	Gain and Loss of Functional Assays	117
	3.8.1 Preparation of Plasmid DNA: Overexpression and Knockdown System	117
	3.8.2 Plasmids Amplification in Bacteria Culture	118
	3.8.2.1 Lysogeny (LB) Agar Plate	118
	3.8.2.2 Terrific Broth (TB) Media	118
	3.8.2.3 Storage of Bacterial Culture Stocks	119
	3.8.2.4 Plasmid DNA Isolation	119
	3.8.3 Overexpression of circSPINT2	120
	3.8.4 Knockdown of circSPINT2	121
	3.8.4.1 Transfection of PLKO.1 Puro in Packaging Cell line (HEK293A)	121

	3.8.4.2	Transduction PLKO.1 Puro-circSPINT2 in H1975	123
3.9		Construction of circRNA-miRNA Interaction	124
	3.9.1	Biotinylated-circRNA Pull-down Assay	124
	3.9.2	Micro RNA (miRNA) Extraction	125
	3.9.3	CDNA Conversion from miRNA	127
	3.9.4	MicroRNA Next Generation Sequencing (miRNA-Seq)	130
	3.9.5	In-Silico Analysis	131
3.10		Animal Model	131
	3.10.1	Establishment of Osimertinib-Resistant Xenograft Model	131
	3.10.2	Fluorescence In-situ Hybridisation (FISH) Assay	133
	3.10.3	Chromogenic Immunohistochemistry (IHC)	133
4.0		RESULTS	135
	4.1	Generation and Characterization of Osimertinib-Resistant Cell Lines	135
	4.2	Comparative circRNA Expression Profiling in Osimertinib-Resistant Clones and Their Parental Cells Using circRNA-Next Generation Sequencing (NGS)	143
	4.3	Characterization of circRNA: circSPINT2 is Downregulated in Osimertinib-Resistant Cell Lines	146
	4.4	CircSPINT2 Overexpression Improves Osimertinib Sensitivity and Reduces NSCLC Cell Aggressiveness	153
	4.5	CircSPINT2 Knockdown in H1975 Cells Promotes Osimertinib Resistance and Enhances NSCLC Tumorigenicity <i>In-Vitro</i>	160
	4.6	CircSPINT2 Promotes Apoptotic Stress in Response to Osimertinib Treatment	166
	4.7	CircSPINT2 Acts as a miR-1296a-3p Sponge to Upregulate RBP1 Expression	168
	4.8	Investigation of circSPINT2/Hsa-miR-1296/RBP1 Axis on Osimertinib-resistant In-vivo Xenograft Model	178
5.0		DISCUSSION	186

5.1	Discovery of Circular RNA (circRNA) as Potential RNA Biomarker Associated with Mechanism of Resistance to Osimertinib	186
5.2	Osimertinib-resistant <i>In-vitro</i> Model	187
5.3	Identification and Characterization of Putative CircSPINT2	192
5.4	Biological Functions Assessment of CircSPINT2	196
5.5	CircSPINT2 as miRNA Sponge	198
5.6	CircSPINT2/hsa-miR-1296-3p/RBP1 Validation in Animal Model	201
6.0	CONCLUSION	204
6.1	Conclusion	204
6.2	Limitations and Future Recommendation	206
	REFERENCES	207
	APPENDICES	248

LIST OF TABLES

Table		Page
2.1	CircRNAs involved in the regulation of lung cancer	79
2.2	CircRNAs implicated in EGFR-TKI resistance.	82
2.3	CircRNAs implicated in Osimertinib resistance	85
3.1	Medium composition of H1975 medium in 500ml	94
3.2	Medium composition of Osimertinib-Resistant medium in 500ml	95
3.3	CircRNA-NGS Specifications	101
3.4	BSA Protein Standards	106
3.5	Protein Assay Dye Mix for Standard Curve	106
3.6	Running Buffer (10x)	107
3.7	Resolving Gel (10%)	108
3.8	Stacking Gel (5%)	108
3.9	Transfer Buffer	108
3.10	1x Phosphate-Buffered Saline with Tween 20 (PBST)	108
3.11	DNA Labelling	110
3.12	Antibody Solution	110
3.13	Step 1- cDNA Synthesis	112
3.14	Step 2 - cDNA Synthesis	112
3.15	Fast Sybr Green Master Mix	113
3.16	TaqMan Fast Advanced Master Mix	113
3.17	RNase R Treatment	115
3.18	Evagreen Supermix	117

3.19	Cycling Condition of Evagreen Supermix					117
3.20	Lipofectamine (Overexpression)	3000	(A)	Per	Reaction	121
3.21	Lipofectamine (Overexpression)	3000	(B)	Per	Reaction	121
3.22	Lipofectamine (Knockdown)	3000	(A)	Per	Reaction	122
3.23	Lipofectamine (Knockdown)	3000	(B)	Per	Reaction	123
3.24	Poly (A) Tailing Per Reaction					128
3.25	Cycling Condition for Poly (A) Tailing					128
3.26	Ligation Adaptor Per Reaction					128
3.27	Cycling Condition for Ligation Adaptor					129
3.28	Reverse Transcription (RT) Per Reaction					129
3.29	Cycling Condition for Reverse Transcription (RT)					129
3.30	miR-Amplification Per Reaction					129
3.31	Cycling Condition for miR-Amp					129
4.1	IC50 (μ M) – H1975, OR4 and HOsiR					140
4.2	IC50 (μ M) – OR4 (EV/OE) and HOsiR (EV/OE)					157
4.3	IC50 (μ M) – PLKO.1, shRNA1 and shRNA2					163

LIST OF FIGURES

Figures		Page
2.1	Treatment Algorithm for NSCLC Patient	15
2.2	Structure of EGFR-Receptor Tyrosine Kinase (RTK)	18
2.3	EGFR-TKI resistance in lung cancer's fuelled by molecular diversity, significantly impedes the effectiveness of treatment strategies	41
2.4	The potential of RNA-based biomarker compared to DNA and Protein biomarkers	45
2.5	CircRNA strength as promising non-invasive biomarker in liquid biopsies	52
4.1	Morphology of H1975 cell line at 60% confluency	137
4.2	Morphologies of Osimertinib-resistant cell lines isolated from single clones at 70% confluency	138
4.3	Morphologies of Osimertinib-resistant cell line isolated from pool clones at 80% confluency	139
4.4	Osimertinib sensitivity assay (AlamarBlue) in H1975, OR4 and HOsiR	140
4.5	Qualitative measurement of Osimertinib efficacy via Colony formation assay in H1975, OR4 and HOsiR	141
4.6	Qualitative observation of tumorigenic potential via tumoursphere formation assay in H1975, OR4 and HOsiR	142
4.7	Qualitative observation of cell migration potential via migration assay in H1975, OR4 and HOsiR	142
4.8	CircRNA transcriptomic profiling in Osimertinib-resistant cell lines	144
4.9	Venn-diagram of circRNA differential expression	145
4.10	CircRNA validation via qRT-PCR in H1975 and OR (OR3, OR4 and OR6) cells	147

4.11	CircSPINT2 expression in HOsiR	148
4.12	Sanger sequencing of circSPINT2	149
4.13	Characterization of circSPINT2 via RNase R treatment in H1975	150
4.14	Characterization of circSPINT2 via Actinomycin D treatment in H1975	151
4.15	Droplet digital PCR (ddPCR) analysis	152
4.16	Overexpression of CircSPINT2 in OR4	154
4.17	Overexpression of CircSPINT2 in HoSiR	155
4.18	Osimertinib sensitivity assay (AlamarBlue) in overexpression system	157
4.19	Qualitative measurement of Osimertinib efficacy via Colony formation assay in overexpression system	158
4.20	Qualitative observation of tumorigenic potential via tumoursphere formation assay in overexpression system	159
4.21	Qualitative observation of cell migration potential via migration assay in overexpression system	160
4.22	Knockdown of CircSPINT2 in parental H1975 cell line	162
4.23	Osimertinib sensitivity assay (AlamarBlue) in knockdown system	163
4.24	Qualitative measurement of Osimertinib efficacy via Colony formation assay in knockdown system	164
4.25	Qualitative observation of tumorigenic potential via tumoursphere formation assay in knockdown system	165
4.26	Qualitative observation of cell migration potential via migration assay in knockdown system	165
4.27	Apoptosis activation by circSPINT2 in Osimertinib resistant cells	167

4.28	Pull-down assay using biotinylated-circSPINT2 probe	169
4.29	MiRNA transcriptomic profiling in pull-down OR4 lysates	170
4.30	MiRNA validation via qRT-PCR in H1975, OR4 and HOsiR cell lines	171
4.31	Hsa-miR-1296-3p in overexpression and knockdown cell lines	172
4.32	In-silico analysis	173
4.33	RBP1 validation via qRT-PCR in overexpression and knockdown cell lines	175
4.34	RBP1 in overexpression and knockdown cell lines	176
4.35	Qualitative analysis of RBP1 in overexpression and knockdown cell lines	177
4.36	Osimertinib-resistance induced xenograft model	179
4.37	Tumour volume measurement in control and Osimertinib-resistance induced xenograft model.	180
4.38	CircSPINT2/hsa-miR-1296-3p/RBP1 axis in animal model	182
4.39	CircSPINT2 localization in xenograft tissues	183
4.40	RBP1 protein expression in xenograft tissues	185
6.10	Summary of the effects and significance of the circSPINT2/miR-1296-3p/RBP1 axis as a regulating factor in Osimertinib-sensitive and Osimertinib-resistant in NSCLC cells.	206

LIST OF ABBREVIATIONS

AD	Adenocarcinoma
AKT	Protein Kinase B
ALK	Anaplastic Lymphoma Kinase
ARCHER 1050	A Randomized, Open-label, Phase 3 Study of Dacomitinib vs. Gefitinib for First-Line Treatment in Patients With Advanced NSCLC Harboring EGFR-Activating Mutations
AXL	AXL Receptor Tyrosine Kinase
BSJ	Back-Splicing Junction
CALCUL1	Cell-cycle associated gene
CART	Charge-Altering Releasable Transporter
CCND1	Cyclin D1
CDH1	Cadherin 1
cDNA	Complementary DNA
CircRNA	Circular RNA
CIRI	Circular RNA Identifier
CRISPR	Clustered Regularly Interspaced Short Palindromic Repeats
CSCs	Cancer Stem Cells
CT	Threshold Cycle
DAPI	4',6-diamidino-2-phenylindole
ddPCR	Droplet Digital PCR
DEPC	Diethylpyrocarbonate
DMSO	Dimethyl sulfoxide
DNA	Deoxyribonucleic Acid

ECM	Extracellular Matrix
EGFR	Epidermal Growth Factor Receptor
EMA	European Medicines Agency
EMT	Epithelial-Mesenchymal Transition
EPCAM	Epithelial Cell Adhesion Molecule
ERK	Extracellular Signal-Regulated Kinase
ETOH	Ethanol
EURTAC	European Tarceva vs. Chemotherapy NEJ-002 - Japan Clinical Oncology Group Study 002
FC	Fold Change
FDA	U.S. Food and Drug Administration
FFPE	Formalin-fixed paraffin-embedded
FGFR3	Fibroblast Growth Factor Receptor 3
FISH	Fluorescent In-Situ Hybridization
FLAURA	A Study of Osimertinib vs. Standard of Care EGFR Tyrosine Kinase Inhibitor Therapy in Participants With Locally Advanced or Metastatic Non-Small Cell Lung Cancer
FUS	FUS Binding Protein
GAPDH	Glyceraldehyde 3-phosphate dehydrogenase
GBM	Glioblastoma
gDNA	Genomic DNA
GLOBOCON	Global Cancer Observatory
HER2	Human Epidermal Growth Factor Receptor 2

H&E	Haematoxylin and eosin
HGF	Hepatocyte Growth Factor
hTERT	Human Telomerase Reverse Transcriptase
HULC	Highly Upregulated in Liver Cancer
IACUC	Institutional Animal Care and Use Committee
ICS	Intronic Complementary Sequences
IHC	Immunohistochemistry
IPASS	IRESSA Pan-Asia Study
IRES	Internal Ribosome Entry Site
JO25567	A Study of Erlotinib Plus Ramucirumab vs. Erlotinib Plus Placebo in Previously Untreated EGFR Mutation-Positive NSCLC
KNIFE	Kmer-based Nested Iterative Fusion Exon Finder
LCa	Lung cancer
LCC	Large Cell Carcinoma
LDCT	Low-dose Computed Tomography
lncRNA	Long Non-Coding RNA
LRIG2	Leucine-Rich Repeats and Immunoglobulin-Like Domains 2
LUAD	Lung Adenocarcinoma
LUX-Lung 3	Lung Cancer with Afatinib in Asian Patients AURA - AZD9291 vs. Platinum-Based Doublet-Chemotherapy in Locally Advanced or Metastatic Non-Small Cell Lung Cancer
m6A	N6-Methyladenosine

MAPK	Mitogen-Activated Protein Kinase
MCS	Multiple Cloning Site
MEK	Mitogen-Activated Protein Kinase Kinase
MET	Mesenchymal-Epithelial Transition
MREs	miRNA Response Elements
mRNA	Messenger RNA
mTOR	Mammalian Target of Rapamycin
MVD	Microvessel density
Napsin A	Napsin Alpha
NELSON	The Dutch-Belgian Randomized lung cancer screening trial
NGS	Next-Generation Sequencing
NSCLC	Non-Small Cell Lung Cancer
NTRK	Neurotrophic Tyrosine Kinase
Oligo(dT)	Oligodeoxythymidine
ORCHARD	A Study of Savolitinib Plus Osimertinib for the Treatment of Patients With EGFRm+ and MET Amplified Advanced NSCLC After Progression on Prior EGFR-TKI Therapy
OR	Osimertinib-Resistant
OS	Overall Survival
PCR	Quantitative Reverse Transcription Polymerase Chain Reaction
PEG	Polyethylene glycol
PEI	Polyethylenimine
PFS	Progression-Free Survival

PI3K	Phosphoinositide 3-Kinase
Poly(A)	Polyadenylation
PTEN	Phosphatase and Tensin Homolog
RAB10	Ras-related protein Rab-10
RB1	Retinoblastoma Protein 1
RBPs	RNA Binding Proteins
RBP1	Retinol Binding Protein 1
RELAY	A Study of Ramucirumab (LY3009806) Plus Erlotinib in Participants With Untreated EGFR-Mutated Advanced NSCLC
RET	Rearranged During Transfection
RIN	RIN: RNA Integrity Number
RNA	Ribonucleic Acid
RNAi	RNA interference
RNase R	Ribonuclease R
RPMI	Roswell Park Memorial Institute
RPN	Ribonucleoproteins
rRNA	Ribosomal RNA
RTK	Receptor Tyrosine Kinases
SCC	Squamous Cell Carcinoma
SCLC	Small Cell Lung Cancer
shRNA	Short hairpin RNA
snRNA	Small Nuclear RNA
TGF-beta	Transforming Growth Factor-beta
TKI	Tyrosine Kinase Inhibitor
TNM	Tumor, Node, Metstasis

TP53	Tumor Protein 53
tRNA	Transfer RNA
TTF-1	Thyroid Transcription Factor 1
Wnt/ β -catenin	Wingless-related integration site/ β -catenin
XIAP	X-Linked Inhibitor of Apoptosis Protein

CHAPTER 1

INTRODUCTION

According to the 2020 cancer statistics from GLOBOCON, lung cancer is a major contributor to global mortality, with approximately 2.2 million new cases diagnosed and 1.8 million cancer-related deaths recorded. The mortality rate for lung cancer surpasses that of any other type of cancer, with colon cancer (9.4%), liver cancer (8.3%), and stomach cancer (7.7%) following closely behind (Sung et al., 2021). Two major types of lung cancer, Small cell lung cancer (SCLC) and Non-small cell lung cancer (NSCLC), have been identified. NSCLC constitutes approximately 85% of all documented lung cancer cases (Herbst et al., 2018) and is further classified into adenocarcinoma (40%), squamous cell carcinoma (25-30%), and larger cell carcinoma (10-15%) based on histology (Schabath and Cote, 2019). Epidermal Growth Factor Receptor (EGFR) mutations are the most common targetable genomic drivers in NSCLC, with adenocarcinoma being the most affected subtype (Lee et al., 2022, Gou et al., 2024). While EGFR mutations in SCLC are rare and found in only 3-14% of LUAD cases, resulting from histological transformation induced by resistance to EGFR TKIs. This leads to SCLC with original EGFR mutations but with low incidence, resulting in poor prognosis and ineffective treatment (Xie et al., 2024).

Predominant and exclusive EGFR mutation subtypes found in NSCLC patients are exon 19 deletions (Del19) and exon 21 (L858R) substitution, which have shown higher survival rates due to their responsiveness to first and second-

generation EGFR Tyrosine Kinase Inhibitors (TKIs) (Yoshimura et al., 2019). However, acquired resistance in patients to EGFR-TKIs treatment has been observed due to the activation of the secondary Thr790Met (T790M) mutation in EGFR Tyrosine Kinase Domain (TKD) (Piotrowska et al., 2018). Third-generation EGFR-TKI Osimertinib (AZD9291) was shown effective against T790M mutations, but resistance often develops after 10-12 months of treatment. The resistance mechanism are driven by increased frequencies of tertiary EGFR mutations (C797S, L718Q, G724S, L692V, E709K, S768I, and L798) (Wu et al., 2020), histological transformation to SCLC (Oh and Kim, 2024), bypass signalling (Chen et al., 2024) and brain metastases (Skakodub et al., 2023). Hence, current treatment options for NSCLC patients are ineffective, and it is crucial to develop precise molecular-targeted therapies to understand the poorly understood pathological mechanism of acquired resistance in NSCLC patients (Dai et al., 2021).

Recent advancements in RNA sequencing and molecular profiling technologies have led to the discovery of a novel type of non-coding RNA, known as circular RNA (circRNA) (Singh et al., 2024, Gong et al., 2024), which has been found to play a role in human diseases, including cancer. Although circRNAs were discovered almost three decades ago, they were originally thought to be the result of errors in the spliceosomal machinery, as they had disorganized exon arrangements (Greene et al., 2017). However, it is now known that circRNAs are formed by a back-splicing process, which is mediated by intronic complementary sequences (ICSs), essential spliceosomal components, and other regulatory RNA binding proteins (RBPs) (Li et al., 2018). Back-splicing results in a covalently closed continuous loop structure that ligates the

3' and 5' ends at the junction site by a phosphodiester bond (Santer et al., 2019). Unlike linear RNAs, circRNAs lack of poly-A tail and are highly resistant to exonuclease RNase R, making them stable in body fluids with an average half-life of 48 hours (Tang et al., 2020, Meng et al., 2017, Li et al., 2024). Present studies have established several molecular functions of circRNAs can regulate alternative splicing process or the translation of mRNA into proteins by sequestering microRNAs and RBPs as well as via RNA-Pol-II-mediated transcription (Ng et al., 2016, Bose and Ain, 2018, Kakumani, 2022, Babayev and Silveyra, 2024). In addition, under certain conditions, circRNAs can be translated independently into proteins if the mRNA contains Internal Ribosome Entry Site (IRES) sequences and N⁶-Methyladenosine (m⁶A) motifs (He et al., 2021, Hwang et al., 2024, He et al., 2024).

The human transcriptome analysis has revealed an increasing number of unique circRNAs, which have diverse functions and are implicated in various cancer hallmarks including angiogenesis, evading cell death, invasion and metastasis (Yarmishyn et al., 2022). Although several circRNAs have been linked to NSCLC progression, there have been few studies exploring their role in EGFR-dependent and EGFR-independent tumour resistance and Osimertinib resistance mechanisms. CircRNA has been demonstrated to influence EGFR-related pathways, such as the MAPK/ERK pathway and miRNA/mRNA interactions, which are essential for EGFR-TKI resistance. Oncogenic C190 was found to modulate the EGFR/MAPK/ERK signalling pathway by sponging miR-142-5p, potentially driving EGFR-TKI resistance in lung cancer patients, but further evidence is needed to clearly define its role in drug resistance (Ishola et al., 2022). Previous study by Chen T et al used microarray analysis to discover

hsa_circ_0043632 and predicted that it may regulate the mechanism of resistance to Osimertinib by interacting with miRNA and mRNA (Chen et al., 2019). In another study by Ma J. et al, hsa_circ_0002130 was selected from the circRNAs related database (CCRDB), which was previously identified in hepatocellular carcinoma (HCC). The authors found that hsa_circ_0002130 was upregulated in OR cell lines and serum exosomes from Osimertinib-resistant NSCLC patients. Additionally, they demonstrated that hsa_circ_0002130 acts as a sponge for miR-498 and targets the expressions of GLUT1, HK2, and LDHA genes, further promoting NSCLC progression (Ma et al., 2020).

In this recent investigation, we discovered a new circular RNA, circSPINT2, linked to Osimertinib resistance by using next-generation sequencing-based transcriptomic analysis. CircSPINT2 is spliced from the SPINT2 gene, forming a backsplice junction from the 5' end of exon 4 to the 3' end of exon 3 and located at chr19:38778515-38779831, with a total nucleotide length of 114 nt. Resistance to digestion with RNase R exonuclease and validation of back splicing junction sequence confirmed that the circSPINT2 is a stable circularized transcript. The findings revealed that circSPINT2 demonstrated characteristics of a tumour suppressor, enhancing sensitivity to Osimertinib and decreasing the viability of OR cells. CircSPINT2 was shown to sequester hsa-miR-1296-3p, resulting in increased expression of RBP1. Collectively, these data suggest that miR-1296-3p may act as an oncogenic miRNA, inhibiting RBP1 expression in cells resistant to Osimertinib. Present results implicated that the circSPINT2/miR-1296-3p/RBP1 axis could be involved in the mechanism of Osimertinib resistance. Therefore, circSPINT2

could serve as a potential non-invasive diagnostic or predictive biomarker for monitoring resistance to Osimertinib in patients with non-small cell lung cancer.

General Objectives:

To identify circRNA as potential biomarker and investigate its regulatory mechanism contributing to the development of Osimertinib resistance.

Specific Objectives:

1. To establish and characterize circRNA profiles in Osimertinib-resistant NSCLC cells.
2. To evaluate its functional roles of putative circRNA in Osimertinib-resistant NSCLC cells.
3. To elucidate circRNA-miRNA-mRNA network involved in mechanism of Osimertinib resistance.

CHAPTER 2

LITERATURE REVIEW

2.1 Lung Cancer: Statistics

Lung cancer (LCa) accounts for approximately 11.4% of the 19.3 million newly diagnosed cases and 18% of the 9.9 million cancer-related deaths, making it a significant contributor to global mortality. GLOBOCAN's 2020 cancer statistics reported that lung cancer's mortality rate exceeds that of any other cancer type, with colon cancer (9.4%), liver cancer (8.3%), stomach cancer (7.7%) and breast cancer (6.9%) being the closest contenders. Among men, lung cancer was responsible for a significant proportion of deaths, accounting for 21.4% of the 5.5 million deaths, followed by liver and colorectal cancers. On the other hand, lung cancer remained the second leading cause of cancer-related deaths among women, after breast cancer, which accounted for 13.7% of the 4.4 million deaths (Sung et al., 2021).

Overall incidence of lung cancer was distributed globally as follows: 58.5% in Asia, 22.4% in Europe, 12.1% in North America, 4.3% in Latin America's, 1.9% in Africa, and 0.81% in Oceania (Sabbula et al., 2023). However, the regions with the highest occurrence of LCa among men worldwide are Eastern and Southern Europe, Eastern Asia, and Western Asia. Among women, the areas with the highest occurrence rates for women are Northern America, Northern and Western Europe, Australia and New Zealand with Hungary having the highest specific rate in a country. Nevertheless, countries

that have already undergone substantial development have recorded greater incidence and mortality rates of LCa in comparison to those that are still undergoing development(Sung et al., 2021).

2.1.1 Lung Cancer: Risk Factors

Present studies reported a strong correlation between the intensity of tobacco smoking and the risk of developing LCa. Smoking accounts for around two-third of global LCa fatalities. In fact, the estimated relative risk of LCa is about 20 fold higher in heavy smokers compared to lifetime never smokers (Health and Services, 2014, Linda et al., 2018). Exposure to passive smoke, which includes both the exhaled smoke from first-hand smokers and smoke from burning cigarettes or pipes, is carcinogenic, thus contributing to the incidence of lung cancer. To date, a total of 69 carcinogens from tobacco smoke were associated with LCa development and those that have been detected in second-hand smoke include nicotine, amines and hydrocarbons (Xue et al., 2014, Beutel et al., 2021).

Some studies have shown that tobacco smoking is not the only reason behind the occurrence of LCa, but also contributed by several other risk factors. A significant proportion of LCa cases, estimated to be 18-25% in men and 2–6% in women, are attributed to exposure to potentially harmful substances in a work environment or known as occupational exposure (Olsson and Kromhout, 2021). Work environment that are considered dangerous include coal mining (McCunney and Yong, 2022), working in iron and steel foundries (Wang et al., 2021b), manufacturing rubber products (Boniol et al., 2017), as well aluminium production (Shaaban et al., 2016). Also, occupation exposure often involves

exposure to substances such as asbestos, diesel exhaust, arsenic, chromium, and cadmium (Shankar et al., 2019, Hosseini et al., 2022, Zou et al., 2022), which can lead to lung inflammation, genetic mutations, and gradual fibrosis, thus contributing to the development of LCa (Cox, 2011, Naccache et al., 2018).

Apart from the above reported risk factors, Radon, a harmful radioactive gas, was also known to cause LCa. Radioactive gas, Radon occurs naturally and is commonly found in high amounts within indoor residences, educational institutions, and places of employment. Main sources of Radon are from soils and rocks around the foundation including building materials, domestic water and fuels (Eidy and Tishkowski, 2020). The radioactive gas released from the ground and into the air, breaks down to form additional radioactive particles further deposited on the airway lining cells inhaled by humans. This further causes damage to DNA and triggers abnormal genetic alterations (Riudavets et al., 2022).

2.1.2 Lung Cancer: Histological Subtypes

Various methods were employed in clinical settings for detecting and screening lung cancer, such as X-ray, white light bronchoscopy (WLB), liquid-based cytological examination (sputum, blood and pleural effusion) and lung tissue biopsies (Ning et al., 2021, Ren et al., 2023). To date, a randomized lung cancer screening trial (NELSON) has shown that low-dose computed tomography (LDCT) is an effective screening method, with a detection rate of 85% and a specificity of 99% compared to no screening (Amicizia et al., 2023).

There are two main histological subtypes that define LCa: Small Cell Lung Cancer (SCLC), which comprises 15% of all cases, and Non-Small Cell Lung Cancer (NSCLC), which accounts for 85%. SCLC arises from the airway lung, and is a highly aggressive type of lung cancer, whereas NSCLC develops in the lung tissues, generally less aggressive (Nicholson et al., 2022).

2.2 Non-Small Cell Lung Cancer (NSCLC)

The most frequently diagnosed histological subtypes of lung cancer worldwide are non-small cell lung cancer (NSCLC), which has a 5-year survival rate of about 15% across all stages (I-IV). Nonetheless, 5-year survival rates are higher if the patients are diagnosed at very early stages (Hong et al., 2022).

Treatment options for NSCLC patients include surgery, chemotherapy, radiotherapy, chemoradiotherapy or combination of these therapies. These treatments are given to patients diagnosed with stage I, II, or III NSCLC with the aim of curing the disease (Zappa and Mousa, 2016, Hopstaken et al., 2021, Petrella et al., 2023). Surgical-pathological procedure is indeed crucial in aiding clinicians with treatment decision-making for NSCLC patients. Therefore, patients who chose surgery as their initial treatment option will undergo a histological assessment to determine clinical stages. In cases of stage IV NSCLC or disease recurrence following initial treatment, systemic therapy is advised for patients. Current advanced systemic therapy recommended for stage IV NSCLC patients includes targeted drug therapy and immunotherapy. NSCLC also can cause predominant somatic mutation in the EGFR tyrosine kinase. As such, EGFR inhibitors are recommended (erlotinib, gefitinib, and afatinib) (Hanna et al., 2021, Fu et al., 2022).

Based on histological assessment, NSCLC is further classified into adenocarcinoma (40%), squamous cell carcinoma (20-30%), and larger cell carcinoma (~10%) (Paik et al., 2019, Anusewicz et al., 2020, Tai et al., 2020, Seong et al., 2020).

2.2.1 Adenocarcinoma (AD)

Adenocarcinoma is a common histological type of non-small cell lung cancer that typically forms a tumour mass between central fibrosis and pleural puckering. This subtype of cancer has glandular differentiation and produces mucin (Zheng, 2016). The appearance of adenocarcinoma can vary, with features such as diffuse lobar consolidation, bilateral multinodular distribution, centrally located mass, and pleural thickening (Sureka et al., 2013). Lung adenocarcinoma can be detected using pneumocytic markers, as well as markers such as Thyroid transcription factor (TTF-1) and Napsin A (Park et al., 2019), which are expressed in over 85% of cases. These markers are useful for detecting adenocarcinoma in limited biopsy samples (Weidemann et al., 2021).

2.2.2 Squamous Cell Carcinoma (SCC)

Squamous cell carcinoma (SCC) arises from the epithelial lining of the bronchi or the main airway of the lung. This occurs due to a high frequency of mutations, which causes significant keratinization. Based on histological verifications, SCC can be categorized into keratinizing, non-keratinizing and basaloid which are also indicative of varying degrees of differentiation. Keratin formation in epithelial cells serves as a defense mechanism to protect the cells from external damages. However, excessive production of keratin indicates

cancerous transformation and often correlates to poor overall survival in patients diagnosed with SCC. Molecular markers p63 and p40 are utilized to aid in distinguishing SCC from other subtypes of NSCLC using immunohistochemistry (IHC) (Galindo et al., 2020, Sabbula et al., 2023).

2.2.3 Large Cell Carcinoma (LCC)

Large cell carcinoma (LCC) accounts for lowest incidence compared to other subtypes of NSCLC and arises from epithelial cells of various part of the lung. LCC is described as rapid growing (tumour volume doubling time: 67-134 days) with poor prognosis (Rajdev et al., 2018). The tumours are undifferentiated and heterogenous as such composed with lack of definite cytologic features. Hence, early diagnosis is unachievable as the clinical symptoms are usually unclear and onset is subtle. Besides, tumour size are large at the point of detection in patients (Siddiqui et al., 2022). Currently there are no definite IHC markers for LLC, however a wide range of combination of diagnostic markers are being used such as CK5/6, TTF-1, p63, p40, CD56, chromogranin A (CgA) and synaptophysin (SYN) (Liang et al., 2022).

2.3 NSCLC-Lung Adenocarcinoma (LUAD): Overview

Lung adenocarcinoma (LUAD) is reported as the most diagnosed lung cancer subtypes and often not detected until it has already spread locally or to other parts of the body. The 5-year mortality rate of LUAD is relatively high, with a range of 51% to 99% depending on the clinical stage (Wu et al., 2022). There were five major histologic features identified in the onset of lung adenocarcinoma: (1) low grade – lepidic predominant, (2) intermediate grade –

acinar, papillary, (3) high grade – solid growth pattern as well as micropapillary predominant (Moreira et al., 2020, Myers and Wallen, 2023). Patients who exhibit a pure lepidic pattern have been found to have a favourable prognosis while acinar subtype is associated with a wide range of prognoses and denoted as the most common, with an estimated prevalence of 40% to 50% of patient diagnoses (Moreira et al., 2020). Even though the criteria used for classification can be subjective at times and can vary between pathologists, leading to inconsistencies in diagnosis, histologic verification is indeed crucial for determining prognosis and treatment options in lung adenocarcinoma cases.

Although tobacco smoking is the most common risk factor, there is a subset of individuals who have never smoked but still develop LUAD (Schabath and Cote, 2019). In addition, there has been a rise in the occurrence of LUAD among the Asian population, particularly in females (Triphuridat et al., 2023). Somatic driver mutations are also contributing factors to the development of LUAD and a series of oncogene drivers were documented by Cancer Genome Atlas (TCGA). These driver mutations are epidermal growth factor receptor (EGFR), kirsten rat sarcoma viral oncogene (KRAS), anaplastic lymphoma kinase (ALK), proto-oncogene, receptor tyrosine kinase met (MET), encoding tyrosine-protein kinase ros (ROS1), Erb-B2 receptor tyrosine kinase 2 (ERBB2), V-Raf murine sarcoma viral oncogene homolog B (BRAF), proto-oncogene tyrosine-protein kinase receptor Ret (RET) and neurotrophic tyrosine kinase, receptor, type 1 (NTRK1) (Vu and Patel, 2019, Kerr et al., 2021).

2.4 NSCLC-LUAD: Treatment Algorithm

In the treatment of advanced lung cancer, targeted therapy is now recommended for tumours that exhibit specific molecular mutations. Molecular profiling should be performed after the initial diagnosis using histological assessment of tumours and imaging, according to current guidelines, so that the most effective therapy can be recommended inclusive of targeted therapy options. Molecular testing in patient are carried out by means of quantitative real-time PCR (qRT-PCR), sanger sequencing, next-gene sequencing (NGS), immunohistochemistry (IHC) and fluorescent in-situ hybridization (FISH) assays (Rajadurai et al., 2023). In fact, NGS technology has been highlighted in recent studies as the most efficient method for molecular profiling with maximum genomic coverage by simultaneously targeting multiple key biomarkers and produces rapid results with the quickest possible turnaround time (Simarro et al., 2023).

Frequent drivers in LUAD, as revealed by predictive molecular testing, are alterations in the EGFR (90%), ALK (5%), and ROS1 (1-2%) genes. This has led to the development of a range of inhibitors such as EGFR tyrosine kinase inhibitors (EGFR-TKIs), ALK inhibitors, ROS1 inhibitors, and immune checkpoint inhibitors (ICIs) (Pembrolizumab, ipilimumab and nivolumab), which are preferred over chemotherapy drugs in the first-line setting. Treatment plans, including combinations of drug therapies, are determined based on the results of genetic testing (Marinelli et al., 2022, Salifu et al., 2023).

Platinum doublet chemotherapy has been shown to have the potential to slow down the progression of the cancer and alleviate symptoms like coughing

and shortness of breath, making it a viable palliative option for patients who have undergone all other available treatments. In fact, the primary goal in treating stage IV lung adenocarcinoma patients remains the extension of survival, and platinum-based chemotherapy continues to be the established approach (Griesinger et al., 2019, Yao et al., 2022). The main chemotherapeutic agents employed for treating advanced NSCLC are platinum analogs, namely cisplatin and carboplatin, in addition to other medication such as pemetrexed, paclitaxel, docetaxel and taxanes (Planchard et al., 2018, Araghi et al., 2023).

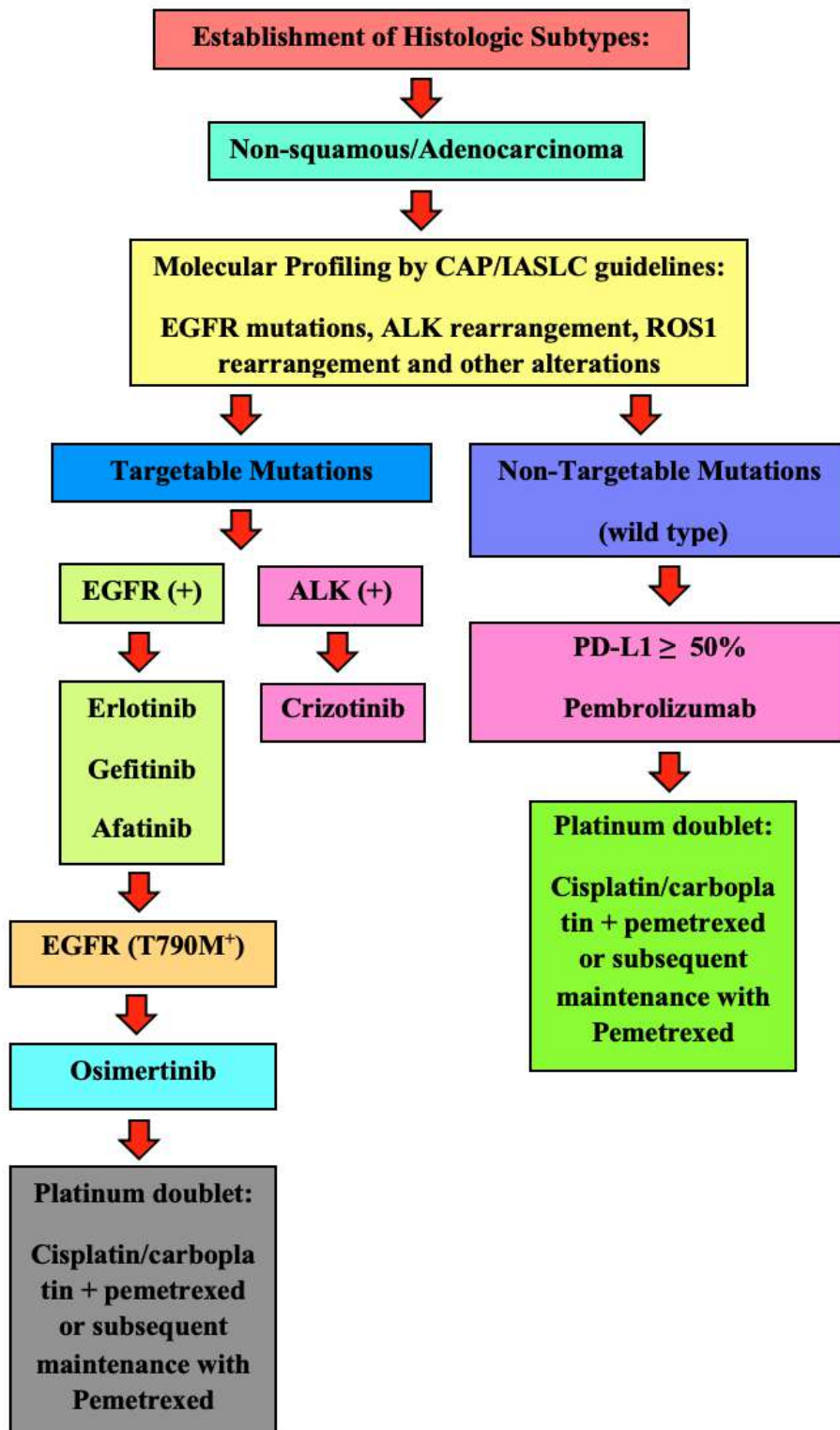


Figure 2.1: Treatment Algorithm for NSCLC Patient (Liam et al., 2020)

2.5 Predominant Driver Mutation in NSCLC-LUAD

While a subset of the molecular profiles and corresponding therapeutic targets have been identified in LUAD patients still EGFR remains as the hotspot driver mutation detected in LUAD tumours. (Jakobsen et al., 2018). It appears that there is a strong correlation between the presence of EGFR mutations in a female of Asian ethnicity (40-50%) and a never-smokers, based on retrospective data analysis (Boustany et al., 2022). However, susceptibility of EGFR mutations in never-smokers LUAD patients remains unclear .

2.6 Epidermal Growth Factor Receptor (EGFR)

The epidermal growth factor receptor (EGFR) is a transmembrane protein that belongs to the receptor tyrosine kinase (RTK) family. The EGFR gene is located across the cell membrane, with one end located inside the cell and the other end projecting outward (Murphrey et al., 2018). This gene is involved in regulating the normal physiology of epithelial cells and that responsible for producing a receptor protein that acts as a binding site for specific molecules called ligands (including EGF, TGF- α , AREG, and EPGN), initiating a sequence of events within the cell that can impact cell growth, division, and survival (Li et al., 2023b). The interaction between ligands and receptors can be compared to the process of fitting keys and locks. In cancers, modifications or mutations in the EGFR gene can cause the receptor to become hyperactive, leading to an excessive expression that can trigger unregulated proliferation and division of cells (Du and Lovly, 2018). EGFR-Wild-type (WT) undergoes ligand dependent signalling pathway, further activates receptor dimerization, autophosphorylation, and the initiation of downstream signalling pathways upon

ligand binding. While, mutant receptors induce either ligand-dependent or ligand-independent dimerization, activating downstream signalling pathways (Holowka and Baird, 2017).

In glioblastoma (GBM), overexpression of EGFR and large internal deletions (EGFRvIII) are frequently observed. These modifications can lead to the constitutive activation of the receptor, which promotes cell proliferation and survival. The overexpression of EGFR in GBM has been associated with poor patient prognosis and resistance to treatment. However, point mutations and small insertions (Exons 18-21) within the kinase domain are predominant in lung adenocarcinoma. These mutations can cause the EGFR protein to become constitutively activated, resulting in uncontrolled cell growth and division. Patients with these mutations tend to have a better response to targeted therapies, such as EGFR tyrosine kinase inhibitors (TKIs) (Uribe et al., 2021).

2.7 Tyrosine Kinase Domain (TKD) of EGFR

Typically, EGFR protein is composed of three major compartments: an extracellular ligand-binding domain, a transmembrane domain and an intracellular kinase domain that builds the juxtamembrane domain, tyrosine kinase domain (TKD) and c-terminal tail (Purba et al., 2017). The TKD of EGFR is responsible for the catalytic activity of the receptor. Its structure is composed of a N-terminal lobe and a C-terminal lobe, connected by a hinge region. The activation of the receptor takes place when the ligands, binds to the extracellular domain of EGFR, inducing the dimerization of EGFR molecules further activating autophosphorylation of tyrosine residues located in the cytoplasmic domain (Metibemu et al., 2019). The autophosphorylation of tyrosine residues

in the TKD leads to the activation of downstream signalling pathways, including the RAS/RAF/MEK/ERK, PI3K/AKT/mTOR, and STAT pathways. These pathways regulate various cellular processes such as cell proliferation, survival, migration, and differentiation (Sudhesh Dev et al., 2021).

The EGFR tyrosine kinase domain (EGFR-TKD) has been targeted for cancer therapy through the development of small molecule inhibitors, such as erlotinib, gefitinib, and afatinib, and monoclonal antibodies, such as cetuximab and panitumumab. These agents inhibit the activity of the EGFR-TKD and downstream signalling pathways, resulting in the inhibition of cell proliferation and induction of cell death (Zubair and Bandyopadhyay, 2023).

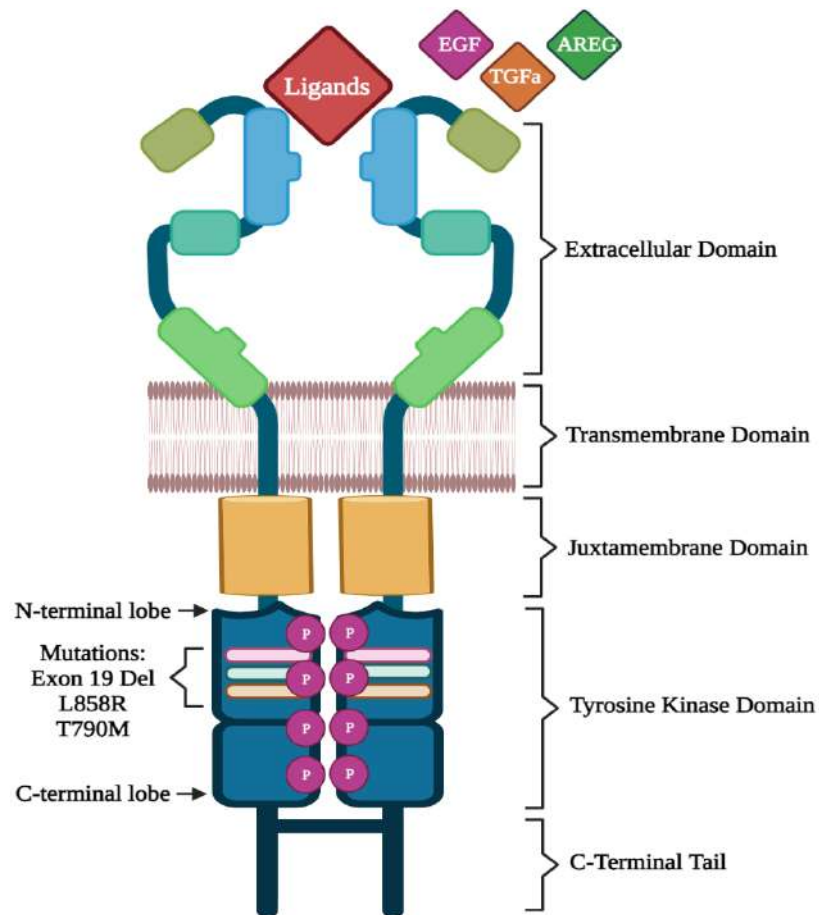


Figure 2.2: Structure of EGFR-Receptor Tyrosine Kinase (RTK)

2.8 EGFR Mutations in NSCLC-LUAD

EGFR hotspot mutations clustered in a specific region of the gene known as the TKD between exons 18-21. It is noteworthy that these mutations are considered exclusive and predominant, meaning that they are the most common and occur only within this particular region. LUAD patients are usually diagnosed for exon 19 deletion and exon 21 (L858R) substitution and these mutations account for approximately 90% of LUAD samples (Zhuo et al., 2017, Xu et al., 2020a). Both of these mutations are sensitising mutations that exhibit longer progression-free periods when treated with EGFR-TKIs. EGFR TKIs are designed to block the activation of the EGFR signalling pathway and, in turn, slow down or stop the growth of cancer cells. Unfortunately, higher concentrations of EGFR-TKI's induced drug selective pressure in some patients causes development of secondary mutations in exon 20 (T790M) (Li et al., 2014a, Vyse and Huang, 2019, Vaclova et al., 2021). Occurrence of T790M in NSCLC patients accounts for 55% of mechanisms of acquired resistance to first- and second-generation EGFR-TKIs (Liao et al., 2019). Currently, emergence of tertiary mutations C797S is now detected in exon 20, responsible for 10-26% of cases where resistance develops against EGFR-TKI third generation (Osimertinib/AZD9291) (Reita et al., 2021).

2.8.1 EGFR Exon 18

Alterations in EGFR exon 18 were classified as rare and uncommon. Mutations in exon 18 take place at codon 709 and 719. These mutations are G719S and E709X, both accounting for 3-4% of all EGFR aberrations (Pretelli et al., 2023). According to previous retrospective studies, patients diagnosed

with exon 18 mutations have demonstrated a lack of response to first-generation EGFR-TKIs. However, they have shown effectiveness when treated with second-generation EGFR-TKIs (Russo et al., 2019).

2.8.2 EGFR Exon 19 Deletion-Insertion (E19 delins)

EGFR exon 19 deletion-insertion (E19delins) is a frequently observed activating mutation, commonly referred to as the classical mutation. Patients who have the E19delins mutation demonstrate positive responses to EGFR-TKIs, making this mutation a robust indicator for favourable clinical outcomes. The primary mutations observed in exon 19 are deletions, whereas point mutations and insertions are rare in patients. However, research studies showed that EGFR exon 19 insertion mutations exhibit a comparable rate of response to TKIs, similar to that of exon 19 deletion mutations (Chen et al., 2022b).

2.8.3 EGFR Exon 20

The exon 20 mutations subtype are rare and observed in approximately 5-10% of lung adenocarcinoma patients with EGFR mutations. Crucial mutations that are present include EGFR exon 20 insertion (E20 ins), T790M, and C797S (Fang et al., 2019, Ou et al., 2023). The E20 ins mutations involved the insertion of base pairs within exon 20, resulting in the activation of the oncogenic EGFR expression. Current studies reported that, E20 ins prevalence are higher among Asian women non-smokers (Wang et al., 2020). Studies have indicated low response rates in lung adenocarcinoma patients with EGFR E20 ins mutations when treated with first and second-generation EGFR-TKIs (Qin et al., 2020). Consequently, this diminishes the therapeutic opportunity for

achieving clinical benefits. Thus, chemotherapy and immunotherapy are often the preferred treatment options in this specific group of patients.

In addition to insertions, gatekeeper mutation of EGFR, Thr790Met (T790M) in exon 20 has also been recognized as an oncogenic driver responsible for acquired resistance. The T790M mutation is characterized by the substitution of threonine (T) with methionine (M) at position 790 of exon 20. The presence of the T790M mutation prevented the first and second-generation EGFR-TKI drugs from binding to the ATP-binding site of the EGFR protein, which contains E19 delins and L858R point mutation. This inhibition ultimately resulted in the failure of treatment in patients (Minari et al., 2016, Ko et al., 2017). However, the FDA later approved Osimertinib as a third-generation EGFR-TKI, which showed significant effectiveness against the T790M mutation in both laboratory tests (*in-vitro*) and clinical studies (AURA 3 clinical trial) (Papadimitrakopoulou et al., 2020, Li et al., 2023d). Despite this success, patients later exhibited inadequate responses to Osimertinib. This was attributed to the emergence of tertiary mutation at exon 20 (C797S) indicating resistance to Osimertinib and other third-generation irreversible mutant-selective EGFR-TKIs such as Rociletinib (CO-1686) and Nazartinib (EGF816) (Cheng et al., 2024).

The EGFR C797S mutation is commonly found in patients with lung adenocarcinoma who are resistant to Osimertinib despite having the T790M mutation. This mutation involves the substitution of cysteine with serine at codon 797 in the ATP binding site of the EGFR protein. Fourth-generation EGFR-TKIs were developed to effectively target C797S mutation. One of these inhibitors is EAI045, an EGFR allosteric inhibitor (He et al., 2021b). EAI045 has demonstrated efficacy against cells carrying the C797S-T790M-L858R co-

mutations when used in combination with the anti-EGFR antibody cetuximab. However, it does not exhibit effectiveness against patients with C796S-T790M-ex19del (Liu et al., 2022b).

2.8.4 EGFR Exon 21 L858R Substitution

The EGFR L858R mutation is a common mutation in patients with lung adenocarcinoma similar to that of E19delins. This mutation involves a substitution of leucine with arginine (L858R) in exon 21. However, compared to patients with E19delins, those with the L858R substitution tend to have less benefit from EGFR-TKIs. L858R mutation is also associated with a weaker immune response, characterized by an increased tumour mutation burden in NSCLC patients (Bruno et al., 2021, You et al., 2022).

2.9 EGFR Tyrosine Kinase Inhibitors (EGFR-TKIs)

It is noteworthy that the majority of activating EGFR mutations in lung adenocarcinoma, approximately 90%, are characterized by either the L858R substitution in exon 21 or in-frame deletions in exon 19. Also, less frequently observed EGFR alterations involve point mutations, insertions, or deletions distributed within exon 18–21 (Wang et al., 2020). These mutations lead to the development of cancer by causing independent activation of growth and anti-apoptotic pathways without the need for external signals. Nevertheless, sensitizing EGFR mutations represent a prevalent form of targetable genomic aberration which is frequently observed in 15% of lung adenocarcinomas among Caucasian population, and in fact even higher among Asian patients (approximately 50%) (Soon et al., 2017).

EGFR-TKIs have emerged as an effective approach in cancer treatment, specifically for advanced NSCLC with common EGFR-sensitizing mutations. Over the past two decades, a significant number of EGFR inhibitors have been developed and made commercially available. These drugs possess distinct characteristics in terms of activity and safety and are categorized into first-, second-, and third generation TKIs. The effectiveness of EGFR-TKIs has consistently improved with each successive generation (Papini et al., 2021, Johnson et al., 2022).

EGFR TKIs gained approval as standard treatment regimen for patients with specific EGFR mutations based on clinical trials. The findings provided evidence of the superiority over platinum-based doublet chemotherapy for lung adenocarcinoma, particularly exon 19 deletions and L858R point mutations (Shah et al., 2022). The approved EGFR-TKIs can be classified into reversible and irreversible inhibitors based on their mode of inhibiting EGFR activity. In the case of reversible inhibitors, they competitively bind to the ATP binding site in EGFR through non-covalent interactions, which involve electrostatic, hydrogen-bonding, and hydrophobic interactions. On the other hand, irreversible EGFR inhibitors create a covalent bond with a cysteine residue in EGFR (Abourehab et al., 2021).

2.10 Trajectory of EGFR-TKIs Development

Initial approval of Gefitinib (first generation EGFR-TKI) was in June 2009 by the European Medicines Agency (EMA) for the treatment of EGFR-mutant NSCLC. In September 2009, the IRESSA Pan-Asia Study (IPASS) trial

demonstrated that Gefitinib was more effective than chemotherapy for Asian NSCLC patients who were light or never smokers (Burotto et al., 2015). Later in December 2009, a randomized phase III trial WJTOG3405 further endorsed the superiority of Gefitinib over chemotherapy in EGFR-mutant NSCLC (Mitsudomi et al., 2010). Subsequently, in June 2010, the NEJ-002 trial provided further confirmation of Gefitinib's efficacy in treating EGFR-mutant NSCLC (Inoue et al., 2011).

In March 2012, the European Tarceva vs. Chemotherapy (EURTAC) trial was conducted, focusing on the European population affected by advanced NSCLC characterized by activating EGFR mutations. This pivotal study demonstrated for the first time that Erlotinib, a first-generation EGFR-TKI, emerged as a superior choice for initial treatment in EGFR-mutant NSCLC patients (Rosell et al., 2012, Gridelli and Rossi, 2012) whereby in May 2013 the FDA approved Erlotinib for EGFR-mutant NSCLC (Khozin et al., 2014). Furthermore, in June 2012, initial findings from the LUX-Lung 3 trial provided preliminary evidence showing that Afatinib, a second-generation EGFR-TKI, exhibited greater efficacy than chemotherapy in treating EGFR-mutant NSCLC (Yang et al., 2012). A year later, both the FDA and EMA subsequently approved Afatinib for use as a first-line treatment option for EGFR-mutant NSCLC (Yu and Pao, 2013).

Furthermore, AURA trial conducted in 2015, conclusively demonstrated the effectiveness and efficacy of Osimertinib in addressing advanced NSCLC with EGFR-T790M mutation that had progressed following initial EGFR-TKI treatments (Yang et al., 2017a, Ito and Hataji, 2018). As a result, the FDA granted accelerated approval to Osimertinib for the treatment of NSCLC with

EGFR T790M mutation and subsequent year (February 2016), the EMA approved Osimertinib for patients with EGFR T790M-mutant NSCLC (Khozin et al., 2017, Karachaliou et al., 2017). In 2018, the FLAURA trial demonstrated the superiority of Osimertinib over first-generation EGFR TKIs when used as the first-line treatment for certain patients (Ricciuti and Chiari, 2018).

In 2017, the ARCHER 1050 study presented compelling evidence supporting the superior effectiveness of Dacomitinib, a second-generation EGFR-TKI, compared to Gefitinib as a first-line treatment option (Wu et al., 2017). Subsequently, in 2018 the FDA granted approval for Dacomitinib as a first-line treatment, followed by the EMA's approval in April 2019 (Shirley, 2018, Nilsson et al., 2021). In fact, several studies recommended the combination of EGFR-TKIs with monoclonal antibodies which benefited NSCLC patients in terms of overall survival. Hence, the JO25567 trial in 2014, while RELAY trial in 2019 demonstrated that combining Erlotinib with Bevacizumab and Ramucirumab (monoclonal antibody) was more effective than using Erlotinib alone in the initial treatment phase (Seto et al., 2014, Wang et al., 2021a).

In 2020, the FDA approved the combination of Ramucirumab (monoclonal antibody) with Erlotinib for use in the first-line treatment setting (Abdelghaffar et al., 2022). This was a significant development in the field of lung cancer treatment. The ORCHARD trial, a phase 2 study, was then carried out in the year 2021, revealed promising results when combining Osimertinib with Savolitinib (MET inhibitor) after patients experienced disease progression on Osimertinib. These combination therapy showed positive results in treating patients who had not responded to EGFR TKIs (Hartmaier et al., 2023).

Up until now, these studies and trials have yielded valuable discoveries in the realm of lung cancer treatment. They have provided potential treatment alternatives (including combinational treatment with chemotherapy and immunotherapy) for patients who had previously encountered disease advancement despite specific therapies. Nevertheless, additional clinical trials are currently underway and require FDA approval, as patients frequently encounter resistance to existing treatments.

2.10.1 First Generation EGFR-TKIs

First generation EGFR-TKIs (gefitinib and erlotinib) are reversible inhibitors that can effectively block the EGFR tyrosine kinase domain through ATP-competitive and reversible mechanisms. Erlotinib and gefitinib have demonstrated considerably longer median progression-free survival (PFS) in comparison to platinum-based chemotherapy when used as initial treatment for patients with metastatic lung cancer carrying sensitizing EGFR mutations (Karachaliou et al., 2019).

2.10.1.1 Gefitinib

Gefitinib (ZD1839/Iressa) is a pioneering oral chemotherapy medication utilized in the treatment of locally advanced or metastatic non-small cell lung cancer (NSCLC) (Tamura and Fukuoka, 2005). This drug belongs to the anilinoquinazoline class and has a molecular weight of 446.90 g/mol (Shamseddine et al., 2005, Alanazi et al., 2020). Functioning as an oral tyrosine

kinase competitive inhibitor, gefitinib exerts its antineoplastic effects by targeting ErbB-1 (EGFR), a subtype of the ErbB family, selectively inhibits ATP binding to the phosphate-binding loop in the intracellular domain of EGFR. As a result, it suppresses EGFR autophosphorylation and blocks downstream signalling pathways, leading to the inhibition of cancer cell proliferation and the induction of apoptosis. Following oral administration, Gefitinib is absorbed at a moderate rate, with an average bioavailability of 60%. Adverse effects linked to excessive dosage were observed, predominantly manifesting as diarrhea and skin rash. During the IRESSA study, there was no escalation in exposure with higher doses, and the adverse events reported were generally of mild to moderate intensity, aligning with the well-established safety profile of IRESSA (Tamura and Fukuoka, 2005).

2.10.1.2 Erlotinib

Erlotinib (Tarceva) is derived from quinazoline class and exhibits antineoplastic properties, with a molecular weight of 429.9 g/mol (Herbst and Sandler, 2008, Reguart et al., 2010). Functioning as a reversible first-generation receptor tyrosine kinase inhibitor, it primarily targets the EGFR within the ErbB receptor family, along with gefitinib. Pfizer originally patented erlotinib in the mid-1990s (Slobbe et al., 2015). This drug bears resemblances to gefitinib, as it contains an aminoquinoline moiety, but it distinguishes itself through specific substitutions, utilizing alkoxy chains for solvent regions and employing cyano-substituted phenyl rings for hydrophobic pockets (Bansal and Malhotra, 2021). Adverse reactions reported more frequently in patients receiving single-agent

erlotinib therapy, in comparison to placebo, include fatigue, as well as others that are typical of the EGFR TKI family. Notably, diarrhoea and rash are common side effects, and chest pain is also often observed (Blackhall et al., 2005).

2.10.2 Second Generation EGFR-TKIs

Second-generation inhibitors (Afatinib and Dacomitinib) are irreversible inhibitors that interact with ErbB family receptors through covalent bonding, leading to the inhibition of ErbB3 transphosphorylation and signalling. These inhibitors were designed to address treatment-resistant conditions by targeting not only T790M but also EGFR-activating mutations and wild-type EGFR (Westover et al., 2018, Bansal and Malhotra, 2021).

2.10.2.1 Afatinib

Afatinib (Gilotrif) belongs to the group of anilinoquinazoline compounds, forms covalent bonds with EGFR, HER2, and HER4, impeding their phosphorylation. This results in inhibition of the tyrosine kinase activity. Furthermore, Afatinib hampers the transphosphorylation process of ErbB3 (HER3), effectively hindering the signalling capacity of the entire ErbB receptor family (Ricciuti et al., 2018). The suggested daily oral intake of Afatinib is 40 mg, and it reaches its highest levels in the bloodstream approximately 2 to 5 hours post ingestion (Wind et al., 2017). The likelihood of afatinib causing or being affected by drug interactions is low, particularly concerning agents that

modify cytochrome P450 enzymes. However, coadministration with potent inducers or inhibitors of the P-glycoprotein transporter could influence how afatinib is processed in the body (Wind et al., 2017). Common adverse effects associated with Afatinib include feelings of nausea, vomiting, fatigue, and the development of a rash (Moosavi and Polineni, 2022).

2.10.2.2 Dacomitinib

Dacomitinib (Vicimpro) with a molecular weight of 469.94 g/mol, an irreversible inhibitor for EGFR, HER2, and HER4. Also categorized as a pan-HER inhibitor whereby its kinase inhibitory effects were evaluated against the wild type of the HER family (Nagano et al., 2019, Kudo et al., 2020). The suggested dose is 45 mg taken orally once daily, and it can be administered with or without meals (Takahashi et al., 2012). In the ARCHER 1050 trial, common adverse effects associated with dacomitinib include diarrhoea, rash, dry skin, decreased appetite, itching, and weight loss (Wu et al., 2017).

2.10.3 Third Generation EGFR-TKIs

The design of third-generation EGFR-TKIs (Osimertinib and Rociletinib) aimed for enhanced effectiveness and targeted specificity. These inhibitors can permanently block the kinase activity of the T790M isoform, while maintaining their efficacy against mutations in exon 19 and 21 (Shi et al., 2022). Importantly, they achieve this without affecting the inhibition of EGFR-WT. The initial third-generation EGFR-TKI in development was WZ4002, which did not advance to

clinical trials. Subsequently, Rociletinib (CO-1686) and Osimertinib (AZD9291) were developed (Andrews Wright and Goss, 2019). Despite their similar potency in inhibiting T790M-mutant EGFR, with minimal impact on the WT receptor, only Osimertinib has received regulatory approval (Yang et al., 2021b).

2.10.3.1 Osimertinib

Osimertinib/AZD9291 (Tagrisso/AstraZeneca), is a monomeric anilino-pyrimidine compound with a molecular weight of 596 g/mol (Gao et al., 2016). Delivered orally, Osimertinib possesses greater potency against Exon19del/L858R/T790M mutations compared to wild-type EGFR, which has propelled its prominent role in the global management of EGFR-positive NSCLC. It effectively blocks the downstream signalling pathways, such as RAS/RAF/MAPK and PI3K/AKT, further inhibiting NSCLC progression (Santarpia et al., 2017). Osimertinib has demonstrated efficacy in treating central nervous system (CNS) metastases originating from NSCLC. Notably, Osimertinib secured FDA and EMA approvals as the pioneering third-generation EGFR TKI (Remon et al., 2018). Adverse effects associated with Osimertinib use have included diarrhoea, skin rash, and paronychia, as reported in patients receiving this treatment (Chu et al., 2018).

2.10.3.2 Rociletinib

Rociletinib, an orally bioavailable irreversible EGFR-TKI, is a derivative of 2,4-diaminopyrimidine. It displays remarkable potency as a TKI,

specifically targeting L858R and deletions in exon 19, as well as the resistant T790M mutation (Yang et al., 2021b, Zubair and Bandyopadhyay, 2023). However, its impact on wild-type EGFR remains limited. Unfortunately, the development of Rociletinib for treating patients with EGFR-mutant NSCLC, particularly those who had previously undergone EGFR-targeted therapy and carried the T790M mutation, was terminated by the sponsor in 2016 . The discontinuation was attributed to undesirable toxicities observed during the TIGER-3 study, including elevated incidences of diarrhoea, hyperglycaemia, QTc prolongation, and cataracts. Following this decision, submissions to regulatory bodies in both the United States and Europe were withdrawn (Yang et al., 2021b).

2.10.4 Fourth Generation EGFR-TKI – EAI045

Patients undergoing treatment with third-generation EGFR-TKIs begin to develop diverse forms of resistance primarily due to the emergence of a tertiary point mutation, C797S in the ATP binding site. Consequently, the introduction of fourth-generation EGFR-TKIs (EAI045) has been initiated for clinical assessment in order to counteract the presence of the C797S (Wang et al., 2017a).

EAI001 a thiazole amide-based compound previously identified through a comprehensive screening of a vast compound library that stands out as a distinctive allosteric inhibitor and showed affinity for mutant EGFR. Despite the presence of the C797S mutation, the drug displays therapeutic benefits due to its unique binding sites on the target (Tripathi and Biswal, 2021). This offers a

promising supplementary treatment strategy in conjunction with ATP-competitive kinase inhibitors. While EAI045 stands as a pioneering fourth-generation EGFR-TKI drug, its maximum effectiveness is attainable solely when combined synergistically with EGFR-targeted monoclonal antibodies like cetuximab. Cetuximab, operating as an ATP competitive inhibitor of EGFR, instigates a reinforcement of structural stability in the EGFR domain upon interaction (Sun et al., 2022).

Currently, research into fourth-generation EGFR-TKIs designed to target C797S mutation is progressing through different experimental phases, and there is no approved drug for clinical utilization (Zhao et al., 2022a).

2.11 Mechanism of Resistance in NSCLC-LUAD

Drug resistance is undeniably an important cancer hallmark, playing a role in the advancement of the disease and impacting individuals with cancer worldwide (Sosa Iglesias et al., 2018). In spite of the advancements seen in clinical outcomes through the introduction of EGFR-TKIs for treating patients with (LUAD carrying EGFR-activating mutations, the prognosis remains unfavourable due to the emergence of resistance mechanisms (Tulpule and Bivona, 2020). At present, the resistance mechanisms initiated by EGFR-TKIs represent a substantial obstacle to the efficacy of treatment strategies due to the molecular heterogeneity present in lung cancer. Mechanism of resistance can be categorized as either intrinsic or acquired, depending on how patients respond to the initial therapy (Wu and Shih, 2018).

2.11.1 Intrinsic Resistance

Intrinsic resistance, alternatively also referred to as primary resistance, manifests when a patient does not exhibit a positive treatment response upon initial EGFR-TKI treatment. This lack of response is accompanied by an absence of discernible enhancements in symptoms, disease management, or overall survival (OS). Intrinsic resistance often arises due to the presence of a non-sensitive EGFR mutation and is predominantly linked to wild-type EGFR (Kobayashi, 2023). Noteworthy mutations associated with intrinsic resistance include exon 19 mutations, exon 20 mutation T790M, and exon 21 mutation (Suryavanshi et al., 2022). Other contributing factors to intrinsic resistance also include KRAS mutations (Luo et al., 2022), BIM polymorphisms (Wakabayashi et al., 2021), activation of NF- κ B signalling (Yu-Chang et al., 2021), and involvement of the tumour microenvironment (Lim and Ma, 2019).

2.11.2 Acquired Resistance

A significant challenge in treating LUAD patients arises from acquired resistance to EGFR-TKIs treatment. According to clinical guidelines, acquired resistance is characterized by tumours harbouring EGFR mutations that respond to TKIs, such as L858R or exon 19 deletions, which additionally demonstrated initial partial or complete response and showed signs of systemic progression thereafter (Nguyen et al., 2009, Passaro et al., 2022). Even though there was notable initial success in patients with specific genetic mutations (exon 19 deletion and L858R), resistance emerged, typically due to the T790M mutation,

around 9 to 14 months after starting treatment (Gaut et al., 2018, Vyse and Huang, 2019). Studies have revealed that prolonged use of first- and second-generation EGFR-TKI drugs (such as gefitinib, erlotinib, and afatinib) leads to the emergence of this resistance (Verusingam et al., 2020). To address this, Osimertinib was developed and approved by the FDA (Remon et al., 2018). It showed promise in targeting the secondary mutation in laboratory and clinical studies, but faced limitations, as subsequent tertiary resistance emerged through new mutations at various genetic locations (C797S, L718/G719, G796/C797, L792, and L798) (Verusingam et al., 2020), highlighting the need for further development of EGFR-TKI drugs and innovative treatment strategies for LUAD patients. Therefore, the unceasing resistance to EGFR-TKIs highlights the complicated evolutionary nature of NSCLC in reaction to EGFR-TKI therapy (Laface et al., 2023).

According to current reports, the emergence of acquired resistance to EGFR-TKI has been linked to bypass signalling (ligand-independent EGFR /non-canonical EGFR signalling pathways) (Gong et al., 2021), histological transformation such as epithelial-mesenchymal transition (EMT) and SCLC transformation (Jin and Yang, 2021), activation of additional oncogenic mutations , as well as the occurrence of brain metastases is also evident (Li et al., 2021).

2.11.2.1 Ligand-independent EGFR Signalling

As NSCLC-LUAD progresses, the ligand-dependent EGFR signalling, drives the signals through its subsequent cascades (RAS-RAF-MEK-ERK-

MAPK and AKT-PI3K-mTOR), fostering cancer cell survival, cell proliferation, increased motility, enhanced migration and promote cellular differentiation (Bahar et al., 2023). However, when certain receptor tyrosine kinases (RTKs) such as HGF/MET, HER2, and AXL, are activated through ligand-independent EGFR signalling manner, they confer resistance to EGFR-TKIs by setting in motion alternative downstream pathways or by activating additional mutations (Liu et al., 2018b). For instance, the interaction between HGF and MET stimulates PI3K/Akt signalling independently of EGFR, prompting diverse biological responses promoting tumour invasiveness, increased metastatic dissemination and reduced anti-apoptosis activities (Spagnolo et al., 2023). This process can curtail the efficacy of EGFR-TKIs in EGFR-mutant NSCLC patients, ultimately resulting in resistance.

Furthermore, the co-existence of an elevated HER2 copy number alongside EGFR contributed to an increased sensitivity to TKIs. Nevertheless, previous research has indicated that HER2 amplification in individuals with EGFR mutations subsequently leads to the onset of acquired resistance to EGFR-TKIs as the tumours become more dependent on HER2 and that bypassed EGFR signalling (Zhao and Xia, 2020).

Previous studies have demonstrated association between elevated AXL protein expression within tumours and unfavourable prognostic outcomes across a range of cancer types (breast cancer, acute myeloid leukemia, and glioblastoma) (Falcone et al., 2020, Wium et al., 2021, Scherschinski et al., 2022). Nonetheless, further research reveals that AXL also plays a role in conferring resistance against Osimertinib in NSCLC, thereby contributing to intrinsic resistance and unfavourable clinical outcomes in patients harbouring

advanced EGFR mutations (Tang et al., 2023). Notably, lung adenocarcinomas with EGFR-activating mutations exhibit a higher prevalence of AXL expression compared to those with wild-type EGFR (Fu et al., 2022). AXL governs downstream signalling pathways, notably MAPK and Akt, thereby promoting NSCLC progression.

Up until now, in multiple clinical contexts, combined approaches involving targeted drug therapy (MET inhibitors, anti-HER2 and AXL inhibitors), monoclonal antibodies and immunotherapy have been investigated to counteract acquired resistance (Gumusay et al., 2020).

2.11.2.2 Histological Transformation

Numerous studies have shown a plausible link between histological transformation and the emergence of resistance to EGFR-TKIs which is significantly correlated to EMT and the transition from LUAD to small cell lung cancer (SCLC) (Shaurova et al., 2020). While histological transformation highly influences patient outcomes due to increased resistance to treatments, the precise mechanisms driving this transformation remain unclear (Lee et al., 2022). As a result, there is a scarcity of data regarding the frequency, factors causing it, underlying mechanisms, effectiveness of treatments, and prospective therapeutic approaches.

EMT is a crucial cellular mechanism regulating normal developmental processes and effective wound healing. However, when there is an abnormal shift from epithelial characteristics to mesenchymal traits, tumour cells acquire the capability to migrate and infiltrate surrounding tissues, ultimately fostering

the spread of cancer, known as metastasis. Hence, EMT-induced morphological alterations can be delineated as a process wherein the tumour cells undergo a transformation, leading to the loss of their epithelial traits and the acquisition of a spindle-like mesenchymal morphology (Ribatti et al., 2020). EMT initiation can be prompted by diverse cellular signals like Wnt/ β -catenin and TGF- β which might bestow an acquired resistance to drugs in cases of LUAD-NSCLC (Hao et al., 2019, Chanvorachote et al., 2022). Recent investigations have also demonstrated that Wnt/ β -catenin and TGF- β fuels EMT by activating the MEK/ERK and PI3K/AKT/mTOR pathways (Bahar et al., 2023). Various transcription factors (ZEB1/2, Slug, Twist 1/2, Snail) and tight junction markers (Vimentin, CDH1, EPCAM) associated with EMT undergo alterations during the development of acquired resistance to EGFR-TKIs (Heery et al., 2017). Additionally, existing research has also indicated the involvement of AXL overexpression contribute to EMT in patients with LUAD (Zhang et al., 2018a).

SCLC transformation arises when surviving persister cells from adenocarcinoma endure the selection pressure exerted by EGFR-TKIs, resulting in their trans-differentiation into cells resembling high-grade neuroendocrine carcinoma. This specific form of lung cancer is characterised as a highly aggressive and malignant tumour, exhibiting an extremely unfavourable prognosis (Leonetti et al., 2021). Previous research has demonstrated a correlation between the development of SCLC transformation and genetic alterations in TP53, RB1, and EGFR among NSCLC patients. Notably, preclinical investigations have indicated that multiple biopsy samples from the same patient display evidence of a transformed SCLC tumour that maintains the original EGFR mutations (Li et al., 2022a). This suggests that these transformed

cells are not entirely de novo clones but rather a changed phenotype of pre-existing cancer cells. The precise mechanisms driving this transformation process remain insufficient.

2.11.2.3 Activation of Additional Oncogenic Mutations

According to findings from the AURA3 clinical trial, the predominant tertiary EGFR mutation observed in patients is C797S (15%) (Gomatou et al., 2023). Interestingly, these patients also retained the T790M mutation. Over time, further tertiary EGFR mutations emerged (L718Q/G719A, G796X, L792H, and S768I) as a result of prolonged treatment (Lin et al., 2018). The clonal evolution of oncogene-dependent non-small cell lung cancer (NSCLC) can lead to diverse molecular changes following treatment failure, thus adding complexity to the mechanisms of molecular resistance. These aberrations can co-occur within the same tumour and coexist alongside EGFR tertiary mutations. Additional driver oncogenes such as MAPK-PI3K mutations (KRAS, PIK3CA, BRAF) (Li et al., 2014b), oncogenic fusions (FGFR3, RET, ALK, NTRK) (Suda and Mitsudomi, 2020), and disruptions in downstream signalling (Loss of PTEN and AKT mutations) (Jacobsen et al., 2017, Liu et al., 2018b) are the outcome of acquired resistance to EGFR-TKIs.

2.11.2.4 Brain Metastases

Studies showed, when comparing patients with EGFR-mutation to those with EGFR wild-type, approximately 70% of the patients with EGFR

mutations experience the emergence of brain metastases, whereas this occurrence is observed in only 38% of the latter (Kelly et al., 2018). The prognosis in cases of brain metastases is unfavourable, which may progress to death within a short span of one to two months. As a result, the presence of brain metastases poses a substantial challenge within the realm of oncological treatment and is associated with the development of acquired resistance to EGFR-TKI (Shao et al., 2022). Importantly, it is noteworthy to know that a low occurrence of the T790M mutation (T790M negative) within central nervous system (CNS) lesions is associated with a poorer prognosis following the acquisition of resistance to EGFR-TKI (Hata et al., 2015, Hata et al., 2015). Based on the currently available body of evidence, patients suffering from NSCLC and EGFR mutations who also have brain metastases exhibit improved overall survival and progression-free survival when subjected to a combined approach of upfront radiotherapy and TKI treatment, as opposed to TKI treatment alone (Sarmey et al., 2022). However, with the ongoing enhancement of long-term survival outcomes in EGFR-mutant NSCLC, the burden posed by brain metastases assumes an increasingly formidable role.

2.12 Unceasing EGFR-TKI Resistance and the Anticipated Corrective

Strategy

Presently, EGFR gene mutations serve as the conventional predictive biomarkers employed to determine the suitability of EGFR-TKI treatment for NSCLC patients. However, continuous treatment in patients induced tumour heterogeneity within NSCLC tumours further contributes to substantial alterations in cellular signalling pathways. Consequently, this leads to the

ongoing emergence of mechanisms of resistance against EGFR-TKI treatment, including the more recent Osimertinib, a third-generation EGFR-TKI (Gregorc et al., 2021).

In the context of NSCLC progression, there is an imperative need for predictive biomarkers capable of identifying Osimertinib-resistance. Available molecular biomarkers should be finely tailored to pinpoint resistance mechanisms, disease progression sites, and the speed of advancement (Rodríguez et al., 2021). Utilization of molecular biomarkers is absolutely important for early detection of lung cancer, leading to improved clinical management decisions by clinicians and clinical outcomes. However, comprehension of the genetic dysregulation and its link to acquired resistance mechanisms for EGFR-TKI treatment seems to be limited. Therefore, the latest advancements in high-throughput techniques such as Next-Generation Sequencing (NGS) might offer enhanced molecular characterization in the future. Application of NGS provides relatively faster, cost-effective genomic analysis of tumour samples from patients which includes the identification of reliable biomarkers and oncogenic drivers that hold utmost clinical significance (Brown et al., 2018).

Simultaneously, obtaining access to tumour tissues is not consistently feasible, particularly in advanced NSCLC and usually serves as routine samples for EGFR mutation analysis (Saito et al., 2017). Invasive procedures like surgery or biopsy become impractical for frequent repetition in order to monitor the development of resistance to EGFR-TKIs (Sun et al., 2015). Considering these limitations, there is a critical necessity to swiftly investigate methods that are more convenient, economically feasible, and non-invasive for monitoring the

effectiveness of EGFR-TKI treatment in NSCLC. Hence, innovative non-invasive methods, often relying on plasma or serum samples, have demonstrated significant potential in monitoring the effectiveness of EGFR-TKI treatment. Present studies indicated that application of blood-based liquid biopsy has emerged as a potential tool in managing NSCLC (Lone et al., 2022, Bertoli et al., 2023).

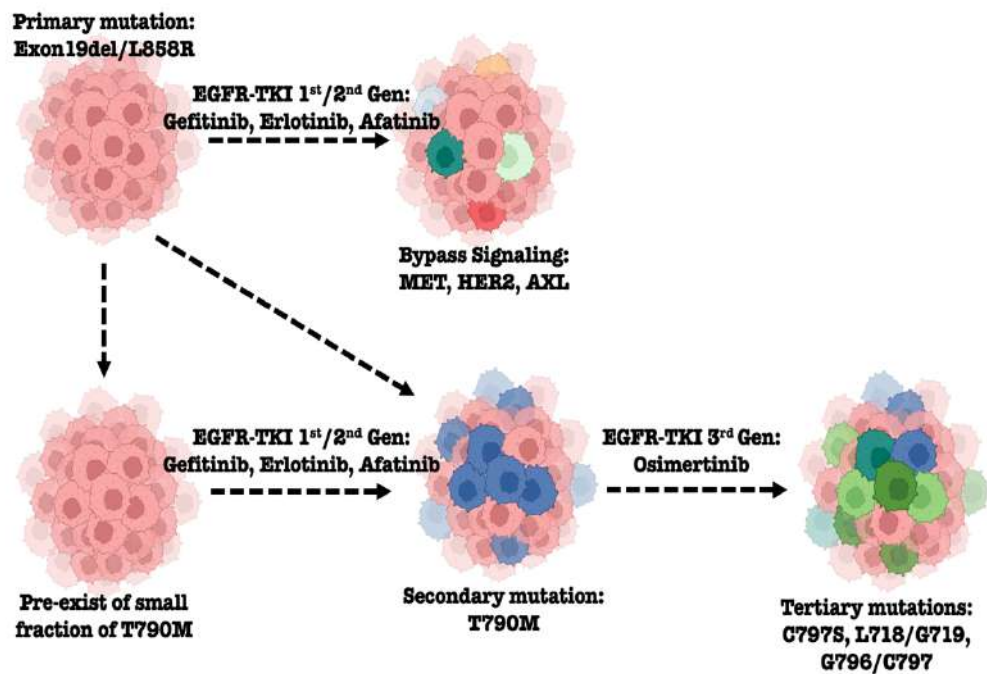


Figure 2.3: EGFR-TKI resistance in lung cancer's fuelled by molecular diversity, significantly impedes the effectiveness of treatment strategies.

2.13 Biomarkers in NSCLC-LUAD Progression

Molecular cancer biomarkers defined by quantifiable molecular cues that signify the potential for cancer risk, the onset of cancer, or the prognosis of patients (Sarhadi and Armengol, 2022). Numerous researchers have diligently worked towards investigating targeted therapeutic biomarkers with the objective of surmounting the acquired resistance to EGFR TKIs. As such, timely and accurate diagnosis of cancer is truly vital with cancer biomarkers. In addition, if the biomarkers prove to be dependable and cost-effective while also contributing to monitoring strategies for cancer risk indication perhaps this could potentially enable patients to receive the most suitable treatment and oversee the advancement, recurrence, and regression of the disease (Ahmad et al., 2023). However, there are numerous challenges that any potential biomarker must overcome, including various stages of validation (such as analytic validity, clinical validity, and clinical utility), before it can be endorsed for clinical use (Parkinson et al., 2014). To date, application of biomarkers involves DNA, RNA and protein based biomarkers in both solid and liquid biopsies. It is crucial to enhance the sensitivity and specificity of these biomarkers, and it is imperative to standardize and validate the techniques used (Khetrapal et al., 2018).

The histopathological identification of lung cancer in compact biopsy samples ascertains the presence of tumour cells within the sample and discerns the particular tumour heterogeneity. Given the invasive nature of biopsies and patient's limited adherence to undergoing multiple such procedures, liquid biopsy holds a distinct advantage (Freitas et al., 2021). Presently, the methods for detecting cancer in NSCLC-LUAD involve analysing tumour tissues,

sputum, and blood samples (Nooreldeen and Bach, 2021). Among these, blood samples hold considerable promise as a source for discovering biomarkers, owing to the infusion of cellular fragments from the tumour into the bloodstream. Consequently, blood can be harnessed as a less intrusive form of liquid biopsy. Blood constitutes an intricate milieu encompassing exosomes (Tamkovich et al., 2019), circulating tumour DNA (Tivey et al., 2022), microRNAs (miRNAs) (Glinge et al., 2017), lipids (Liu et al., 2020), peptides (Guo et al., 2021), as well as a variety of cells including cancer associated fibroblast, endothelial cells and immune cells, thus contributing to its complexity. Recent research has reported on RNA biomarkers, known as long noncoding RNAs and circular RNAs, play crucial functions in driving cancer development, fostering tumour formation, and sustaining ongoing cell proliferation. These biomolecules were shown to be expressed in liquid biopsies and hold the potential to serve as promising candidates for identifying and indicating the presence of lung cancer (Cao et al., 2021).

2.14 RNA Biomarkers

Recent breakthroughs in RNA biomarker research have led to the involvement of highly effective techniques for detecting RNAs in cancer. As compared to DNA, which remains relatively stable, it differs from RNA which is subjected to constant state of change, reflecting the overall health of the cell, organ, and individual. Such criteria makes RNA biomarkers a valuable resource for acquiring high-throughput and real-time insights into cellular conditions and regulatory processes, setting them apart from DNA biomarkers. Moreover, RNA

is present in higher copy numbers within a cell, providing extensive information compared to DNA (Xi et al., 2017, Martinez-Dominguez et al., 2021).

Compared to protein biomarkers, RNA biomarkers exhibit greater sensitivity and specificity (Bae et al., 2022). Cutting-edge methods such as PCR and NGS allowed for the amplification and precise detection of even trace amounts of RNA sequences, ensuring high sensitivity. Not to mention, the cost of detecting RNA biomarkers is relatively lower than that of protein biomarkers, as the latter requires specific antibodies for protein detection. Nevertheless, the simplicity of RNA isolation from various bodily fluids extended their potential as a potential non-invasive biomarker (Nagasaka et al., 2021).

At present, two primary types of RNA-based biomarkers which are coding RNAs and non-coding RNAs, are widely studied in cancer studies (Slack and Chinnaiyan, 2019, Li and Liu, 2019). Transcriptional and post-transcriptional mechanisms can yield a variety of RNA molecules, whether or not they have the ability to code for proteins. Conventionally, messenger RNAs (mRNAs), which encode proteins, constitute about 2% of the human genome by carrying the translatable genetic code (Rönnau et al., 2014). While non-coding RNAs, composed of 20% of the human genome, play a pivotal role in regulating vital biological processes (Peng et al., 2016). Non-coding RNAs also exhibited diversity and can be categorized based on their size and structure into groups such as, small non-coding RNAs (sncRNA), long non-coding RNAs (lncRNAs) and circular RNAs (circRNAs) (Chao et al., 2022). Collectively, these RNA biomarkers enable early disease detection, analysis of differential gene expression, accurate tracking of drug responses, and informative assessments.

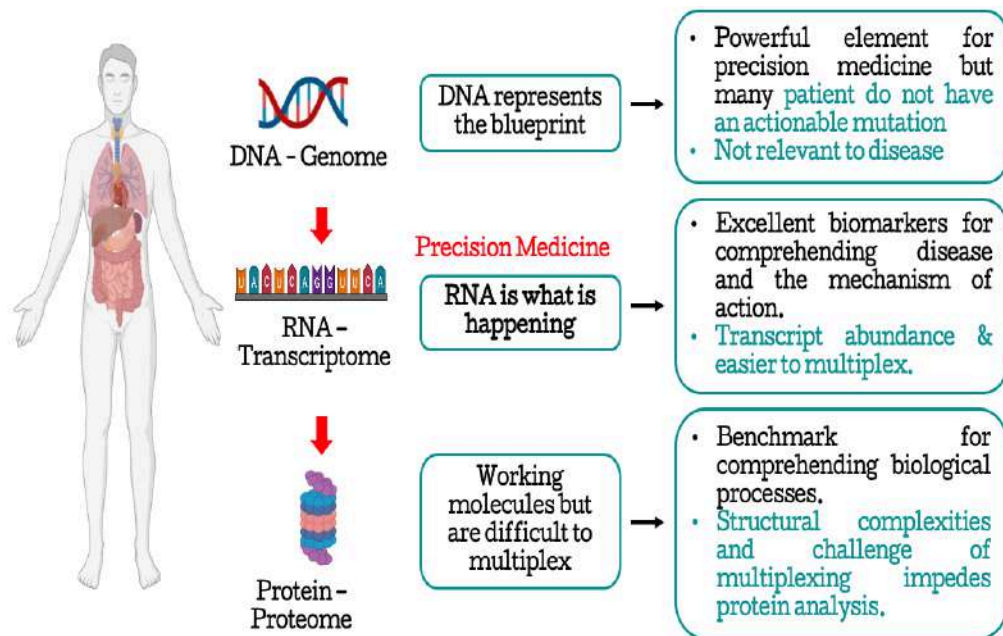


Figure 2.4: The potential of RNA-based biomarker compared to DNA and Protein biomarkers

2.14.1 Messenger RNA (mRNA)

Messenger RNA (mRNA) is a single-stranded ribonucleic acid molecule which harbors the encoded instructions for orchestrating protein synthesis and is known as transcripts. The category of mRNA stands as the most diverse class of RNA, encompassing an abundance of distinct mRNA molecules within a cell at any particular juncture. The length of mRNA molecules displays significant variation and isn't constrained to a fixed length of around 1000 nucleotides (Landeras-Bueno et al., 2021). Certain mRNAs are shorter, whereas others extend considerably longer. Commonly referred to as transcripts, mRNAs exhibit a spectrum of stability. The stability of mRNAs within eukaryotic cells is subjected to diverse factors, encompassing the presence of regulatory components in the mRNA sequence and the interactions with various proteins

that can either enhance its stability or accelerate its degradation. It's indeed accurate that the instability and scarcity of certain mRNA molecules can pose difficulties when considering their application as biomarkers in liquid biopsies or other diagnostic contexts (Wang and Farhana, 2020).

2.14.2 Micro RNA (miRNA)

At present, numerous distinct miRNAs, a type of small non-coding RNA, have been recognized. Extensively researched across a spectrum of diseases, miRNAs have been investigated in various categories, specifically in cancers, hereditary conditions, and more. MiRNAs typically consist of nucleotide sequences spanning from 18 to 24 nucleotides and predominantly participate in regulating gene expression by initiating mRNA translation and fostering mRNA degradation (Sohel, 2016). The process of biogenesis involves the generation of mature miRNAs from extended primary transcripts through a sequence of nucleases. These mature miRNAs are then integrated into an RNA-induced silencing complex, which identifies target mRNAs through base pairing that's complementary. This complex fosters the degradation of target mRNAs or hinders their translation, depending on the extent of complementarity between the miRNA and its target (Lao and Le, 2020). MiRNAs have been detected in bodily fluids like plasma blood, exosomes, cerebrospinal fluid, and urine (Lusardi et al., 2017, Beylerli et al., 2023). In contrast to coding mRNAs, miRNAs typically exhibit greater stability and resilience against degradation. The stability levels, however, exhibit notable variation across different miRNAs, with half-lives spanning from approximately 4 hours to 24 hours. Studies have demonstrated that miRNAs exhibit resistance to degradation even when kept at

room temperature for a duration of up to 24 hours (Glinge et al., 2017, Karl-Frédéric et al., 2021).

2.14.3 Long Non-Coding RNA (lncRNA)

Transcription of genomes leading to the emergence of numerous long non-coding RNAs (lncRNAs), among which a larger ratio resides within the nucleus when contrasted with mRNAs. Nevertheless, notable conservation patterns have been identified within both the exonic and promoter regions of these lncRNAs. Despite their length of around 200 nucleotides and their lack of protein-coding capacity, these lncRNAs play significant roles in cellular functions (Mattick et al., 2023).

2.14.4 Circular RNA (circRNA)

The circRNAs can manifest as non-coding RNAs or even protein-coding RNAs, the latter having been recently uncovered. Their sizes span a broad range, from exceedingly small approximately 100 nucleotides to more extensive than 4 kilobases (Zhang et al., 2018c). Biological function of circRNAs in various cellular mechanisms includes the sequestration of microRNA and protein, regulation of transcription, translation into proteins facilitated by the presence of internal ribosome entry site (IRES), and regulation of DNA methylation. Nonetheless, despite the surging interest in circRNAs, the specific functional capacities of the majority of circRNAs remain elusive (Sun and Yang, 2023b).

2.15 Latest Breakthrough: Circular RNAs (circRNAs)

CircRNAs were initially considered as by-products of abnormal splicing and were largely overlooked (Santer et al., 2019). However, a significant turning point occurred when the existence of single-stranded, covalently closed circRNAs was initially documented in 1976 within viroids. These viroids consist of relatively short sequences, ranging from 246 to 430 nucleotides, and display impressive self-complementarity, allowing them to form circular, non-coding RNA molecules through base pairing (Sanger et al., 1976, Yang et al., 2021d). Shortly thereafter, in 1979, Hsu and co-authors made a ground breaking discovery by confirming the presence of circRNAs in human HeLa cells through the use of electron microscopy (Hsu and Coca-Prados, 1979, Patop et al., 2019).

RNA sequencing has emerged as a highly efficient and commonly employed method for quantifying circular RNAs (circRNAs) for the past ten years. This is achieved through the identification and quantification of sequence reads that align with back-splicing junctions (BSJs) (Zhang et al., 2022). In a ground-breaking investigation, Salzman and colleagues demonstrated the extensive presence of circRNAs in the human transcriptome using RNA-seq from various human cell types. Furthermore, their RNA-seq data revealed that circRNAs represent the dominant transcript isoform in hundreds of human genes (Salzman et al., 2012).

2.15.1 Biogenesis of circRNAs

Canonical splicing event is a critical process in eukaryotes that regulates gene expression by rearranging coding and noncoding gene fragments through ribonucleoproteins (RPN) known as spliceosomes. These fragments, referred to as exons, join together to produce mature linear mRNA transcripts, while introns are simultaneously removed from pre-mRNA (Will and Lührmann, 2011, Kiegle et al., 2018). However, interference during pre-mRNA processing can redirect nascent RNA towards an alternative back-splicing pathway, ultimately forming circRNAs. Despite the distinct back-splicing events compared to the canonical splicing of linear RNAs, circRNA biogenesis can unexpectedly take place at canonical splice sites as well, resulting in a regulatory interplay where they vie for the same splicing sites. Hence, pre-mRNAs are alternatively referred to as circRNA precursors (Zhou et al., 2020).

Circular RNAs (circRNAs) represent a significant category of functional RNA molecules characterized by their continuous loop configuration, formed through back-splicing. Back-splicing is an alternative splicing event that creates a closed loop structure by connecting an upstream (5') splice donor site to a downstream (3') splice acceptor site through exon skipping. This looping is facilitated by the flanking intron sequences on both the splice donor and splice acceptor sites, promoting the efficient circularization of various exons (Quan and Li, 2018). Within these introns, reverse complementary motifs (RCMs) like Alu elements, form loops in pre-mRNA through base pairing, assisting in the back-splicing process (Ragan et al., 2019). Studies in humans have revealed that 88% of circular RNAs (circRNAs) possess ALU repeats in their adjacent introns,

which are likely to facilitate back-splicing processes (Patop et al., 2019). On the other hand, the RNA-binding protein Quaking (QKI) has been demonstrated to promote back-splicing, generating numerous circular RNAs (circRNAs) akin to RCMs. This occurs through QKI binding to adjacent introns, facilitating the formation of loops (Conn et al., 2015).

Following circRNA biogenesis, the majority of exonic circRNAs (EcircRNAs) are transported to the cytoplasm, while intronic (ciRNAs) and intron-exon circRNAs (EiciRNAs) predominantly remain localized within the nucleus (Wang and Fang, 2018, Misir et al., 2022). CircRNAs predominantly originate from exonic regions. EcircRNAs can be formed from either a single exon or multiple exons within pre-mRNA transcript, constituting approximately 85% of the total circRNAs generated (Fontemaggi et al., 2021). Moreover, circRNA can also be derived solely from intronic regions or a combination of both exonic and intronic elements. A subset of intronic lariats manages to escape the debranching process in the course of splicing, leading to the formation of stable ciRNAs. In contrast, EiciRNAs are typically derived from genes with highly active promoter regions (Feng et al., 2023). Circular RNAs (CircRNAs) are notably enriched and stably expressed within exosomes or extracellular vesicles. This observation suggests the potential involvement of extracellular vesicles in clearance mechanisms or their role as mediators in intercellular communication within the context of cancer (Seimiya et al., 2020).

2.15.2 Characteristics of circRNAs

CircRNA have lack of a 5' end cap and a 3' end poly (A) tail which means this distinctive circular composition safeguards circRNAs against degradation by exonucleases, bolstering their biophysical stability in comparison to conventional linear mRNA molecules (Li et al., 2020). It is important to highlight that the majority of circRNAs have a half-life exceeding 48 hours, which stands in stark contrast to linear mRNA, where the average half-life is typically just 10 hours. Research findings have indicated that the average half-life of circRNAs is roughly five times longer than that of mRNAs in most species (Meng et al., 2017, Xie et al., 2020). Furthermore, circRNAs demonstrate specificity with regard to tissue types, developmental stages, and age groups. RNA sequencing studies conducted on human tissues have unveiled that as much as 50% of circRNAs exhibit pronounced tissue specificity, with increased expression levels observed in fetal tissues compared to adult tissues (Cai et al., 2019, Misir et al., 2022). Moreover, it's noteworthy that circRNAs exhibit a level of sequence conservation across various species. For instance, out of the 15,849 circRNAs identified in mice, 4522 of them share analogous sequences with those found in humans. This observation serves as compelling evidence that circRNAs are not merely the by-product of erroneous splicing, as previously believed (Cheng et al., 2021).

As such circRNA was proposed as a reliable diagnostic, prognosis and disease monitoring biomarker which can be used to evaluate the effectiveness of treatments. The robustness of circRNA characteristics facilitates the identification of these entities in different human bodily fluids, thereby

augmenting the capacity of circRNAs to function as non-invasive biomarkers of diagnostic significance (Visci et al., 2020). Current studies showed that circRNAs are extensively involved in multiple signalling pathways and some of which have already been well-characterized for their pivotal roles in human diseases including cancer pathogenesis (Papatsirou et al., 2021).

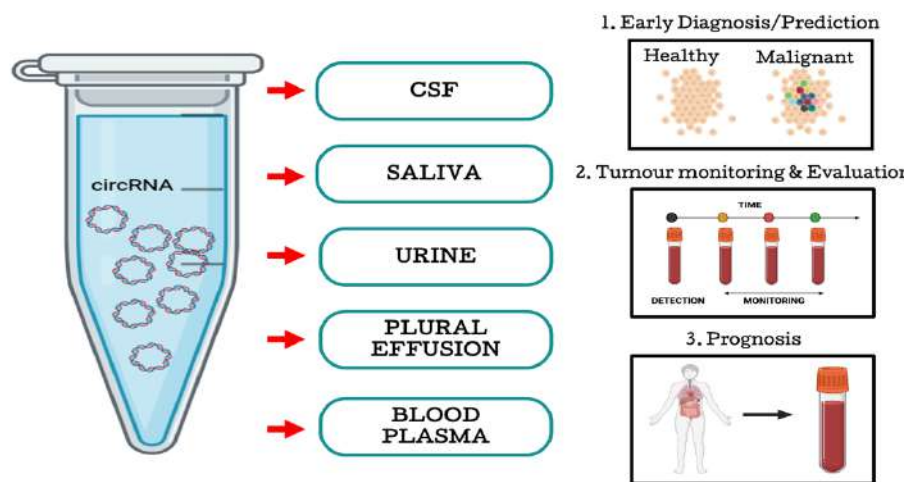


Figure 2.5: CircRNA strength as promising non-invasive biomarker in liquid biopsies

2.15.3 Biological Function of circRNAs

CircRNAs govern a spectrum of biological and molecular functions, which include regulation of splicing and transcription, miRNA sponges, protein scaffolds, and facilitating protein translation (Zhong et al., 2018).

2.15.3.1 Regulation of Splicing and Transcription

Transcription and splicing processes are interconnected, occurring concurrently, and mutually influencing each other. Recent research has demonstrated that RNA polymerase II (RNA pol II) is responsible for transcribing circRNAs, and it is probable that their formation is influenced by the spliceosome. RNA polymerase II is a pivotal enzyme in the tightly regulated gene transcription process, significantly impacting mRNA levels and pre-mRNA splicing. CircRNAs interact with RNA polymerase II in the promoter region of their host genes, and through this pathway, they can effectively regulate and modulate gene transcription (Liu et al., 2017). The rate of RNA polymerase II elongation plays a key role in splicing outcomes, with a slower rate favouring the recognition of weaker splice sites, leading to the inclusion of alternative exons (Muniz et al., 2021). Additionally, the speed of RNA Pol II affects splicing efficiency, and it has been linked to the regulation of circular RNA (circRNA) production, which contributes to the diversity of the transcriptome. In a 2015 study, it was discovered that an EIciRNA known as circEIF3J engages with RNA Pol II and U1 spliceosomal RNA, a small nuclear RNA (snRNA) present in the nucleus. This interaction subsequently enhances the transcription of the genes from which these circEIF3J molecules originate (Li et al., 2015). In a study conducted by Zhang Y et al. in 2013, it was shown that ci-ankrd52 interacts with the RNA Pol II elongation complex. When these circular RNAs (circRNAs) were suppressed, it resulted in reduced transcription levels of Ankyrin Repeat Domain 52 (ANKRD52) proteins (Zhang et al., 2013). This discovery unveils a

novel mechanism through which circRNAs contribute to the regulation of gene expression.

2.15.3.2 miRNA Sponge

CircRNAs contain numerous miRNA-binding sites as such play a crucial role in regulating microRNA by acting as miRNA sponges. This sequestration of miRNAs by circRNAs is primarily achieved through the presence of miRNA response elements (MREs), which serve as sites for miRNA binding and integration. As a result, circRNAs effectively inhibit the endogenous activity of miRNAs by competitively binding to and preventing them from exerting their regulatory functions (Verduci et al., 2019).

2.15.3.3 Protein Decoy/Sponge

While most research on circular RNAs (circRNAs) suggests that they influence downstream genes by functioning as miRNA sponges, some recent studies have proposed that circRNAs also serve as protein decoys, thereby altering activities of the target protein and subsequently affecting downstream genes or pathways. CircRNAs interaction with proteins modulate multiple cellular physiology including tumorigenesis such as cell proliferation and migration, angiogenesis as well as apoptosis (Seimiya et al., 2022). As previously demonstrated by Ashwal-Fluss et al., it was shown that circ-Mbl possesses the capacity to specifically bind to the Muscleblind (MBL) protein and that alterations in MBL protein levels were observed to have an impact on the

biosynthesis of circ-Mbl. This suggests that circ-Mbl may potentially play a role in the regulation of gene expression by engaging in competition with the process of linear splicing (Ashwal-Fluss et al., 2014). On another note, Circ-transportin 3 (TNPO3) was also shown to act as a protein decoy, effectively sequestering insulin-like growth factor 2 binding protein 3 (IGF2BP3). This interaction involving circRNA serves as a protein sponge and has the effect of interfering with the MYC/SNAIL axis, further contributing to the suppression of both proliferation and metastasis in gastric cancer (Yu et al., 2021).

2.15.3.4 CircRNA Facilitates Protein Translation

Typically in a cap-dependent protein translation pathway, the translation initiation factors collectively referred to as eukaryotic initiation factor 4F (eIF4F) enlist eIF4G to assemble the 43S pre-initiation complex, which includes the 40S ribosomal subunit and the eIF complex. Subsequently, eIF4F recognizes the 5'-terminal 7-methylguanosine (m7G) cap of mRNA molecules to trigger the initiation of the translation process (Park et al., 2013, Malka-Mahieu et al., 2017).

The initiation of translation for circRNAs involved a cap-independent mechanism due to their deficiency in both a 5' cap and a 3' end. Currently, two proposed mechanisms have been advanced to elucidate cap-independent protein translation. The initial mechanism that was substantiated indicates that circRNAs necessitate internal ribosome entry sites (IRES) in order to undergo translation. In the context of cap-independent protein translation mechanisms, circRNAs carry an open reading frame (ORF) along with an IRES that enables

it to directly recruit ribosomes to initiate translation (Fan et al., 2022). Study by Wang, Y. and Wang, Z in 2015, demonstrated that circRNAs as the primary source of protein translation, as opposed to the by-products resulting from linear splicing. In their experimental approach, the authors inserted IRES in a circRNA minigene reporter located at the upstream of the GFP's start codon within a single exon encoding two GFP fragments in a reversed sequence. The authors then hampered the production of functional GFP protein by inducing a mutation at the 5' splice site, leading to a complete disruption of the back-splicing junction and also introduced a mutation into the coding region of the GFP sequence, causing a frameshift mutation (Wang and Wang, 2015).

Prior to IRES, another alternative mechanism for the translation of proteins from circular RNAs (circRNAs), is through N⁶-methyladenosine (m⁶A) mediated ribosome entry sites, known as MIREs (Zhang et al., 2020b, Prats et al., 2020). YTHDF3, a widely recognized m⁶A reader protein, was observed to potentiate the recruitment of eIF4G2 to m⁶A sites, thereby driving the initiation of protein translation (Meyer, 2019). The deletion of YTHDF3 results in the inhibition of circRNA translation. Furthermore, absence of an inherent IRES in circRNAs but with presence of a single m⁶A site is adequate to drive translation (He et al., 2021). Previous study by Yang and colleagues, have shown a notable enrichment of m⁶A-predicted motifs within circRNAs. Additionally, consistent findings from m⁶A RNA immunoprecipitation (m⁶A-RIP) have identified a higher proportion of m⁶A sites within the m⁶A methylome. Their data provides compelling evidence for the presence of circRNA translation mechanisms dependent on m⁶A reader proteins (Yang et al., 2017b). Subsequently in 2017, Zhou et al. identified a proportion of m⁶A methylation-

altered circular RNAs (circRNAs) in human embryonic stem cells using a genome-wide mapping platform (Zhou et al., 2017). In 2019 Zhao, Jiawei, et al. detected circE7, a circular RNA encoded by human papillomaviruses (HPVs), which was found enriched in the cytoplasm and carries m6A modifications, ultimately facilitating the translation of the E7 oncoprotein. These findings robustly affirm the inherent capacity for protein translation of circRNAs (Zhao et al., 2019).

2.16 CircRNA Detection and Analysis Methods

CircRNA was first identified through electron microscopy (Sanger et al., 1976) and subsequently confirmed through high-throughput RNA sequencing (Salzman et al., 2012). In recent years, the field has advanced significantly in the development of sequencing pipelines, bioinformatics tools and molecular techniques, greatly simplifying the systematic detection of circRNAs. Presently, the identification, quantification, and analysis of circRNAs consist of a broad spectrum of methods, ranging from low- to high-throughput techniques such as qRT-PCR, sanger sequencing, NGS, FISH assay, northern blotting, droplet digital PCR (ddPCR), overexpression/silencing and pull-down assay (Pandey et al., 2020). In addition, databases designed for circRNA identification are accessible, simplifying circRNA studies such as CircInteractome, circNet and circBase (Aghaee-Bakhtiari, 2018).

2.16.1 CircRNA Sequencing (circRNA-seq)

Detection of circRNAs from NGS analysis are dependent on the identification of reads mapped to back-splice junctions (BSJs), which are subsequently normalized based on certain sequencing depth, measured as reads per billion mapped bases. Due to the relatively lower expression levels of circRNAs when compared to their linear mRNA during analysis, effective circRNA detection required a high sequencing depth, paired-end reads and long-read sequencing parameters (Wang et al., 2017b, Zhang et al., 2020c). Findings reported by Wang et al. in 2017, an analysis of 90 million raw reads only yielded approximately 88 circRNAs, indicating that sequencing depth of higher reads (above 500 million reads) will certainly enhance the probability of capturing circRNAs with low abundance (Guria et al., 2019). Paired-end sequencing confers an advantage for circRNAs with improved large-genome assemblies and the determination of the relative positions of reads within the genome, thereby significantly enhancing its efficiency compared to single-end sequencing (Nielsen et al., 2022). On another note, long-read sequencing is recommended in the circRNA sequencing pipeline since most circRNAs are of multiple exonic origin, made of thousands of nucleotides in length. As such, long-read parameters are able to detect full-length sequences and the precise exon configurations of circRNAs compared to short-read sequencing (Hossain et al., 2022).

Additionally, circRNA sequencing involves non-polyadenylated transcripts during library preparation, which distinguishes it from the typical sequencing of mRNA or miRNA. CircRNA enrichment is crucial to enhance the

sequencing depth especially for circRNAs with low abundance. Therefore, circRNA enrichment methods were highlighted in previous studies on its importance prior to library preparation and subsequent computational analysis (Shi et al., 2022a).

2.16.1.1 CircRNA Enrichment

Current circRNA enrichment methodologies engaged in circRNA sequencing include the removal of ribosomal RNA (rRNA), polyadenylation (poly (A)⁺RNA and linear mRNA degradation.

Depletion of rRNA was the initial approach adapted in RNA-seq to improve transcriptome coverage. During the rRNA depletion process, highly abundant rRNA species are effectively eliminated while preserving all types of coding and non-coding RNAs including circRNAs. Subsequent studies have demonstrated that the polyadenylation of mRNA (Poly(A)⁺ RNA) selection method holds superior efficiencies compared to rRNA depletion, offering improved exonic coverage and more accurate quantification of protein-coding transcripts (Zhao et al., 2018). Polyadenylation involves the addition of Poly(A) tail to the 3' terminus of mRNAs for enrichment relative to other RNA types, including rRNA and transfer RNA (tRNA). Poly(A)⁺ RNA selection requires relatively low sequencing depth and is the preferred technique for the detection of alternative splicing events (Pandey et al., 2019). In circRNA sequencing depleting Poly(A)⁺ RNA enhances the abundance of circRNA expression and thus eases the precision of computational analysis. Another widely utilized approach in the circRNA enrichment process involved the use of Ribonuclease

R (RNase R), an exoribonuclease enzyme, for the depletion of linear RNA. Rnase treatment enhance the efficiencies of circRNA detection despite its greater demand for total RNA input. The Rnase R enzyme cleaves and degrades double-stranded RNA with 3' overhangs that consist of total nucleotides length lesser than seven nucleotides. This degradation occurs because mRNAs lack the protective cap structure at their 3' tail region in contrast to their 5' ends (Xiao and Wilusz, 2019).

Despite the existing techniques, Pandey, Poonam R and group introduced an effective circRNA enrichment flow referred to as RAPD (RNase R treatment followed by polyadenylation and poly(A)+ RNA depletion) for enhancing circRNA sequencing and analysis. The authors subjected the total RNA from human HeLa cells and mouse C2C12 cells to RNase R treatment and subsequently polyadenylation the remaining RNA. Following polyadenylation, they depleted poly(A)+ RNAs using oligo(dT) beads, which resulted in high enriched population of circular RNAs, effectively eliminating linear RNAs. The purified circRNA fraction was then subjected to pair-end sequencing and full-length circRNA sequencing. Analysis of the sequencing data indicated a substantial depletion of linear exons, while exonic circRNAs remained intact (Pandey et al., 2019).

2.16.1.2 CircRNA Library Preparation

Library preparation is a process whereby genomic DNA (gDNA) or complementary DNA (cDNA) will be fragmented into smaller and specific sized fragments which is a crucial step in a sequencing workflow (Head et al., 2014).

As such, insert length required during sequencing depends on the NGS instrument being used. Insert lengths exceeding 600 base pairs are suitable for the HiSeq 2500 and MiSeq, while 350 base pairs for the HiSeq 3000 (Motazedizadeh et al., 2017, Gohl et al., 2019, Zhao et al., 2021). Prior to library construction, the ligation step has been integrated by inserting specialized adapters at both ends of the fragments. The adapters consist of a comprehensive sequences that can hybridize with sequencing primers, followed by the use of an enzyme to connect these specialized adapters to both ends of the DNA fragments (Head et al., 2014). To prepare the blunt ends of each DNA strand for ligation to the sequencing adapters, adenine (A) bases are added. Simultaneously, each adapter possesses a 'T'-base overhang, which offers a complementary overhang for attaching the adapter to the A-tailed fragmented DNA (Son and Taylor, 2011, Kapp et al., 2021).

2.16.1.3 CircRNA Computational Analysis

Multitude computational analysis methods have been introduced to streamline the analysis of circRNA expression by utilizing various algorithms and pipelines. Current algorithms hold a remarkable capability in detecting and predicting the back splicing junctions (BSJ) of circRNAs based on RNA-seq data (Zhang et al., 2020a). The underlying principles of these algorithms can be categorized into two major sections: segmented-based, which involve mapping sequencing reads against a reference genome (hg38 human genome) (Shin et al., 2019) while pseudo-reference-based are dependent on candidate-based approaches (Sekar et al., 2020). A common approach involves segmented-based tools, which identify BSJs by aligning reads to the reference genome and are

generally considered as de novo tools. In contrast, pseudo-reference tools involve gene annotation files to identify the junction reads. As such, existing circRNA algorithms widely used to identify circRNAs are CIRCexplorer3, KNIFE, CIRI, circFinder, circParser and CircleSeq. Majority of these algorithms are efficient in detecting circRNAs derived from exons and introns (Jeck et al., 2013, Szabo et al., 2015, Gao et al., 2015, Ma et al., 2019, Nedoluzhko et al., 2020).

2.16.2 Fluorescence In-Situ Hybridization (FISH) Assay

In situ hybridization techniques enable the detection of precise distribution of gene expression in the nucleus and cytoplasm region. Fluorescence in situ hybridization (FISH) is a technique that involves the binding of DNA or RNA probes, incorporated with fluorescent reporter signals targeting specific sequences in a given sample. Subsequently, FISH enables the visualization of localization of target DNA and RNA within cells by merging high-resolution microscopy such as confocal microscopy. FISH assay have been extensively applied in the field of cytogenetics and it is now widely acknowledged as a dependable diagnostic and research tool in the realm of genetic diseases (Shakoori, 2017).

FISH probes exhibit a high degree of specificity for their intended target DNA/RNA sequences and categorized into four primary types of probes which includes chromosome painting probes, whole genomic DNA probes, repetitive-sequence probes (telomeric and centromeric sequences), and gene-specific probes. Consequently, recent studies have shown that FISH can be employed to analyse circular RNAs (circRNAs) by using fluorescently labeled probes that

span the circRNA back-splice junctions (BSJs). These fluorescent signals can be computationally identified, making FISH a standard method for characterizing circRNAs (Zirkel and Papanonis, 2018). Typically, circRNA FISH probes are designed as a combination of 15-20 nucleotides in length and are labelled with a single fluorophore at their 3' end (Koppula et al., 2022).

2.16.3 CircRNA Affinity Pull Down Assay

Affinity pull-down assay is an *in-vitro* method employed to investigate interactions between protein-RNA complexes, protein-protein interactions, and mRNA-miRNA. Recent research has demonstrated affinity pull-down assay in the context of circRNA studies to elucidate the interactions with miRNA and RNA-binding proteins (RBPs) (Pandey et al., 2020). Current investigations into circRNA have reported that microRNAs function as "microRNA sponges," and also highlighted the binding capabilities of proteins with circRNAs. Hence, affinity pull-down assay facilitate in the effort to discover the role of circRNA as a regulatory role in modulating the functions of these miRNAs and RBPs, thereby influencing post-transcriptional processes of downstream mRNAs (Yang et al., 2021, Liu et al., 2021a).

CircRNA was derived from the entire sequence of its host gene (linear RNA), with the only distinguishing feature being the circRNAs BSJ. Therefore, the principle of the affinity pull-down assay involves the use of specific designed biotinylated antisense oligonucleotides that selectively recognizes the target circRNA's BSJ (Liu and Chen, 2022). This biotinylated antisense oligonucleotide hybridizes with the unique BSJ of the circRNA, thereby

decreasing the probabilities of capturing linear RNAs during the pull-down process. Streptavidin-coated beads are incorporated in the next step facilitating the pull-down procedure, followed by the elution of lysates containing circRNA-miRNA or circRNA-protein complexes (Das et al., 2021). The retrieved pull-down lysates are then subjected to further analyses, by qRT-PCR, western blotting, sequencing, and mass spectrometry (MS), depending on the requirements of the research. If low-abundance circRNAs are of interest, it is recommended to overexpress the circRNA in the samples before conducting the pull-down, thus enhancing the identification of interacting molecules.

2.16.4 Northern Blot

Northern blotting has been established as a standard technique for the validation of multiple RNA isoforms, including the identification and quantification of circular RNAs (circRNAs). The methodology for circRNA identification via Northern blotting requires antisense probes that are complementary to sequences spanning the BSJ within the circRNAs of interest. Subsequently, these probes are loaded onto a denatured agarose gel containing formaldehyde, and hybridization is further carried out. However, Northern blotting in demand for a substantial quantity of RNA, involves multiple procedural steps, exhibits high background noise, and employs radioactively labeled probes. Moreover, the disadvantage of this method is characterized by labor-intensiveness, and time consumption. Also, the primary drawback of Northern blotting is its lower sensitivity compared to by qRT-PCR, making it

suitable for detecting only the most highly abundant circular RNAs (Schneider et al., 2018, Wang and Shan, 2018).

2.16.5 CircRNA Overexpression System

In-vitro overexpression platform or gain of function assay has been commonly used to investigate the effects of circRNAs in disease and cancer research. However, it is worth noting that, overexpression system approach may be implausible at times as it may not represent the spatial and temporal expression patterns of the native circRNAs, downstream gene/protein targets. Therefore, it is important to assess the circRNA to linear RNA ratio generated and a validation of the accurate formation of the back-splice junction (BSJ) prior to overexpression and downstream analysis (Mecozzi et al., 2022).

Overexpression systems using plasmids vectors have been adapted as a common method to study the functions of circRNAs. To date, known functions including sponging microRNAs/proteins, protein translation and modulation of transcription and splicing through plasmid vectors induced overexpression have been widely reported. Plasmids vectors drive back splicing by employing either naturally occurring or artificially introduced inverted repeats (ALU repeats). In order to construct plasmids that express circRNAs, it is important to include exons that of the circular RNA structure, which are surrounded by Alu sequences (Obi and Chen, 2021). These repeat elements of Alu sequences then promote the circularization of the expressed transcript by joining the splice sites into close proximity, thereby facilitating the formation of a backsplicing-like structure (Wilusz, 2015). Plasmid vectors constructed for circRNA overexpression

systems mimic the natural biogenesis pathway which generates both linear and circular RNAs that occur during splicing events. Even though overexpression plasmid vector is commonly employed in circRNA studies, some research has indicated that overexpressing a circRNA of interest can be a more intricate endeavour than circRNA silencing (Liu et al., 2018a). In fact, the delivery of circRNA plasmid vectors has been found to be efficient through the use of genomic integration constructs and transposon-based methods, in contrast to the Lentiviral approach for circRNA delivery.

Overexpression of circRNAs can also be done by transfecting cells with artificial circRNAs generated from *In-Vitro* Transcription (IVT), also known as *In-Vitro* RNA synthesis method (Obi and Chen, 2021). It is an intracellular transcription process synthesizing RNA molecules in a cell-free system. Artificial circRNAs are generated *in-vitro* by T7 RNA polymerase based transcription primed with a GMP, followed by ligation with T4 RNA ligase which works well for relatively short circRNAs (up to ~300 nt) (Nielsen et al., 2022). Even though transfection of *in vitro*-generated circRNAs is sufficient with an appropriate length, amount, circ-to-linear ratio, the amount may not entirely recapitulate endogenous circRNA function (Ho-Xuan et al., 2020). However, present research using this system have indicated a restricted immune reaction to unmodified circRNAs, proposing that these repercussions could be prevented through stringent purification of *in vitro*-produced circRNAs prior to transfection. Previous studies also reported that T7 transcription is known to produce relatively small amounts of dsRNA that can trigger an innate immune response (Nelson et al., 2020). Similar to overexpression systems using plasmids vectors, the stability of transfected circRNAs needs to be monitored throughout

the experiments to ensure that effects attributed to circRNAs are not driven by linear forms.

2.16.6 CircRNA Knockdown System

Loss-of-function assay is equally important in investigating the functional roles of circRNAs in diseases. Robust methodologies such as RNA interference (RNAi), CRISPRi, CRISPR/Cas9, and CRISPR/Cas13 are being used to selectively silence gene expression (He et al., 2021a, Ishola et al., 2022, Feng et al., 2023).

Mechanism of RNAi involves when cytoplasmic double-stranded RNA (dsRNA) is being cleaved by the Dicer enzyme, producing small interfering RNA (siRNA) fragments typically 21–23 total nucleotide length (Zhang et al., 2023b). These siRNAs incorporate with the RNA-induced silencing complex (RISC), inclusive of endonuclease argonaute 2 (AGO2). AGO2 within the RISC cleaves the sense strand of the siRNA, leaving the guide strand (antisense) associated with the RISC. Eventually, the RISC–siRNA complex degrades complementary mRNA, leading to target gene silencing (Dana et al., 2017). Synthetic siRNA and short hairpin RNA (shRNA) activation are common strategies for gene knockdown in mammalian cells. Synthetic siRNA sequence targets and cleaves complementary mRNA directly upon introduction into cells, bypassing Dicer-mediated processing, resulting in transient silencing. While shRNAs introduced into mammalian cells via viral plasmid vectors undergo transcription by RNA pol III. Prior to transcription, the shRNA sequence is cleaved by Dicer into siRNA duplexes further initiates silencing effect. ShRNA

generates stable expression compared to siRNA as it can integrate into the host genome (Sheng et al., 2020). Therefore, the options between siRNA and shRNA methods are dependent on the requirement for transient or stable integration and time constraint.

Recent studies have incorporated Clustered Regularly Interspaced Short Palindromic Repeats (CRISPR technique) and RNAi for gene silencing known as CRISPR interference (CRISPRi) (Larson et al., 2013, Katti et al., 2022). This method differs from the conventional CRISPR/Cas9 system which required guide RNAs (gRNA) to guide Cas9 nuclease for DNA editing. As for CRISPRi, a modified variant dCas9 enzyme was used, along with a single guide RNA (sgRNA). Instead of DNA cleavage, dCas9 binds to a designated genomic site, obstructing transcription and consequently suppressing targeted gene expression (Replege et al., 2022). Additionally, Cas13 enzymes from the CRISPR-associated protein family demonstrated RNA-editing abilities differ from Cas9's DNA targeting. Similar to Cas9, they rely on RNA guidance but cleaves targeted mRNA instead (Abudayyeh et al., 2017, Palaz et al., 2021). As such, the CRISPR/Cas9 system employs guide RNAs (gRNA) to disrupt circRNAs by interfering with the intron pairing around circularized exons (He et al., 2021a). Meanwhile, the CRISPR-Cas13 approach precisely distinguishes circRNAs from linear mRNAs further reducing off-target effects (Ishola et al., 2022). Instead of targeting intronic sequences or gene loci as with CRISPR/Cas9, CRISPR/Cas13 directly aims at the back-splice junction of circRNAs (Feng et al., 2023).

Indeed, the RNAi system provides a feasible approach to knockdown circRNAs. Nevertheless, potential off-target effects necessitate the design of at

least two distinct knockdown sequences strategically positioned to target BSJs with slight variations to evaluate effectiveness in reducing the circRNAs to linear RNAs ratio. Incorporating scrambled sequences as controls is crucial in these experiments (Modrzejewski et al., 2020, Chen et al., 2021b).

2.17 CircRNA Implication in Cancer Hallmark

There are ample studies that have highlighted the involvement of circRNAs in cancer hallmark: either promoting or inhibiting cancer pathogenesis. As such circRNAs can be classified as oncogenic circRNA or tumour suppressive circRNA (Radanova et al., 2021).

Oncogenic circRNAs were shown to dysregulate molecular mechanisms crucial for safeguarding the cellular and tissue homeostasis through a phenomenon associated with cancer hallmarks. Instead, tumour suppressive circRNAs may play a role in inhibiting cancer properties and potentially halt tumour growth (Ando et al., 2021). The impact of circRNAs on molecular signalling pathways that modulates cancer hallmarks includes the sustaining proliferative signalling, resistance to cell death, sustained angiogenesis, insensitivity to antigrowth signals, acquired limitless cell division potential, activation of tissue invasion and metastasis cascade (Yarmishyn et al., 2022).

2.17.1 Sustaining Proliferative Signalling

Proliferation is an important hallmark for cancer development and tumour metastasis. Uncontrolled cell proliferation takes place when the normal

cell homeostasis is disrupted by abnormal signalling cascade and tumour microenvironment. CircRNAs were shown to regulate multitude signal transduction pathways driving tumorigenesis further promoting unlimited proliferation (Zhong et al., 2018).

As such, high expression of hsa_circ_0079557 was recently detected in colorectal cancer (CRC) tissues and in a series of CRC cell lines (SW480 and SW620). In this study, the authors documented that high hsa_circ_0079557 expression was responsible for promoting cell proliferation while, in contrast, inhibiting hsa_circ_0079557 expression reduced proliferation capacity in both *in-vitro* and *in-vivo*. The authors demonstrated that hsa_circ_0079557 regulates Cyclin D1 (CCND1), a prominent gene responsible in cell cycle progression by sponging miR-502-5p. This study concluded that hsa_circ_0079557 promotes cell proliferation in CRC via miR-502-5p/ CCND1 axis (Yu et al., 2023).

In a separate study, hsa_circRNA_0001776 was shown to inhibit endometrial cancer (EC) progression via miR-182/LRIG2 axis. Jia, Y and colleagues, discovered that the hsa_circRNA_0001776 expression was lower in patients diagnosed with grade 3 EC compared to grade 1 and grade 2 while low survival rate was also observed in patients with low hsa_circRNA_0001776 expression. As such, overexpression hsa_circRNA_0001776 showed suppression of glycolysis metabolism in EC. This study further highlighted the role of an oncogenic miR-182 potentially reversed the inhibitory function of hsa_circRNA_0001776 by suppressing tumour suppressive LRIG2 by activating cell proliferation and glycolysis pathways in EC (Jia et al., 2020).

2.17.2 Resistance to Cell Death

Once the oncogenic pathway is triggered, cancer cells evade apoptosis, resisting cell death leading to tumour progression and eventual metastasis. CircRNAs were also known to contribute to these pathways in multiple cancer types (Liu et al., 2021b).

In a study reported by Duan, X et al., circ_0001658 was shown to be upregulated in gastric cancer (GC) tissues and cell lines. When the authors knockdown circ_0001658 in AGS and HGC27 GC cell lines, there's a decrease in cell viability, autophagy but elevated apoptosis. Here, the authors described miR-182 as a known tumour suppressor in GC while Ras-related protein Rab-10 (RAB10) possess oncogenic potential in cervical cancer and are involved in autophagy. Hence, silencing circ_0001658 enhanced the apoptotic potential, downregulated RAB10 expression level by restoring miR-182 in GC cells. Therefore, in this study the authors concluded that circ_0001658 function as oncogenic circRNA inhibiting apoptosis through miR-182/RAB10 signalling axis in GC (Duan et al., 2022).

Another study by Tan, Y et al. demonstrated circZFR, an oncogenic circRNA modulates apoptosis signalling and cell cycle pathway in colorectal cancer (CC). Additionally, the authors elucidated the mechanism of circZFR/miR-147a/CACUL1 in CC cells and its role in apoptosis. CircZFR was highly upregulated in CC cell lines. The authors discovered that knockdown of circZFR, upregulated miR-147a which subsequently impedes cell proliferation and promotes G1/S phase cell cycle arrest. Furthermore, silencing of circZFR increases pro-apoptotic protein expression such as BAX, PARP and cleaved

Caspase-9 indicating elevated apoptotic activity in CC cells. In this study, the authors predicted CALCUL1 (cell-cycle associated gene) is a target of mir-147a based on ENCOR1 database prediction method. In accordance with previous studies, CACUL1 functions as a tumour promoter and is often highly expressed in CC tissues. Owing to the fact that, circZFR sponges miR-147a, silencing of this circRNA also downregulated CACUL1 promoting apoptosis, reducing cell viability and cell proliferation as well as hampered cell-cycle progression in CC cell lines (Tan et al., 2022).

2.17.3 Sustained Angiogenesis

In cancer, angiogenesis is a process where new blood vessels formed around tumours, subsequently support tumour growth and metastasis by supplying additional nutrients and oxygen. Currently, a series of circRNAs were implicated in sustaining angiogenesis further promoting cancer growth. In contrast, a number of circRNAs have also been documented to be involved in the suppression of angiogenesis (Jiang et al., 2021b).

CircSMARCA5 was reported to interact with SRSF1 (a potential oncoprotein) regulating the pro-angiogenic and anti-angiogenic factors in GBM. In this study, the authors found circSMARCA5 was downregulated in GBM subtypes but high expression of SRSF1 and its downstream target VEGFA mRNA as compared to unaffected brain parenchyma samples. Similar expression pattern was also consistent in the GBM cell lines (A172, CAS-1 and U87MG). On top of that, their data also showed that the VEGFA pre-mRNA isoforms ratio, Iso8a (pro-angiogenesis) to-Iso8b (anti-angiogenesis) was

significantly higher in GBM biopsies compared to UC samples. Prior to overexpressing circSMARCA5 in U87MG, the ratio of Iso8b increases over Iso8a indicating reduction in angiogenic potential. Subsequently the authors also reported that the blood vascular microvessel density (MVD) negatively correlated to circSMARCA5, as such positively correlated to SRSF1 expression in GBM patient cohort. Also, circSMARCA5 contributed to poor OS and PFS in GBM. Therefore, Barbagallo and group demonstrated that circSMARCA5 attenuated the angiogenic potential in GBM by modulating SRSF1 and subsequently regulating VEGFA indirectly (Barbagallo et al., 2019).

While, high expression of oncogenic circFOXP1 was detected in osteosarcoma against normal tissues and consistently expressed in a series of osteosarcoma cell lines (U2OS, MG-63, HOS, SAOS-02). According to the authors' survival analysis, it was observed that the 5-year survival rate among osteosarcoma patients with high circFOXP1 expression was comparatively low. Later evidence demonstrated by Zhang H et al. indicating CircFOXP1 promotes angiogenesis in osteosarcoma via miR-127-5p/CDKN2AIP signalling axis. Subsequently, the authors elucidated on how circFOXP1 exert its regulatory function on CDKN2AIP as the mechanism responsible in promoting angiogenesis in osteosarcoma. Luciferase assay showed circFOXP1 significantly binds to miR-127-5p. Furthermore, miR-127-5p and circFOXP1 expression were negatively correlated in clinical samples. These findings indicated that circFOXP1 sponges miR-127-5p in osteosarcoma tissues samples. However, CDKN2AIP was then denoted as a target of miR-127-5p. All in all, the data showed that circFOXP1 sponges miR-127-5p, upregulates CDKN2AIP in promoting angiogenesis in osteosarcoma (Zhang et al., 2021a).

2.17.4 Insensitivity to Antigrowth Signals

Tumour suppressor genes (TSGs) serve as a key factor to monitor and impede uncontrolled cell growth and prevent abnormal cell transformation (Wang et al., 2018). Countless TSGs such as tumour protein (TP53), retinoblastoma (RB), epithelial cadherin (CDH1), phosphatase and tensin homolog (PTEN), and adenomatous polyposis coli (APC) have been known for playing an important role in guarding the genome by activating apoptosis, hinder cell-cycle progression, and induce DNA repair mechanisms (Eshghifar et al., 2017, Shenoy, 2019, Chen et al., 2020, Hu et al., 2021). However, aberrant genomic mutations and activation of oncogenes propel the initiation of tumorigenesis, promoting tumour growth (Rivlin et al., 2011). Numerous research have elucidated the role of circRNAs in either promoting or inhibiting cell proliferation, invasion, migration, and metastasis (Chen et al., 2019b) (Huang et al., 2019) which includes the regulatory impact of circRNAs on TSG and how they might facilitate or impede the evasion of growth suppressors.

He, J et al. reported that circ-MAPK4 (has_circ_0047688) attenuated the phosphorylation of p38/MAPK4 while sponging tumour suppressive miR-125a-3p in glioma tissues. The authors found the circ-MAPK4 was highly expressed in glioma tissues compared to its non-tumour tissue counterpart. Previous studies have demonstrated when p38/MAPK4 is phosphorylated, it inhibits tumour cell proliferation and promotes cellular apoptosis. In this study, the authors confirmed by knocking down circ-MAPK4 expression, the size of glioma xenograft tumours reduced in *in-vivo* while TUNEL assay indicated increased

cell apoptosis. Likewise, miR-125a-3p expression exhibited negative correlation upon silencing of circ-MAPK4 (He et al., 2020).

Whereas, circRNA CDR1as was shown to promote apoptosis by positively regulating p53 in glioma cells. The researchers revealed that CDR1as safeguards p53's function by intersecting the p53/MDM2 protein complex. When MDM2 (a negative regulator of p53) binds to p53, it suppresses p53's transcription, activates its degradation and further initiates cancer progression. In fact, deactivating circRNA CDR1as, induces DNA damage in gliomas, setting off the progression of oncogenic processes (Lou et al., 2020).

2.17.5 Acquired Limitless Cell Division Potential

Normal cells have a limited lifespan owing to decreased cell division process over time after multiple rounds of divisions, ultimately leading to cellular inactivity. This limitation is driven by the reduction of telomeres, a protective cap at the ends of DNA, activating either cellular senescence or apoptosis. Senescence and apoptosis mechanisms are important as they thwart cells from perpetually existing and accumulating mutations during the cellular repair mechanism (Chakravarti et al., 2021).

Telomeres consist of repeating short sequences of 'TTAGGG' which essentially serve as a 'circadian clock', ensuring a controlled replicative capacity while protecting chromosome ends from damage (Trybek et al., 2020). Telomeres length in a normal cell is regulated by catalytic enzymes of telomerase known as human telomerase reverse transcriptase (hTERT) as such abnormal telomere shortening results in inevitable genome instability and DNA

damage occurs. If DNA damage becomes uncontrollable and disrupts telomere function, the normal cells transform into cancer cells. Abnormal activation of hTERT activity affects telomeres and enables the immortalization of cancer cells (Leão et al., 2018).

Multiple studies have highlighted the involvement of circRNA and its interactions with hTERT in cancer pathogenesis. In a study conducted by Zhang, X. L et al., they observed increased expression levels of hsa_circ_0020397 alongside downregulation of miR-138 within colorectal cancer (CRC) cells. These interactions promoted cellular viability and invasion while concurrently inhibiting apoptosis. The researchers demonstrated that hsa_circ_0020397 sequesters miR-138, confirming the negative correlation between these entities through luciferase assays. Furthermore, it was reported that miR-138 modulates the expression of target genes TERT and PD-L1, both of which play crucial roles in the advancement of CRC. Silencing of TERT or PD-L1 using siRNA system resulted in the downregulation of hsa_circ_0020397, implicating its involvement in suppressing CRC cell viability, apoptosis, and invasion via the upregulation of miR-138 (Zhang et al., 2017).

In a recent study led by Jiang, X and colleagues, it was discovered that circular MEG3 (CircMEG3) impedes the growth of liver cancer stem cells (CSCs) by reducing telomerase activity through HULC and Cbf5. Previous studies have indicated that the long non-coding RNA MEG3 capable of forming CircMEG3, downregulated in human liver cancer and possess a tumour suppressor role. HULC has been identified as being deregulated in cancer and has potential as a biomarker, whereas Cbf5 is an essential component of the telomere synthase H/ACA ribonucleoprotein (RNP). In this research, the authors

have demonstrated that CircMEG3 has reduced expression levels and was negatively correlated with the expression of the telomerase-associated gene Cbf5 in human liver cancer. Furthermore, their RNA-seq confirmed that CircleMEG3 suppresses the activity of HULC, METTL3, and Cbf5. On the other hand, the protein chip analysis also corroborated the RNA-seq data whereby HULC actually elevated the levels of METTL3 and Cbf5. Alongside with their *in-vitro* data their discoveries strongly suggest that CircMEG3 hinders the progression of liver cancer (Jiang et al., 2021c).

2.17.6 Activation of Tissue Invasion and Metastasis Cascade

Cancer invasion and metastasis occurs when cancer cells detached from the primary tumour, spreading to nearby organs, and forming secondary and/or tertiary tumours (Martin et al., 2013). Genetics, epigenetics, and various unknown aetiology contribute to this process. Activation of invasion-metastasis in cancer patients leads to disease recurrences, treatment resistance, and increased mortality rates (Kilmister et al., 2022). Studies shows that aberrations in the extracellular matrix (ECM) triggered a stepwise cancer progression which starting with altered ECM dynamics, then invasion, entry into blood or lymphatic vessels (intravasation), and exiting from these vessels (extravasation) (Walker et al., 2018). Loss of cell to matrix interactions and increased blood vessels formation facilitate cancer cell detachment promoting invasion of nearby tissues, and migration to the blood and lymph systems. Eventually, these cells settle in distant organs, forming new tumour foci (Winkler et al., 2020). However, ECM has the capability to modulate EMT transcription factors, thereby regulating the

process of EMT. As such, the involvement of EMT in invasion and metastasis cascade was also significantly demonstrated by ample studies. During the EMT process, cancer cells acquired cellular plasticity which leads to the adoption of a mesenchymal-like phenotype from the epithelial state. Such abnormal transformations into mesenchymal-like phenotypes promote the capacity for cell motility, enhanced migration and invasion properties (Lu and Kang, 2019).

At present, there are substantial evidence supporting the involvement of circRNA-miRNA-mRNA network in either promoting or inhibiting the invasion-metastasis cascade via EMT in cancer progression. Zhang, R et al. have shown the oncogenic properties exhibited by circ_0001666/miR-1251/SOX4 regulatory axis in pancreatic cancer (PC). Their study revealed that this circ_0001666 facilitates EMT, cell proliferation and invasion in PC. They demonstrated that overexpression of miR-1251 reduced the oncogenic effects of circ_0001666 further inhibiting SOX4 expression, as corroborated by both *in-vitro* and *in-vivo* data (Zhang et al., 2021b). As previously comprehended, circRNA modulates the regulation of protein translation by sequestering RNA-binding proteins (RBPs) (He et al., 2021a). However, there is limited understanding regarding the role of circRNA-RBP interactions in promoting invasion and metastasis in cancer (Jiang et al., 2021a). Drawing from existing research, a novel circ0005276 has been identified in prostate cancer, known to promote cell proliferation, EMT, and migration via FUS binding protein (FUS). The binding of circ0005276-FUS activates the X-linked inhibitor of apoptosis protein (XIAP), which is the host gene of circ0005276. The authors of this study demonstrated that circ0005276-FUS positively regulates XIAP transcription, thereby promoting metastasis in their *in-vivo* animal (Feng et al., 2019).

2.18 CircRNA in Lung Cancer (NSCLC)

In recent times, a substantial number of data has demonstrated the involvement of circRNAs in the modulation of NSCLC in cancer hallmarks, significantly contributing to the initiation, progression, infiltration, and metastasis of tumours (Table 2.1). These circRNAs have been extensively documented as promising biomarkers with potential applications in prognosis, prediction, monitoring, and diagnosis (Li et al., 2022b).

Table 2.1: CircRNAs involved in the regulation of lung cancer.

No	CircRNA	Cancer Hallmark	Oncogene/ Tumour Suppressor	Reference
1	circXPO1	Promote Proliferation	Oncogene	(Huang et al., 2020a)
2	circPRKCI	Evading Tumour Suppressor	Oncogene	(Qiu et al., 2018)
3	hsa_circ_0001946	Evading Immune Checkpoint	Oncogene	(Zhang et al., 2018b, Yao et al., 2019)
4	circFGFR1	Evading Immune Checkpoint	Oncogene	(Zhang et al., 2019)
5	circ-CPA4	Evading Immune Checkpoint	Oncogene	(Hong et al., 2020)
6	hsa_circ_0000190	Promote Proliferation	Oncogene	(Luo et al., 2020)
7	hsa_circ_0007142	Evading Immune	Oncogene	(Ma et al., 2020)
8	circMET	Proliferation/Metastases/ Immune Evasion	Oncogene	(Pei et al., 2020)
9	CiRS-7 (CDR1as)	Inhibits cell apoptosis and promote proliferation	Oncogene	(Xu et al., 2020b)

10	circHIPK3	Promote Proliferation	Oncogene	(Guo et al., 2020)
11	circZFR	Evading Tumour Suppressor, promote Proliferation	Oncogene	(Ren et al., 2020)
12	circFGFR1	Proliferation / Migration	Oncogene	(Tan et al., 2021)
13	circFAT1(e2)	Promote Migration and invasion	Oncogene	(Dong et al., 2021)
14	circ_0015278	Promote cell apoptosis and inhibit proliferation, invasion and EMT	Tumour suppressor	(Ye et al., 2021)
15	circWHSC1	Promote Migration and invasion, Inhibit apoptosis	Oncogene	(Shi et al., 2021)
16	hsa_circ_000881	Inhibit migration and invasion	Tumour suppressor	(Huang et al., 2021)
17	hsa_circ_0002483	Promote proliferation and invasion	Oncogene	(Wan et al., 2021)
18	circ_0000317	Inhibit proliferation, migration and invasion	Tumour suppressor	(Xia and Zhang, 2022)
19	hsa_circ_0070659	Promote proliferation, migration and invasion	Oncogene	(Meng et al., 2022)
20	hsa_circ_0000520	Promote Migration and invasion	Oncogene	(Han et al., 2022)
21	circ_0001998	Promote proliferation and invasion	Oncogene	(Shi and Ju, 2022)
22	circ-0002727	Promote proliferation, migration and invasion	Oncogene	(Li et al., 2023c)

23	circATP9A	Promote proliferation and Immune Evasion	Oncogene	(Yao et al., 2023)
24	circRANGAP1	Promote cell migration	Oncogene	(Zhao et al., 2023)
25	circ_0129047	Promote cell apoptosis and inhibit proliferation	Tumour suppressor	(Xia et al., 2023)

2.18.1 CircRNA in EGFR-TKI Resistance Lung Cancer (NSCLC)

Recent breakthrough of mRNA vaccines targeting SARS-CoV-2 has significantly proclaimed its application as an excellent RNA-based therapeutic and a robust platform for experimenting various diseases (Li et al., 2023a). RNA biomarkers confer dynamic insights into cellular states and regulatory mechanisms, providing more comprehensive information inclusive of superior sensitivity and specificity. Besides, circRNAs have demonstrated superiority over traditional DNA and protein biomarkers and thus denoted as a promising RNA biomarker revolutionizing disease diagnostics, prognosis, predictive and monitoring, particularly in cancer.

Existing evidence has suggested that circRNAs prominently influence EGFR TKI-resistant lung cancer by regulating signalling pathways. Studies have shown, circRNA potentially affects pathways related to EGFR such as MAPK/ERK pathway (known as a key mechanism in EGFR-TKI resistance) and miRNA/mRNA axis. As such, oncogenic C190 was shown to modulate EGFR/MAPK/ERK signalling pathway by sponging miR-142-5p driving EGFR-TKI resistance in lung cancer patients. Yet, in this study, evidence remains inadequate to evidently elucidate its role in drug resistance (Ishola et al.,

2022). On the flip side, high expression of hsa_circ_0004015 offset the downregulation of miR-1183, fostering resistance to gefitinib. The authors reported that increased hsa_circ_0004015 level correlates with poor OS and increased invasion indicated by TNM staging of lung cancer patients (Zhou et al., 2019). Table 2.2 summarizes circRNAs involved in EGFR-TKI resistance in lung cancer and its molecular mechanisms.

Table 2.2: CircRNAs implicated in EGFR-TKI resistance.

No	CircRNA	EGFR-TKIs	Molecular Signalling Pathway	Reference
1	hsa_circ_0004015	Gefitinib	miR-1183/ PDPK1	(Zhou et al., 2019)
2	circSETD3	Gefitinib	miR520h/ ABCG2	(Huang et al., 2020b)
3	circRNA_102481	Gefitinib, Erlotinib	miR-30a-5p/ ROR1	(Yang et al., 2021a)
4	circHIPK3	Gefitinib	-	(Zhao et al., 2022b)
5	circKIF20B	Gefitinib	miR-615-3p/ MEF2A	(Wei et al., 2023)

2.19 Understanding the role of circRNA in Mechanism of Resistance to Osimertinib

Although numerous studies have highlighted circRNAs diagnostic and prognostic significance in lung cancer, limited research has explored their association with EGFR-TKIs resistance. As discussed earlier, when EGFR mutation-positive NSCLC patients are continuously exposed to Osimertinib, they develop tertiary EGFR mutations, becoming resistant to treatments (Li et

al., 2023d). The mechanism developed along the course of treatment hampers the efficacy of EGFR-TKIs and without comprehending why this happens.

A number of studies have elucidated how circRNAs contribute to Osimertinib resistance and the associated signalling pathways involving miRNA/mRNA (listed in Table 2.3) from different sources, including cell lines specific to LUAD (HCC827 and H1975), as well as tumour tissues. To date, these circRNAs were primarily reported as promoting cancer (oncogenic) rather than suppressing tumour growth (tumour suppressor). Nevertheless, more research is required to explore circRNA encoding proteins or translatable circRNAs that may suppress tumour growth which could lead to valuable diagnostic markers.

Therefore, circRNA can represent as a promising RNA biomarker for investigating resistance to Osimertinib since it has been shown to highly involved in cellular functions such as miRNAs and RBPs, transcription regulation, IRES-mediated translation, and DNA methylation regulation, marking them as valuable contributors to RNA-based research and applications (Chen et al., 2021a). As such, an *in-vivo* study conducted by Liu et al. revealed that although Osimertinib selectively inhibits EGFR signalling pathway it isn't sufficient to completely hinder downstream phosphorylation of AKT and ERK1/2 activity. On the other hand, silencing hsa_circ_0005576 followed by Osimertinib treatment, there was a significant inhibition of AKT and ERK1/2 phosphorylation with improvised sensitivity to Osimertinib (Liu et al., 2022a). Elucidating the interactions of circRNAs with other RNA species, RBPs associated with EGFR signalling pathways (both canonical and non-canonical)

as well as EGFR mutations in Osimertinib resistance concede potential insights into understanding resistance mechanisms.

Table 2.3: CircRNAs implicated in Osimertinib resistance.

No	CircRNA	Molecular Signalling Pathway	Oncogene/ Tumour Suppressor	Sample Source	Reference
1	hsa_circ_0043632	miR-492/TIMP2	Oncogene	LUAD cell lines	(Chen et al., 2019)
2	hsa_circ_0002130	miR-498/ GLUT1/HK2/LDHA	Oncogene	serum exosomes	(Ma et al., 2020b)
3	hsa_circ_0005576	miR-512-5p/IGF1R	Oncogene	LUAD cell lines	(Liu et al., 2022a)
4	hsa_circ_0007312	miR-764/MAPK1	Oncogene	tumour tissues; LUAD cell lines	(Dai et al., 2022)
5	circKRT17	METTL3/circKRT17/EIF4A3/YAP1	Oncogene	tumour tissues; LUAD cell lines	(Ji et al., 2022)
6	circPDLIM5	-	Tumour suppressor	LUAD cell lines	(Chen et al., 2023)
7	circPPP4R1	-	Oncogene		
8	circRBM33	DNMT1/IL-6	Oncogene	LUAD cell lines	(Pan et al., 2023)

2.20 Future Application of CircRNA as Diagnostic, Prognosis, Predictive And Monitoring Biomarker in Osimertinib Resistance

Liquid biopsy method has consistently proven advantageous against tissue biopsies for diagnosing cancer, owing to its non-invasive approach, remarkable sensitivity and specificity. Notably, circRNAs exhibit high stability in liquid samples and are resistant to degradation by exoribonuclease enzymes with longer life-span than other RNA species. This distinctive characteristic confers potential as reliable tumour markers, where it can be easily detectable in bodily fluids (Pisignano et al., 2023).

Aligned with diagnostic testing, the NGS platform has significantly contributed to the profiling of circRNA expression patterns. NGS technology has the potential to streamline the identification of NSCLC patients prone to high resistance against Osimertinib (Ruan et al., 2023, Chen et al., 2023). Moreover, the use of highly sensitive and accurate ddPCR method facilitates the detection of circRNAs and the screening of circRNAs that indicate the differential expression patterns in both resistant and non-resistant groups which serves as a robust diagnostic and prognostic tool (Luo et al., 2020).

In addition, exploring the potential of circRNA as a biomarker (Sun and Yang, 2023a) in patients with LUAD undergoing 1st/2nd/3rd EGFR-TKIs treatment holds promise in monitoring and predicting the emergence of resistance to Osimertinib and post-treatment outcomes, including the potential disease recurrence. CircRNA can be used to monitor intratumor heterogeneity and the evolutionary transition contributing to Osimertinib resistance in NSCLC patients with EGFR mutations. Hence, circRNA indeed serves as a promising

predictive marker for the occurrence of metastasis following Osimertinib resistance (Souza et al., 2023). Indeed, circRNA may prove valuable in tailoring personalized therapies that may be used to target circRNA and its downstream RNA and protein biomolecules abnormalities present in patients facing resistance to Osimertinib.

2.21 Future Application of CircRNA as Therapeutic Target in Osimertinib Resistance

Breakthroughs in RNA cell-based therapy have led to the establishment of mRNA vaccines, coupled with nano-materials and charge-altering releasable transporters (CARTs) for RNA delivery systems in human clinical application for prevention and treatment of various diseases including cancer (Haabeth et al., 2018, Zhang et al., 2023c, Chehelgerdi and Chehelgerdi, 2023). However, there are studies reported that, current use of mRNA as delivery target and vaccines may activate immune response and exhibit significant instability during *in-vivo* delivery (Zhang et al., 2023a).

Utilizing therapeutic proteins derived from circRNAs instead, may supersede the limitation encountered during mRNA-based therapies. Engineered circRNAs consist of coding regions that enable translation of untranslated regions, vaccine antigens, promoters, and RNA spacers (Xie et al., 2023). Previous studies have reported that circRNA vaccines produce therapeutic proteins similar to mRNA vaccines via IRES-mediated translation pathway and effectively activate cellular immunity but with low immunogenicity compared to mRNA-based vaccines (Bai et al., 2022). In

addition, existing studies suggested that circRNA vaccines exhibit prolonged protein translation, lasting up to approximately 7 days, surpassing the duration of linear mRNA vaccines upon *in-vivo* delivery (Chen et al., 2022a, Wan et al., 2023). In a most recent study by Amaya et al. demonstrated the innate immune responses triggered by circOVA when encapsulated in CARTs delivered *in-vivo*. The authors revealed that immunization with CART-encapsulated circRNA, encodes specific antigen which enhances antigen presentation, potent cellular immunity, and facilitates successful tumour clearance. Furthermore, CART-circRNA vaccine was tested for its anti-tumour efficacy in mice subcutaneously transplanted with Syngeneic B16-F10-OVA melanoma cells. The circRNA vaccine group demonstrated significant inhibition of tumour growth compared to the untreated group. Their findings implicated that circRNA immunization holds promise as an effective cancer immunotherapy for inhibiting *in-vivo* tumour growth (Amaya et al., 2023).

On another note, nano-materials technology serves as an effective vehicle for targeting circRNA being both as carriers and delivery systems. CircRNA can be introduced without encapsulation or with encapsulation within nanoparticle-based delivery systems, such as lipid-based or polymer-based nanoparticles. Several studies have demonstrated the application of circRNA as a therapeutic target within nano-material delivery systems. In 2017, Du et al. demonstrated the tumour suppressive role of circ-Foxo3 in breast carcinoma. The authors showed that delivery of circ-Foxo3 plasmid conjugated with gold nanoparticles could inhibit xenograft tumours in mice model (Du et al., 2017). Meanwhile, Muller et al. demonstrated Polyethylenimine-based nanoparticles (PEI) carrying circular RNA decoys inhibit oncomiR miR-21-5p subsequently

impairs the oncogenic potential in lung adenocarcinoma. The authors confirmed the therapeutic efficacy of circular miR-21-5p decoys delivered via PEI nanoparticles in an *in-vivo* setting (Müller et al., 2020).

On the whole, circRNA not only holds potential as a diagnosing, prognostic, monitoring, and predictive biomarker but also could be employed as a promising clinical molecular therapeutic target for treating NSCLC patients who acquired resistance to Osimertinib due to its stability and its sponging capacity to miRNAs and proteins. As such, similar technology through circRNA vaccines alongside with nano delivery technology and CART delivery could be applied to target circRNA and its downstream pathway involving miRNAs and RBPs either by inhibition of oncogenic circRNAs that promote Osimertinib resistance, or alternatively, by inducing overexpression of tumour suppressive circRNAs inhibiting Osimertinib resistance and metastasis in NSCLC patients.

CHAPTER 3

MATERIALS AND METHODOLOGY

3.1 Overview of Methods

Commercial H1975 (CRL-5908) cell line carrying L858R/T790M EGFR mutations used in this study was purchased from American Type Culture Collection (ATCC), Manassas, VA. This cell line was established from a non-smoking female diagnosed with lung adenocarcinoma (NSCLC), displays resistance to both 1st and 2nd generation EGFR-TKIs but responds to Osimertinib (AZD9291). The characteristics and properties of H1975 cell lines were previously validated by ATCC. Osimertinib-resistant clones (OR3,OR4 and OR6) were derived from H1975 as described in previous study (Verusingam et al., 2020). All OR clones were characterized and validated prior to circRNA-seq. In this study, H1975AZDR cells/HOsiR (pool clone of Osimertinib-resistant cell line) was also included in the experiments which was kindly provided by Dr Chou Yu-Ting from National Tsing Hua University, Taiwan. CircRNAs identified from differential expression profiling were validated and characterized through a series of different methods, including qRT-PCR, RNase R treatment, Actinomycin assay, and ddPCR. Subsequently, putative circRNA selected from transcriptome analysis was further subjected to gain and loss of functional assays and assessed for tumorigenicity properties using drug sensitivity assay, colony formation assay, tumour sphere formation,

migration assay and western blot analysis. Apoptosis activity was quantified using flow cytometry and micro-western blot array. Further, proof of concept experiments were carried out to establish miRNA/mRNA axis pathway of target circRNA using biotinylated pull-down assay and miRNA-seq. In-silico analysis was used to predict mRNA associated with miRNA which was selected for downstream analysis. Osimertinib resistant *in-vivo* mouse model further was established to corroborate the outcome of circRNA/miRNA/mRNA axis with *in-vitro* findings. Xenograft tumours harvested from the mouse model were subjected to qRT-PCR, IHC staining, FISH analysis and Western blot analysis. Mycoplasma screening was carried out in all cell lines used in this study via Polymerase Chain Reaction (PCR). All samples in active cell cultures were confirmed free of bacterial and mycoplasma contamination. Active cell cultures were maintained for not more than 10 weeks prior thawing from cryogenic storage. An overview of the methods used is illustrated in the flowchart provided below (Figure 3.1).

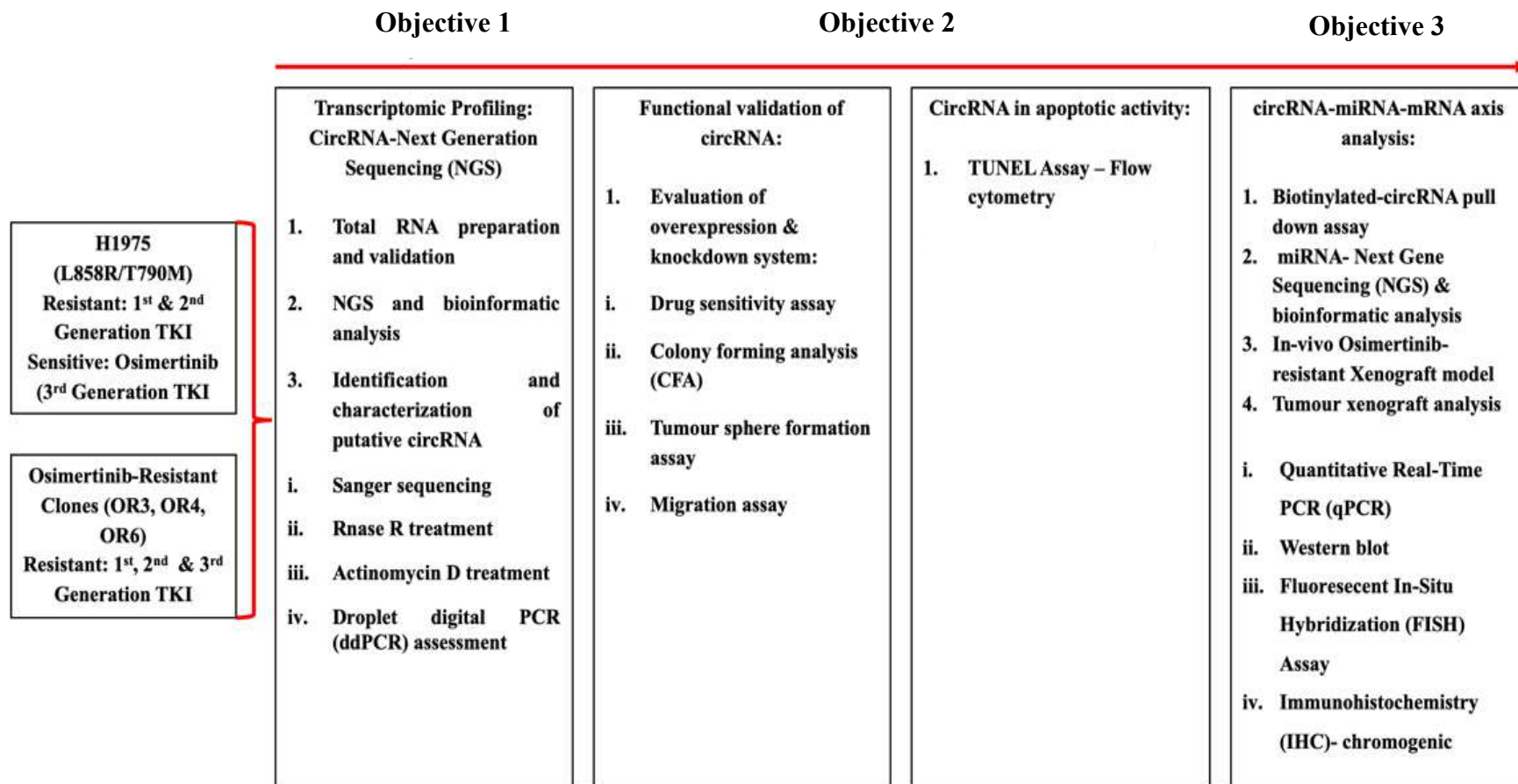


Figure 3.1 Overview methods and experimental design of the study.

3.2 Cell Culture and Maintenance of Cell lines

3.2.1 Maintenance of H1975 Cell Line in Active Cell Culture

H1975 cell line thawed in a water bath (Memmert, Germany) at 37°C upon receiving from ATCC. The cryogenic vial was removed from the water bath within two minutes and was gently wiped clean with 70% ethanol (ETOH) according to proper aseptic techniques in a bio-safety cabinet (Esco, Singapore). Cells from the cryogenic vial ($\sim 1 \times 10^6$ cells) were removed using pasteur pipette and transferred into 50ml conical tube with 15ml of Roswell Park Memorial Institute (RPMI) 1640 medium (Gibco/Invitrogen, Grand Island, NY, USA) complemented with 10% of heat-inactivated Fetal Bovine Serum (FBS) (Gibco/Invitrogen, Grand Island, NY, USA), 2mM L-Glutamine (Gibco/Invitrogen, Grand Island, NY, USA) and 1% penicillin/streptomycin (Gibco/Invitrogen, Grand Island, NY, USA). Complete growth medium components of H1975 are described in Table 3.1. H1975 cells were pelleted by centrifugation at 2000 RPM for 5 minutes. Supernatant was carefully removed using 1ml precision pipette (Eppendorf, Hamburg, Germany) without disrupting the cell pellet. The pellet was then re-suspended in 5ml of new complete RPMI medium using gentle pipetting before evenly seeded into 1:2 tissue-treated 10cm cell culture dish. The H1975 cell line was cultured in a CO₂ incubator at 37°C and 5% CO₂ atmosphere. (Eppendorf, Hamburg, Germany). Active cell cultures were examined 24 hours after thawing and subsequently daily, using the Olympus Microscope IX73 (Olympus, Japan) to ensure the attachment of the cells on

cell culture dish and to assess for any possible contamination. Complete growth medium

was changed every alternate day followed by washing in 1x PBS each time, in order to remove cell debris and dead cells. Cells were harvested by using 1ml of 0.25% trypsin-EDTA (Gibco/Invitrogen, Grand Island, NY, USA) and passaged ($\sim 1 \times 10^5$ cell/10cm culture dish) every three days upon reaching 80-90% confluency.

Table 3.1: Medium composition of H1975 medium in 500ml

Components	Working Concentration	To Prepare 500ml Medium
RPMI 1640	90%	450ml
Heat-Inactivated FBS	10%	50ml
L-Glutamine (200mM)	2mM	5ml
Penicillin/streptomycin (100x)	1%	5ml

3.2.2 Maintenance of Osimertinib-Resistant Cell Lines in Active Cell

Culture

Approximately 1×10^5 of Osimertinib cells (OR3, OR4 and OR6) expanded from single clone were seeded into 10cm culture dish for maintenance. All OR cell lines were maintained in RPMI 1640 medium (Gibco/Invitrogen, Grand Island, NY, USA) supplemented with 10% of heat-inactivated Fetal Bovine Serum (FBS) (Gibco/Invitrogen, Grand Island, NY, USA), 2mM L-Glutamine (Gibco/Invitrogen, Grand Island, NY, USA), 1% penicillin/streptomycin (Gibco/Invitrogen, Grand Island, NY, USA) and 1.5 μ M Osimertinib/AZD9291 (Selleckchem, Houston, TX, USA). Complete growth medium components of OR cell lines are described in Table 3.2. OR

cell lines were cultured in standard cell culture condition (37°C and 5% CO² atmosphere). All cell lines in active culture were examined daily, using the Olympus Microscope IX73 (Olympus, Japan) to confirm the attachment of the cells on cell culture dish for any unexpected cell death due to Osimertinib and contamination. Medium was changed every two days followed by gentle washing in 1x PBS each time, in order to remove cell debris and dead cells. OR cells were trypsinized in 0.25% trypsin-EDTA (Gibco/Invitrogen, Grand Island, NY, USA) prior to subcultured (~2 x 10⁵ cell/10cm culture dish) every four days upon reaching 80-90% confluency.

Table 3.2: Medium composition of Osimertinib-Resistant medium in 500ml

Components	Working Concentration	To Prepare 500ml Medium
RPMI 1640	90%	450ml
Heat-Inactivated FBS	10%	50ml
L-Glutamine (200mM)	2mM	5ml
Penicillin/streptomycin (100x)	1%	5ml
Osimertinib/AZD9291(1mM)	1.5µM	7.5µL

3.2.3 Maintenance of circRNA Overexpressed and Knockdown Cell

Lines

All modified cell lines generated from overexpression system (OR4-EV, OR4-OE, HOSiR-EV, and HOSiR-OE) and knockdown system (PLKO.1, shRNA1, and shRNA2) were maintained in a complete growth medium identical to that used for H1975 cells (Table 3.1). Complete growth medium was changed for both overexpression and knockdown cell lines every two days followed by washing with 1x PBS each round to remove cell debris and dead cells. The cell lines were all cultured in a CO² incubator at

37°C and 5% CO² atmosphere (Eppendorf, Hamburg, Germany). Active cell cultures were observed daily, using the Olympus Microscope IX73 (Olympus, Japan) to prevent unexpected cell detachment and to monitor for any possible contamination. Cells were trypsinized using 0.25% trypsin-EDTA (Gibco/Invitrogen, Grand Island, NY, USA) before passaging every three days for overexpressed system (~1 x 10⁵ cell/10cm culture dish) and four days for knockdown system (~2 x 10⁵ cell/10cm culture dish) upon reaching 80-90% confluency.

3.3 Generation of Osimertinib-Resistant Cell Lines

3.3.1 Step-wise Dose Escalation Method

A total of 1 x 10⁶ H1975 cells were seeded in a 10cm cell culture dish, and the cells were treated with Osimertinib in a dose escalation manner starting from an initial concentration of 500nM. RPMI complete medium supplemented with Osimertinib were replaced every alternate day and drug exposure dose was increased by 500nM every 5 days until day 15 at the final concentration of 1.5µM. Osimertinib treated cells were sub-cultured and maintained for two months in RPMI medium supplemented with 1.5µM Osimertinib until the cells were able to resume normal growth and proliferate without extreme cell death. Osimertinib treated H1975 cells were further seeded in a 96-well plate using a limiting dilution method for single cell isolation to attain monoclonality. Heterogenous H1975 Osimertinib treated cells were diluted across 96-well plates to generate cell per unit volume seeded in the wells. Single cell clones were maintained and expanded in active culture for approximately four months in RPMI medium supplemented with 1.5µM Osimertinib. Three single clones from respective

wells of 96-well plate (OR3, OR4 and OR6 clones) were characterized as described by (Verusingam et al., 2020) and selected for further analysis.

3.4 Transcriptomic Profiling of circRNA – Next Generation Sequencing (NGS)

3.4.1 Total RNA Extraction

TRIzol (Invitrogen, Grand Island, NY, USA) extraction method is a conventional method in molecular biology for RNA isolation from cells, tissues and condition medium. In this study TRIzol was used to extract total RNA for RNA-seq and other downstream work such as qRT-PCR and ddPCR. TRIzol is composed of guanidine isothiocyanate and phenol forming a monophasic solution which can effectively solubilize RNA, DNA, and proteins. The protocol of total RNA extraction using TRIzol reagent as described below:

Firstly, a total of 1×10^6 cultured cells were collected from 10cm cell culture dish. The adherent cells were trypsinized and centrifuged in 15ml tubes at 2000 RPM, 5minutes. Upon centrifugation, cells were washed in 1x PBS, transferred to 1.5ml tubes before moving forward to TRIzol RNA extraction. Each 1×10^6 cultured cells required 1ml of TRIzol reagent for complete homogenization. Cells were lysed completely using mechanical disruption technique by vigorously pipetting up and down using 1ml precision pipette. BCP (1-Bromo-3-chloropropane) solution was applied next, to the homogenized cells, vigorously vortex (30 seconds) and incubated at room temperature (22°C, 5 minutes) for phase separation. After the homogenates separated into organic and aqueous phases, the top transparent layer containing RNA were transferred to a clean 1.5ml tube without disrupting the other layers. Next, 200µL of Isopropanol

per sample were added and mixed homogeneously using a vortex before centrifugation at 4°C and 140000 RPM for 20 minutes. The RNA pelleted by centrifugation were then rinsed twice with 70% ETOH and air-dried in a biosafety cabinet for 30 minutes. Subsequently, the RNA pellets were resuspended in 30µL of diethylpyrocarbonate (DEPC) treated water and thoroughly mixed using 100µL precision pipette. The concentration and purity of total RNA were measured using Implen NanoPhotometer N60 (Munich, Germany). The ratio of A260/A280 for pure RNA was defined in the range of 1.8-2.0.

3.4.2 Circular RNA Next Gene Sequencing (circRNA-seq)

As for circRNA sequencing, TruSeq Stranded Total RNA Library Prep Gold kit by Illumina (San Diego, CA, USA) (according to manufacturer's protocol) was used for high-quality RNA libraries preparation. CircRNA-NGS specification as listed in Table 3.3. High-quality total RNA from two biological replicates of each sample (1975, OR3, OR4 and OR6) were used as the starting materials in this study. Total RNA input required for each sample ranging from 0.1–1 µg of total RNA. Prior to NGS, total RNA were subjected to 2100 Bioanalyzer (Agilent, Germany) to assess the RNA integrity. Samples with a RIN (RNA integrity Number) of 8-10 were prioritized for sequencing input. The overview of the process includes depletion and fragmentation of RNA, synthesize first strand cDNA, synthesize second strand cDNA, adenylate 3' ends, ligate adapters, enrich DNA fragments, and the last step involves normalization

and pool libraries. The protocol of circRNA sequencing using Illumina platform as described below:

In the first step, total RNA undergoes rRNA depletion and fragmentation step to break it into smaller, more adaptable fragments. After depletion of ribosomal RNA (rRNA), total RNA were subjected to purification, fragmentation, and priming for cDNA synthesis. The efficacy of rRNA depletion is gauged by comparing the rRNA peaks in the input sample before and after depletion using a 2100 Bioanalyzer (Agilent, Germany). Successful depletion is confirmed by the disappearance of ribosomal rRNA peaks on the analyser.

In the next step, following fragmentation, the first strand of cDNA was synthesized. RNA fragments from the previous step were converted into complementary DNA (cDNA) using SuperScript II Reverse Transcriptase according to manufacturer's protocol (Gibco/Invitrogen, Grand Island, NY, USA). During reverse transcription, cleaved RNA fragments primed with random hexamers into first strand cDNA. Actinomycin D were then added to the First Strand Synthesis Act D Mix to prevent uncontrolled DNA-dependent synthesis and to permit RNA-dependent synthesis further enhancing strand specificity in the final product. Continuing from the first strand cDNA synthesis, the second strand of cDNA was again synthesized to generate double-stranded cDNA molecules. In this step, the RNA template was removed, leaving behind complimentary copies of the original RNA. The resulting double-stranded cDNA serves as the template for subsequent library construction. Also, at this step the strand specificity is maintained to preserve information of the original RNA strand.

During Adenylation 3' end, the cDNA molecules undergo end repair to produce blunt ends and in order to prevent the blunt fragments from ligating to each other during adapter ligation, adenine (A) nucleotide is added to their 3' ends. While, thymine (T) nucleotide was added to the 3' end of the adapter instead, forming a complementary overhang for efficient ligation to the fragment. The A-tailing procedure was done by running the thermocycler 'ATAIL70' program which prepares the cDNA fragments for adapter ligation and subsequent amplification. Next, adapters were ligated to the A-tailed cDNA fragments produced from the previous step. The adapters used, enable the identification of individual samples during the sequencing process. The ligation was executed in a strand-specific manner, whereby the adapters are attached to the appropriate cDNA strand. Consequently, the ligated cDNA fragments in the library were enriched through PCR amplification using Illumina PCR Primer Cocktails (PPC) according to the manufacturer's protocol. The resulting enriched libraries were checked and quantified according to the Illumina sequencing library qPCR quantification guide. Optimization of the cluster densities on flow cells during sequencing were performed to ensure precise quantification of DNA libraries. In the final step, to normalize and pool libraries, the DNA templates were prepared for cluster generation. Barcoded indexed DNA libraries were aligned to a concentration of 10 nM in the Diluted Cluster Template (DCT) plate and subsequently combined in equal volumes within the Pooled DCT (PDP) Plate. As for the non-indexed DNA libraries, normalization to 10 nM in the DCT plate was then performed independently. The raw fastq files were aligned to the reference genome (Putative spliced circRNA sequences, <http://www.circbase.org/cgi-bin/downloads.cgi>), Then we performed circRNA

quantification and differential expression analysis by using RStudio (<https://posit.co/download/rstudio-desktop/>).

Table 3.3: CircRNA-NGS Specifications

Platform	Illumina
Sequencer	HiSeq 2500
Output	12 GB/samples (~ 40 million reads)
Read	150 pair-end
Insert size	250 – 300 bp
Library	TruSeq Stranded Total RNA Library Prep)

3.5 Characterization of Osimertinib Resistance Properties

3.5.1 Drug Sensitivity Assay (AlamarBlue)

All cell lines were cultured in their respective complete growth medium prior to drug sensitivity assay and maintained in the logarithmic growth phase at the time of assay to acquire reliable results. Approximately, 3×10^3 cells per well were seeded in 96-wells plate and allowed to adhere on plate overnight. The cells were treated with Osimertinib/AZD9291 (Selleckchem, Houston, TX, USA) at various concentrations ranging from 0.001 to 10 μ M, along with DMSO (Sigma, St. Louis, MO, USA) as control, which was added one day after cell seeding. Treated cells were exposed to Osimertinib/AZD9291 (Selleckchem, Houston, TX, USA) for 48 hours at 37 °C in the presence of 5% CO₂. After 48 hours, AlamarBlue reagent (Thermo Fisher Scientific, Waltham, MA, USA) was diluted in the cell culture medium at a concentration as per manufacturer's protocol which was at 1:10 dilution. The medium was removed and replaced

with 100 μ L of diluted AlamarBlue (Thermo Fisher Scientific, Waltham, MA, USA) followed by further incubation for 3 hours. Thereafter, absorbance of the cells was measured at 560 nm (excitation wavelength) and 590 nm (emission wavelength) using SpectraMax M3 Multi-Mode Microplate Reader (USA). Absorbance values from the microplate reader were used to calculate the percentage of cell viability and statistical analysis (Verusingam et al., 2020).

3.5.2 Colony Formation Assay (CFA)

Cells were seeded in 6-well plates at a density of 1×10^4 cells, and treated with various concentrations of Osimertinib (Selleckchem, Houston, TX, USA) ranging from 0.001 to 10 μ M and DMSO (Sigma, St. Louis, MO, USA) as control, a day after cell seeding. All treated cells were maintained at 37°C in the presence of 5% CO₂ for 10 days until colonies formed. Meanwhile, medium containing Osimertinib (Selleckchem, Houston, TX, USA) including DMSO (Sigma, St. Louis, MO, USA) for control well were changed every alternate day. Following this, on day 10 the medium was removed and the cells were fixed with 1 mL fixative solution for 15 minutes. The fixative used was a mixture of methanol and acetic acid glacial in a 3:1 ratio. The fixed cells were then stained with 0.5% crystal violet (Sigma, St. Louis, MO, USA) for 10 minutes. Excess crystal violet was removed and each well was washed with ddH₂O and allowed to dry overnight. Thereafter, cells were visualized and compared between Osimertinib-treated and the control wells for further analysis.

3.5.3 Migration Assay

In this study, a transwell cell culture insert of 8µm pore-size polycarbonate membrane (Corning, New York, USA) was used to assess cell migration. The upper chamber of the transwells were seeded with a total of 5×10^3 cells, while the lower chamber were not seeded with any cells but only consist of complete cell growth medium supplemented with 20% heat-inactivated FBS, to create a chemoattractant gradient for cell migration. After an incubation period of 16 hours, those cells that successfully invaded the membrane and attached to its lower surface were subjected to nucleic acid stain, Propidium iodide (Thermo Fisher Scientific, Waltham, MA, USA). In order to visualize the invaded cells, the bottom membrane surfaces were fixed with methanol for an hour. As a final step, the cells were stained with Propidium iodide (Thermo Fisher Scientific, Waltham, MA, USA) for a duration of 30 minutes. Images of the stained cells were taken using Olympus Microscope IX73 (Olympus, Japan).

3.5.4 Tumour Formation Assay

All cell lines were cultured in their respective complete growth medium prior to tumour sphere formation assay and maintained in the logarithmic growth phase at the time of assay to acquire reliable results. The adherent cells were trypsinized and centrifuged in 15ml tubes at 2000 RPM, 5minutes. Approximately, 1×10^3 cells per well were plated in 24-well ultra-low attachment plates in 500µL of DMEM-F12 (Gibco/Invitrogen, Grand Island, NY,

USA) supplemented with EGF (20 ng/mL) and bFGF (20 ng/mL) and 4 mg/mL insulin (Dai et al., 2019). Subsequently, 500µL of DMEM-F12 containing (EGF, bFGF, and insulin) (R&D Systems, Minneapolis, MN, USA) were every three days up to day 12. Images of the tumour sphere were taken on day 12 using Olympus Microscope IX73 (Olympus, Japan).

3.5.5 Western Blot

3.5.5.1 Protein Lysis

Cells from both Osimertinib-treated and control groups were scraped from a 10cm cell culture dish using a cell scraper, collected in 1.5ml tubes and washed with 1x PBS. Subsequently, the cells were pelleted through centrifugation at 2000 RPM for 10 minutes. While, as for mouse xenograft, the tissues were subjected to flash freezing method using liquid nitrogen, homogenised using mortar and pestle and then washed in 1x PBS before centrifugation at 2000 RPM for 10 minutes. Supernatants were completely removed after centrifugation. A total volume of 50-80µL of Ripa lysis buffer (Thermo Fisher Scientific, Waltham, MA, USA) were added to all samples, mixed up and down by mechanical disruption force using precision pipette, and vortexed for 30 seconds to ensure complete lysis. Lysis buffer supplemented with 1x protease inhibitor (Selleckchem, Houston, TX, USA) , 1x Phosphatase Inhibitor Cocktail (Selleckchem, Houston, TX, USA) and 1mM Dithiothreitol (DTT) (Thermo Fisher Scientific, Waltham, MA, USA) to prevent protein degradation. The samples were then incubated on ice for about 30 minutes. Following this, samples were all centrifuged at 14000 rpm for 20 minutes (4°C).

Supernatants containing protein lysate were transferred to a clean 1.5ml tube and protein concentration were quantified using Bradford assay.

3.5.5.2 Protein Quantification

First, a protein standard curve was generated to quantify the unknown protein samples. In order to generate protein standard curve, five dilution points were prepared from the stock solution of BSA (Sigma, St. Louis, MO, USA) at 1mg/ml. Dilution points (1:2 in ratio) were prepared at various concentrations from 0 – 1mg/ml as shown in Table 3.4.

Protein quantification was carried out using Bio-Rad Protein Assay Dye Reagent Concentrate (Bio-Rad, Hercules, CA, USA). Overall, the protein assay dye reagent was diluted to 1x solution in a double distilled water (ddH₂O) at a ratio of 1:5 (200ul of protein assay dye and 798 μ l of dH₂O). Total of 2 μ l of Bovine Serum Albumin (BSA) (Sigma, St. Louis, MO, USA) from each dilution point were mixed into 1x protein assay dye to generate a standard curve (as listed in Table 3.5). Subsequently, 2 μ l of unknown protein samples were mixed into 1x protein assay dye to measure the protein concentrations. All protein standards and protein samples were assayed in four replicates using a Microtiter plate (200 μ l of protein dye mix per replicate).

The absorbance value of BSA and unknown proteins were measured at 595 nm using SpectraMax M3 Multi-Mode Microplate Reader (USA). Absorbance values of BSA, from each dilution point, were used to generate a linear regression graph and to determine the slope and y-intercept values. Following this gradient of the straight line equation, $Y = Mx + C$ was employed to calculate

the concentration of the unknown proteins (Y = absorbance values, M = slope, and C = y-intercept).

BSA Dilution Point	BSA Concentration (1mg/ml)	BSA Concentration in 2 μl (ug)
1	1.0	2.0
2	0.5	1.0
3	0.25	0.5
4	0.125	0.25
5	0.0625	0.125

BSA Concentration in 2 μl (ug)	2.0	1.0	0.5	0.25	0.125
Protein Assay Dye (μ l)	200	200	200	200	200
ddH ₂ O (μ l)	798	798	798	798	798
BSA(μ l)	2	2	2	2	2
Total (μ l)	1000	1000	1000	1000	1000

3.5.5.3 SDS-Polyacrylamide Gel (PAGE) Electrophoresis

Protein samples measured via Bradford assay, were mixed in a 6x protein loading buffer (bromophenol blue) and denatured by heating at 95°C for 10 minutes in a ThermoMixer C (Eppendorf, Hamburg, Germany). Subsequently, 10% SDS-PAGE gel was loaded into the Mini-PROTEAN Tetra vertical electrophoresis tank (Bio-Rad, Hercules, CA, USA) with 1x running buffer (Table 3.6). Preparation of resolving gel (10%) and stacking gel as shown in Table 3.7 and 3.8 respectively.

A total of 50 μ g of protein per well were loaded to 10% SDS-PAGE gel. Pre-stained protein marker (ARROWTEC, New Taipei City, Taiwan) included in each SDS-PAGE gel. Loaded protein samples in SDS-PAGE gel were run at 70

V for 15 minutes and 110 V for another 90 minutes until the dye front reached the bottom of the gel. Meanwhile, 1x transfer buffers were prepared for the protein transfer process (Table 3.9). Next, upon completion of SDS-PAGE electrophoresis, the gel was removed from gel cassettes, then assembled sequentially in between filter paper and 0.45- μ m nitrocellulose membrane. The transfer sandwiches were fixed in a transfer cassette before loaded into a vertical electrophoresis tank for electroblotting. Protein transfers were run in a 1x transfer buffer at 400mA for 2 hours. To visualize the efficiencies of protein transfer, the blots were stained in Ponceau S for 5 minutes and thoroughly washed in 1x PBST (Figure 3.10) prior to blocking step. Consequently, the membrane blots were blocked in 5% milk for 1 hour, washed in 1x PBST before moving forward to primary antibodies incubation overnight at 4°C. Blots were washed three times (5 minutes each) in PBST solution and then incubated in secondary antibodies conjugated to a detection enzyme for 1 hour. GAPDH (Cell Signaling Technology, Danvers, MA, USA) was used as the housekeeping gene. Proteins of interest on blots were detected by the UVP ChemiDoc system (Thermo Fisher Scientific, Waltham, MA, USA).

Table 3.6: Running Buffer (10x)

Components	Stock Solution (1L)
Tris-Base	30.3g
Glycine	144.4g
SDS	10.0g
ddH ₂ O	800ml

*Adjust volume to 1L.

Table 3.7: Resolving Gel (10%)

Components	To Prepare 20ml
ddH ₂ O	7.9
30% Acrylamide Mix	6.7
1.5M Tris-HCL (pH 8.8)	5.0
Sodium Dodecyl Sulfate (SDS) 10%	0.2
10% Ammonium Persulfate (APS)	0.2
Tetramethylethylenediamine (TEMED)	0.008

Table 3.8: Stacking Gel (5%)

Components	To Prepare 5ml
ddH ₂ O	3.4
30% Acrylamide Mix	0.83
1.5M Tris (pH 6.8)	0.63
Sodium Dodecyl Sulfate (SDS) 10%	0.05
10% Ammonium Persulfate (APS)	0.05
Tetramethylethylenediamine (TEMED)	0.006

Table 3.9: Transfer Buffer

Components	Stock Solution (10x)	Working Solution (1x)
Tris-Base	30.3g	100ml of 10x Transfer
Glycine	144.1g	Buffer
Methanol	-	200ml
ddH ₂ O	800ml	700ml

*Adjust volume of 10x Transfer buffer to 1L.

*Working solution (1L)

Table 3.10: 1x Phosphate-Buffered Saline with Tween 20 (PBST)

Components	To Prepare 1L
1x PBS	100ml
ddH ₂ O	900ml
Tween 20	1ml

3.6 Validation of Apoptosis Activity

3.6.1 Tunel Assay (BrdU and 7-AAD Staining)

Approximately, $1-2 \times 10^5$ cells per 10cm cell culture dish were seeded and allowed to adhere on plate overnight. All cell lines were cultured in their respective complete growth medium prior to Osimertinib/AZD9291 (Selleckchem, Houston, TX, USA) treatment and maintained in the logarithmic growth phase at the time of assay to acquire reliable results. The cells were treated with $1.5\mu\text{M}$ Osimertinib/AZD9291 (Selleckchem, Houston, TX, USA) inclusive of DMSO (Sigma, St. Louis, MO, USA) as control for each cell line. Osimertinib/AZD9291 (Selleckchem, Houston, TX, USA) and DMSO (Sigma, St. Louis, MO, USA) were added a day after cell seeding. All treatments were carried out for 48 hours at 37°C in the presence of 5% CO_2 . After 48 hours, 1×10^6 cells were harvested by trypanization in 1 mL of 1x PBS and cells were pelleted by centrifugation at 2000 RPM (5 minutes).

Cell pellets were fixed with 5 mL of 4% paraformaldehyde (PFA) (Sigma, St. Louis, MO, USA) and incubated on ice for 15 minutes, before centrifugation for 5 minutes at $300 \times g$ under 4°C . Supernatant containing PFA were then discarded and the cells were washed in 5 mL of ice-cold 1x PBS and repeated twice. Next, 5 mL of ice-cold 70% ETOH were added to the cells and left for incubation overnight at -20°C .

ETOH fixed cells were collected after overnight incubation and 1 mL aliquots of each sample were transferred into 1.5ml tubes and centrifuged at 1000 RPM for 5 minutes. Supernatants containing ETOH were carefully removed and the cells were resuspended in 1 mL of wash buffer. Washing steps

were repeated twice and further mixed heretogenously in 50 μ L of DNA labeling solution as shown in Table 3.11. All samples were incubated for 60 minutes at 37°C in a ThermoMixer C (Eppendorf, Hamburg, Germany). After incubation in the labelling solution, 1 mL of rinse buffer was added to each tube, centrifuged for 5 minutes (300 x g) at 4°C . The rinsing steps were repeated twice. Next, 100 μ L of antibody solution as described in Table 3.12, were added to the cells and incubated in the dark for 30 minutes at room temperature. Prior to flow cytometry analysis, all samples were resuspended in 500 μ L of 7-AAD/RNase A solution in 12 x 75 mm FACS tubes and incubated in the dark for 30 minutes at room temperature. The cells were analyzed by flow cytometry (BD FACSCanto II (Franklin Lake, NJ, USA) with excitation/emission values as per recommended by manufacturer’s protocol (BrdUred - 488/576 nm) and 7-AAD - 488/655 nm). Data displayed in dot plots or histograms representing either BrdU or 7-AAD staining).

Table 3.11: DNA Labelling

Components	Working Volume/Reaction (μL)
TdT reaction buffer	10.0
TdT enzyme	0.75
Br-dUTP	8.0
ddH ₂ O	32.25
Total Volume	51.0

Table 3.12: Antibody Solution

Components	Working Volume/Reaction (μL)
Anti-BrdU-Red	5.0
Rinse Buffer	95.0
Total Volume	100.0

3.7 Characterisation of circRNAs

3.7.1 Gene Expression Study

3.7.1.1 CDNA Synthesis from Total RNA

Reverse transcription was performed using SuperScript™ II Reverse Transcriptase (Thermo Fisher Scientific, Waltham, MA, USA) according to manufacturer's protocol, to convert total RNA to cDNA for subsequent downstream analysis such as qRT-PCR. A total of 3µg of RNA was converted to cDNA in each 20µL reaction volume. Before the preparation of the reverse transcriptase master-mix, all components were thawed on ice and briefly centrifuged to bring down the residual liquid from the sides of the tubes.

In the first step, total RNA, 100 ng/µL of random hexamer, dNTP Mix (10 mM each) and RNase free water were mixed in a microcentrifuge tube (14µL per/sample) as listed in Table 3.13. The mixtures were subjected to thermal cycler heat (Eppendorf, Hamburg, Germany) for 65°C for 5 minutes, followed by 1 minute quick incubation on ice.

As in second step, the samples were collected for brief centrifugation and added with 5X First-Strand Buffer (4 µL), 0.1 M DTT (2 µL) and 1 µL of reverse transcriptase enzyme per samples as shown in Table 3.14. All components were mixed by pipetting and incubated in a thermal cycler (Eppendorf, Hamburg, Germany) at 25°C for 10 minutes, 42°C for 50 minutes and inactivated by heating at 70°C for 15 minutes. All cDNA samples were kept at 4°C for short term storage and for long term storage, the cDNAs were placed in a minus 20°C freezer.

Table 3.13: Step 1-cDNA Synthesis

Components	Working Volume/Reaction (μL)
RNA	3 μg
Random Primer (100 ng/ μl)	1.0
10mM dNTP	1.0
ddH ₂ O	-
Total	14.0

Table 3.14: Step 2-cDNA Synthesis

Components	Working Volume/Reaction (μL)
5x Buffer	4.0
0.1M DTT	1.0
RT Enzyme	1.0
Total	6.0

3.7.1.2 Quantitative Real-Time Reverse Transcription PCR (qRT-PCR)

All cell lines including *in-vivo* tumour xenografts used in this study were subjected to circRNA, miRNA and mRNA quantification via qRT-PCR. Sybr green was used as the designated fluorescent reporter to quantify the circRNA and mRNA expression during PCR cycle. The TaqMan system was used to quantify miRNA expressions. PCR amplification efficiencies and primers used in this study were optimised during the course of study. GAPDH was used as a housekeeping gene for mRNA expression while hsa-mir-191-5p as endogenous control for miRNA expression throughout the experiments .

As for circRNA and mRNA quantification, The Fast SYBR Green Master Mix (Thermo Fisher Scientific, Waltham, MA, USA) was used as stated in the manufacturer's protocol. Briefly, the qRT-PCR cycle was performed for

40 cycles at 95°C for 3 seconds and annealing at 60°C for 30 seconds with initial enzyme activation temperature at 95°C for 30 seconds. Whereas, TaqMan Fast Advanced Master Mix (2X) was used to quantify miRNA expression as described in the manufacturer’s protocol. The qRT-PCR cycle denoted for miRNA comprises initial enzyme activation at 95°C for 20 seconds, denaturing and annealing for 40 cycles at 95°C for 1 second and 60°C for 20 seconds respectively. All qRT-PCR were executed using QuantStudio 3 Real-Time PCR System. Master mix PCR reactions were shown in Table 3.15 and 3.16 and lists of primers used in this study were attached in Appendix A.

Table 3.15: Fast Sybr Green Master Mix

Components	Working Volume/Reaction (µL)
Fast Sybr Green (2x)	5.0
cDNA	1.0
Forward Primer (10 µM)	0.5
Reverse Primer (10 µM)	0.5
RNase free water	3.0
Total	10.0

Table 3.16: TaqMan Fast Advanced Master Mix

Components	Working Volume/Reaction (µL)
TaqMan Fast Advanced (2x)	10.0
TaqMan Advanced miRNA Probe (20x)	1.0
RNase free water	4.0
Total	15.0

3.7.1.3 Calculation and Analysis

All expressions of circRNA, miRNA and mRNA were calculated using comparative CT Method ($\Delta\Delta CT$) normalised against GAPDH as endogenous control for circRNA and mRNA while hsa-mir-191-5p as endogenous control for miRNA. The experiments were performed in triplicates to confirm the accuracy and reproducibility of data acquired. Fold change of expressions were generated based on threshold cycles values (CT) generated from qRT-PCR. Paired t-Tests were included as the statistical data analysis method in this study. Experiments were conducted at the 95% confidence level and presented as mean \pm standard deviation (SD) or mean \pm standard error of mean SEM. The differences in the control and treated group were considered significant at $P < 0.05$, $P < 0.01$ and $P < 0.001$ where appropriate. Data are described and plotted into histograms in the Results sections.

3.7.2 Ribonuclease R (RNase R) Treatment

RNase R (Lucigen, Middleton, WI, USA) treatment was used to deplete linear RNA and purify circular RNA instead, for studies involving alternative splicing and gene expression studies. Treatment with RNase R was applied to the total RNA of all samples used in this study prior to circRNA expression studies according to the manufacturer's protocol as described in Table 3.17. Total of 10 μ g of RNA from each sample was subjected to 20 units of RNase R (Lucigen, Middleton, WI, USA) treatment, coupled up with 1 \times Reaction Buffer, and RNase free water. The components were incubated for 2 hours at 37 $^{\circ}$ C in a thermal cycler heat (Eppendorf, Hamburg, Germany). Subsequently, the purified circRNA was retrieved using acid phenol-chloroform (5:1) method

(Ishola et al., 2022). RNase R treated and mock samples were subjected to qRT-PCR analysis.

Table 3.17: RNase R Treatment

Components	Working Volume/Reaction (μL)
Total RNA	10ug
RNase R (20 Unit/ μL)	1.0
RNase R buffer (10x)	2.0
RNase free water	Top up to final volume
Total	20.0

3.7.3 Actinomycin D Assay

Actinomycin D (Sigma, St. Louis, MO, USA) was used to study the half-life, stability and resistance to exonuclease degradation of circRNAs at both cellular and extracellular level. First, the stock solution of Actinomycin D (Sigma, St. Louis, MO, USA) was prepared in DMSO (Sigma, St. Louis, MO, USA) following the manufacturer's protocol.

Prior to treatment with Actinomycin D, H1975 were maintained in active culture upon 80-90% confluency. H1975 cells were treated with Actinomycin D (Sigma, St. Louis, MO, USA) at a concentration of 2 $\mu\text{g}/\text{mL}$ for specified time intervals (0h, 4h, 8h, 12h, and 24h). The untreated cells at 0 hour were considered as the control group. Subsequently, the cells were subjected to RNA extraction, further converted into cDNA. CircRNA and linear RNA expression upon Actinomycin D treatment were assessed using qRT-PCR.

3.7.4 Droplet Digital PCR (ddPCR)

Droplet digital PCR (ddPCR) enables quantification of 20000 droplets in a total of 20 μ L which provides high sensitivity and specificity for liquid biopsy quantification. In this study, quantification of circRNA was accessed in the condition medium of H11975, OR4 and HOSiR via ddPCR using Evagreen Supermix as described in the manufacturer's protocol (Bio-Rad, Hercules, CA, USA). Eva green was used as the designated fluorescent reporter to quantify the circRNA expression during the PCR cycle. GAPDH was used as a housekeeping gene for circRNA expression throughout the experiments.

Total RNA of 3 μ g converted to cDNA in 20 μ L cDNA synthesis components according to the manufacturer's protocol (Bio-Rad, Hercules, CA, USA). Synthesized cDNA (approximately 1 μ l/per reaction) and ddPCR master mix containing Evagreen Supermix (1x), Forward primer, Reverse primer and RNase free water as shown in Table 3.18, were loaded into DG8 cartridge for droplet formation using the QX200 Droplet System (according to the manufacturer's protocol) (Bio-Rad, Hercules, CA, USA). The oil droplets from DG8 cartridge were then transferred to a 96-well plate and subjected to Bio-rad C1000 Touch Thermal Cycler. Cycling condition as listed in Table 3.19. Final PCR products were quantified and analysed using QX200 Droplet Reader (Bio-Rad) and QuantaSoft software Bio-Rad, Hercules, CA, USA)(Luo et al., 2020).

Table 3.18: Evagreen Supermix

Components	Working Volume/Reaction (μL)
2x ddPCR Evagreen Supermix	10.0
Forward Primer	1.0
Reverse Primer	1.0
RNase free water	10.0
Total	20.0

Table 3.19: Cycling Condition of Evagreen Supermix

Cycling Step	Temperature ($^{\circ}\text{C}$)	Time	Ramp	Number of Cycle
Enzyme Activation	95	5 min		1
Denaturation	95	30 sec		40
Annealing/Extension	60	1 min		40
Signal Stabilization	4	5 min		1
	90	5 min		1
Hold	4	∞		1

3.8 Gain and Loss of Functional Assays

3.8.1 Preparation of Plasmid DNA: Overexpression and Knockdown System

Plasmid vector backbone pcDNA3.1(+) ZKSCAN1 MCS Exon vector (#69901) (Addgene, Watertown, MA, USA) was used to establish overexpression system in OR4 and HOsiR cell lines. Meanwhile, Lentiviral PLKO.1-Puro (#8453) (Addgene, Watertown, MA, USA) were transfected in HEK293FT cell line before transduction in H1975. Packaging plasmids pMD2.G (#12259) and psPAX2 (#12260) were used to produce Lentivirus for transduction. All vector backbones used in these experiments were purchased

from Addgene plasmid repositories. Cloning and E.coli transformation were performed using TOPO TA Cloning Kit (Thermo Fisher Scientific, Waltham, MA, USA) and NEB® Stable Competent E. coli (High Efficiency) according to manufacturer's protocol. Plasmid clones were amplified in Ampicillin treated Lysogeny broth (LB) (Sigma, St. Louis, MO, USA) agar plates, expanded in Terrific broth (TB) (Sigma, St. Louis, MO, USA) and subsequently extracted for downstream analysis. Plasmid maps as per documented in Appendix B-F.

3.8.2 Plasmids Amplification in Bacteria Culture

3.8.2.1 Lysogeny (LB) Agar Plate

Lysogeny (LB) agar was made of high nutrient components to grow Escherichia coli (E. coli), DH5α strain. A total of 40g of LB Broth with agar (Miller - L3147) homogenously mixed in 1L of ddH₂O, according to manufacturer's protocol (Sigma- Aldrich, USA). The broth was autoclaved at 121°C for 20 minutes. Ampicillin (100ug/ml) (Sigma- Aldrich, USA) were added into LB agar medium when the temperature drops to 55°C. Supplemented LB agar mediums were mixed thoroughly without any bubble formation and were poured into sterile 100mm petri dishes. LB agar medium in petri dishes were allowed to solidify for 2 hours in a laminar hood and subsequently wrapped with aluminium foil for storage at 4°C to prevent degradation of antibiotics.

3.8.2.2 Terrific Broth (TB) Media

E.coli containing plasmid DNA were amplified in 1L of Terrific broth (T0918) (Sigma- Aldrich, USA) on a shaking incubator at 37°C overnight, not exceeding 16 hours. TB medium was prepared according to manufacturer's

protocol, whereby 47.6 g of TB powder supplemented with 8ml of sterile glycerol was dissolved in 1L of ddH₂O and autoclaved at 121°C for 20 minutes. Ampicillin (100ug/ml) (Sigma- Aldrich, USA) were added into the TB medium when the temperature dropped to 55°C and the medium was stored at room temperature prior to use.

3.8.2.3 Storage of Bacterial Culture Stocks

All E.coli containing plasmid DNA were stored in -80°C freezer to be amplified when needed. A few selected bacteria clones were selected from LB agar plate and cultured in 5ml (each clone in a single 15ml tube) of TB broth (37°C) overnight, not more than 16 hours. The stocks were made of 200µl of autoclaved glycerol and 800µl of transformed E.coli.

3.8.2.4 Plasmid DNA Isolation

In this study, all plasmid DNA was isolated from transformed E.coli using Qiagen Plasmid Maxi Kit according to the manufacturer's protocol. E.coli containing plasmid DNA cultured in TB, were collected after 16 hours of incubation and pelleted in 50ml tubes via centrifugation at 6000 x g for 30 minutes at 4°C. Bacterial pellets were then vigorously mixed using 1ml precision pipette in 10ml of Buffer P1 supplemented with RNase A and LyseBlue (ratio of 1:1000). Buffer P2 (10ml) was then added into the mixture and thoroughly mixed by inverting the tubes five times and incubated at room temperature for 5 minutes. The mixtures were in blue colour due to LyseBlue reagent. Next, pre-chilled Buffer P3 (10ml) were added in, mixed thoroughly by inverting the tubes five times until the solution turned colourless and incubated for 20 minutes on

ice. Subsequently, all tubes containing samples were subjected to centrifugation at 20,000 x g for 30 minutes (4°C). Meanwhile, during centrifugation, the empty QIAGEN-tips (column) were equilibrated with 10ml of Buffer QBT, and the buffer were allowed to clear by gravity flow. After centrifugation, the supernatants were collected (excluding the precipitation) and loaded into Qiagen-tip columns. Buffer QC were applied into the column and washed twice (30ml each time). The buffers were removed by gravity flow. Plasmid DNA were eluted in 15ml of Buffer QF into a new 50ml tube and precipitated in 10.5ml of 70% ETOH by centrifugation (20,000 x g) for 1 hour at 4°C. Plasmid DNA pellets were air-dried for 30 minutes in a laminar hood and reconstituted in 100-300uL of RNase free water depending on the size of pellets.

3.8.3 Overexpression of circSPINT2

Osimertinib-resistant parental cell lines (OR4 and HOsiR) were cultured in RPMI complete medium prior to circRNA overexpression and maintained in the logarithmic growth phase at the time of assay. The cell lines were maintained in a CO² incubator at 37°C and 5% CO² atmosphere. Approximately, 3 x 10⁵ cells were seeded in 6cm culture dish and allowed to adhere on plate overnight. The next day, OR4 and HOsiR cell lines were transfected with 10µg of pcDNA3.1(+) ZKSCAN1-circSPINT2 overexpression plasmid using Lipofectamine 3000 Transfection Reagent (Invitrogen, Grand Island, NY, USA) in 3.5ml of RPMI medium. Transfection components were prepared and incubated for 15 minutes prior to use as shown in Table 3.20 and 3.21. OR4 and HOsiR cell lines transfected with empty vector backbone pcDNA3.1(+) ZKSCAN1 MCS Exon vector which serves as control. After, 24 hours, the

medium containing Lipofectamine 3000 were removed and replaced with RPMI complete medium supplemented with Neomycin (400 ug/ml) (Gibco/Invitrogen, Grand Island, NY, USA) as selection antibiotic for selecting stable strains. Transfected cells were maintained in Neomycin for 1 week whereby medium were changed every alternate days. Subsequently, the transfected cells were harvested for qRT-PCR to assess circRNA overexpression effect. In due course, overexpression established cell line (OR4-EV, ORV-OE, HOsiR-EV and HOsiR-OE) were maintained in culture for downstream assays.

Table 3.20: Lipofectamine 3000 (A) Per Reaction

Components (A)	OR4-EV (μL)	OR4-OE (μL)	HOsiR- EV	HOsiR- OE
Opti-MEM	238	237.5	237.0	238.5
pcDNA3.1 – Empty Vector	2.0	-	3.0	1.5
pcDNA3.1 – circSPINT2	-	2.5		
P3000	10.0	10.0	10.0	10.0
Total	250.0	250.0	250.0	250.0

Table 3.21: Lipofectamine 3000 (B) Per Reaction

Components (B)	OR4-EV (μL)	OR4-OE (μL)	HOsiR- EV	HOsiR- OE
Lipofectamine 3000	10.0	10.0	10.0	10.0
Opti-MEM	240.0	240.0	240.0	240.0
Total	250.0	250.0	250.0	250.0

*Components A and B were mixed thoroughly and incubated for 15 minutes.

3.8.4 Knockdown of circSPINT2

3.8.4.1 Transfection of PLKO.1 Puro in Packaging Cell line (HEK293A)

Approximately 3×10^6 HEK293A cells were seeded in a 10cm culture dish, and allowed to adhere on plate overnight. HEK293A confluency on the day

of transfection was achieved at 80% – 90%. After 24 hours, HEK293A cells were transfected with pLKO.1-shRNA-circSPINT2 plasmid (10 μ g), together with packaging plasmids pMD2.G (5 μ g) (Addgene, Watertown, MA, USA) and psPAX2 (5 μ g) (Addgene, Watertown, MA, USA) in 6ml of RPMI medium using Lipofectamine 3000 Transfection Reagent (Invitrogen, Grand Island, NY, USA). In this study, two shRNA plasmids (shRNA1 and shRNA2) with different circSPINT2 sequences were designed for knockdown. Prior to transfection, Lipofectamine 3000 components (Life Technologies, USA) were prepared and incubated for 15 minutes. Transfection components and plasmids used were summarised in Tables 3.22 and 3.23 respectively.

Fresh Dulbecco's Modified Eagle Medium (DMEM) high glucose medium supplemented with 10% FBS, 1% penicillin/streptomycin and 1% L-glutamine (Gibco/Invitrogen, Grand Island, NY, USA) were replaced after 24 hours of post-transfection. Lentivirus-containing supernatants were collected from HEK293A at 72 hours post-transfection, centrifuged at 2000 RPM for 15 minutes and filtered using a 0.45 μ m syringe filter to remove cell debris. Polybrene (8 μ g/ml) was added into lentivirus-containing supernatant to enhance transduction efficiencies.

Table 3.22: Lipofectamine 3000 (A) Per Reaction

Components (A)	PLKO.1 (μL)	shRNA1 (μL)	shRNA2 (μL)
Opti-MEM	467.05	467.2	465.6
PLKO.1 Puro – Empty Vector	1.55	-	-
PLKO.1 Puro – circSPINT2	-	1.4	3
pMD2.G	0.8	0.8	0.8
psPAX2	0.6	0.6	0.6
P3000	30.0	30.0	30.0
Total	500.0	500.0	500.0

Table 3.23: Lipofectamine 3000 (B) Per Reaction

Components (B)	PLKO.1 (μL)	shRNA1 (μL)	shRNA2 (μL)
Lipofectamine 3000	20.0	20.0	20.0
Opti-MEM	480.0	480.0	480.0
Total	500.0	500.0	500.0

3.8.4.2 Transduction PLKO.1 Puro-circSPINT2 in H1975

Osimertinib sensitive parental cell line (H1975) maintained in the logarithmic growth phase at the time of assay in a CO₂ incubator at 37°C and 5% CO₂ atmosphere. Approximately, 6×10^4 cells/well were seeded in a 6-well plate and allowed to adhere on plate overnight. The next day, 2ml of Lentivirus supernatants (shRNA1 and shRNA2) were added to each well of H1975. Upon transduction, the plates were subjected to spinfection at 800 x g for 1 hour (32°C). H1975 cell lines transduced with empty vector backbone of PLKO.1 Puro, serves as control. Mediums were changed after 24 hours post-transduction to RPMI medium supplemented with Puromycin (Invivogen, Toulouse, France) at 2 μ g/ml for stable strain selection. Fresh mediums with Puromycin (Invivogen, Toulouse, France) were changed every alternate day for 1 week. After 7 days, Puromycin (Invivogen, Toulouse, France) was removed and the established knockdown cell lines were expanded in culture. Subsequently, shRNA1 and shRNA 2 clones were harvested for qRT-PCR to assess circRNA knockdown effect prior to downstream experiments.

3.9 Construction of circRNA-miRNA Interaction

3.9.1 Biotinylated-circRNA Pull-down Assay

Interactions between circRNA and miRNA in this study were investigated using Pierce Pull-Down Biotinylated Interaction Kit (Thermo Fisher Scientific, Waltham, MA, USA) according to manufacturer's protocol. The pull-down assay procedures involved preparation of streptavidin for immobilization, bait RNA binding protein immobilization, Biotin blocking, prey RNA/Protein Capture, spin column wash and elution. CircSPINT2 biotinylated (Thermo Fisher Scientific, Waltham, MA, USA) probe was used in this study, while a biotinylated negative mimic probe served as a control (Appendix G). The protocol of pull-down assay as described below:

A total of 150 μ L (each reaction) Streptavidin magnetic beads were resuspended in 350 μ L of TBS binding buffer and transferred into spin column. The column were placed in a collection tube and gently inverted for 5 times and centrifuged for 90 seconds at 1250 x g. Supernatants were discarded upon centrifugation. The washing step was repeated three times. Approximately, 50 μ M of Biotinylated-circSPINT2 probe were resuspended in TBS buffer and loaded into spin column. The mixtures of Streptavidin magnetic beads and biotinylated probe were incubated overnight at 4 $^{\circ}$ C on a carousel rotating shaker. The next day, the column tubes were centrifuged for 90 seconds at 1250 x g and supernatants were discarded. Biotin blocking solution (250 μ L per sample) were added to spin column, inverted five times and incubated at room temperature for 5 minutes. TBS buffer (250 μ L) were then added in and inverted five times and subsequently centrifuged at 1250 x g for 90 seconds. This step was repeated three times and supernatants were removed each time upon centrifugation.

Approximately, 1×10^7 of OR4 cells were harvested from 15cm cell culture dish and lysed in 120 μ L of co-IP lysis buffer prior to pull-down assay. Approximately, 100 μ L of the lysates were mixed homogeneously in 400 μ L TBS buffer, Streptavidin and biotinylated probe mixtures. The components in spin columns were incubated overnight at 4°C on a carousel rotating shaker. Thereafter, the spin columns were collected the next day and centrifuged at 1250 x g for 90 seconds to remove the supernatant. A total of 400 μ L of wash buffer were added to each column, inverted 5 times, incubated for 3 minutes and centrifuged at 1250 x g for 90 seconds. The washing step were repeated three times. In the final step, 10 μ L of neutralization buffer were loaded into each spin column with new collection tube followed by 200 μ L of elution buffer. Spin columns were incubated at room temperature for 5 minutes prior to centrifugation at 1250 x g for 2 minutes. Pull-down lysates were subjected to miRNA-seq and qRT-PCR analysis.

3.9.2 Micro RNA (miRNA) Extraction

In this study miRNeasy mini kit (Qiagen, Germany) was used to extract miRNAs for small RNA-seq and other downstream work such as qRT-PCR as per the manufacturer's protocol. The protocol of miRNA isolation using miRNeasy mini kit as described below:

A total of 1×10^6 adherent cells were harvested by trypsinization from 10cm culture dish, pelleted by centrifugation (2000 RPM, 5 minutes) and transferred to 1.5ml tubes. QIAzol lysis buffer (700 μ L) was added to the cell pellets and mixed homogeneously using mechanical disruption force by

vigorously pipetting up and down using 1ml precision pipette. The mixtures were vortexed for 30 seconds and left for incubation at room temperature for 5 minutes before the addition of 140 μ L of chloroform. Next, the mixtures were vortexed again for 15 seconds and left for another round of incubation for 3 minutes at room temperature. Subsequently, the samples were centrifuged for 20 minutes at 14,000 RPM and 4°C. The samples were separated into three phases which consist of an upper layer (aqueous phase) containing RNA, a white interphase layer and the bottom layer (organic phase). Approximately, 350 μ L of the upper aqueous phase were then transferred to a new 1.5ml collection tube. Following this, 525 μ L of 100% ETOH were added into aqueous phase and mixed thoroughly by pipetting up and down. These mixtures (700 μ L) were then transferred into an RNeasy Mini spin column and centrifuged at 14,000 RPM for 20 seconds at room temperature. Flow-through were discarded upon centrifugation. As in washing steps, a total of 500 μ L Buffer RPE was added to the samples and centrifuged for 20 seconds. Flow-through were discarded upon centrifugation. Another 500 μ L Buffer RPE were added to the spin column and centrifuged for 2.5 minutes to completely dry the spin column membrane. Spin column were transferred to a new 1.5ml collection tube and 20-30 μ L of RNase-free water were added directly onto the spin column membrane. The spin column were incubated for 1 minute at room temperature before centrifugation at 14000 RPM for 2 minutes to elute the miRNA. The concentration and purity of miRNA were measured using Implen NanoPhotometer N60 (Munich, Germany).

3.9.3 CDNA Conversion from miRNA

TaqMan Advanced miRNA cDNA Synthesis Kit was used in this study according to manufacturer's protocol (Thermo Fisher Scientific, Waltham, MA, USA) to convert 1 µg of RNA to cDNA for subsequent downstream analysis such as qRT-PCR. The cDNA synthesis process involved poly(A) tailing, adaptor ligation, reverse transcription (RT) and miR-amplification (miR-Amp). Before the preparation of the cDNA synthesis master-mix, all components were thawed on ice and briefly centrifuged to bring down the residual liquid from the sides of the tubes while 50% PEG 800 was allowed to thaw at room temperature.

Master mix preparation for poly (A) tailing step as outlined in Table 3.24. A total of 2 µL of RNA were thoroughly mixed in 3 µL of poly (A) tailing components. The mixtures were vortexed for 30 seconds and briefly centrifuged. Subsequently, the samples (5 µL/reaction) were subjected to thermal cycler heat (Eppendorf, Hamburg, Germany). Standard cycling as shown in Table 3.25. Next, master mix for ligation adaptor were prepared as listed in Table 3.26. Ligation Reaction Mix (10 µL/sample) were added to 5 µL of poly(A) tailing reaction product. The mixtures (15 µL/sample) were vortexed and briefly centrifuged prior to heat in thermal cycler (Eppendorf, Hamburg, Germany). Standard cycling as shown in Table 3.27. Subsequently, 15 µL/sample of RT reaction mix (as shown in Table 3.28) were added to ligation adaptor product. The reaction containing 30 µL/sample were vortexed for 30 seconds, briefly centrifuged and subjected to thermal cycler heat (Eppendorf, Hamburg, Germany). Standard cycling as shown in Table 3.29. As for the final step, miR-Amp reaction were prepared as listed in Table 3.30. 45 µL of miR-Amp reaction

and 5 μL were thoroughly mixed in a new PCR tube. The mixtures of 50 μL /sample were subjected to thermal cycler heat (Eppendorf, Hamburg, Germany). Standard cycling as shown in Table 3.31. All remaining RT reaction samples and synthesized cDNA samples were kept in a minus 20°C freezer.

Table 3.24: Poly (A) Tailing Per Reaction

Components	Working Volume/Reaction (μL)
RNA	1 μg in 2 μL
10x Poly (A) Buffer	0.5
ATP	0.5
Poly (A) Enzyme	0.3
RNase Free Water	1.7
Total	5.0

Table 3.25: Cycling Condition for Poly (A) Tailing

Components	Temperature	Time
Polyadenylation	37°C	45 minutes
Stop Reaction	65°C	10 minutes
Hold	4°C	∞

Table 3.26: Ligation Adaptor Per Reaction

Components	Working Volume/Reaction (μL)
5x DNA Ligase Buffer	3.0
50% PEG 8000	4.5
25x Ligation Adaptor	0.6
RNA Ligase	1.5
RNase Free Water	0.4
Total	10.0

Table 3.27: Cycling Condition for Ligation Adaptor

Components	Temperature	Time
Ligation	16°C	60 minutes
Hold	4°C	∞

Table 3.28: Reverse Transcription (RT) Per Reaction

Components	Working Volume/Reaction (μL)
5x RT Buffer	6.0
dNTP Mix (25mM each)	1.2
20x Universal RT Primer	1.5
10x RT Enzyme Mix	3.0
RNase Free Water	3.3
Total	15.0

Table 3.29: Cycling Condition for Reverse Transcription (RT)

Components	Temperature	Time
Reverse Transcription	42°C	15 minutes
Stop Reaction	85°C	5 minutes
Hold	4°C	∞

Table 3.30: miR-Amplification Per Reaction

Components	Working Volume/Reaction (μL)
2x miR-Amp Master Mix	25.0
20x miR-Amp Primer Mix	2.5
RNase Free Water	17.5

Table 3.31: Cycling Condition for miR-Amp

Components	Temperature	Time	Cycles
Enzyme Activation	95°C	5 minutes	1

Denature	95°C	3 seconds	14
Anneal/Extend	60°C	30 seconds	
Stop Reaction	99°C	10 minutes	1
Hold	4°C	Hold	∞

3.9.4 MicroRNA Next Generation Sequencing (miRNA-Seq)

Small RNA libraries preparation for miRNA sequencing was performed using TruSeq Small RNA Library Prep Kit by Illumina (San Diego, CA, USA) (according to manufacturer's protocol). High-quality RNA of biotinylated circRNA pull down lysate from OR4 were used as the starting material in this study. RNA input required for miRNA sequencing ranging from 10-50ng of purified miRNA. Prior to NGS, RNA were subjected to 2100 Bioanalyzer (Agilent, Germany) to assess the RNA integrity. Samples with a RIN (RNA integrity Number) of 8-10 were prioritized for sequencing input. The overview of the process includes ligate adapters, reverse transcription and amplification of libraries, purification of cDNA constructs, library checking, and the last step involves normalization of libraries. The protocol of miRNA sequencing using Illumina platform as described below:

First, total RNA undergoes a small RNA enrichment process using miRNeasy mini kit (Qiagen, Germany) as described by manufacturer's protocol. Next, in the adapter ligation step, the 3' and 5' RNA were ligated to the small RNA molecules. Adapters and ligase were mixed in small RNA samples, allowing for the specific binding of the adapters to the ends of the small RNAs. Purification was carried to remove unligated adapters and other contaminants from the ligated product to ensure efficient downstream library preparation. Ligated small RNAs were then subjected to reverse transcription to synthesize

cDNA. In this step, reverse transcription reaction integrated primers, complementary to the ligated adapters which converts RNA into cDNA and provide unique labelling to each sample. PCR-amplification of cDNA was completed to enrich small RNA fragments with ligated adapters. Subsequently, small RNA libraries generated were purified using magnetic bead-based purification to remove PCR primer-dimers and other non-relevant artifacts. In the final step, prior to sequencing, normalization and quality control of library preparation were assessed using 2100 analyzer (Agilent, Germany) to ensure the libraries meet the criteria for size distribution and sequencing input.

3.9.5 In-Silico Analysis

The interaction between microRNA and tumour suppressor gene was constructed by connecting microRNA targets (<https://mirdb.org/>) and filtering tumour suppressor-associated genes, which are classified by GO annotation (<https://string-db.org/>). The nodes of genes are coloured according to their expression in the NGS results. The network was plotted by using Cytoscape 3.10.0 (<https://cytoscape.org/>).

3.10 Animal Model

3.10.1 Establishment of Osimertinib-Resistant Xenograft Model

In this study, Osimertinib-resistant *in-vivo* xenograft model were established by subcutaneous injections of H1975 cell line into NOD-SCID mice (6–8 weeks old, Jackson Laboratory). The animal work conducted has been subjected to approval (IACUC NO: 2020-010) from both Taipei Veteran General Hospital (TVGH) and National Yang-Ming Chiao Tung University Ethics &

Code of Conduct. The procedures of *in-vivo* experiments conducted in this study as described below:

First, 1×10^6 cells of H1975 cell line were seeded in 15cm cell culture dish, cultured in RPMI growth medium and maintained in the logarithmic growth phase. The cells were harvested by trypsinization upon reaching 70-80% confluency and pelleted by centrifugation at 2000 RPM for 10 minutes. Approximately, 5×10^6 H1975 cells were resuspended in 100 μ L of 1 x PBS and injected subcutaneously into both left and right lower flanks of NOD-SCID mice (each side 100 μ L). Tumour diameters were measured using a calliper and tumour volume were monitored and calculated (Tumour Volume = Length x Width x Height x 0.5). Once, the tumours reached an average-size of 50mm³, the mice were treated with 5 mg/ml of Osimertinib/AZD9291 (Selleckchem, Houston, TX, USA), 5 times per week using an oral gavage. Control/vehicle group were established simultaneously and given 1xPBS instead. In this study three mice per group were employed (n=3). Osimertinib-resistant xenografts were established over 21 days under continuous Osimertinib treatment *in-vivo*. Mice were euthanized when the tumour volume reached approximately 1000 mm (Tumour Volume = Length x Width x Height x 0.5). Xenograft tumours were harvested, fixed with 4% formalin and further subjected to Paraffin-embedded (FFPE) tissues slide preparation (~2 μ M thickness each slices). The tissue slides were then employed for haematoxylin and eosin (H&E) staining, FISH analysis, qRT-PCR and western blot. Tumour volume of all xenografts as detailed in Appendix H.

3.10.2 Fluorescence In-situ Hybridisation (FISH) Assay

The tumour xenografts FFPE slides (Osimertinib treated and vehicle group) were first heated on a block at 60°C for one hour, then subjected to deparaffinization and rehydration using a series of xylene (5 minutes), gradient ETOH concentrations (100%, 95%, 70% and 50%) for 10 minutes each and ddH₂O for 5 minutes. Next, Proteinase K (0.6 U/mL) (Sigma, St. Louis, MO, USA) was applied to the samples for 30 minutes at 37 °C in a humidified chamber. Following this, the samples were treated with a 30 µM of Cy3-tagged fluorescent probe (Integrated DNA Technologies, Coralville, IA, USA) (Appendix I) overnight at 42 °C and washed with 2X SSC buffer (three times) (Thermo Fisher Scientific, Waltham, MA, USA). Subsequently, the samples were immersed in 100 mg/mL RNase A solution (Thermo Fisher Scientific, Waltham, MA, USA) diluted in 2X SSC (Thermo Fisher Scientific, Waltham, MA, USA) at 37 °C for 30 minutes, washed in 1X PBS, and then incubated in 1X PBS containing DAPI (1:10,000 dilution). Finally, the slides were rinsed three times in 1X PBS, mounted in mounting medium, and imaged using FV3000 confocal laser scanning microscopes from (Olympus, Japan)

3.10.3 Chromogenic Immunohistochemistry (IHC)

FFPE tissue slides were deparaffinized and rehydrated using a series of xylene (5 minutes), gradient ETOH concentrations (100%, 95%, 70% and 50%) for 10 minutes each and ddH₂O for 5 minutes. Tissues sections were then treated with peroxidase blocking solution for 10-15 minutes and washed with wash

buffer to remove remaining residual blocking solution prior to overnight incubation at 4 °C, with primary antibody using anti-human RBP1 polyclonal (Catalog # PA5-28713, Thermo Fisher Scientific, Waltham, MA, USA) (Appendix J). Incubation with secondary antibody and chromogen substrates were performed according to manufacturer's protocol (Catalog # K5007; Dako, Agilent Technologies, CA, USA).

CHAPTER 4

RESULTS

6.1 Generation and Characterization of Osimertinib-Resistant Cell Lines

The H1975 cell line was derived from a non-smoking female diagnosed with lung adenocarcinoma (NSCLC) and harbours the L858R/T790M mutations. Studies have shown that, this cell line is resistant to first and second generation EGFR-TKIs. The cells display a morphologically homogeneous epithelial-like appearance and adhere to cell culture flasks. H1975 cell line was prominently used in immuno-oncology studies and to investigate EGFR-TKIs resistant properties targeting T790M in lung cancer research. Typically, H1975 cells demonstrate stable proliferation rate and reaches 70% - 80% confluency within three days in active cell culture (Figure 4.1).

Osimertinib-resistant (OR) clones were derived using a stepwise dose-escalation method. Recommended *in-vitro* dosage by FDA, which ranged from 480 nM–1.8 μ M was used to induced resistance in H11975 cell line. As such, H1975 cell line was treated *in-vitro* with an increasing dose of Osimertinib, from 500 nM to 1.5 μ M in a sequential manner, until stable cell growth without significant cell death was observed in active culture. Subsequently, single cell clone was established through limiting dilution in a 96-well format. Each clone was expanded under a final concentration of 1.5 μ M Osimertinib and three clones (OR3, OR4 and OR6) were selected based on their survival for over 6 months under Osimertinib selective pressure and *in-vitro* characterization

(Verusingam et al., 2020). Significant morphological differences were observed in parental H1975 cell line and the OR cells. OR cells derived, exhibit elongated and spindle-shaped characteristics resembling fibroblast-like cells (Figure 4.2). Prior to transcriptomic analysis, protein expression levels of EGFR signalling pathway and its downstream signalling pathways, AKT and ERK were characterised in H1975 and its OR counterparts. Despite the distinguishable morphological alterations in OR cell lines, EMT associated markers were also examined. Based on the western blot protein analysis, the absence of phosphorylated EGFR expression in all OR cells was observed (including those treated with Osimertinib and the control DMSO) which implicated the potential acquisition of resistance through EGFR-independent signalling. Additionally, Osimertinib treatment effectively inhibited phospho-ERK and phospho-AKT expression in the parental H1975 cells, but the inhibitory effect was not effective in the OR cell lines. Overall, the data suggested that OR cells generated in this study, bypassed the canonical EGFR signalling by retaining ERK and AKT signalling. Besides, reduction in epithelial protein expression (E-Cadherin and EpCAM) and an increase in mesenchymal protein markers (Vimentin and CD44) in the OR cells was observed. These findings substantiated with the observed morphological alterations in OR cells. The OR (OR3, OR4 and OR6) cells characterisation data as listed in Appendix K.

On another note, H1975AZDR cells/HOsiR cell line (Figure 4.3) used in this study, also showed significant resistance to Osimertinib and distinct morphological difference against parental H1975. However, this cell line was derived from pool clone of Osimertinib induced resistance and exhibited

fibroblast like morphology (Figure 4.3). HOSiR cell line was kindly provided by our collaborator, Dr Chou Yu-Ting (Kuo et al., 2020)..

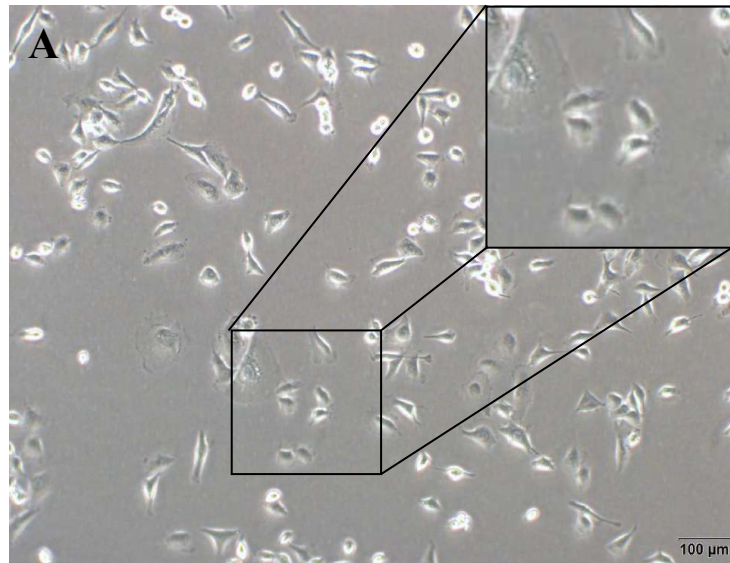
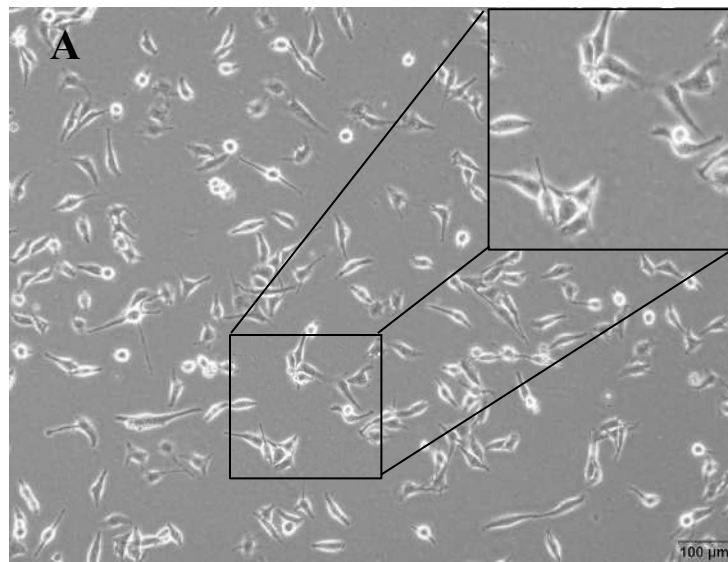


Figure 4.1 Morphology of H1975 cell line at 60% confluency. (A) Lung adenocarcinoma cell harbouring L858R/T790M mutation exhibiting epithelial morphology. Olympus inverted microscope, magnification: 10x.



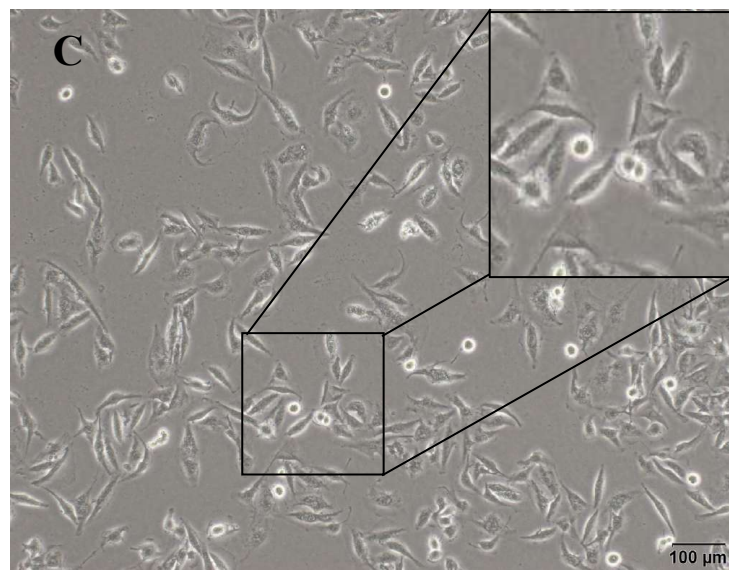
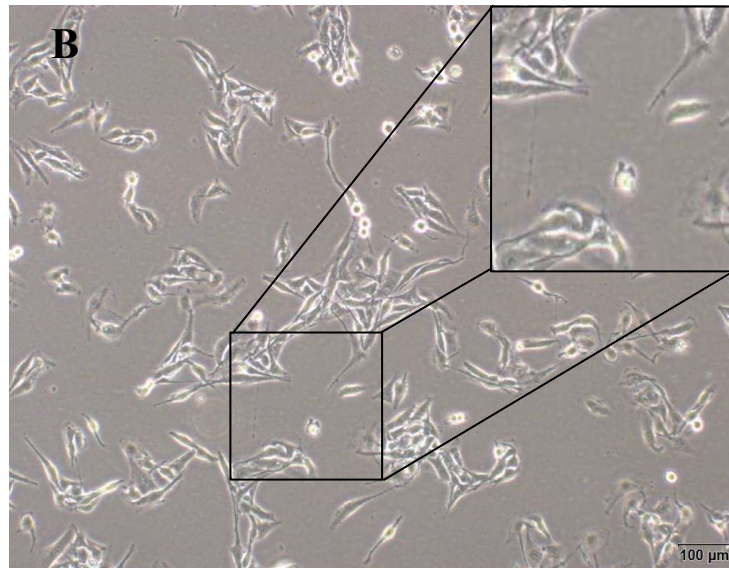


Figure 4.2 Morphologies of Osimertinib-resistant cell lines isolated from single clones at 70% confluency. (A) OR3 (B) OR4 and (C) OR6, all Osimertinib-resistant cells exhibiting elongated fibroblast like morphology. Olympus inverted microscope, magnification: 10x.

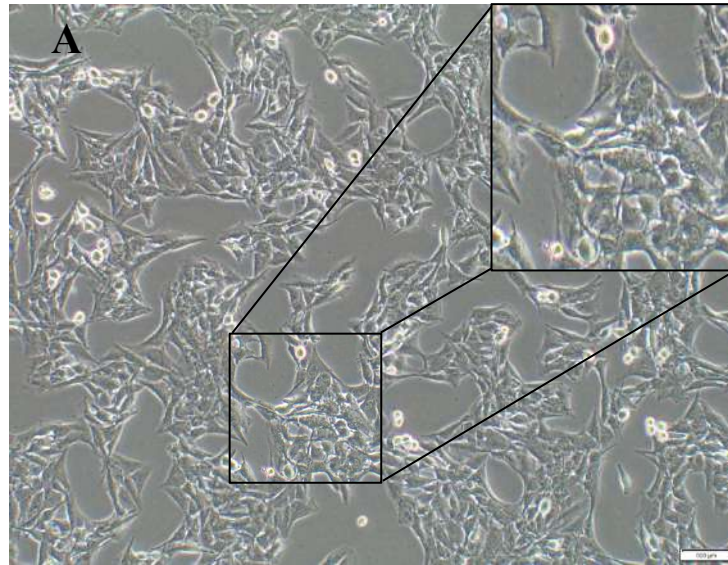


Figure 4.3 Morphologies of Osimertinib-resistant cell lines isolated from pool clones at 80% confluency. (A) HOSiR cell line exhibited elongated and fibroblast like morphology compared to its parental H1975. Olympus inverted microscope, magnification: 10x.

Osimertinib's efficacy in H1975, OR4, and HOSiR was concurrently confirmed using the AlamarBlue assay to quantify the cell viability before subjected to circRNA characterization and downstream assays. The AlamarBlue assay employed in this study, uses the Resazurin fluorescence dye, characterized by its non-toxic nature and cell-permeable properties, which is crucial for the accurate quantification of cell viability. H1975, OR4, and HOSiR cells were exposed to Osimertinib concentrations ranging from 0.001 to 10 μM for 48 hours. DMSO treated cell were included as control. Notably, the established OR cell exhibited higher IC_{50} values compared to the parental counterpart. The IC_{50} values for OR4 and HOSiR were 3.97 μM and 3.98 μM , respectively, whereas the parental H1975 displayed a lower IC_{50} value of 0.07 μM Figure 4.4). This

discrepancy suggested that OR cells are less responsive to Osimertinib compared to H1975.

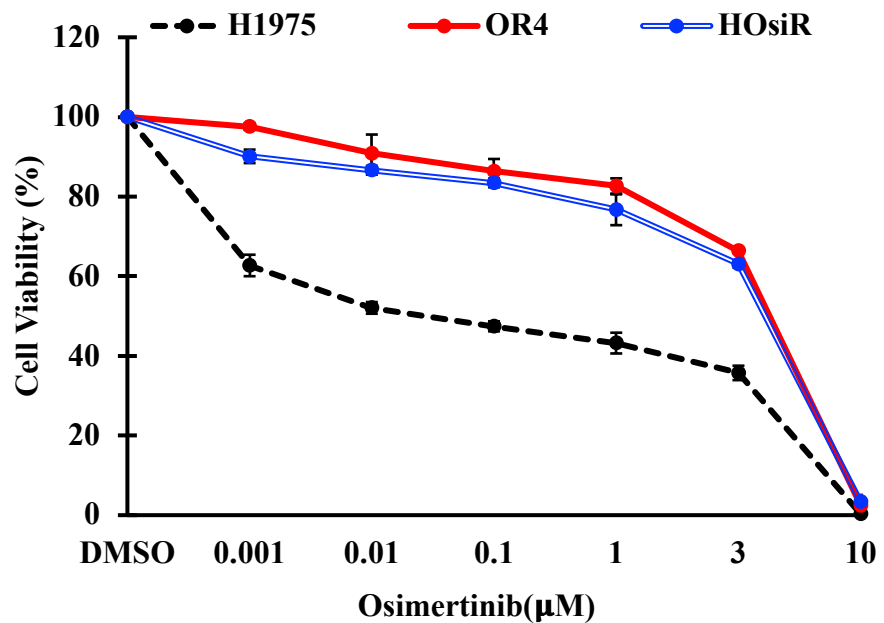


Table 4.1: IC ₅₀ (µM) – H1975, OR4 and HOsiR			
Cell Lines	H1975	OR4	HOsiR
IC ₅₀ (µM)	0.07 ± 0.03	3.97 ± 0.17	3.98 ± 0.15

Figure 4.4 Osimertinib sensitivity assay (AlamarBlue) in H1975, OR4 and HOsiR. Quantitative measurement of Osimertinib efficacy in OR cell lines and the parental H1975 cell line at 48 hours. Data are presented as the mean ± SEM (n = 3). Statistical differences are indicated with * for P < 0.05, ** for P < 0.01 and *** for P < 0.001 using paired t-test.

In alignment with the drug sensitivity assay, the colony formation assay demonstrated high clonogenic survival in OR4 and HOsiR cells following Osimertinib treatment, suggesting the development of acquired resistance. As illustrated in Figure 4.5, a dosage of 0.1 µM Osimertinib effectively inhibited

the clonal expansion of the H1975 cell line but was insufficient to suppress the *in-vitro* clonal growth of OR4 and HOsiR cells.

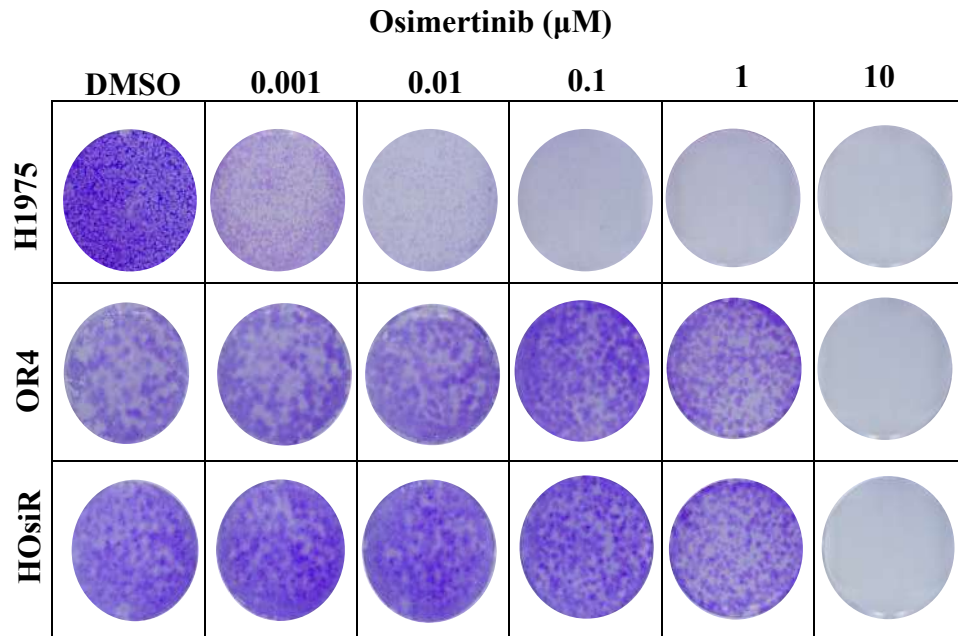


Figure 4.5 Qualitative measurement of Osimertinib efficacy via Colony formation assay in H1975, OR4 and HOsiR. Osimertinib response in OR cell lines and the parental H1975 cell line at 48 hours.

To further validate the findings of the drug sensitivity assay, tumoursphere formation assay was conducted to assess resistance properties in the H1975, OR4, and HOsiR cell lines. The OR cells demonstrated a significantly higher capacity for sphere formation in culture compared to the H1975 cell line (Figure 4.6), indicative of enhanced tumorigenic potential, self-renewal and clonogenicity. Tumourspheres derived from OR4 and HOsiR cells were rounder and more compact compared to those formed by H1975 cells.

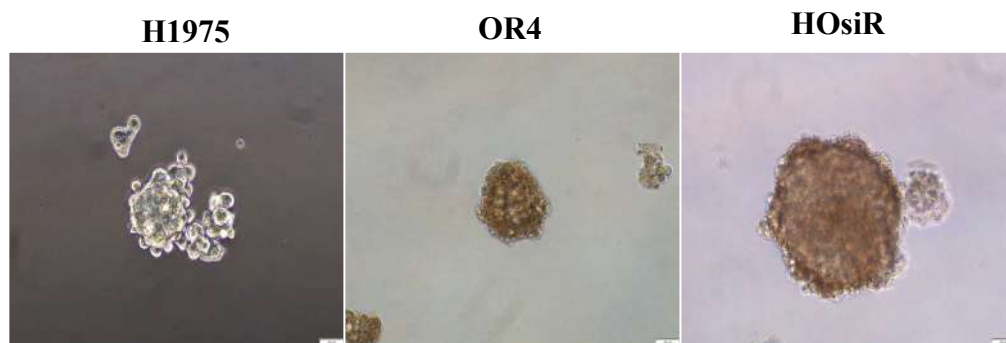


Figure 4.6 Qualitative observation of tumorigenic potential via tumoursphere formation assay in H1975, OR4 and HOsiR. Tumorigenic potential in OR cell lines and the parental H1975 cell line. Olympus inverted microscope, magnification: 20x.

Next, Propidium iodide (PI) was used to stain cells that migrated to outer side of culture insert. OR cells exhibited higher migration potential indicative of their tumorigenic potential. As shown in Figure 4.7, a higher number of nuclei stained with Propidium iodide (PI) were observed in OR4 and HOsiR. This indicates an increased population of cells that potentially migrated across the transwell membrane, suggesting their invasive properties

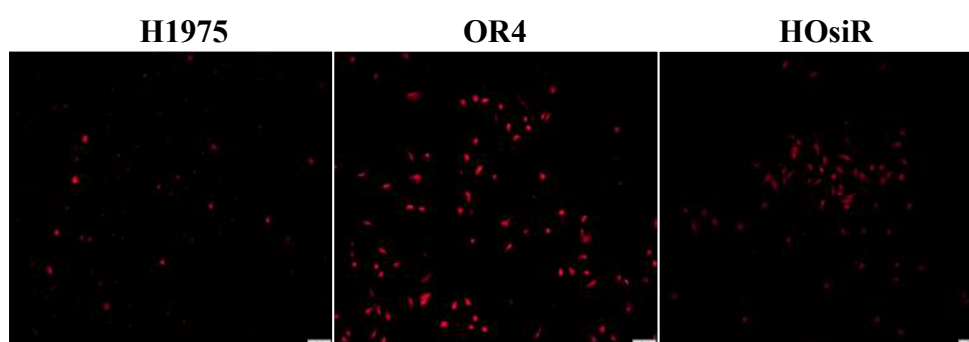


Figure 4.7 Qualitative observation of cell migration potential via migration assay in H1975, OR4 and HOsiR. Migration potential in OR cell lines and the parental H1975 cell line at 16 hours. Olympus inverted microscope, magnification: 10x.

All in all, Osimertinib-resistant cell lines demonstrated not only a greater drug resistance potential (Figure 4.5) but also an increased capacity for efficient tumoursphere formation (Figure 4.6) and enhanced migration ability compared to the parental H1975 cell line (Figure 4.7).

4.2 Comparative circRNA Expression Profiling in Osimertinib-Resistant Clones and Their Parental Cells Using circRNA-Next Generation Sequencing (NGS)

Initial success in patients with sensitizing EGFR mutations is often hindered by T790M resistance due to EGFR-TKI selective pressure. This highlights the need for further EGFR-TKI development and innovative treatment approaches, revealing the complex evolution of NSCLC under EGFR-TKI therapy. Therefore, a high-intracellular-abundance RNA biomarker is crucial to gain dynamic insights into cellular states and regulatory processes, ensuring superior sensitivity and specificity. CircRNAs have demonstrated such potential as a biomarker with diverse predictive values across different cancers, offering advantages like stability, tissue specificity, sensitivity, and reproducibility.

Derivatives of OR cells derived in this study, exhibited resistance to Osimertinib treatment, making them as valuable resources for elucidating Osimertinib resistance mechanisms, understanding tumour evolution during prolonged drug exposure, and investigating associated signalling pathways (Verusingam et al., 2020). Three OR clones were subjected for circRNA sequencing to establish comparative circRNA transcriptomic profile analysis associated to Osimertinib resistance. Clustered heat map showed differential

circRNAs expression of both up-regulation and down-regulation in OR cells versus parental H1975 cells (fold change [FC] ≥ 2.0 ; $P < 0.05$) (Figure 4.8). Approximately, 84140 of circRNAs were identified during transcriptomic analysis. Whereas, a total of 280 overlap circRNAs were up-regulated in the Osimertinib-resistant group while 199 were down-regulated compared with the parental control (Figure 4.9).

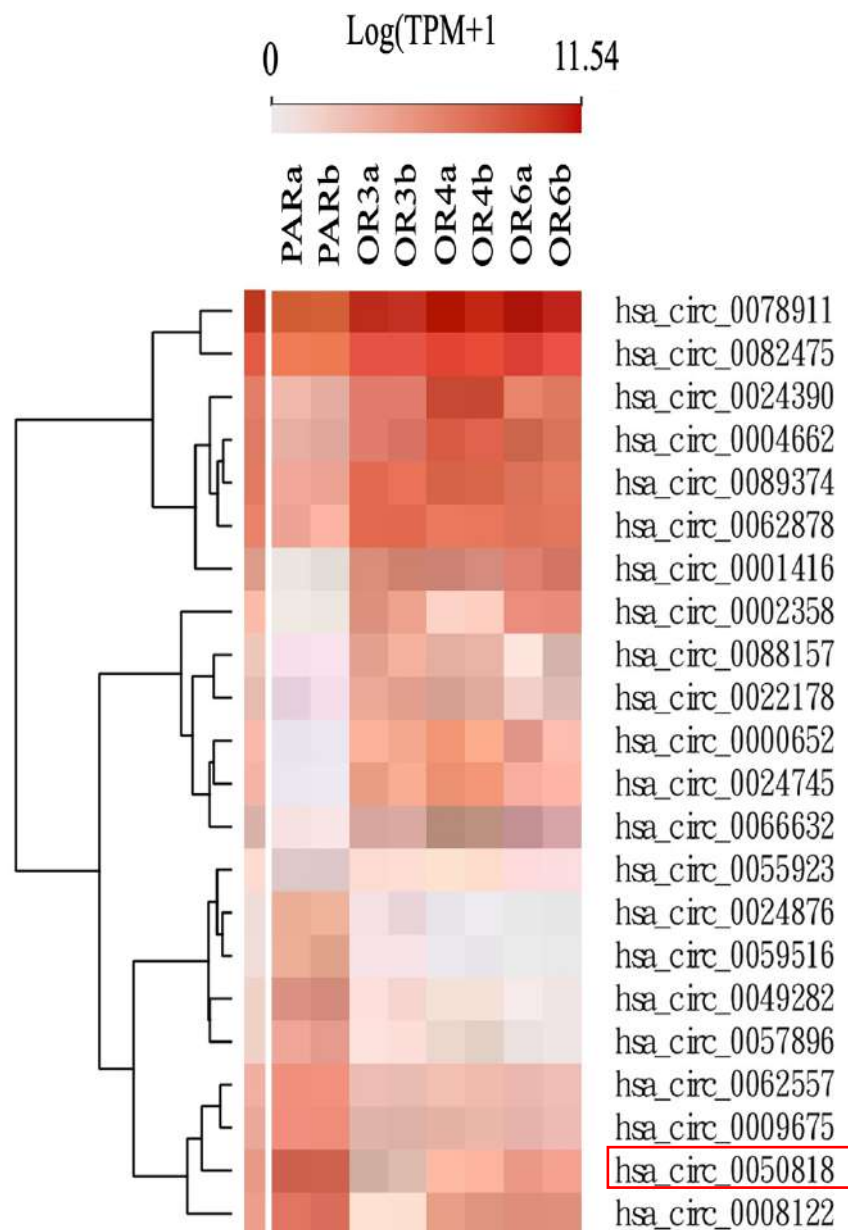


Figure 4.8 CircRNA transcriptomic profiling in Osimertinib-resistant cell lines. Heat map shows expression clustering between parental H1975, and Osimertinib -resistant (OR3, OR4 and OR6) cell lines.

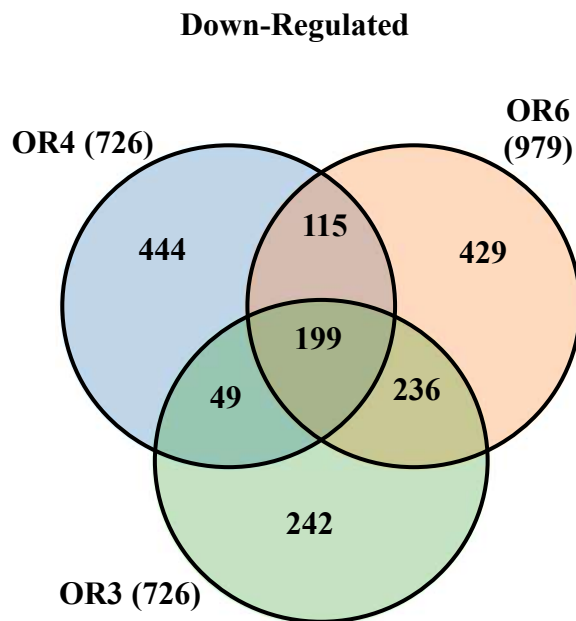
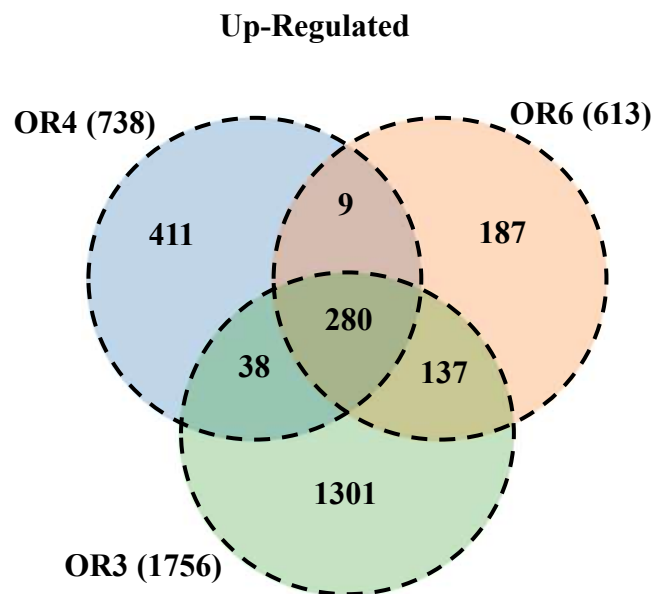


Figure 4.9 Venn-diagram of circRNA differential expression. Overlap of circRNAs differential expression in OR3, OR4 and OR6 cell lines.

4.3 Characterization of circRNA: circSPINT2 is Downregulated in Osimertinib-Resistant Cell Lines

Based on whole transcriptomic analysis results, 10 circRNAs were chosen (top 5 up-regulated circRNAs and top 5 down-regulated circRNAs) for qRT-qPCR validations (Appendix L). CircRNAs validation through qRT-qPCR demonstrated that the differential expression patterns of 5 up-regulated and 3 down-regulated circular RNAs (circRNAs) remained consistent with the circRNA-seq data. (4.10). However, two down-regulated circRNAs (hsa_circ_0059516 and hsa_circ_0057896) were not significant with high $P > 0.05$. While, for hsa_circ_0024390 the high error bars of the standard deviations exhibit considerable overlap and thus may not represent a conclusive circRNA expression within OR samples. Also, down-regulated circRNAs (hsa_circ_0049282, hsa_circ_0024876 and hsa_circ_00508818) expressions were significant in the OR group compared to H1975 with p-value of $P < 0.001$. The remaining portion of the circRNAs holds substantial significance expression as confirmed by qRT-PCR validations with p-values of $P < 0.05$. The p-values were computed through Paired t-tests to compare Osimertinib-sensitive group (H1975) and Osimertinib-resistant group (OR3, OR4 and OR6).

Hsa_circ_0050818 or herewith named as circSPINT2 was selected as target circRNA molecule in this study because its host gene, SPINT2 has been previously known as tumour suppressor, inhibiting metastasis in lung cancer (Ma et al., 2019). Hence, circSPINT2 was postulated to hold tumour suppressive function and may replace SPINT2 as a potential biomarker in Osimertinib resistance NSCLC patients.

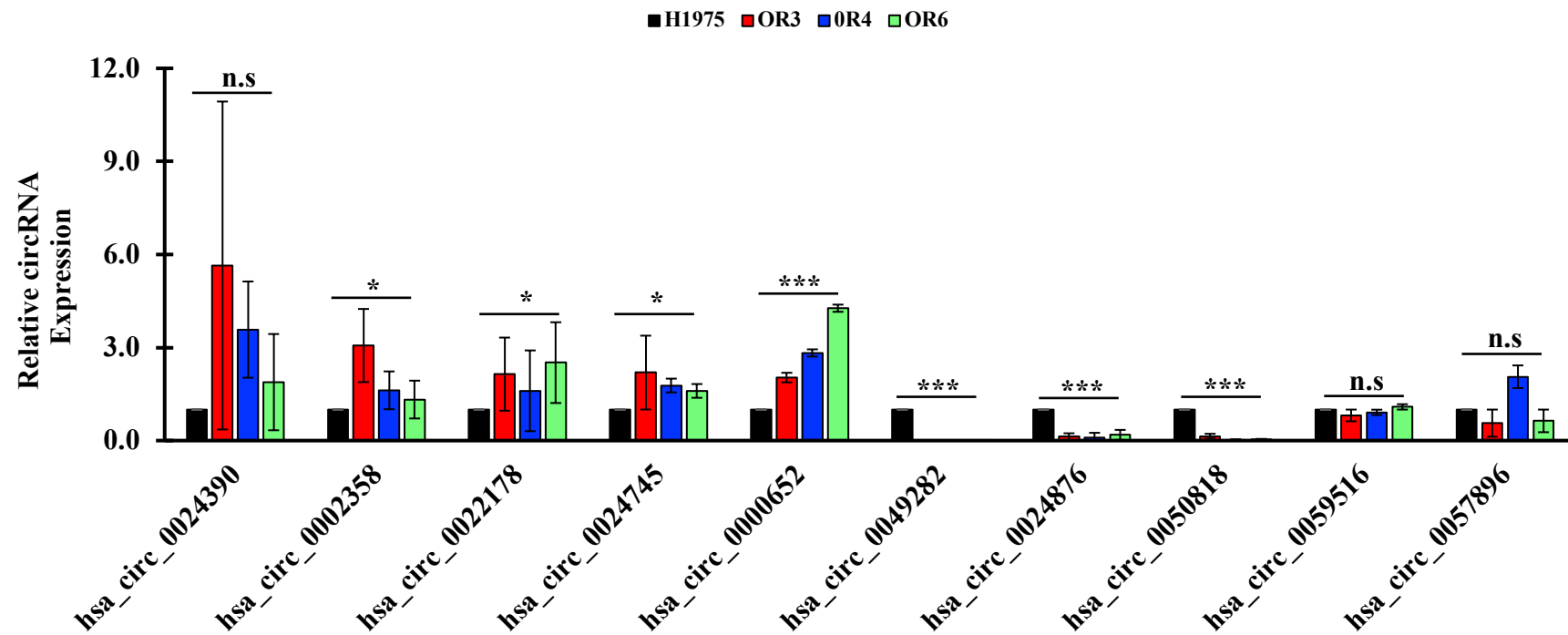


Figure 4.10 CircRNA validation via qRT-PCR in H1975 and OR (OR3, OR4 and OR6) cells. Ten circRNAs selected from transcriptomic analysis validated using qRT-PCR. Data are presented as the mean \pm SEM (n = 3). Statistical differences are indicated with * for $P < 0.05$, ** for $P < 0.01$ and *** for $P < 0.001$ using paired t-test.

When circSPINT2 expression was assessed in the HOSiR cell line using qRT-PCR, the findings were consistent with those observed in Osimertinib-resistant clones. The results demonstrated a significant downregulation of circSPINT2 in HOSiR cells ($P < 0.001$, Figure 4.11). These data suggest that circSPINT2 may play a role in the mechanism of acquired resistance to Osimertinib.

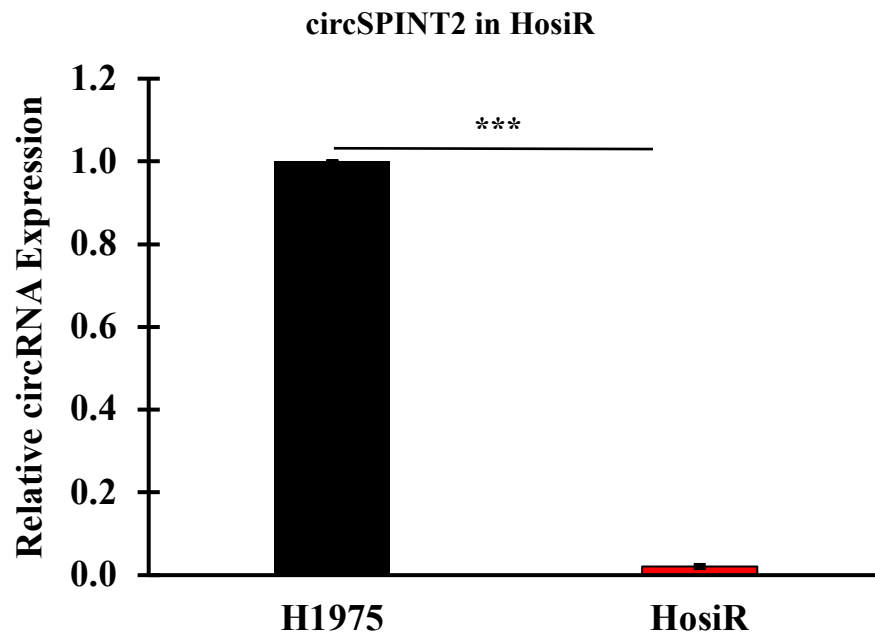


Figure 4.11 CircSPINT2 expression in HOSiR. Relative CircSPINT2 expression via qRT-PCR analysis between H1975 and HOSiR. Data are presented as the mean \pm SEM ($n = 3$). Statistical differences are indicated with * for $P < 0.05$, ** for $P < 0.01$ and *** for $P < 0.001$ using paired t-test.

Subsequently, amplified PCR product of circSPINT2 of H1975 acquired through qRT-PCR was subjected to Sanger sequencing. The Sanger sequencing technique provides confirmation of the specific location of back-splice junction site. Hence based on the sequencing results, CircSPINT2 is derived from the Exon 3 and 4 of SPINT2 gene transcript through a 5'-3' backsplicing (4.12). The location of circSPINT backsplicing junction was also verified in

Circinteractome and Circbase databases. Divergent primers were designed to amplify and detect the sequence at the backspliced exon junction of circSPINT2 (Appendix A).

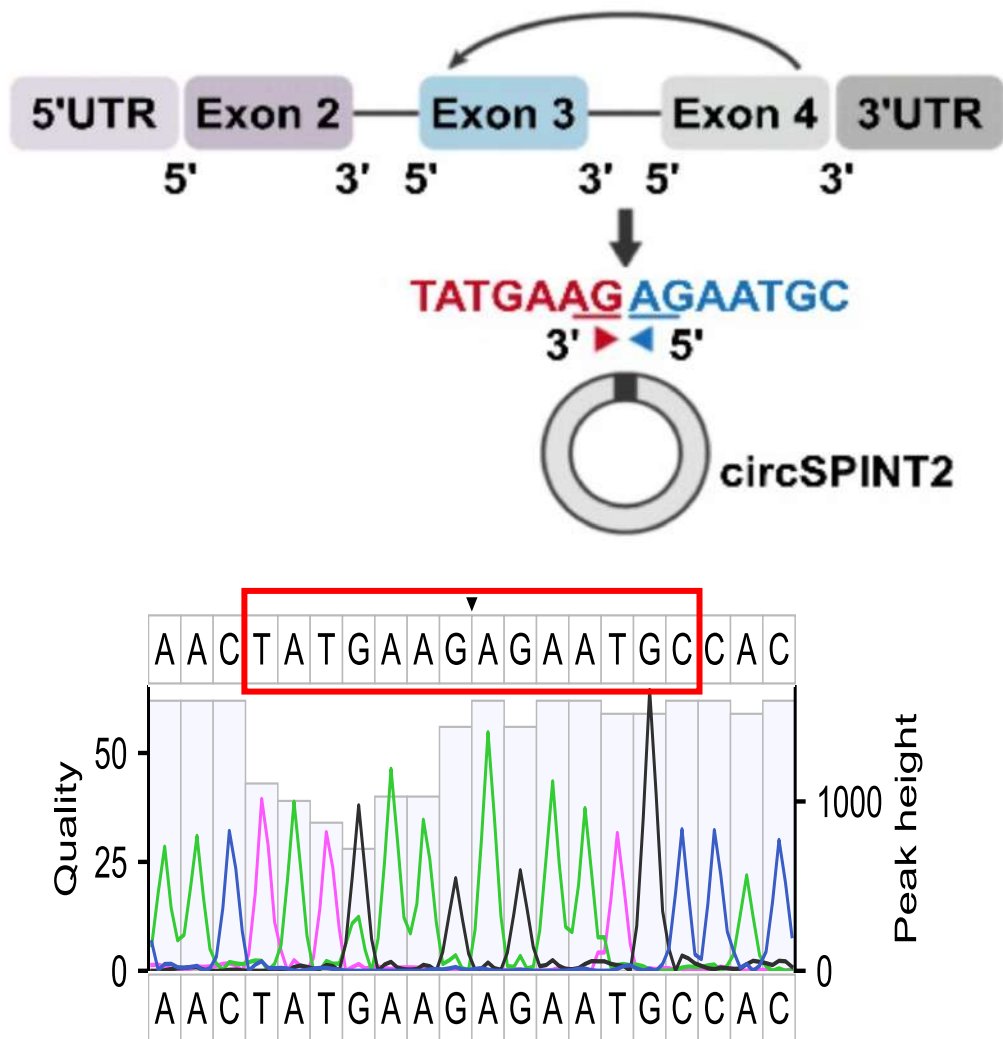


Figure 4.12 Sanger sequencing of circSPINT2. Sanger sequencing confirms the backsplicing junction of circSPINT2 in H1975 PCR product.

To further confirm that the detected transcript was circSPINT2 rather than its linear counterpart, total RNA from H1975 cells were subjected to RNase R treatment, an exonuclease that degrades linear RNA but had no effect on circRNAs. H1975 cell line was treated with RNase R and a mock sample (without RNase R treatment). The enzyme resulted in the degradation of

SPINT2 mRNA, wherein the expression level became almost not detectable, while circSPINT2 remained unaffected (Figure 4.13). The RNase R treated samples were normalized to mock group. Divergent primer was used to amplify circSPINT2 expression while convergent primer was used to detect SPINT2 expression (Appendix A). This result also implicated that circSPINT2 is a circularised transcript exhibiting resistance to exonucleolytic activity.

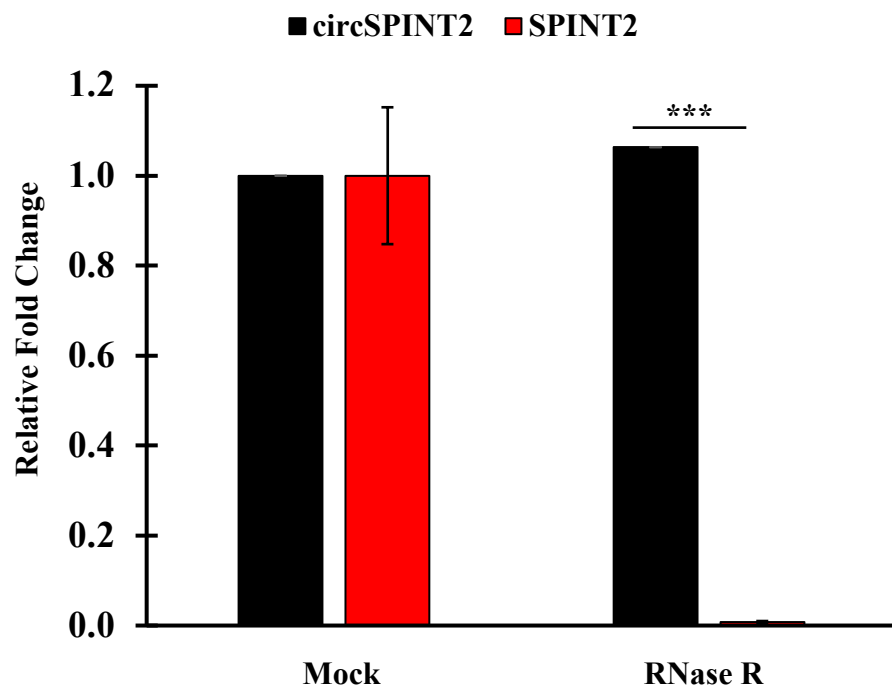


Figure 4.13 Characterization of circSPINT2 via RNase R treatment in H1975. RNase R degrades linear RNA transcript as indicated by relative fold change between circSPINT2 and SPINT2. Data are presented as the mean \pm SEM (n = 3). Statistical differences are indicated with * for $P < 0.05$, ** for $P < 0.01$ and *** for $P < 0.001$ using paired t-test.

Actinomycin D was used to inhibit RNA transcription in the H1975 cell line to assess the stability of circSPINT2. SPINT2 mRNA and circSPINT2 expressions were quantified at 0 hour, 4 hours, 8 hours, 12 hours and 24 hours. The data indicated circSPINT2 has a longer half-life compared to its host gene

SPINT2 (Figure 4.14) with statistically significant p-values ($P < 0.001$). Overall, RNase R and actinomycin assays confirmed that circSPINT2 indeed a stable circularized circRNA transcript.

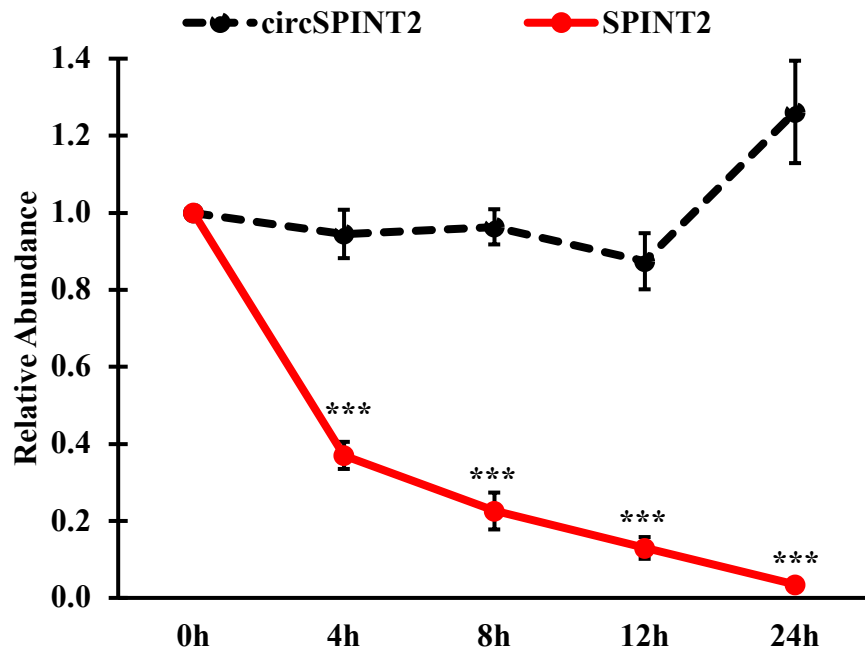


Figure 4.14 Characterization of circSPINT2 via Actinomycin D treatment in H1975. Actinomycin D treatment confirms the stability of circSPINT2 in H1975 Cell line. Data are presented as the mean \pm SEM ($n = 3$). Statistical differences are indicated with * for $P < 0.05$, ** for $P < 0.01$ and *** for $P < 0.001$ using paired t-test.

Notably, the application of circRNAs as biomarkers in liquid biopsies has been of great interest in recent studies. Thus, the abundance of circSPINT2 in the cell-conditioned media was evaluated using droplet digital PCR (RT-ddPCR) system. The ddPCR enables absolute quantification for quantifying low target input with improved sensitivity and precision for liquid biopsy analysis. The samples are partitioned into 20,000 nanoliter-sized droplets, whereby each droplet was collectively computed as an 'Event Number' in ddPCR analysis.

Total secreted RNA were extracted from cell-conditioned media of H1975, OR4 and HOsiR, further quantified for circSPINT2 expression with ddPCR. Divergent circSPINT2 primer sequence was applied in the ddPCR experiment. The condition medium of H1975 displayed an average total event count of 11,984, whereas OR4 demonstrated 35 events and HOsiR showed 81.5 events, all with statistically significant p-values ($P < 0.001$). As such, CircSPINT2 expression pattern was consistent as off in the cell lines whereby significantly low circSPINT2 positive droplets were detected in OR4 and HOsiR conditioned medium compared to H1975. Also, the result revealed that circSPINT2 can be detected in the extracellular environment.

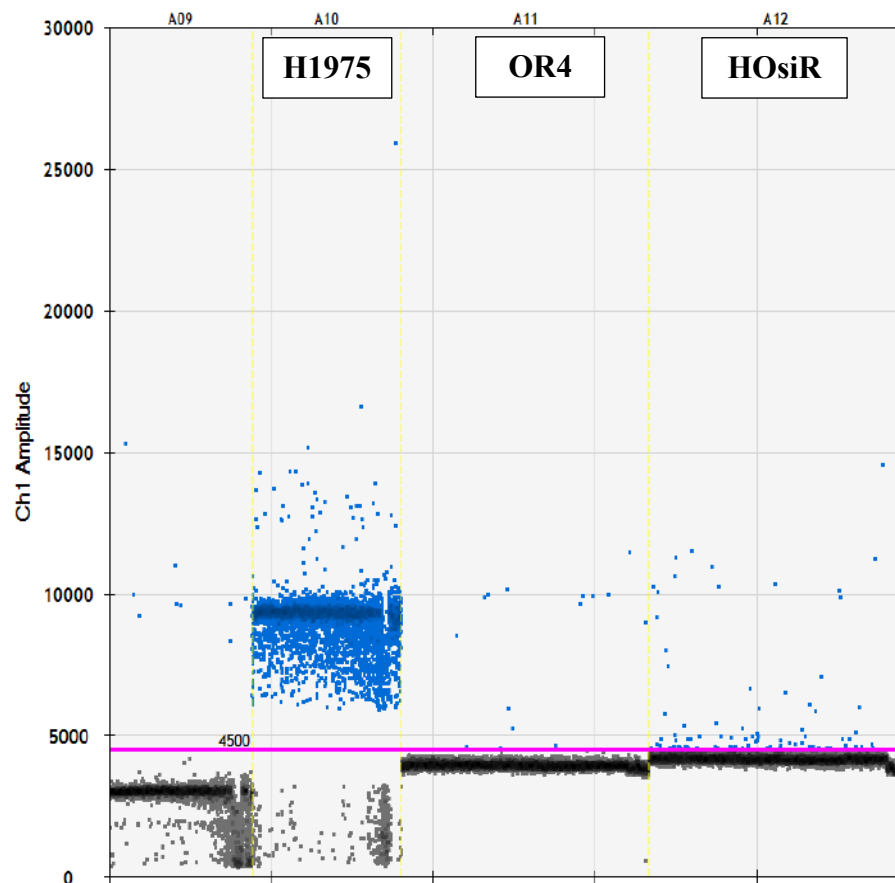


Figure 4.15 Droplet digital PCR (ddPCR) analysis detected the presence of circSPINT2 in the medium conditioned of H1975 and OR cells. Data are presented as the mean \pm SEM ($n = 2$).

4.4 CircSPINT2 Overexpression Improves Osimertinib Sensitivity and Reduces NSCLC Cell Aggressiveness

In an effort to explore the potential involvement of circSPINT2 in Osimertinib resistance, the functional implication and biogenesis of this circRNA were investigated through gain-of-function assay in OR4 and HOSiR cell lines. Exogenous expression of circSPINT2 was executed by transient transfection with pcDNA3.1(+) ZKSCAN1 MCS exon overexpression vector consisting circSPINT2 backsplice junction sequence (Ishola et al., 2022). Overexpression leads to a senescence-like state with enhanced adherence to cell culture flasks. OR4-OE and HOSiR-OE cells undergo significant changes, transitioning from a spindle fibroblast shape to an enlarged morphology (Appendix M). While, transfection efficiencies were assessed through qRT-PCR and data was calculated using $\Delta\Delta$ CT method between the control/empty vector group (EV) and overexpression group (OE). The qRT-PCR data in Figure 4.16 showed up-regulation of circSPINT2 expression in the overexpressed OR4 cell line (OR4-OE) compared to the control group (OR4-EV) with fold change of 4.5×10^5 . Similar overexpression effect was documented in HOSiR-OE cell line with 1.7×10^5 fold change against its control (HOSiR-EV) (Figure 4.17). SPINT2 expression in OR4-OE and HOSiR-OE in comparison to their control group (OR4-EV and HOSiR-EV) were not significant with respective p-values of $P=0.086$ and $P=0.06$. As such, circSPINT2 was successfully overexpressed in OR4 and HOSiR without any noticeable impact on the host gene, SPINT2 mRNA

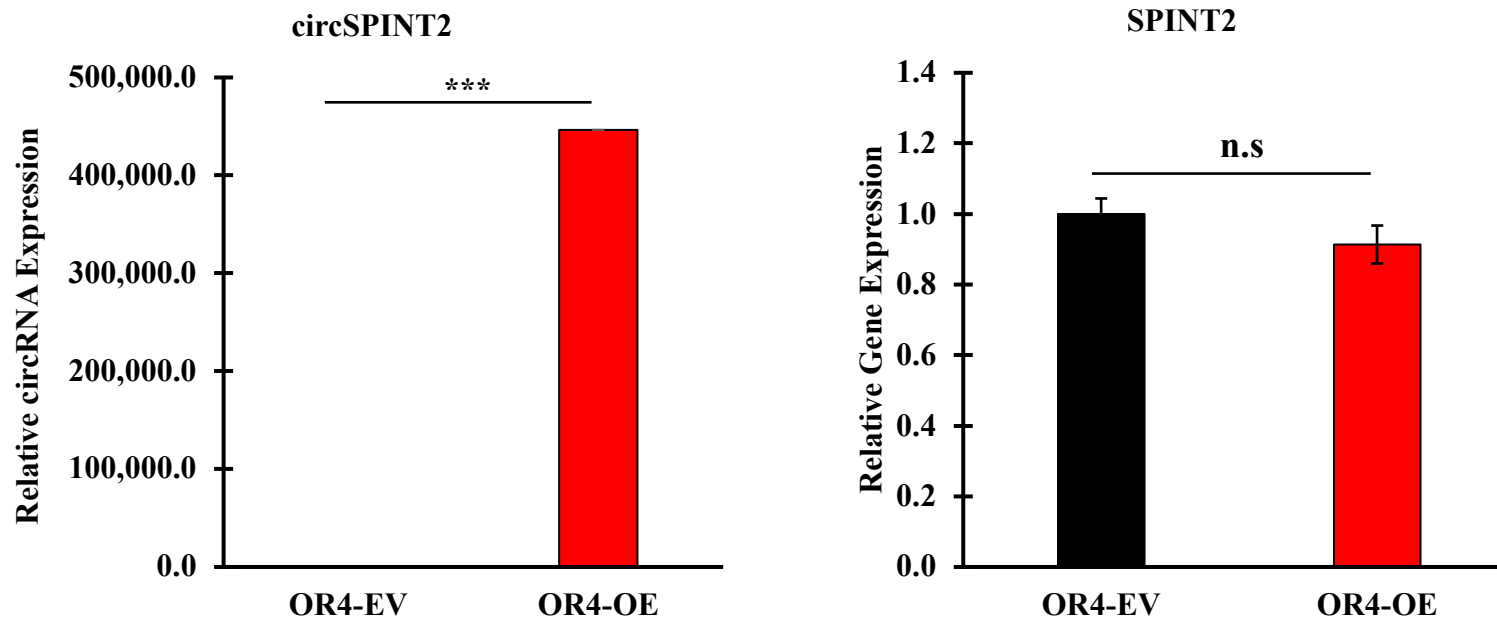


Figure 4.16 Overexpression of CircSPINT2 in OR4. Analysis of circSPINT2 overexpression treatment and its effect on SPINT2 expression via qRT-PCR in OR4. Data are presented as the mean \pm SEM (n = 3). Statistical differences are indicated with * for P < 0.05, ** for P < 0.01 and *** for P < 0.001 using paired t-test.

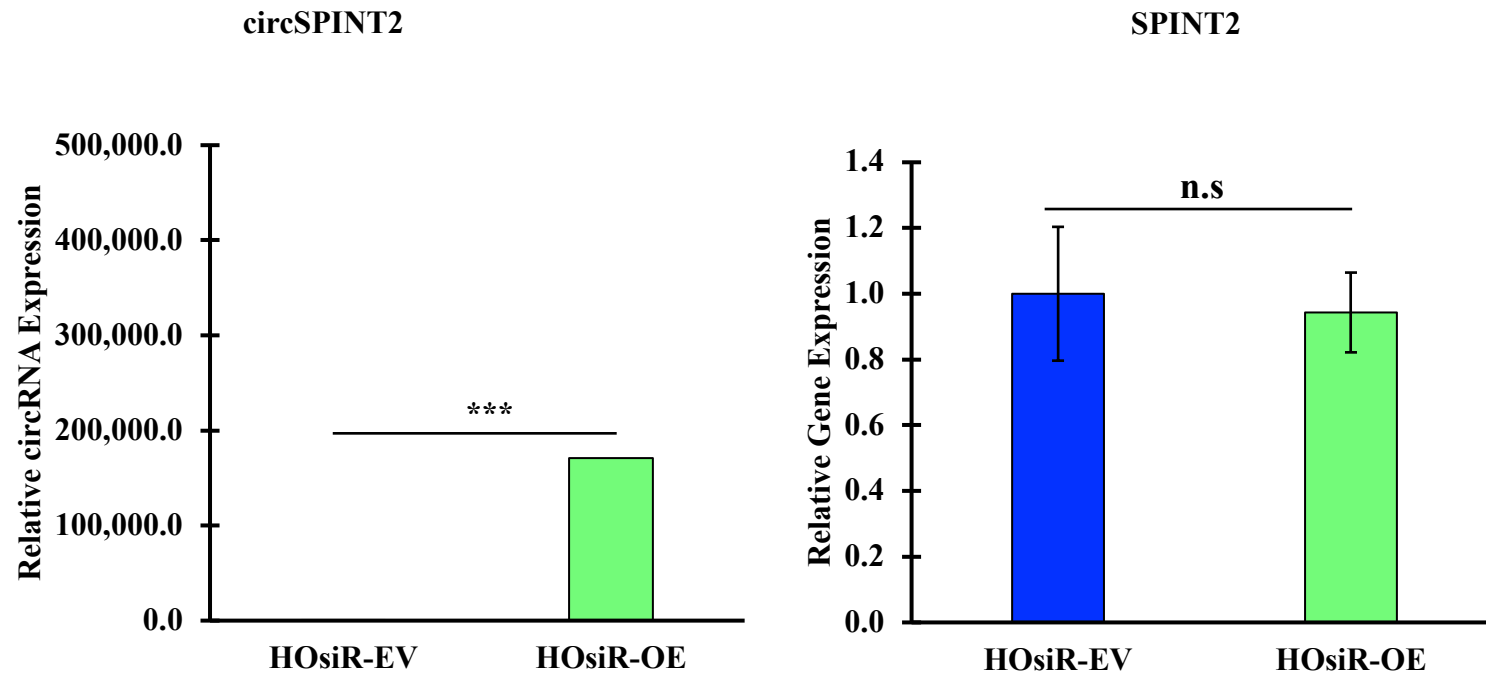


Figure 4.17 Overexpression of CircSPINT2 in HoSiR. Analysis of circSPINT2 overexpression treatment and its effect on SPINT2 expression via qRT-PCR in HOsiR. Data are presented as the mean \pm SEM (n = 3). Statistical differences are indicated with * for $P < 0.05$, ** for $P < 0.01$ and *** for $P < 0.001$ using paired t-test.

Thereafter, the effect of circSPINT2 overexpression in Osimertinib resistance and tumorigenic potential were investigated through Osimertinib sensitivity assay, tumoursphere formation capacity, and *in-vitro* migration potential. Drug sensitivity assay using AlamarBlue was employed to quantitate the cell viability under different dosages (0.001 μ M, 0.01 μ M, 0.1 μ M, 3 μ M and 10 μ M) of Osimertinib, inclusive of control treated with DMSO. Data showed that, overexpression of circSPINT2 resulted in lower survival rate of cells in both cell lines (OR4-OE & HOsiR-OE) compared to their respective empty vector controls (OR4-EV & HOsiR-EV). Consistently, the IC₅₀ values of OR4-OE (0.33 ± 0.07) and HOsiR-OE (0.45 ± 0.36) were relatively lower than the EV group (OR4-EV = 3.96 ± 0.37 , HOsiR-EV = 3.88 ± 0.13), suggesting increased drug sensitivity in OR4 and HOsiR cells by circSPINT2 overexpression (Figure 4.18).

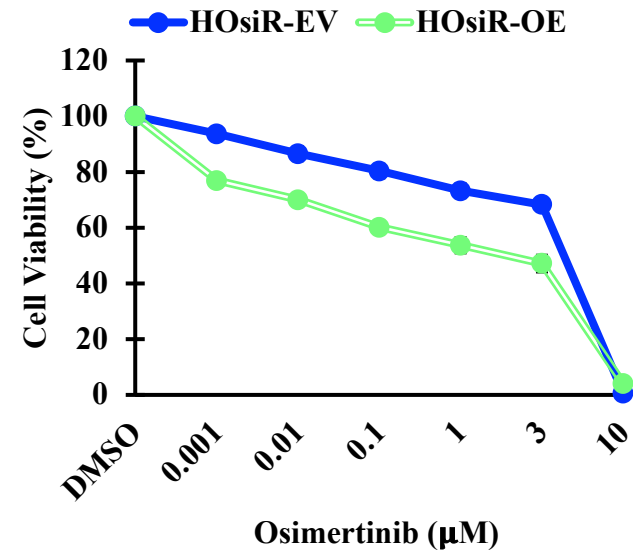
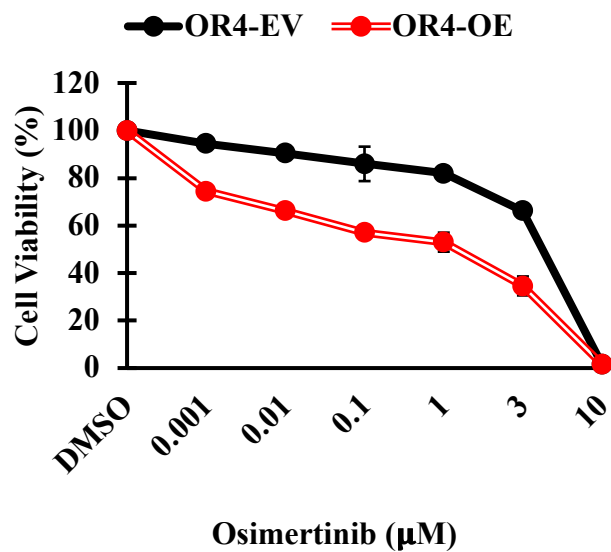


Table 4.2: IC ₅₀ (µM) – OR4 (EV/OE) and HOsiR (EV/OE)				
Cell Lines	OR4-EV	OR4-OE	HOsiR-EV	HOsiR-OE
IC ₅₀ (µM)	3.96 ± 0.37	0.33 ± 0.07	3.88 ± 0.13	0.45 ± 0.36

Figure 4.18 Osimertinib sensitivity assay (AlamarBlue) in overexpression system. Quantitative measurement of Osimertinib efficacy in overexpression cell lines at 48 hours. Data are presented as the mean ± SEM (n = 3). Statistical differences are indicated with * for P < 0.05, ** for P < 0.01 and *** for P < 0.001 using paired t-test.

Notably, colony formation assay corresponds similarly to drug sensitivity assay, by which low clonogenic survival observed in OR4-OE & HOsiR-OE following Osimertinib treatment. As represented in Figure 4.19, a dosage of 0.1 μM of Osimertinib was sufficient to inhibit the *in-vitro* expansion of OR4-OE and HOsiR-OE, similar effect observed in H1975 cell line. Upon circSPINT2 overexpression, tumourspheres derived from OR4-OE and HOsiR-OE exhibited a deviation from the typically round and densely packed morphology as observed in the control cells (Figure 4.20). Thus, inefficient tumoursphere formation ability exhibited by circSPINT2 overexpression cells indicated reduction of cancer associated stemness properties.

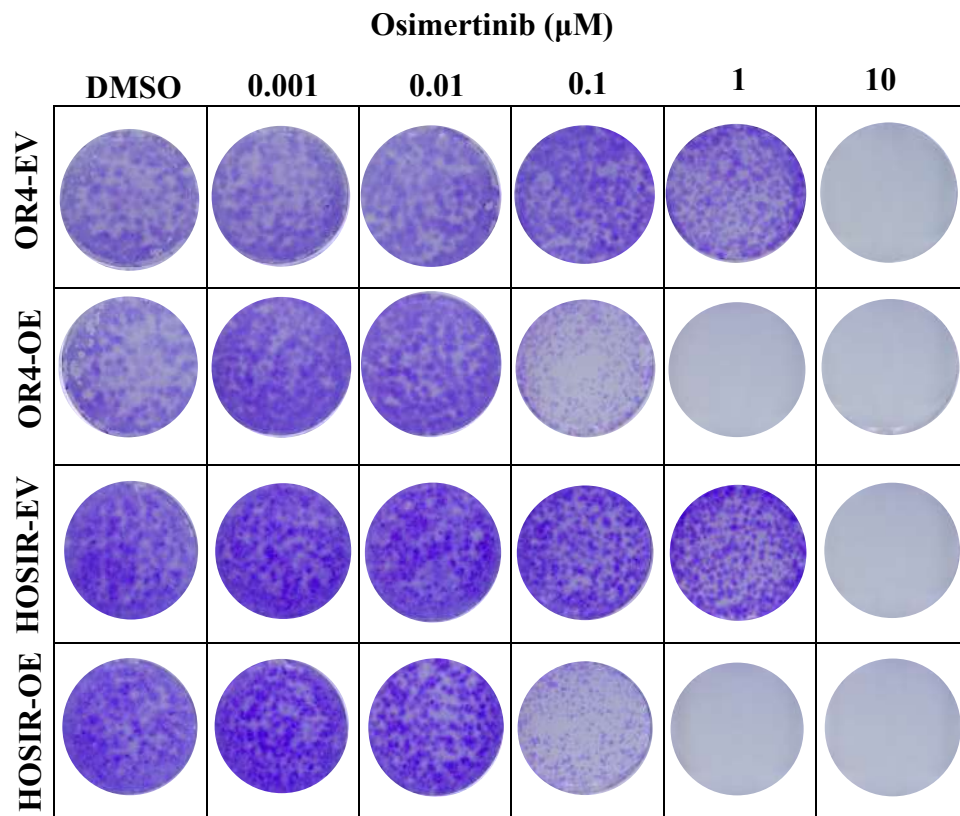


Figure 4.19 Qualitative measurement of Osimertinib efficacy via Colony formation assay in overexpression system. Osimertinib response in OE cell lines and the control/EV at 48 hours.

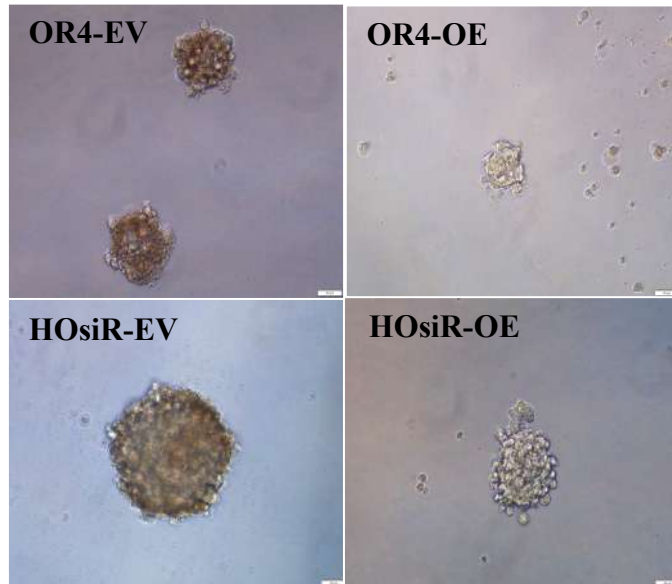


Figure 4.20 Qualitative observation of tumorigenic potential via tumoursphere formation assay in overexpression system. Tumorigenic potential in OE cell lines and the control/EV. Olympus inverted microscope, magnification: 20x.

Additionally, higher number of nuclei stained with Propidium iodide (PI) were observed in OR4-OE and HOsiR-OE indicating reduced migratory properties in both OE cells compared with their respective EV controls (Figure 4.21). Collectively, these results demonstrated that overexpression of circSPINT2 sensitised OR cells to Osimertinib treatment and decreased the tumorigenic potential *in-vitro*.

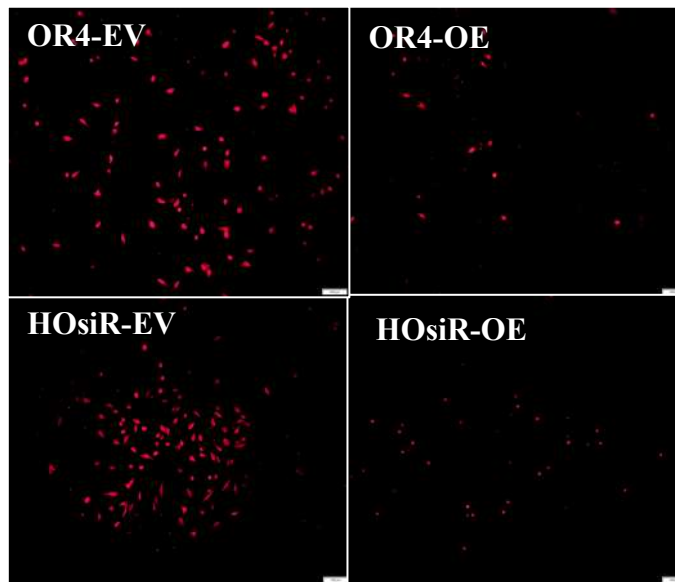


Figure 4.21 Qualitative observation of cell migration potential via migration assay in overexpression system. Migration potential in in OE cell lines and the control/EV at 16 hours. Olympus inverted microscope, magnification: 10x.

4.5 CircSPINT2 Knockdown in H1975 Cells Promotes Osimertinib Resistance and Enhances NSCLC Tumorigenicity *In-Vitro*

Given that circSPINT2 has demonstrated inhibitory properties *in-vitro* when overexpressed, a hypothesis has been formulated based on the observed phenomenon. The circSPINT2 overexpression data suggested that an opposite effect may be anticipated if circSPINT2 was knocked down, potentially leading to an increase in resistance to Osimertinib. Thus, loss of function assay was demonstrated to confirm the silencing effect of circSPINT2 in H1975 cell line using circSPINT2-lentiviral shRNA vector (PLKO.1-Puro). Two shRNA clones (shRNA1 & shRNA2) were constructed whereby both shRNA vectors were successfully knocked down circSPINT2 without interfering its host gene

expression. Knockdown of circSPINT2 transforms the morphology of H1975 cells from an epithelial to a spindle fibroblast shape in shRNA2, resembling the changes observed in OR cells (Appendix N). However, no significant morphological changes were observed in shRNA1. The qRT-PCR data representing transduction efficiencies in Figure 4.22 showed down-regulation of circSPINT2 expression in shRNA1 (FC = 0.24) and shRNA2 (FC = 0.18) compared to the control group with p-values $P < 0.05$. Even though shRNA1 and shRNA2 acquired almost similar transduction efficiencies, shRNA2 exhibited significant effect in the biological assays. Importantly, knockdown of circSPINT2 was achieved in H1975 without any noticeable impact on the host gene, SPINT2 mRNA.

Drug sensitivity assay indicated that knockdown cell lines (shRNA1 = 0.09 ± 0.01 and shRNA2 = 3.59 ± 0.2) led to a reduction in Osimertinib efficacy corroborated by the cell survival rate and IC_{50} values compared to PLKO.1 (0.03 ± 0.0). However, in line with the knockdown efficiency, shRNA2 cell line exhibited greater Osimertinib efficacy with higher IC_{50} values than cells transduced with shRNA1 (Figure 4.23).

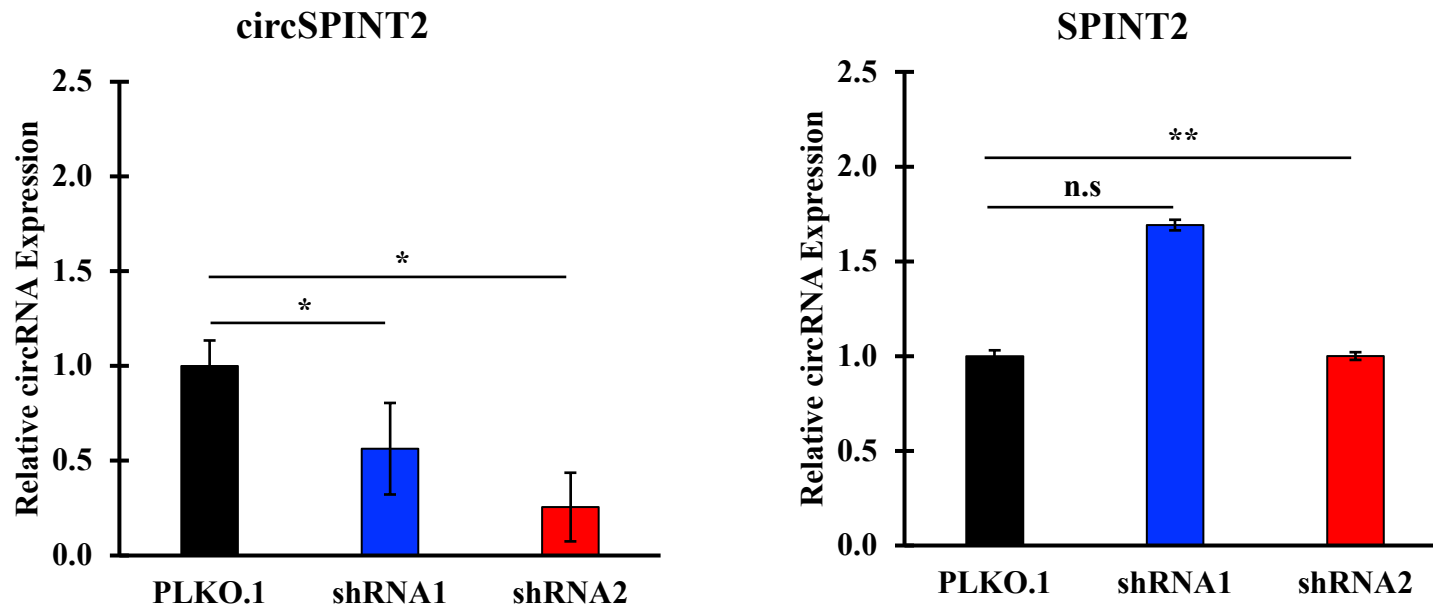


Figure 4.22 Osimertinib sensitivity assay (AlamarBlue) in knockdown system. Quantitative measurement of Osimertinib efficacy in knockdown cell lines at 48 hours. Data are presented as the mean \pm SEM (n = 3). Statistical differences are indicated with * for P < 0.05, ** for P < 0.01 and *** for P < 0.001 using paired t-test.

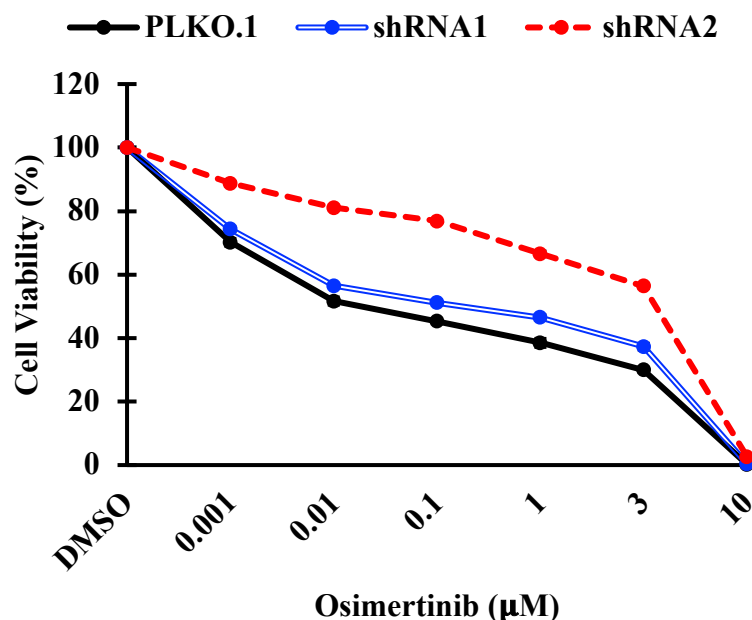


Table 4.3: IC₅₀ (µM) – PLKO.1, shRNA1 and shRNA2

Cell Lines	PLKO.1	shRNA1	shRNA2
IC ₅₀ (µM)	0.03 ± 0.0	0.09 ± 0.01	3.59 ± 0.2

Figure 4.23 Osimertinib sensitivity assay (AlamarBlue) in knockdown system. Quantitative measurement of Osimertinib efficacy in knockdown cell lines at 48 hours. Data are presented as the mean ± SEM (n = 3). Statistical differences are indicated with * for P < 0.05, ** for P < 0.01 and *** for P < 0.001 using paired t-test.

Similarly, knockdown of circSPINT2 enhanced clonogenic growth of cells under Osimertinib treatment, increased tendency to form tumoursphere, as well as increased migratory capacity. As shown in Figure 4.24, none of the Osimertinib dosages were effective on shRNA2 as compared to shRNA1 and control/PLKO.1. The Osimertinib efficacy observed in shRNA2 were similar to that of in OR4 and HOsiR cell lines. On another note, ShRNA2 cells were able to form rounded-shaped and compact tumourspheres indicatives of their tumorigenic potential (Figure 4.25). As shown in Figure 4.26, higher number of nuclei stained with Propidium iodide (PI) were observed in shRNA2,

resembling the invasive potential observed in OR4 and HOSiR. It has to be noted that in consistent with the better circSPINT2 knockdown efficiency, shRNA2 demonstrated superior effects in these functional assays than shRNA1. These results suggest that down-regulation of circSPINT2 induced Osimertinib resistance and encouraged tumorigenicity *in-vitro*.

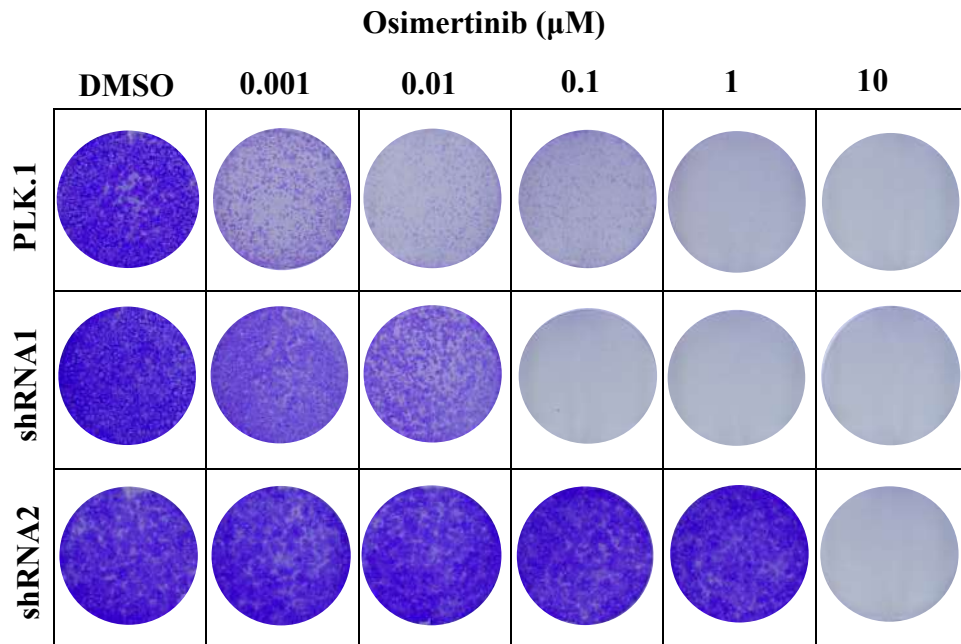


Figure 4.24 Qualitative measurement of Osimertinib efficacy via Colony formation assay in knockdown system. Osimertinib response in shRNA1, shRNA2 cell lines and the control/PLKO.1 at 48 hours.

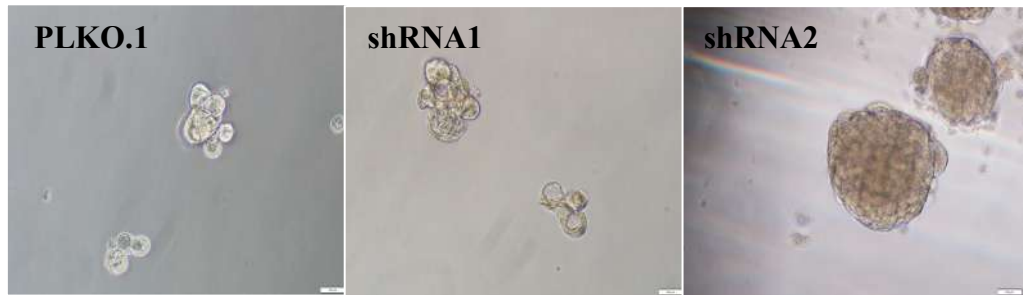


Figure 4.25 Qualitative observation of tumorigenic potential via tumoursphere formation assay in knockdown system. Tumorigenic potential in shRNA1, shRNA2 cell lines and the control/PLKO.1. Olympus inverted microscope, magnification: 20x.

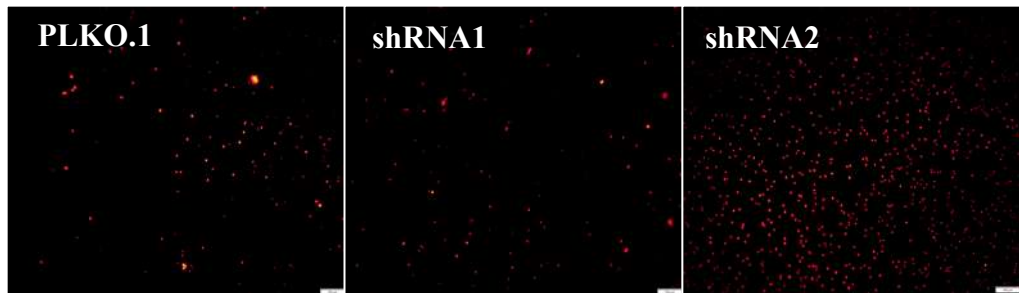


Figure 4.26 Qualitative observation of cell migration potential via migration assay in knockdown system. Migration potential in shRNA1, shRNA2 cell lines and the control/PLKO.1 at 16 hours. Olympus inverted microscope, magnification: 10x.

4.6 CircSPINT2 Promotes Apoptotic Stress in Response to Osimertinib Treatment

Alteration of apoptosis is one of the major causes that render cancer cells resistance against therapeutic treatments. Previous experiments revealed that high circSPINT2 expression confers sensitivity to Osimertinib treatment, as such the effect of circSPINT2 in apoptosis and its association to Osimertinib response were investigated. DNA fragmentation in apoptotic cells were quantified using TUNEL assay kit and apoptosis positive cell were stained with 7-Aminoactinomycin D (7-AAD) using flow cytometry. Percentage of apoptotic cell population were measured in parental (H1975, OR4, HOsiR), overexpression and knockdown cell lines (Figure 4.27). All cells were treated with 1.5 μ M Osimertinib for 48 hours while the control counterparts with DMSO respectively. As expected, when treated with Osimertinib, more than 50% of apoptotic population were detected in H1975 (57.5%, $P < 0.05$) but not in both OR cell lines OR4 (0.08%, $P = 0.19$) and HOsiR (0.03%, $P = 0.7$). In accordance to drug response assays, higher percentage of apoptosis was observed in Osimertinib-treated OE cells (OR4-OE = 39% , HOsiR-OE = 23%) when compared with their respective EV controls. On the other hand, knockdown of circSPINT2 decreased the apoptotic population induced by Osimertinib treatment, with a better extent in shRNA2 (0%, $P = 0.2$) cells compared to shRNA1 (30.8%, $P = 0.09$). The data also showed that DMSO has no effect on all cell lines. This results further explains the phenomenon of increased apoptosis in circSPINT2 overexpressed OR cells, and also indicates that circSPINT2 augments Osimertinib induced cell death in lung adenocarcinoma cell lines.

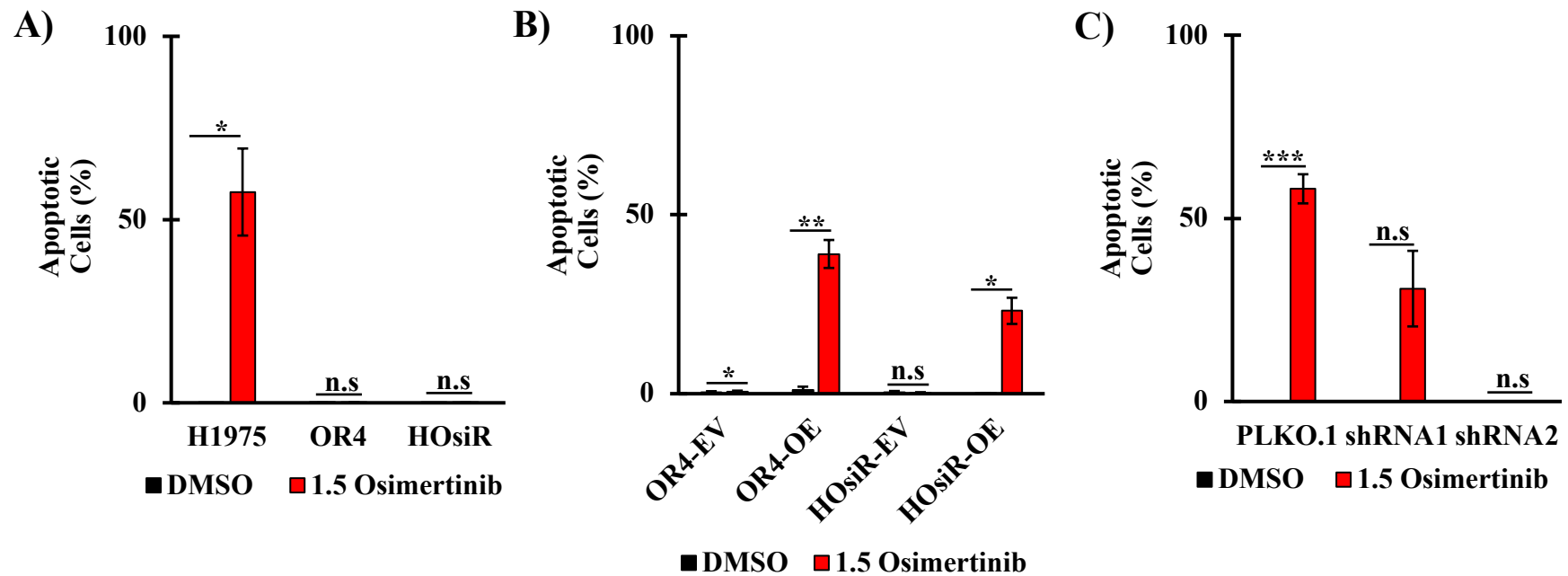


Figure 4.27 Apoptosis activation by circSPINT2 in Osimertinib resistant cells. Quantification of apoptotic cells by flow cytometry indicated in the (A) H1975, OR4, HOsiR, (B) overexpression (OR4-EV & OR4-OE) and (C) knockdown (H1975-PLKO.1, shRNA1 and shRNA2) group. Data are presented as the mean \pm SEM (n = 3). Statistical differences are indicated with * for P < 0.05, ** for P < 0.01 and *** for P < 0.001 using paired t-test.

4.7 CircSPINT2 Acts as a miR-1296a-3p Sponge to Upregulate RBP1 Expression

Sequestration of miRNA is one of the most common methods of circRNA to regulate gene expression (Hansen et al., 2013). To delineate the downstream mechanism of circSPINT2-mediated cell survival and drug sensitivity, the potential miRNA targets of circSPINT2 that may contribute to Osimertinib resistance and tumorigenesis were elucidated. Biotin-circRNA pull down assay was performed to determine circSPINT2 associated miRNA-mRNA regulatory network. Following incubation of 3' biotinylated-circSPINT2 complexes in OR4 cell lysates, labelled circSPINT2 was pulled down using streptavidin-coated beads. Thereafter, qRT-PCR analyses confirmed that circSPINT2 expression was higher in the circSPINT2-captured fractions, exhibiting a fold change of 1.82 ($P < 0.05$) compared to labelled control probe indicative of efficient biotinylated-circSPINT2 probe pull-down (Figure 4.28).

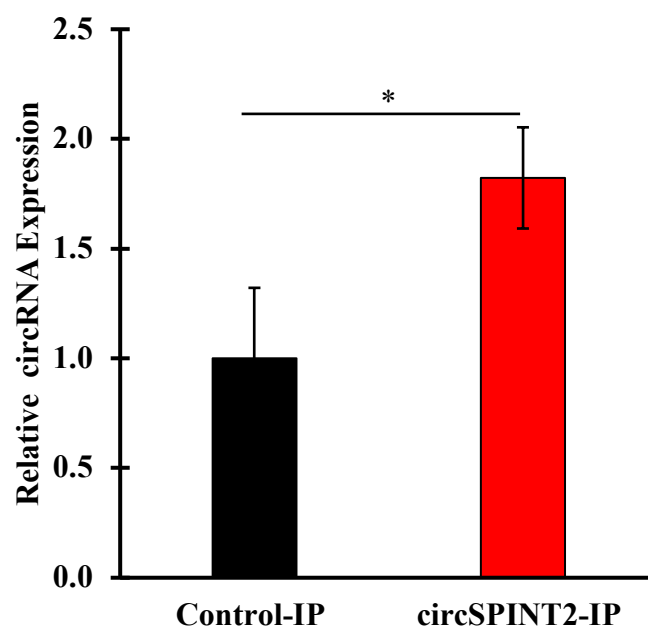


Figure 4.28 Pull-down assay using biotinylated-circSPINT2 probe. Pull-down lysates from OR4 lysates, validated by qRT-PCR. Data are presented as the mean \pm SEM (n = 3). Statistical differences are indicated with * for $P < 0.05$, ** for $P < 0.01$ and *** for $P < 0.001$ using paired t-test.

RNA isolated from pull-down lysates of circSPINT2-captured fractions (circSPINT2-IP) and labelled control probe were subsequently subjected to miRNA sequencing analysis. Comparative miRNA transcriptomic profile analysis were performed, aiming to identify the miRNAs sequestered by circSPINT2. Heatmap analysis exhibits differential miRNAs enriched in pull down lysates (Figure 4.29). Clustered heat map showed differential miRNAs expression of both up-regulation and down-regulation in circSPINT2-IP versus control-IP (fold change [FC] ≥ 2.0 ; $P < 0.05$). Approximately, 1961 of miRNAs were identified during transcriptomic analysis.

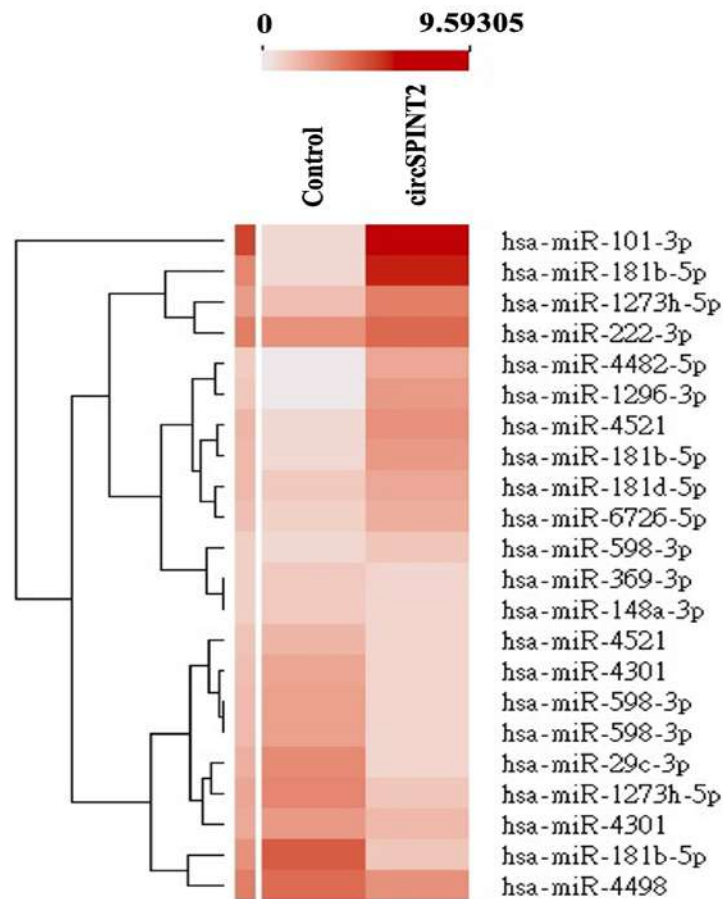


Figure 4.29 MiRNA transcriptomic profiling in pull-down OR4 lysates. Heat map shows expression clustering between the control-IP and the circSPINT2 biotinylated probe containing pull-down lysates.

In total of four miRNAs (down-regulated: miR-148a-3p, miR-29c-3p, up-regulated: miR-1296-3p and miR-101-3p) were validated from pull-down lysates. Notably, miR-1296-3p was consistently found to be highly expressed in OR4 (FC: 9.5, $P < 0.01$) and HOsiR (FC: 4.3, $P < 0.05$) as shown in Figure 4.30. Therefore, miR-1296-3p role in the sequestration by circSPINT2 was elucidated in the overexpression and knockdown system. Following this, the qRT-PCR analysis revealed a down-regulation of miR-1296-3p in cells overexpressing

circSPINT2, OR4-OE (FC: 0.2, $P < 0.001$) and HOSiR-OE (FC: 0.3, $P < 0.05$) while exhibiting an up-regulation shRNA2 (FC: 7.4, $P < 0.01$) in comparison to their respective control counterparts (Figure 4.31). A similar trend of miR-1296-3p down-regulation observed in Osimertinib-resistant cell lines (OR4, HOSiR), was also evident in shRNA2 cells. These findings suggest a potential role of miR-1296-3p as an oncomiR. Hence, the low expression of circSPINT2 in Osimertinib-resistant cells may lead to the insufficient sponging potential of circSPINT2 with miR-1296-3p, consequently resulting in an increase in its expression.

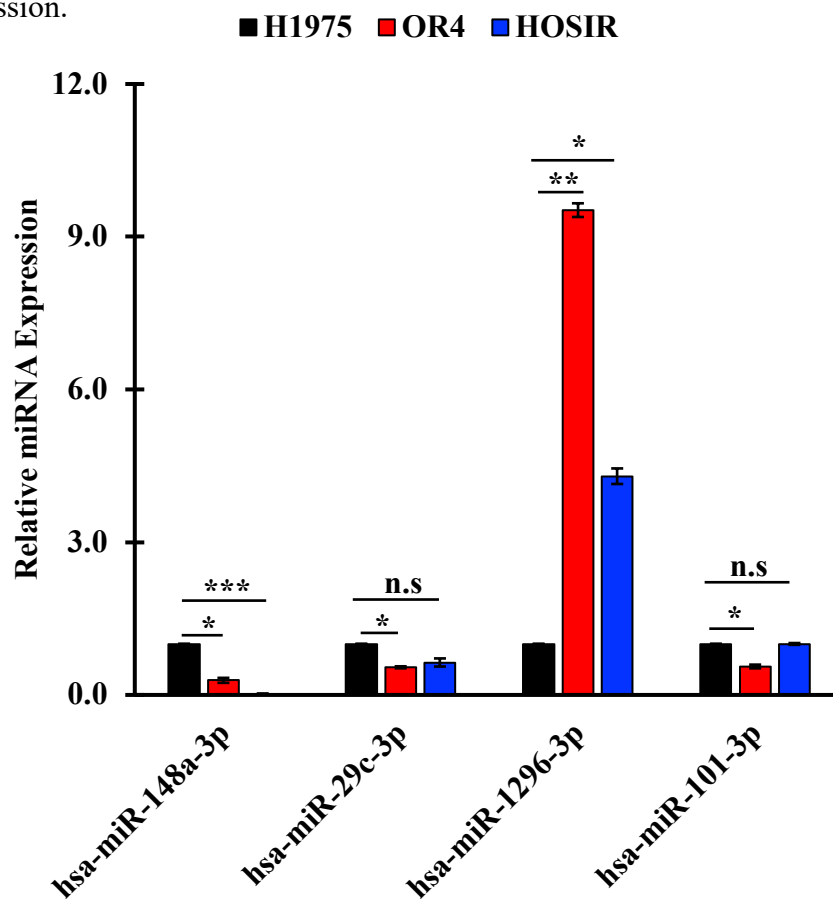


Figure 4.30 MiRNA validation via qRT-PCR in H1975, OR4 and HOSiR cell lines. Four miRNAs were selected from transcriptomic analysis, validated using qRT-PCR. Data are presented as the mean \pm SEM ($n = 3$). Statistical differences are indicated with * for $P < 0.05$, ** for $P < 0.01$ and *** for $P < 0.001$ using paired t-test.

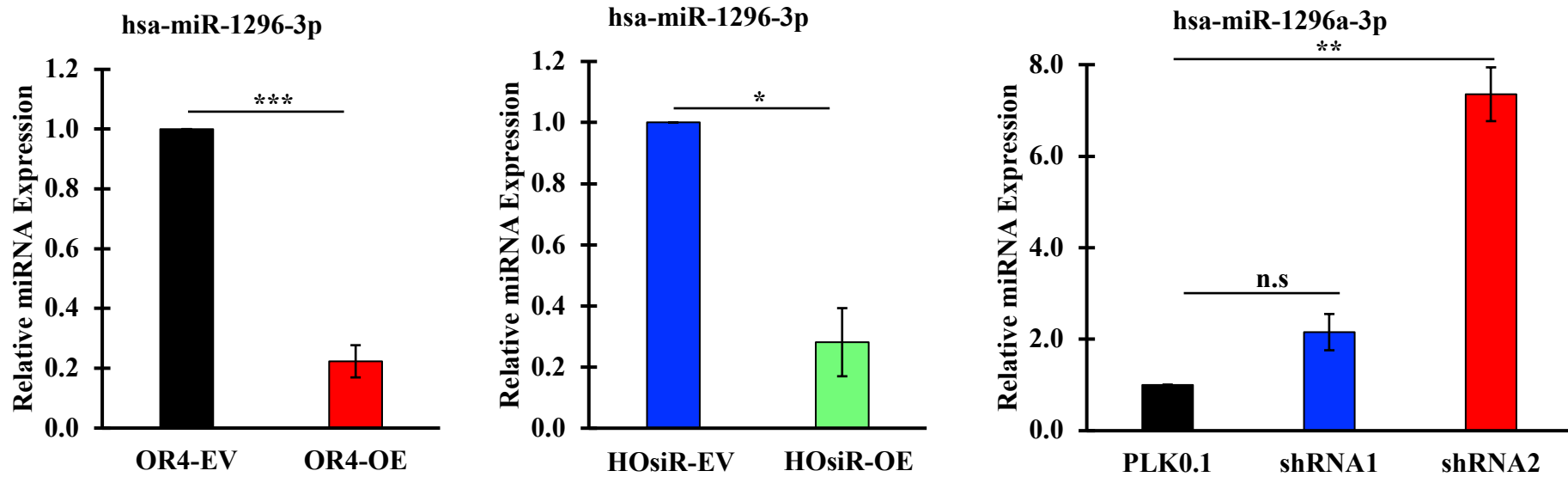


Figure 4.31 Hsa-miR-1296-3p in overexpression and knockdown cell lines. Hsa-miR-1296-3p were selected as miRNA target and validated using qRT-PCR. Data are presented as the mean \pm SEM (n = 3). Statistical differences are indicated with * for P < 0.05, ** for P < 0.01 and *** for P < 0.001 using paired t-test.

Subsequently, the potential downstream gene target of miR-1296-3p was predicted through In-silico analysis to establish circSPINT2/has-miR-1296-3p/mRNA involved in Osimertinib resistance. Two gene targets namely Retina-Binding Protein 1 RBP1 and High Mobility Group AT-Hook 2 (HMGA2) were predicted based on the analysis (figure 4.32). RBP1 was previously shown to hold tumour suppressive role in lung, colon, rectal and liver cancer (Ferlosio et al., 2020, Liu et al., 2021, Yokoi et al., 2017), whereas HMGA2 prominently reported as oncogenes in multiple cancer types (Xu et al., 2020, Zhang et al., 2019).

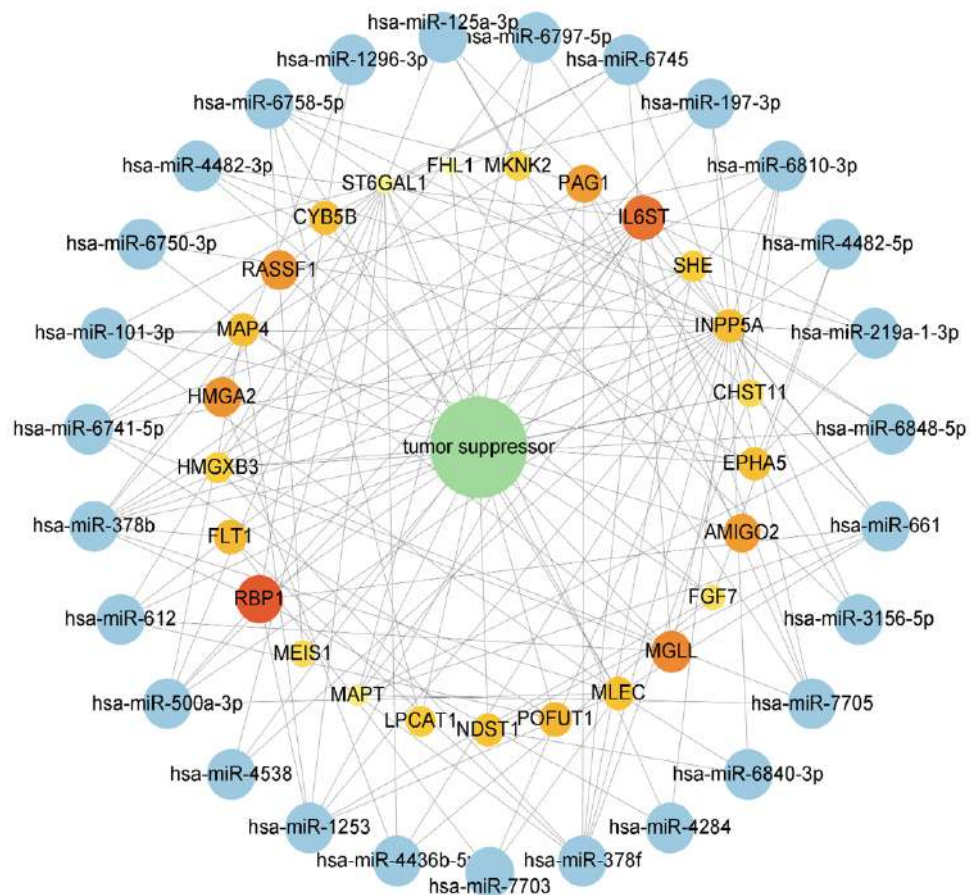


Figure 4.32 In-silico analysis. In-silico analysis of miRNAs and predicted hub genes.

Next, RBP1 and HMGA2 (Figure 4.33) expressions were validated in parental and OR cell lines. As expected, tumour suppressive RBP1 was down-regulated in OR4 and HOsiR cell lines at mRNA and protein levels. The data further implicated that miR-1296-3p, acting as an oncomiR in OR cells, potentially exerts inhibition effect on the expression of RBP1. Conversely, RBP1 was up-regulated in both OR4-OE (FC: 3.6, $P < 0.01$) and HOsiR-OE (FC: 6.0, $P < 0.05$) cells in comparison to their respective control counterparts (Figure 4.34). Also, RBP1 was significantly down-regulated in shRNA2 (FC: 0.14, $P < 0.001$) compared PLKO.1 and shRNA1 (Figure 4.34). Consistent trend of RBP1 down-regulation observed in Osimertinib-resistant cell lines (OR4, HOsiR) which was also evident in shRNA2 cells. Hence, an increase in tumour suppressive RBP1 expression occurred when a high level of circSPINT2 effectively sequestered miR-1296-3p, a phenomenon confirmed through both overexpression and knockdown systems. Western blot qualitative analysis on RBP1 protein expression further corroborated the qRT-PCR results (Figure 4.35). In general, the expression patterns of miR-1296-3p and RBP1 remained consistent across the parental cell lines, as well as in both the overexpression and knockdown systems.

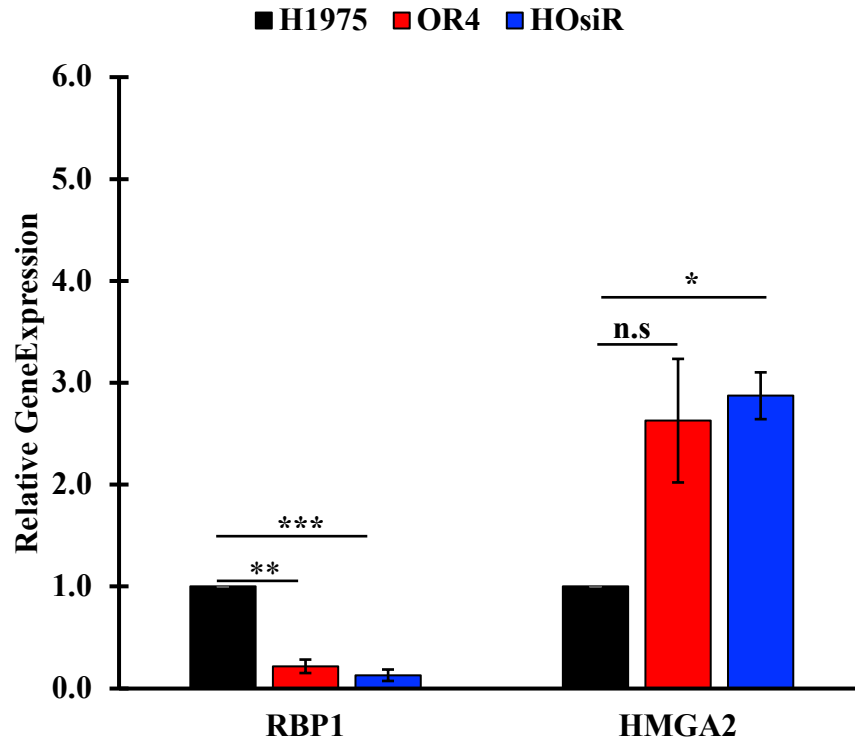


Figure 4.33 RBP1 validation via qRT-PCR in overexpression and knockdown cell lines. RBP1 and HMGA2 from in-silico analysis validated using qRT-PCR. Data are presented as the mean \pm SEM (n = 3). Statistical differences are indicated with * for P < 0.05, ** for P < 0.01 and *** for P < 0.001 using paired t-test.

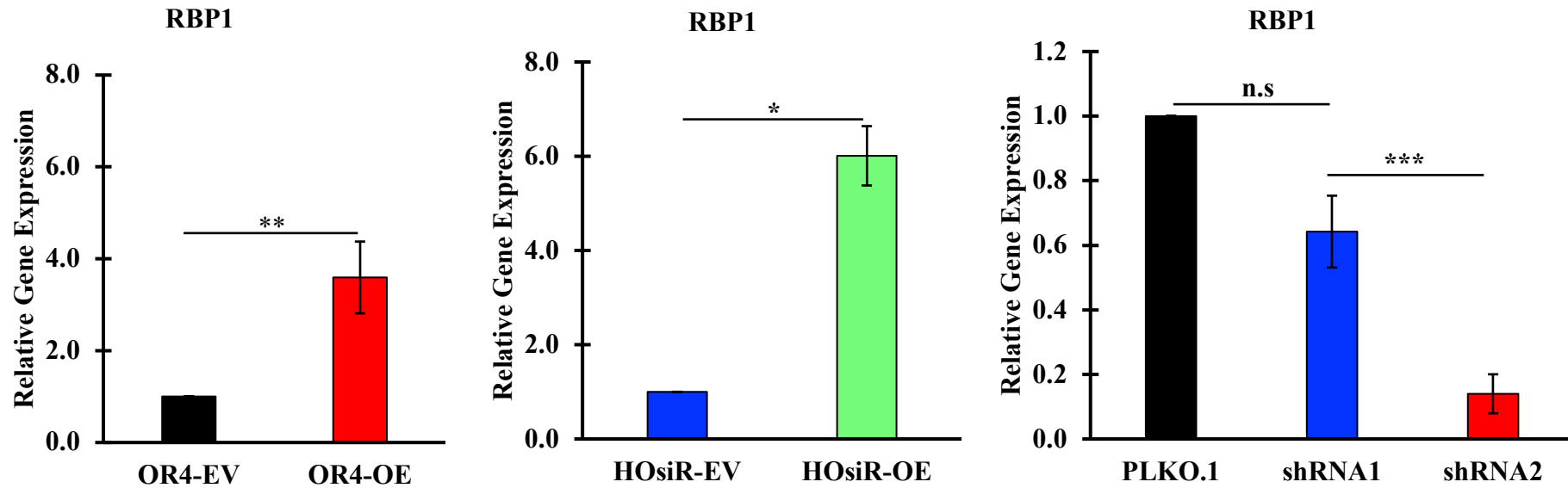


Figure 4.34 RBP1 in overexpression and knockdown cell lines. RBP1 as were selected as miR-1296-3p downstream target validated using qRT-PCR. Data are presented as the mean \pm SEM (n = 3). Statistical differences are indicated with * for P < 0.05, ** for P < 0.01 and *** for P < 0.001 using paired t-test.

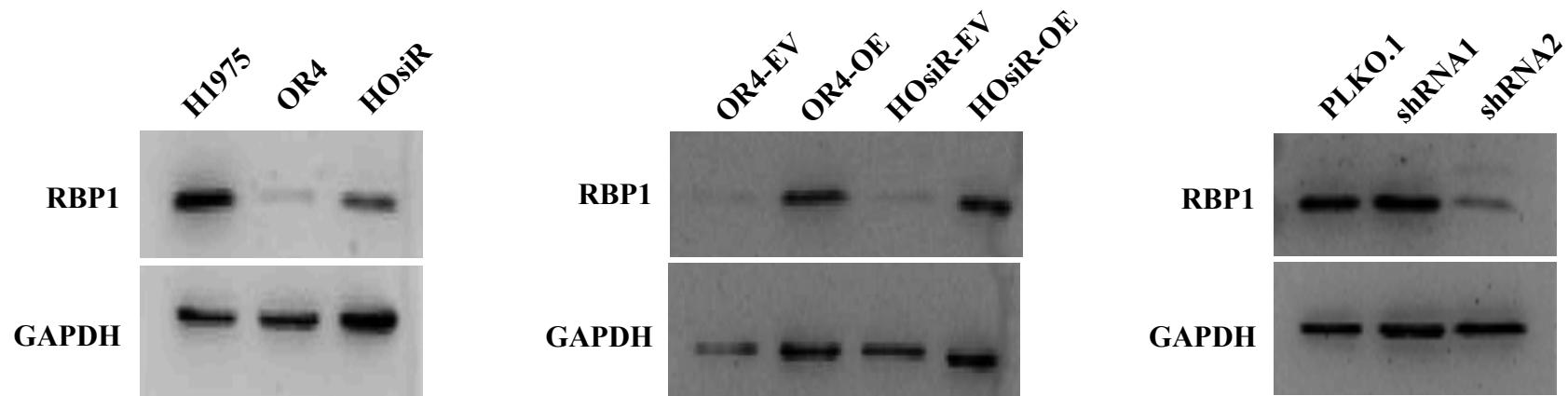


Figure 4.35 Qualitative analysis of RBP1 in overexpression and knockdown cell lines. Western blots showing RBP1 protein expression in parental cell lines (H1975, OR4, HosIR), OR cell lines overexpressing circSPINT2 (OE) and empty vector (EV) controls, and in H1975 cells with circSPINT2 knockdown (shRNA1, shRNA2) compared to vector control (pLKO.1).

4.8 Investigation of circSPINT2/Hsa-miR-1296/RBP1 Axis on Osimertinib-resistant *In-vivo* Xenograft Model

Nevertheless, the functional role of circSPINT2 in Osimertinib resistance were investigated in a xenograft tumour model. H1975 xenograft were first established via subcutaneous injection into both flanks of NOD-SCID mice. Once the tumours reached an average-size of 50mm³, mice were treated with 5 mg/ml Osimertinib, 5 times per week via oral gavage method. Control/vehicle group was established simultaneously and given 1xPBS instead (Figure 4.36). Monitoring of the tumour size showed that the xenograft tumour growth was halted or slightly regressed at the beginning of Osimertinib treatment. However, after day 21 the tumours exhibited sustained exponential growth, reaching a stage where the tumour xenografts were deemed to have developed resistance to Osimertinib. Xenograft tumours in the vehicle group were harvested upon reaching approximately 1000 mm³, while the tumours in treatment group were harvested at day 30 for further characterization (Figure 4.37).

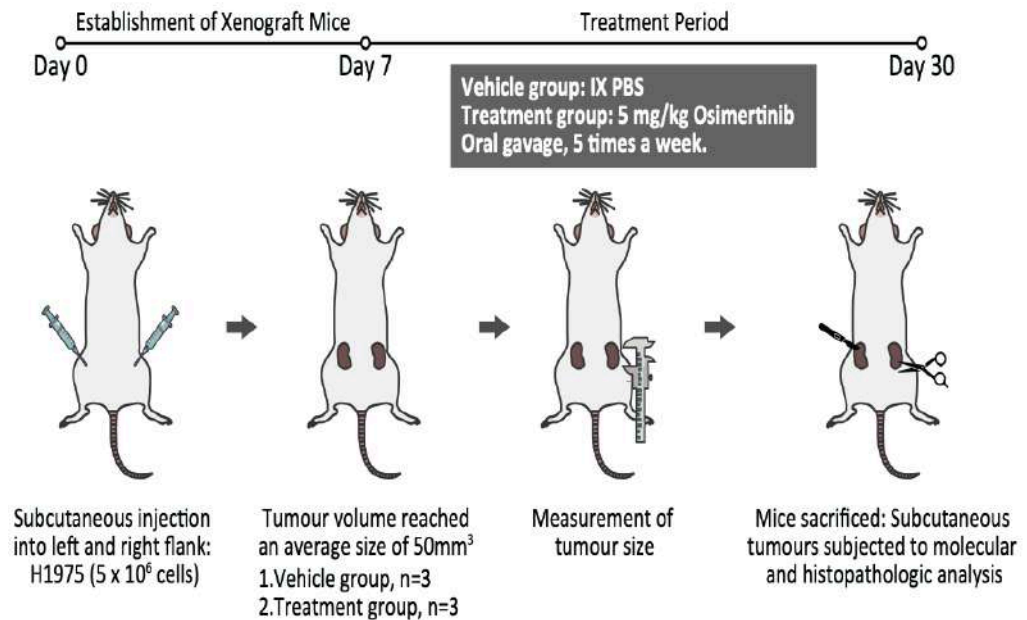


Figure 4.36 Osimertinib-resistance induced xenograft model. *In-vivo* Osimertinib-resistant H1975 xenografts established on day 7 by injecting the cells subcutaneously into the flanks of NOD-SCID mice on both sides. NOD-SCID mice (n=3) with tumours of average volume 50mm^3 was treated with Osimertinib at a concentration of 5mg/ml, administered five times per week. The control/vehicle group (n=3) received 1xPBS. On the 30th day, tumours were collected from the treatment group to conduct additional analysis and examination.

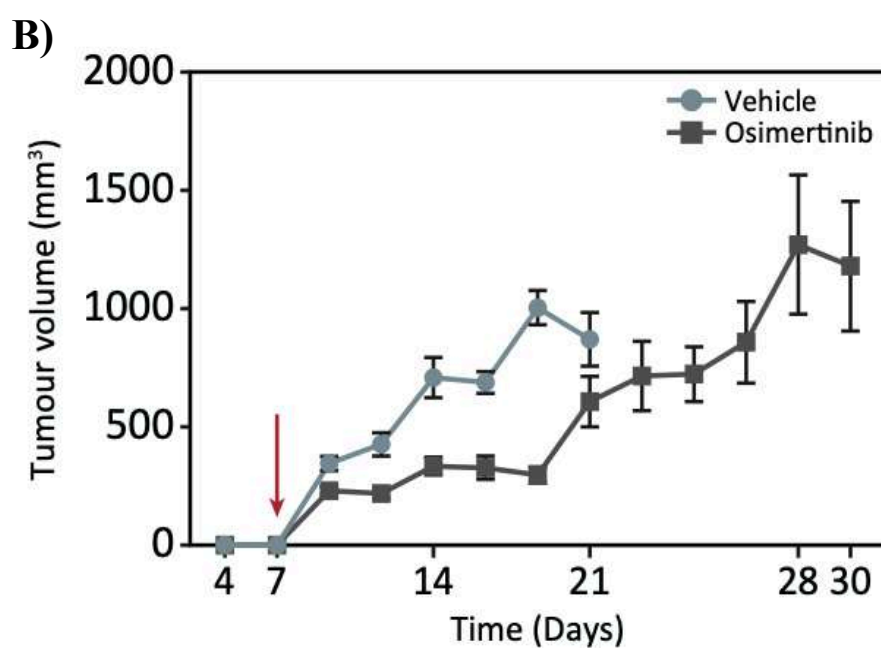
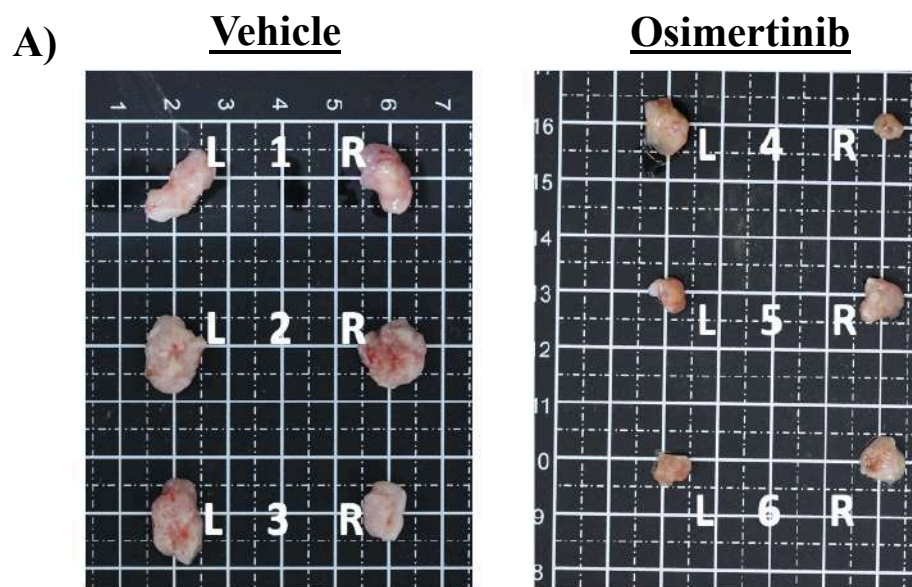


Figure 4.37 Tumour volume measurement in control and Osimertinib-resistance induced xenograft model. (A) Photographs of excised xenografts from vehicle (1-3) and treatment groups (5-6) from the left (L) and right (R) sides post-sacrifice. (B) Tumour growth dynamics in xenografts from the indicated experimental groups.

Overall, the qRT-PCR analysis of circSPINT2 (FC: 0.4, $P < 0.001$), hsa-mir-1296-3p (FC: 3.3, $P < 0.01$) and RBP1 (FC: 0.2, $P < 0.05$) expression levels in xenograft tissues indicated a downregulation of circSPINT2 and RBP1, followed by an upregulation of hsa-mir-1296a-3p in Osimertinib-resistant xenografts compared to the vehicle-treated control xenografts (Figure 4.38). These expression patterns aligned with the *in-vitro* expression profiles.

Subsequently, fluorescence in situ hybridization (FISH) assay using specific RNA probe designed to span circSPINT2's backsplicing junction was used to detect circSPINT2 in the xenograft tissues. The data revealed circSPINT2-cy3 localized in the cytoplasm and was found to be reduced in xenograft tumours of treatment group (Figure 4.39), suggesting a potential association with the resistant characteristics of the tissue.

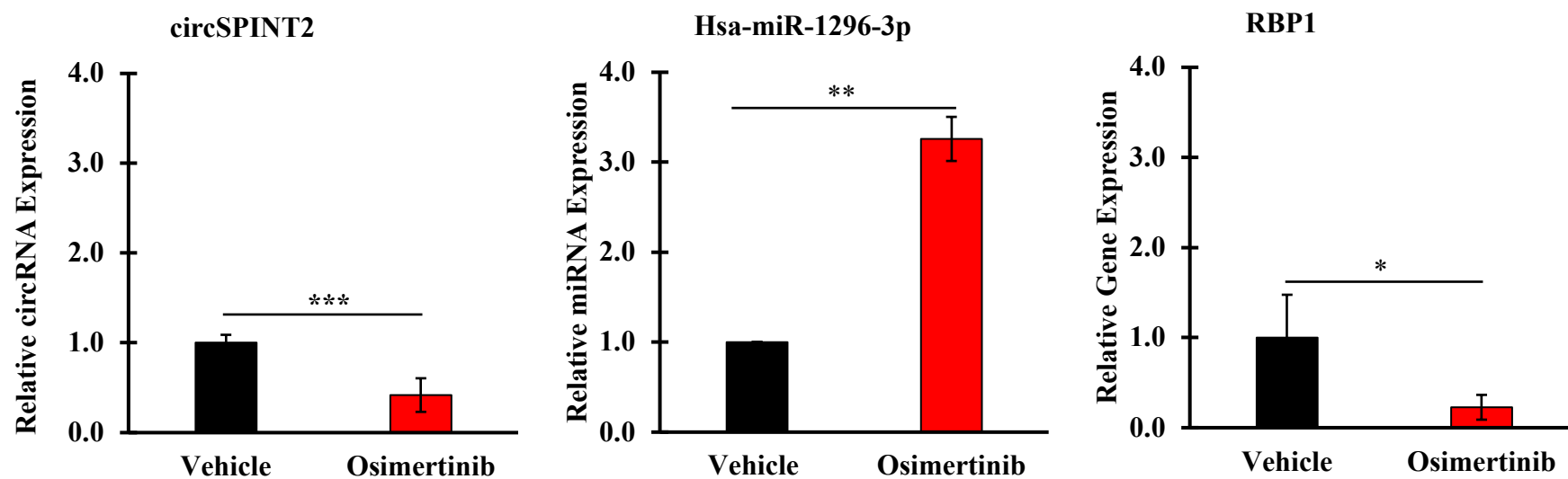


Figure 4.38 CircSPINT2/hsa-miR-1296-3p/RBP1 axis in animal model. CircSPINT2/hsa-miR-1296-3p/RBP1 expressions were validated using qRT-PCR in Osimertinib induced resistance xenograft. Data are presented as the mean \pm SEM (n = 3). Statistical differences are indicated with * for P < 0.05, ** for P < 0.01 and *** for P < 0.001 using paired t-test.

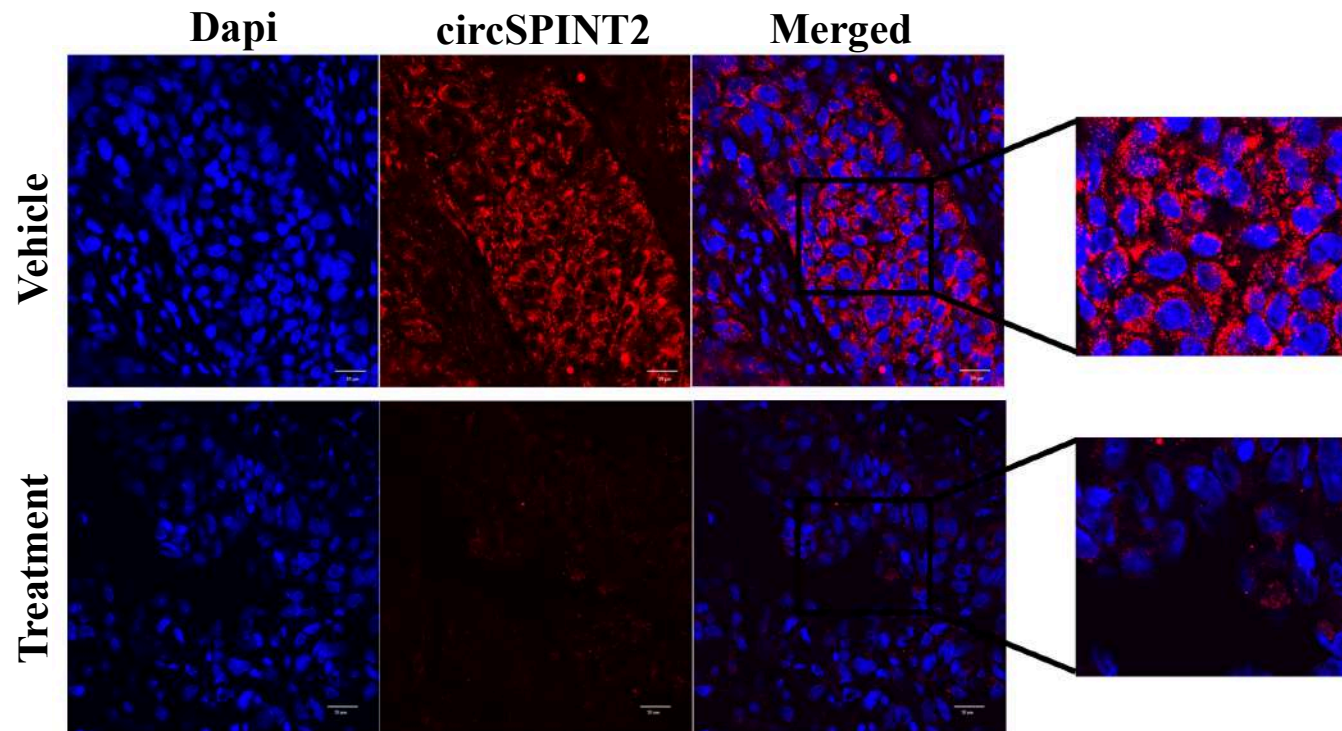


Figure 4.39 CircSPINT2 localization in xenograft tissues. FISH analysis showing circSPINT2 levels and cytoplasmic localization in subcutaneous tumours. Images captured using FV3000 confocal laser scanning microscopes from (Olympus, Japan) at 60x.

Similarly, qualitative analysis via western blot and chromogenic IHC analysis of RBP1 protein expression further confirmed that RBP1 was downregulated in the Osimertinib treated xenograft tumours (Figure 4.40). These results were consistent with *in-vitro* data. In light of the findings, it was observed that Osimertinib-resistant xenograft tumours displayed an elevated potential for drug resistance and a decreased rate of apoptosis. These findings indicated that the continuous administration of Osimertinib leads to the suppression of circSPINT2 expression, thereby contributing to the development of Osimertinib resistance. Ultimately, the results from this study revealed that re-establishment of circSPINT2 expression in the Osimertinib-resistant lung adenocarcinoma cells can enhance cellular sensitivity to Osimertinib, resulting in a decrease in tumorigenicity.

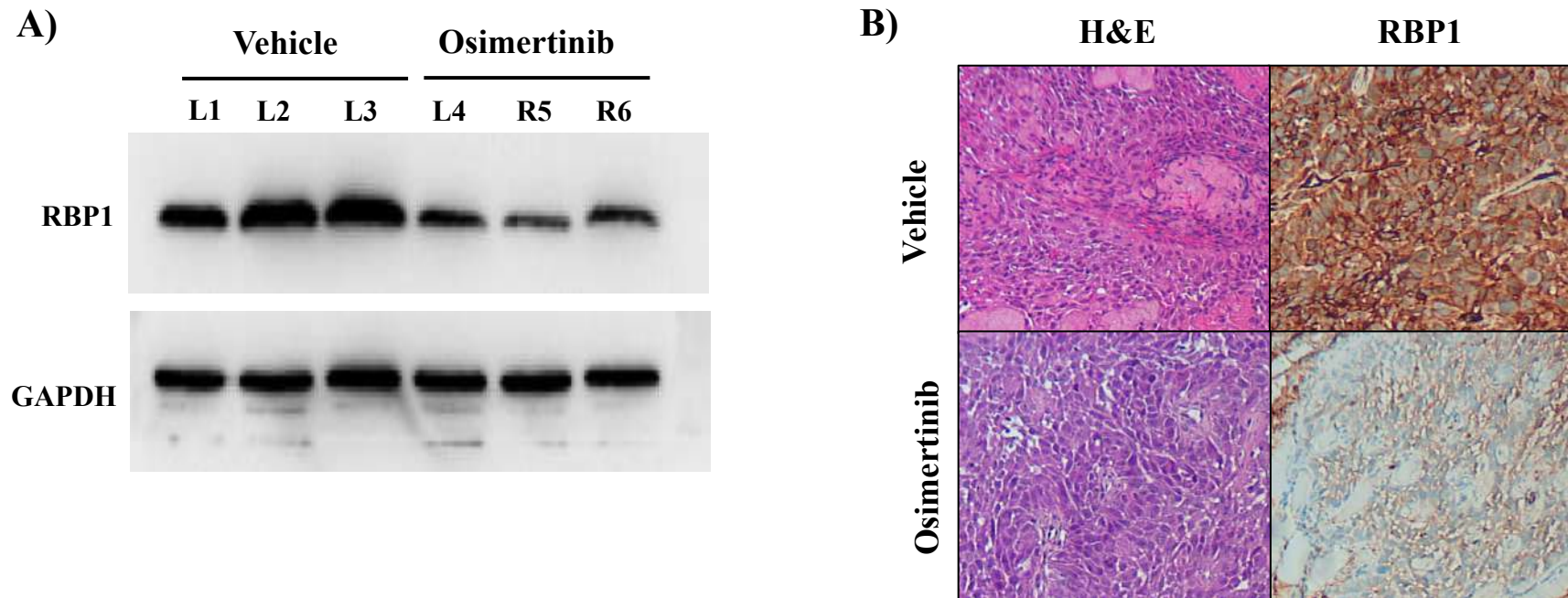


Figure 4.40 RBP1 protein expression in xenograft tissues. (A) Immunoblot analysis of RBP1 expression in vehicle- and osimertinib-treated xenografts, with triplicate samples for each group (L1-L6), GAPDH as the loading control. (B) IHC staining of RBP1 in vehicle- and Osimertinib-treated xenografts. Images captured using Olympus light microscope at 20x.

CHAPTER 5

DISCUSSION

5.1 Discovery of Circular RNA (circRNA) as Potential RNA Biomarker Associated with Mechanism of Resistance to Osimertinib

In this study, the aims are to establish circRNA profiles and to identify a novel circRNA involved in the mechanism of resistance to Osimertinib (a third-generation EGFR-TKI) in NSCLC. CircRNA, a unique biomolecule has been demonstrated to retain a stable circularized structure resistant to exonuclease degradation. Additionally, circRNAs also displayed a prolonged lifespan in both cellular and extracellular environment when compared to other RNA and protein biomolecules. Previous studies have reported the association between the abundance of circRNAs and their role in driving cancer progression and inducing resistance in multiple cancer types, including lung adenocarcinoma, a subtype of NSCLC. Notably, circRNAs have recently highlighted as a major focus of scientific interest, with exploration for their potential as RNA biomarkers, personalized medicines, and cancer vaccines (Ren et al., 2024, Goia et al., 2024).

In subsequent section of this study, a novel hsa_circ_0050818/circSPINT2 discovered through transcriptomic sequencing analysis, down-regulated in Osimertinib-resistant (OR) cell lines (Figure 4.8 and Figure 4.10). The downstream investigation revealed that overexpression of circSPINT2 holds tumour suppressive characteristics potentially confer

sensitivity to Osimertinib treatment via hsa-miR-1296-3p/RBP1 axis in both *in-vitro* and *in-vivo*. To date, this study was the first to demonstrate on tumour suppressive circRNA in Osimertinib-resistant lung adenocarcinoma cells and that circSPINT2 has not been reported to be involved in lung adenocarcinoma progression.

5.2 Osimertinib-resistant *In-vitro* Model

Emergence of unceasing EGFR-TKIs resistance reveals the complexity of NSCLC evolution in response to EGFR-TKI treatment at present. Even so the patients responded to 1st/2nd-generation EGFR-TKIs ultimately, they acquired EGFR T790M secondary mutation owing to selective drug pressure during the course of treatment (Takeda and Nakagawa, 2019, Ferro et al., 2024). Improvised treatment as shown in FLAURA clinical trial, demonstrated Osimertinib (3rd generation EGFR-TKI) was more efficacious in NSCLC patients with EGFR T790M-positive before they succumb to treatment resistance (Wang et al., 2021). Onset of tertiary mutations at various codons (C797S, L792, G796/C797, L798 and L718/G719) due to Osimertinib resistance in NSCLC patients highlights the need for continued advancements in EGFR-TKI development and underscored the need for novel therapeutic strategies (Shah and Lester, 2020, Rotow et al., 2024). A series of fourth generation EGFR-TKI such as EAI054, JBJ-04-125-02, CH7233163 and BLU-945 have been developed recently, targeting tertiary EGFR mutations, but there are no evidence on the clinical efficacies (Shi et al., 2022, Fu et al., 2022). Lack of reliable monitoring or predictive biomarkers that could be used to identify EGFR-TKIs

resistance remain to be a major hurdle to cures and affects patient's quality of life in lung adenocarcinoma patients.

Extensive search for biomarkers in NSCLC had revealed significant implications of circRNAs in tumorigenesis and treatment resistance. CircRNAs were denoted as a potential RNA biomarker as it was proven to be stable than linear mRNA and can be detected in patient's blood, cerebrospinal fluid, saliva, exosomes and urine samples (Zhang et al., 2018b, Wang et al., 2022b, He et al., 2019). Likewise, circRNAs were widely reported in multiple cancer types as a potential prognostic, predictive, monitoring and diagnostic biomarkers. Thus far, a number of circRNAs and its downstream biological processes identified in Osimertinib-resistant (OR) cell lines and patient tissue samples. These circRNAs (hsa_circ_0002130 (Ma et al., 2020), hsa_circ_0005576 (Liu et al., 2022), hsa_circ_0007312(Dai et al., 2022) and circKRT17(Ji et al., 2022)) were up-regulated in OR cells exhibiting oncogenic potential further promote NSCLC progression.

Additionally, a series of OR clones were established from H1975 (EGFR L858R/T790M) mutant cell line via stepwise dose-escalation method and limiting dilution (Verusingam et al., 2020), to be employed as OR *in-vitro* model. Existing studies showed that *in-vitro* stepwise dose-escalation method indeed reproducible, unswerving and economical compared to immediate high drug concentration exposure (Jiang et al., 2013, Yamaoka et al., 2017). In this study, H1975 was used to derived Osimertinib-resistant cell lines owing to the fact that this cell line carries double mutations (L858R and secondary mutation T790M) (Demuth et al., 2018, Sanchez Rios et al., 2019). Higher IC₅₀ values were achieved in the Osimertinib-resistant cell lines generated from H1975 indicating

acquired resistance to Osimertinib (Appendix L) (Figure 4.4). The OR cell lines established in this study were shown to bypass EGFR signalling pathways and exhibited EMT switch. The Western blot analysis showed that Osimertinib derivatives subjected to both DMSO/control and Osimertinib treatments exhibited activation of ERK and AKT but did not show activation of phosphorylated-EGFR (Appendix L). The findings suggested that the stepwise dose-escalation Osimertinib treatment was responsible for activating ligand-independent EGFR/non-canonical EGFR signalling pathways, as detailed in Appendix L. Typically, activation of ligand-dependent EGFR signalling was denoted as the primary event during the progression of NSCLC, leading to the transduction of its downstream pathways within RAS-RAF-MEK-ERK-MAPK and AKT-PI3K-PTEN-mTOR (Rao et al., 2017, Takács et al., 2020). The activation modulates various cellular processes, including cancer proliferation, migration, angiogenesis, enhanced motility and metastasis (Yuan et al., 2014). In a study by Zhang et al have reported that activation of HGF/MET signalling from ligand-independent EGFR signalling pathway initiates ERK and AKT signalling pathways contributing to EGFR-TKI resistance in NSCLC (Zhang et al., 2018a). In another study by Jafarnejad et al has also described the role of HGF/MET pathways in the activation of AKT and ERK in hepatocellular carcinoma (Jafarnejad et al., 2019). On another note, it was reported that Osimertinib resistance leads to rewiring of the AXL signalling pathway, activating ligand-independent EGFR signalling. AXL was implicated as a significant bypass signalling mechanism in Osimertinib resistance. Kim et al. demonstrated that Osimertinib-resistant induced in HCC827 cells resulted in the activation of both AXL and MET, followed by the deactivation of

phosphorylated-EGFR. Consequently, the expression levels of phosphorylated Akt and ERK were found to be elevated in HCC827 induced Osimertinib resistance (HCC827-osi) compared to its parental HCC827 counterpart (Kim et al., 2019). Even though, the Osimertinib-resistant cell lines derived in this study showed evident bypass signalling switch, subsequent in-depth analysis are required to elucidate the specific non-canonical pathways involved.

Furthermore, existing studies showed that acquired resistance to EGFR-TKI facilitates phenotypic transformation as such EMT transformation. OR cell lines derived in this study, exhibited morphological changes upon Osimertinib-resistance induction. Typical morphology of H1975 (Figure 4.1) cell line signified by an epithelial-like morphology, however exposure to increasing Osimertinib *in-vitro* induced a morphological transformation from epithelial into mesenchymal like-cells (elongated cell shapes and loss of tight junction). OR derivatives (OR3, OR4 and OR6) showed significant morphological transformation as shown in Figure 4.2. HOSiR cell line used in this study also showed evident morphological changes, as this cell line was derived from H1975 via *in-vitro* continuous Osimertinib treatment (Figure 4.3). Morphological changes driven by EMT is a well-defined phenomenon occur during drug resistance, often associated with poor prognosis in NSCLC patients (Poh et al., 2018, Li et al., 2020). Upon the acquisition of drug resistance properties and the transition to a mesenchymal-like phenotype, cancer cells acquired enhanced invasion and migration capabilities, ultimately progressing into metastatic cancer cells. Previous studies have shown successful EGFR-TKIs treatment restored cell adhesion molecules (EpCAM and E-Cadherin) expression substantially enhanced survival rate with favourable prognosis in NSCLC

patients (Pan et al., 2018, Huang et al., 2020). However in this study, loss of EpCAM and E-Cadherin protein expression were observed in OR cell lines indicating loss of epithelial like features (Appendix L). Also, high Vimentin expression supported the morphologic changes observed in the OR derivatives (Appendix L). Vimentin is an intermediate filament protein expressed in mesenchymal like cells and highly expressed in cancer cells promoting cell motility and metastasis. In fact, high expression of Vimentin has been correlated to poor prognosis in NSCLC patients (Richardson et al., 2018). Whereas, in a recent investigation by Suda et al. discovered, CD44 highly expressed in lung adenocarcinoma patient samples who acquired resistance to gefitinib or afatinib. The authors proposed that CD44 could serve as a predictor for EMT and function as a mesenchymal marker (Suda et al., 2018). Overall, loss of EpCAM and E-Cadherin, coupled with high expressions of Vimentin and CD44 in the Osimertinib-resistant (OR) cell lines derived in this study, aligned with existing research. These observation collectively suggest that successful induction of Osimertinib resistance has occurred in the OR cell lines (Figure 4.5 – Figure 4.7). Hence, these cell lines model were used to elucidate putative tumour suppressive circRNA, downstream miRNA as well as signalling pathways possibly associated with acquired resistance to Osimertinib. As such, circRNAs modulated in OR cell lines may represent the tumour evolution induced during prolonged drug selective pressure and associated with acquired resistance to Osimertinib (Ma et al., 2020b, Li et al., 2022).

5.3 Identification and Characterization of Putative CircSPINT2

Canonical circRNAs are products resulted from back splicing of pre-mRNAs wherein the splicing could take place at exons, introns or combination of both exon-intron (ElciRNA) (Eger et al., 2018, Xie et al., 2017, Hwang and Kim, 2024). The fusion of 5' splice donor site to upstream 3' splice acceptor forms circularized closed loop structure with no 5' cap and 3' poly A tail (Ebbesen et al., 2017). Relatively, circRNAs signified by unique back splice sequence which are distinguishable from its host gene counterpart (Panda and Gorospe, 2018).

CircSPINT2 identified via circRNA-seq in this study, was significantly down-regulated in the OR cell lines against its control, H1975 (Figure 4.8 - Figure 4.11). The putative circRNA originated from chr19:38778515-38779831 and was spliced at exon 4 – exon 3 of serine peptidase inhibitor, kunitz type 2 (SPINT2) gene (Figure 4.10). Backsplicing junction sequence of circSPINT2 with total sliced length of 114nt was confirmed by Sanger sequencing (Figure 4.12). CircSPINT2 was chosen as a target biomolecule in this study because its host gene, SPINT2 has been previously recognized for its role as a tumour suppressor in various cancer type. Linear mRNA, SPINT2 has been implicated as tumour suppressor in NSCLC and glioblastoma (Liu et al., 2019). SPINT2 gene was reported to suppress epithelial and mesenchymal (EMT), tumour growth, metastasis and invasion in these cancer types (Yamamoto et al., 2018). In glioblastoma, SPINT2 downregulation activates HGF/c-MET pathway further initiate tumour progression (Liu et al., 2019). The hypermethylation promoter region in SPINT2 gene leads to epigenetic silencing during

tumorigenesis (Liu et al., 2019). Consequently, the down-regulation of SPINT2 initiates the activation of the HGF/c-MET axis, thereby facilitating the progression of cancer. In a recent study by Ma, Zhiqiang, et al. reported that SPINT2 gene is a downstream target of Serine/Threonine/Tyrosine Kinase 1 (STYK1) gene in NSCLC. STYK1 was reported as EMT regulator that promotes cancer metastasis. The authors revealed that high expression of STYK1 inhibited SPINT2 expression whereas, overexpression of SPINT2 was able to reverse STYK1 impact on NSCLC progression *in-vitro* and *in-vivo* respectively (Ma et al., 2019). Consistent with existing evidence highlighting the role of SPINT2 in cancer progression, it was hypothesized that circSPINT2 might possess tumour suppressive functions, potentially serving as a replacement for SPINT2 as a biomarker in NSCLC patients exhibiting resistance to Osimertinib. In this study, the regulatory interactions between circSPINT2 and SPINT2 as well as its downstream pathways was not evaluated. In fact, the study primarily focused on elucidation of the functional role of circSPINT2 involved in mechanism of resistance to Osimertinib inclusive of miRNA sponging and its indirect mRNA target.

On another note, circSPINT2 discovered in this study was characterised for its stability against exonucleolytic degradation (RNase R) (Figure 4.13) and Actinomycin D treatment (Figure 4.14). Exonuclease enzyme known to digests all linear RNA forms with a 3' single- stranded region of greater than 7 nucleotides or otherwise with Poly(A) tail (Pandey et al., 2019). However, due to circularized structure of circRNA without 5' end cap and a 3' end poly(A) tail, confers protection against enzymatic degradation by RNase R exonucleases. Studies have shown circRNAs exist in plasma blood over 48 hours than linear

counterpart with approximately 10 hours (Meng et al., 2017). In one of the pioneering study by Pandey et al. have demonstrated a method for circRNA enrichment, by using RNase R treatment followed by polyadenylation and poly(A)⁺ RNA depletion (RAPD) for improving circRNA sequencing and analysis outcome. Subsequently, ample of studies have shown circRNA resisting RNase R enzymatic degradation. In a recent study conducted by Guan, Sisi, et al., an oncogenic circular RNA WHSC1, identified in NSCLC, exhibited resistance to RNase R treatment, in contrast to its linear counterpart. These findings underscore the circRNA's intrinsic stability against RNase R degradation (Guan et al., 2021). In another investigation by Wang, Yunfei, et al., revealed that circCAMSAP1 identified in NSCLC tumour tissues displayed superior stability compared to its linear counterpart CAMSAP1. Their qRT-PCR analysis showed that the circCAMSAP1 expression remained unchanged prior to RNase R digestion, in contrast to linear CAMSAP1 (Wang et al., 2022a).

Also, the stability of circSPINT2 was confirmed through Actinomycin D treatment. Actinomycin D is an established method known to inhibit gene transcription (Hama Faraj et al., 2024). Generally, during the transcription process, Actinomycin D inhibits DNA-dependent RNA polymerase activity such as DNA replication and RNA elongation alongside with activation of caspase enzymes (Ferreira et al., 2020). Conversely, upon inhibition of new transcription by Actinomycin D, circRNA maintains its stability throughout the course of treatment, whereas linear RNA undergoes degradation. Growing number of studies have demonstrated the effect of Actinomycin D on circRNA stability including in a study exemplified by Chi, Yongbin, et al. The authors showed that circ_103820 identified in NSCLC retained its stability of exceeding

24 hours upon Actinomycin D treatment. In contrast, the linear transcript displayed a half-life ranging from 4 to 8 hours (Chi et al., 2021). Similar to that of the existing studies, circSPINT2 also exhibited a half-life over 24 hours while its linear RNA only stable up to 4 hours (Figure 4.14). These findings implicated that circSPINT2 indeed resistant to both RNase R digestion (Figure 4.13) and Actinomycin D treatment compared to its linear form SPINT2 and subsequently confirmed as a stable circularized transcript.

The detection of circRNAs was not only confined to tissues but also have been significantly identified in bodily fluids. Previous studies have highlighted the presence of circRNAs in human plasma blood, platelets, cerebral spinal fluids (CSFs), urine, saliva and even detected in exosomes, suggesting their potential as biomarkers in liquid biopsies (Zhou et al., 2021, Wang et al., 2022b, Zhang et al., 2023, Lee et al., 2024). Existing studies also disclosed that exosomes encapsulate circRNAs at higher concentrations than those found in the cytoplasm, facilitating their transport to extracellular environment and crosstalk between adjacent or distant cells (Li et al., 2015, Banerjee et al., 2024). Previous study by Luo YH, et al., have proven hsa_circ_0000190 secretion from lung cancer cell lines into external condition medium was consistent in patients plasma samples (Luo et al., 2020). In a separate study, Peng, Ziyi, and colleagues documented a significant down-regulation of circTOLLIP in NSCLC tumour tissues and cell lines. The authors demonstrated that circulating circTOLLIP displayed lower expression in the blood samples from NSCLC patients compared to healthy patients and those with benign lung disease. The consistent circTOLLIP expression pattern in both tumour tissues and blood samples underscored its potential as a valuable (Peng et al., 2021) biomarker in liquid

biopsies. High expression of circRNA-002178 in exosomes from the serum of LUAD patients was identified by Wang J. and group. The authors revealed that circRNA-002178 promotes PDL1 via sequestering miR-34 in LUAD samples. As such, the authors also suggested that circRNA-002178 encapsulated within exosomes could be incorporated into T cells to modulate PD1 expression via sequestering miR-28-5p instead. Therefore, circRNA-002178 holds potential applications as a tumor biomarker and therapeutic target, with the to promote both PD1 and PDL1 expression in cancer and immune cells (Wang et al., 2020a). In this study, consistent circSPINT2 expression pattern as in OR cell lines was also detected in the condition medium of OR cells *in-vitro* (Figure 4.15). This data further confirmed that circSPINT2 can be secreted into the extracellular environment. Expression level of circSPINT2 in OR patient's liquid biopsies worth to be explored in clinical settings, particularly in the subsequent phases of the study involving patient blood plasma or exosomes.

5.4 Biological Functions Assessment of CircSPINT2

Given the significant down-regulation of circSPINT2 in Osimertinib-resistant cells, its functional role was further investigated through both overexpression and knockdown systems (shRNA). In this study, plasmid vectors were employed to perform the biological functional assays. As for circSPINT2 overexpression plasmids, it is crucial to incorporate exons forming the circular RNA structure which was flanked by Alu sequences (Obi and Chen, 2021, Choi and Nam, 2024). Alu sequences act as a repeat elements, promoting the circularization of the expressed transcript by bringing the splice sites into close

proximity, thereby facilitating the formation of a backsplicing-like structure (Wilusz, 2015). Besides, available studies showed that overexpression plasmid vectors designed for circRNA enable to mimic the natural biogenesis pathway, generating both linear and circular RNAs during splicing events (Liu et al., 2018). Whereas, the delivery of circRNA plasmid vectors for both overexpression and knockdown has been shown to be efficient using transposon-based methods and constructs incorporated with the Lentiviral for genomic integration (Mecozzi et al., 2022, Feng et al., 2023). As such, ShRNA plasmid vectors for knockdown were chosen in this study due to its stable integration upon transduction while pcDNA3.1(+) ZKSCAN1 MCS Exon vector with Alu repeats was constructed to overexpress circSPINT2 (Liang and Wilusz, 2014, Kelly et al., 2024). After delivering the circSPINT2 plasmids into the cells, confirming the circRNA to linear RNA ratio and validating the accurate formation of the back-splice junction (BSJ) before biological assays and downstream analysis are crucial (Mecozzi et al., 2022). Likewise, in this study, the data implicated that there were no notable changes in SPINT2 expression following both the overexpression and knockdown of circSPINT2 (Figure 4.16 & Figure 4.17) (Figure 4.22).

Thereafter, the overexpressed and knockdown products were subjected to biological assays. Functional role of circSPINT2 were explored via drug sensitivity assay, tumour sphere formation and migration potential *in-vitro* to confirm its association with mechanism of Osimertinib resistance. Results showed, circSPINT2 plays an important role as tumour suppressive circRNA by improving sensitivity to Osimertinib, suppressing *in-vitro* proliferation and promotes apoptosis. The findings implicated that overexpression (Figure 4.18 – Figure 4.21) of circSPINT2 confer sensitivity to Osimertinib and reduced

tumorigenic potential while knockdown of circSPINT2 indicated opposite effects (Figure 4.23 – Figure 4.26).

There are now ample of studies implicated the role of tumour suppressive circRNAs in cancer hallmarks, even though not directly associated with EGFR-TKI resistance (Dawoud et al., 2024, Zhou et al., 2024). In a study exemplified by Wei S, et al., high expression of circPTPRA was shown to regulate cellular adhesion by repressing EMT via miR-96-5p and its downstream tumour suppressor gene, RSSF8 (Wei et al., 2019). Another study by Wang Y, et al. demonstrated, overexpression of circSLC7A6 elevated a series of downstream tumour suppressor gene targets of miR-21 expressions, also inhibited invasion and proliferation ability in NSCLC cell lines (Wang et al., 2020b). In further evidence, Nan A, et al. have implicated circNOL10 function in apoptosis activation. The authors have shown overexpression of circNOL10 increased expression of pro-apoptotic proteins further attenuated proliferation and cell cycle progression in lung adenocarcinoma cells (Nan et al., 2019). Prior to apoptosis protein expression, high apoptotic population were quantified in circSPINT2 overexpressed OR cells using TUNEL assay by dead cell exclusion staining method (Figure 4.27). The data corroborated with the *in-vitro* AlamarBlue and colony formation assays.

5.5 CircSPINT2 as miRNA Sponge

CircRNAs exert multiple biological function to regulate protein and gene expressions in cancer pathogenesis. As such circRNA act as a competitive endogenous RNA (ceRNA) by sequester miRNAs away from their target

mRNAs to modulate gene expression (Yang et al., 2022). The association of circRNA/miRNA/mRNA interactions according to competitive endogenous RNA (ceRNA) mechanism occur when the circRNA showed an increased expression with a concurrent decrease in the expression of targeted miRNAs and an up-regulation in the expression of downstream mRNAs. In contrary, decreased expression of circRNA is anticipated to correspond with high expression of miRNAs and a decrease in the expression of downstream mRNAs. This pattern exhibited the regulatory interplay among circRNA, miRNAs, and mRNAs, elucidating the potential regulation. In this study, biotinylated affinity pull-down assays played a crucial role in uncovering the regulatory functions of circSPINT2 in modulating the activities of hsa-miR-1296-3p (Figure 4.28 & Figure 4.29) consequently influencing the post-transcriptional processes of downstream mRNA (Yang et al., 2021, Liu et al., 2021b). Typically, the underlying principle of the pull-down assay involves the use of designed biotinylated antisense circSPINT2 binding site junction (BSJ) engineered probe to selectively recognize the binding site of the target miRNA (Liu and Chen, 2022). Therefore, by sequencing the miRNAs present in the biotinylated-circSPINT2 probe pull-down lysates, hsa-miR-1296-3p was identified and could be potentially sequestered by circSPINT2 (Figure 4.28 & Figure 4.29). Several studies have reported conflicting results and have suggested that hsa-miR-1296-3p may have tumour suppressive effects cancer metastasis (Deng et al., 2020, Zhang et al., 2021). However, previous study by Yang XW et al. demonstrated that hsa-miR-1296-3p enhances hepatocellular carcinoma cell proliferation and tumorigenicity by targeting the metastasis suppressor gene FOXO1 (Yang et al., 2014). Moreover, similar study by Tao Y et al. confirmed that hsa-miR-1296-

3p promotes cell proliferation, migration and invasion in colorectal cancer cells by targeting the tumour suppressor gene, SFPQ (Tao et al., 2018). The data presented in the previous session indicated that knockdown of circSPINT2 enhanced resistance to Osimertinib (Figure 4.18 & Figure 4.19). Up-regulation of miR-1296-3p expression has been consistently observed in the OR cells and in the knockdown circSPINT2 group that have developed resistance to Osimertinib (Figure 4.30 & Figure 4.31). This information provide insights into the function of hsa-miR-1296-3p and its role as oncogenic miRNA in Osimertinib resistance. Subsequently, the downstream target of miR-1296-3p, which could potentially exert an indirect impact on Osimertinib resistance was explored. The bioinformatic analysis constructed in this study indicated that Retinol Binding Protein 1 (RBP1; also known as CRBP1) is one of the downstream targets of miR-1296-3p (Figure 4.32). RBP1 is a gene that is involved in the transport and metabolism of retinoids, which are essential for cellular differentiation and proliferation (Yu et al., 2022). Lower RBP1 expression was associated with the development of various cancer pathogenesis although higher expression were documented in lung cancer (Jerónimo et al., 2004, Liu et al., 2021a, Doldo et al., 2014, Doldo et al., 2015). In a study by Ferlosio A et al. demonstrated that RBP1 overexpression in H460 human NSCLC cell line, reduced the cell proliferation and clonogenicity through suppression of AKT signalling pathway (Ferlosio et al., 2020). In addition, force expression of RBP1 was found to enhance the cellular sensitivity of rectal cancer cells to radiation treatment (Yokoi et al., 2017). Knocking down circSPINT2 leads to upregulation of miR-1296-3p expression, which in turn downregulates RBP1 expression and promotes the development of Osimertinib resistance while

overexpression of circSPINT2 exhibited opposing outcome (Figure 4.33 & Figure 4.34). RBP1 expression was also consistent at protein level (Figure 4.35). Overall, the findings indicated that miR-1296 potentially serves as an oncogenic miRNA, inhibiting the expression of RBP1 in cells resistant to Osimertinib.

5.6 CircSPINT2/hsa-miR-1296-3p/RBP1 Validation in Animal Model

In an effort to investigate *in-vitro* observations involving the interaction of circSPINT2/hsa-miR-1296-3p/RBP1 in an *in-vivo* animal model, Osimertinib-resistant tumour xenograft was established in NOD-SCID mice (Figure 4.36). H1975 xenografts were established through subcutaneous injection into both flanks of nude mice. NOD-SCID mice were given 5mg/ml Osimertinib continuously for five times per week over a total of 30 days, when the xenograft tumours reaches at an average size of 50mm³. Xenograft tumours in the control/vehicle group were harvested earlier once they reached approximately 1000mm³. In contrast, at day 30, tumours from the treatment group were collected for further characterization. The data comprising tumour volume measurement for 30 days indicated a tumour suppressive effect resulted from Osimertinib treatment from day 7 to day 21 (Figure 4.37) . However, subsequent tumour growth, observed up to day from day 21 onwards, indicating signs of resistance. Previous study by Emdal, Kristina B., et al. have also attempted to investigate acquired resistance to Osimertinib by establishment of long-term Osimertinib treatment in tumour xenograft models. The authors subcutaneously injected 5×10^6 of H1975-HGF (HGF overexpression) and HCC827-ER1 (MET amplification) cell lines into the flanks of female BALB/c nude mice (6–8 weeks

old). Osimertinib treatment initiated when the tumour xenografts reaches approximately 400–600 mm³. Osimertinib, administered daily via oral gavage, at a dose of 5 mg/kg. Their results showed that all tumours derived from H1975-HGF and HCC827-ER1 displayed resistance to Osimertinib treatment (Emdal et al., 2017). In another study by La Monica, Silvia, et al., also demonstrated *in-vivo* Osimertinib-resistance induced xenograft model but the course of Osimertinib treatment were continued for approximately 60 days. The authors subcutaneously injected PC9T790M cell line into female Balb/c-Nude mice, and upon reaching an average size of around 150mm³, the nude mice were randomly assigned to three types of treatment groups. Upon *in-vivo* continuous Osimertinib treatment in mice, the tumour suppression was effective for the initial 45 days, after which resistance developed (La Monica et al., 2019).

As expected, qRT-PCR validation of circSPINT2/hsa-miR-1296-3p/RBP1 expressions were similar to that of *in-vitro* data (Figure 4.38). FISH analysis exhibited circSPINT2 expression was detected in the cytoplasmic region of the Osimertinib-resistant induced xenograft tissues (Figure 4.39). Correspondingly, low RBP1 protein expression was noted in the in the Osimertinib-resistant induced xenograft tissues compared to the control/vehicle group (Figure 4.40). Based on these results, circSPINT2/hsa-miR-1296-3p/RBP1 axis in the animal model may have correlation in the development of Osimertinib resistance. In light of the results obtained in this investigation, it was observed that Osimertinib-resistant xenograft tumours displayed an elevated potential for drug resistance and a decreased rate of apoptosis. Consequently, these data indicated that the continuous administration of Osimertinib leads to the suppression of circSPINT2 expression, thereby contributing to the

development of Osimertinib resistance. Ultimately, the outcome of this research unveiled the involvement of circSPINT2 in enhancing sensitivity to Osimertinib, resulting in a decrease in tumorigenicity.

CHAPTER 6

Conclusion

6.1 Conclusion

Osimertinib/AZD9291 demonstrated inefficiencies within 12 month of treatment regimen among T790M in positive LUAD (a predominant subtype of NSCLC) patients as they acquired resistance through tertiary EGFR mutations (Yi et al., 2022). Continuous resistance highlights the complex evolution of NSCLC in response to EGFR-TKI therapy, underlining the desperate need for a biomarker to elucidate the mechanism behind acquired resistance to Osimertinib (Santoni-Rugiu et al., 2019). Traditional biomarkers comprising DNA and protein biomarkers may not fully mirror the information of the disease as effectively as RNA biomarker and are lack of sensitivity and specificity (Xi et al., 2017).

CircRNA discovered recently, serves as an excellent RNA biomarker owing to its high sensitivity and specificity in both solid and liquid biopsies. Its distinctive circular structure permits elusion from degradation by exoribonuclease enzymes, resulting in an extended half-life exceeding 48 hours (Xie et al., 2020, Wang et al., 2023). Besides, circRNA's strength is stable in nature and extended half-lives renders it potential as a valuable biomolecule for investigating the acquired mechanisms of resistance to Osimertinib. Also, its robust characteristics improves the detectability in diverse body fluids,

expanding its potential as a non-invasive diagnostic biomarker in liquid biopsies (Zhang et al., 2021).

To sum up, this study reveals that downregulation of circSPINT2 is essential for LUAD to develop resistance to the third-generation EGFR-TKI, Osimertinib (Fig 6.1). CircSPINT2 enhances drug sensitivity by promoting drug-induced apoptosis and sponging miR-1296-3p, which subsequently increases RBP1 expression. Both in vitro and in vivo models show that Osimertinib-resistant cells exhibit reduced circSPINT2 levels, reducing apoptosis upon Osimertinib treatment. Restoring circSPINT2 expression in resistant cells significantly improves drug efficacy by enhancing Osimertinib-induced apoptosis. Since circSPINT2 can be secreted, it may serve as a therapeutic biomarker for risk assessment, screening, prognosis, and monitoring of Osimertinib resistance in a clinical setting. However, further research using clinical samples is necessary to assess its clinical relevance and potential applications. In conclusion, this report provides experimental evidence of a tumour-suppressive circRNA that can increase cellular sensitivity to third-generation EGFR-TKIs, potentially influencing the future detection and treatment of Osimertinib resistance.

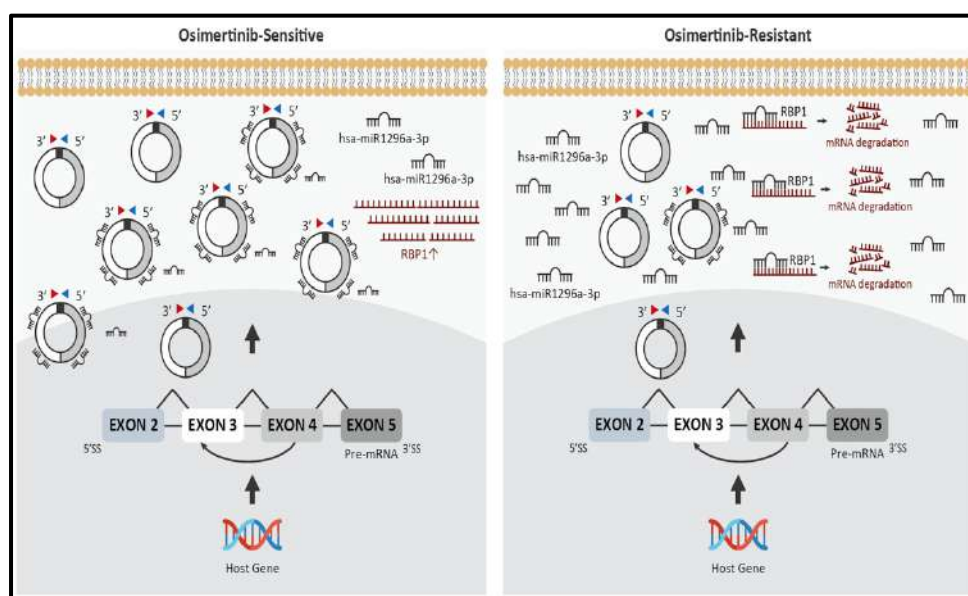


Figure 6.1 Summary of the effects and significance of the circSPINT2/miR-1296-3p/RBP1 axis as a regulating factor in Osimertinib-sensitive and Osimertinib-resistant in NSCLC cells.

6.2 Limitations and Future Recommendation

The *in-vivo* Osimertinib-resistant model was established within a 30-day timeframe in this study. Prolong the induction period (>30-60 days) could postulate a more conclusive understanding of the resistance mechanisms and the evolution over time. Additionally, the validation of circSPINT2/miR-1296-3p/RBP1 has not been carried out in clinical samples acquired from NSCLC patients with T790M and are resistant to Osimertinib. Indeed, it is essential to confirm the relevance of these molecular interactions in clinical settings to corroborate the clinical significance and potential as biomarkers for Osimertinib resistance in NSCLC patients. Therefore, further validation of circSPINT2 in clinical samples are warranted to substantiate the findings between pre-clinical observations and clinical pertinency.

REFERENCES

- ABOUREHAB, M. A. S., ALQAHTANI, A. M., YOUSSEF, B. G. M. & GOUDA, A. M. 2021. Globally Approved EGFR Inhibitors: Insights into Their Syntheses, Target Kinases, Biological Activities, Receptor Interactions, and Metabolism. *Molecules*, 26.
- ABUDAYYEH, O. O., GOOTENBERG, J. S., ESSLETZBICHLER, P., HAN, S., JOUNG, J., BELANTO, J. J., VERDINE, V., COX, D. B. T., KELLNER, M. J., REGEV, A., LANDER, E. S., VOYTAS, D. F., TING, A. Y. & ZHANG, F. 2017. RNA targeting with CRISPR–Cas13. *Nature*, 550, 280-284.
- AGHAEE-BAKHTIARI, S. H. 2018. Online Databases and Circular RNAs. *Adv Exp Med Biol*, 1087, 35-38.
- AHMAD, A., IMRAN, M. & AHSAN, H. 2023. Biomarkers as Biomedical Bioindicators: Approaches and Techniques for the Detection, Analysis, and Validation of Novel Biomarkers of Diseases. *Pharmaceutics*, 15, 1630.
- ALANAZI, A., ALSHEHRI, S., ALTAMIMI, M. & SHAKEEL, F. 2020. Solubility determination and three dimensional Hansen solubility parameters of gefitinib in different organic solvents: Experimental and computational approaches. *Journal of Molecular Liquids*, 299, 112211.
- AMAYA, L., GRIGORYAN, L., LI, Z., LEE, A., WENDER, P. A., PULENDRAN, B. & CHANG, H. Y. 2023. Circular RNA vaccine induces potent T cell responses. *Proceedings of the National Academy of Sciences*, 120, e2302191120.
- AMICIZIA, D., PIAZZA, M. F., MARCHINI, F., ASTENGO, M., GRAMMATICO, F., BATTAGLINI, A., SCHENONE, I., STICCHI, C., LAVIERI, R., DI SILVERIO, B., ANDREOLI, G. B. & ANSALDI, F. 2023. Systematic Review of Lung Cancer Screening: Advancements and Strategies for Implementation. *Healthcare (Basel)*, 11.
- ANDO, T., KASAMATSU, A., KAWASAKI, K., HIROSHIMA, K., FUKUSHIMA, R., IYODA, M., NAKASHIMA, D., ENDO-SAKAMOTO, Y. & UZAWA, K. 2021. Tumor Suppressive Circular RNA-102450: Development of a Novel Diagnostic Procedure for Lymph Node Metastasis from Oral Cancer. *Cancers (Basel)*, 13.
- ANDREWS WRIGHT, N. M. & GOSS, G. D. 2019. Third-generation epidermal growth factor receptor tyrosine kinase inhibitors for the treatment of non-small cell lung cancer. *Transl Lung Cancer Res*, 8, S247-s264.
- ANUSEWICZ, D., ORZECZOWSKA, M. & BEDNAREK, A. K. 2020. Lung squamous cell carcinoma and lung adenocarcinoma differential gene expression regulation through pathways of Notch, Hedgehog, Wnt, and ErbB signalling. *Scientific Reports*, 10, 21128.

ARAGHI, M., MANNANI, R., HEIDARNEJAD MALEKI, A., HAMIDI, A., ROSTAMI, S., SAFA, S. H., FARAMARZI, F., KHORASANI, S., ALIMOHAMMADI, M., TAHMASEBI, S. & AKHAVAN-SIGARI, R. 2023. Recent advances in non-small cell lung cancer targeted therapy; an update review. *Cancer Cell International*, 23, 162.

ASHWAL-FLUSS, R., MEYER, M., PAMUDURTI, N. R., IVANOV, A., BARTOK, O., HANAN, M., EVANTAL, N., MEMCZAK, S., RAJEWSKY, N. & KADENER, S. 2014. circRNA biogenesis competes with pre-mRNA splicing. *Mol Cell*, 56, 55-66.

BABAYEV, M. & SILVEYRA, P. 2024. Role of circular RNAs in lung cancer. *Frontiers in Genetics*, 15.

BAE, J., YANG, S.-H., KIM, A. & KIM, H. G. 2022. RNA-based biomarkers for the diagnosis, prognosis, and therapeutic response monitoring of prostate cancer. *Urologic Oncology: Seminars and Original Investigations*, 40, 105.e1-105.e10.

BAHAR, M. E., KIM, H. J. & KIM, D. R. 2023. Targeting the RAS/RAF/MAPK pathway for cancer therapy: from mechanism to clinical studies. *Signal Transduction and Targeted Therapy*, 8, 455.

BAI, Y., LIU, D., HE, Q., LIU, J., MAO, Q. & LIANG, Z. 2022. Research progress on circular RNA vaccines. *Front Immunol*, 13, 1091797.

BANSAL, R. & MALHOTRA, A. 2021. Therapeutic progression of quinazolines as targeted chemotherapeutic agents. *European Journal of Medicinal Chemistry*, 211, 113016.

BARBAGALLO, D., CAPONNETTO, A., BREX, D., MIRABELLA, F., BARBAGALLO, C., LAURETTA, G., MORRONE, A., CERTO, F., BROGGI, G., CALTABIANO, R., BARBAGALLO, G. M., SPINA-PURRELLO, V., RAGUSA, M., DI PIETRO, C., HANSEN, T. B. & PURRELLO, M. 2019. CircSMARCA5 Regulates VEGFA mRNA Splicing and Angiogenesis in Glioblastoma Multiforme Through the Binding of SRSF1. *Cancers (Basel)*, 11.

BANERJEE, S., SHARMA, V. & DAS MUKHOPADHYAY, C. 2024. Exploring emerging concepts of exosomes for the diagnosis, prognosis, and therapeutics of brain cancers. *Extracellular Vesicle*, 3, 100038.

BERTOLI, E., DE CARLO, E., BASILE, D., ZARA, D., STANZIONE, B., SCHIAPPACASSI, M., DEL CONTE, A., SPINA, M. & BEARZ, A. 2023. Liquid Biopsy in NSCLC: An Investigation with Multiple Clinical Implications. *Int J Mol Sci*, 24.

BEUTEL, M. W., HARMON, T. C., NOVOTNY, T. E., MOCK, J., GILMORE, M. E., HART, S. C., TRAINA, S., DUTTAGUPTA, S., BROOKS, A., JERDE, C. L., HOH, E., VAN DE WERFHORST, L. C., BUTSIC, V., WARTENBERG, A. C. & HOLDEN, P. A. 2021. A Review of Environmental Pollution from the

Use and Disposal of Cigarettes and Electronic Cigarettes: Contaminants, Sources, and Impacts. *Sustainability*, 13, 12994.

BEYLERLI, O., ENCARNACION RAMIREZ, M. D. J., SHUMADALOVA, A., ILYASOVA, T., ZEMLYANSKIY, M., BEILERLI, A. & MONTEMURRO, N. 2023. Cell-Free miRNAs as Non-Invasive Biomarkers in Brain Tumors. *Diagnostics*, 13, 2888.

BLACKHALL, F. H., REHMAN, S. & THATCHER, N. 2005. Erlotinib in non-small cell lung cancer: a review. *Expert Opin Pharmacother*, 6, 995-1002.

BONIOL, M., KOECHLIN, A. & BOYLE, P. 2017. Meta-analysis of occupational exposures in the rubber manufacturing industry and risk of cancer. *Int J Epidemiol*, 46, 1940-1947.

BOSE, R. & AIN, R. 2018. Regulation of Transcription by Circular RNAs. *Adv Exp Med Biol*, 1087, 81-94.

BOUSTANY, Y., LARAQUI, A., EL RHAFFOULI, H., BAJJOU, T., EL MCHICHI, B., EL ANAZ, H., AMINE, I. L., CHAHDI, H., OUKABLI, M., SOUHI, H., ELOUAZZANI, H., RHORFI, I. A., ABID, A., MAHFOUD, T., TANZ, R., ICHOU, M., ENNIBI, K., BELKADI, B. & SEKHSOKH, Y. 2022. Prevalence and Patterns of EGFR Mutations in Non-small Cell Lung Cancer in the Middle East and North Africa. *Cancer Control*, 29, 10732748221129464.

BROWN, N. A., AISNER, D. L. & OXNARD, G. R. 2018. Precision Medicine in Non-Small Cell Lung Cancer: Current Standards in Pathology and Biomarker Interpretation. *American Society of Clinical Oncology Educational Book*, 708-715.

BRUNO, R., ALÌ, G., POMA, A. M. & FONTANINI, G. 2021. Non-small cell lung cancer molecular characterization of advanced disease with focus on sex differences: a narrative review. *Precision Cancer Medicine*, 4.

BUROTTO, M., MANASANCH, E. E., WILKERSON, J. & FOJO, T. 2015. Gefitinib and erlotinib in metastatic non-small cell lung cancer: a meta-analysis of toxicity and efficacy of randomized clinical trials. *Oncologist*, 20, 400-10.

CAI, H., LI, Y., NIRINGIYUMUKIZA, J. D., SU, P. & XIANG, W. 2019. Circular RNA involvement in aging: An emerging player with great potential. *Mechanisms of Ageing and Development*, 178, 16-24.

CAO, B., LIU, G., ZHANG, W., SHI, Y. & WEI, B. 2021. Role of circular RNAs and long non-coding RNAs in the clinical translation of gastric cancer (Review). *Int J Mol Med*, 47, 77-91.

CHAKRAVARTI, D., LABELLA, K. A. & DEPINHO, R. A. 2021. Telomeres: history, health, and hallmarks of aging. *Cell*, 184, 306-322.

- CHANVORACHOTE, P., PETSRI, K. & THONGSOM, S. 2022. Epithelial to mesenchymal transition in lung cancer: potential EMT-targeting natural product-derived compounds. *Anticancer Research*, 42, 4237-4246.
- CHAO, H. M., WANG, T. W., CHERN, E. & HSU, S. H. 2022. Regulatory RNAs, microRNA, long-non coding RNA and circular RNA roles in colorectal cancer stem cells. *World J Gastrointest Oncol*, 14, 748-764.
- CHEHELGERDI, M. & CHEHELGERDI, M. 2023. The use of RNA-based treatments in the field of cancer immunotherapy. *Molecular Cancer*, 22, 106.
- CHEN, C., WEI, H., ZHANG, K., LI, Z., WEI, T., TANG, C., YANG, Y. & WANG, Z. 2022a. A flexible, efficient, and scalable platform to produce circular RNAs as new therapeutics. *bioRxiv*, 2022.05. 31.494115.
- CHEN, H.-H., ZHANG, T.-N., WU, Q.-J., HUANG, X.-M. & ZHAO, Y.-H. 2021a. Circular RNAs in lung cancer: recent advances and future perspectives. *Frontiers in oncology*, 11, 664290.
- CHEN, J., PENG, Y., ZHANG, H., WANG, K., ZHAO, C., ZHU, G., REDDY PALLI, S. & HAN, Z. 2021b. Off-target effects of RNAi correlate with the mismatch rate between dsRNA and non-target mRNA. *RNA Biol*, 18, 1747-1759.
- CHEN, L., LIU, S. & TAO, Y. 2020. Regulating tumor suppressor genes: post-translational modifications. *Signal Transduction and Targeted Therapy*, 5, 90.
- CHEN, Q., JIA, G., ZHANG, X. & MA, W. 2024. Targeting HER3 to overcome EGFR TKI resistance in NSCLC. *Frontiers in Immunology*, 14, 1332057.
- CHEN, T., LUO, J., GU, Y., HUANG, J., LUO, Q. & YANG, Y. 2019. Comprehensive analysis of circular RNA profiling in AZD9291-resistant non-small cell lung cancer cell lines. *Thorac Cancer*, 10, 930-941.
- CHEN, X., GU, J., HUANG, J., WEN, K., ZHANG, G., CHEN, Z., WANG, Z. 2023. Characterization of circRNAs in established osimertinib-resistant non-small cell lung cancer cell lines. *Int J Mol Med*, 52, 102.
- CHEN, X., MAO, R., SU, W., YANG, X., GENG, Q., GUO, C., WANG, Z., WANG, J., KRESTY, L. A., BEER, D. G., CHANG, A. C. & CHEN, G. 2019b. Circular RNA circHIPK3 modulates autophagy via MIR124-3p-STAT3-PRKAA/AMPK α signaling in STK11 mutant lung cancer. *Autophagy*, 1-13.
- CHEN, Y., XU, J., ZHANG, L., SONG, Y., WEN, W., LU, J., ZHAO, Z., KONG, W., LIU, W., GUO, A., SANTARPIA, M., YAMADA, T., CAI, X. & YU, Z. 2022b. A multicenter-retrospective study of non-small-cell lung carcinoma harboring uncommon epidermal growth factor receptor (EGFR) mutations: different subtypes of EGFR exon 19 deletion-insertions exhibit the clinical characteristics and prognosis of non-small cell lung carcinoma. *Translational Lung Cancer Research*, 11, 238-249.

CHENG, D., WANG, J., DONG, Z. & LI, X. 2021. Cancer-related circular RNA: diverse biological functions. *Cancer Cell International*, 21, 11.

CHENG, Z., CUI, H., WANG, Y., YANG, J., LIN, C., SHI, X., ZOU, Y., CHEN, J., JIA, X. & SU, L. 2024. The advance of the third-generation EGFR-TKI in the treatment of non-small cell lung cancer (Review). *Oncol Rep*, 51.

CHI, Y., ZHENG, W., BAO, G., WU, L., HE, X., GAN, R., SHEN, Y., YIN, X. & JIN, M. 2021. Circular RNA circ_103820 suppresses lung cancer tumorigenesis by sponging miR-200b-3p to release LATS2 and SOCS6. *Cell Death Dis*, 12, 185.

CHOI, S.-W. & NAM, J.-W. 2024. Optimal design of synthetic circular RNAs. *Experimental & Molecular Medicine*, 56, 1281-1292.

CHU, C. Y., CHOI, J., EABY-SANDY, B., LANGER, C. J. & LACOUTURE, M. E. 2018. Osimertinib: A Novel Dermatologic Adverse Event Profile in Patients with Lung Cancer. *Oncologist*, 23, 891-899.

CONN, SIMON J., PILLMAN, KATHERINE A., TOUBIA, J., CONN, VANESSA M., SALMANIDIS, M., PHILLIPS, CAROLINE A., ROSLAN, S., SCHREIBER, ANDREAS W., GREGORY, PHILIP A. & GOODALL, GREGORY J. 2015. The RNA Binding Protein Quaking Regulates Formation of circRNAs. *Cell*, 160, 1125-1134.

COX, J. L. A. 2011. An Exposure-Response Threshold for Lung Diseases and Lung Cancer Caused by Crystalline Silica. *Risk Analysis*, 31, 1543-1560.

DAI, C., LIU, B., LI, S., HONG, Y., SI, J., XIONG, Y., WU, N. & MA, Y. 2021. Construction of a circRNA-miRNA-mRNA Regulated Pathway Involved in EGFR-TKI Lung Adenocarcinoma Resistance. *Technology in Cancer Research & Treatment*, 20, 15330338211056809.

DAI, C., MA, Z., SI, J., AN, G., ZHANG, W., LI, S. & MA, Y. 2022. Hsa_circ_0007312 Promotes Third-Generation Epidermal Growth Factor Receptor-Tyrosine Kinase Inhibitor Resistance through Pyroptosis and Apoptosis via the MiR-764/MAPK1 Axis in Lung Adenocarcinoma Cells. *J Cancer*, 13, 2798-2809.

DAI, F. Q., LI, C. R., FAN, X. Q., TAN, L., WANG, R. T. & JIN, H. 2019. miR-150-5p Inhibits Non-Small-Cell Lung Cancer Metastasis and Recurrence by Targeting HMGA2 and β -Catenin Signaling. *Mol Ther Nucleic Acids*, 16, 675-685.

DANA, H., CHALBATANI, G. M., MAHMOODZADEH, H., KARIMLOO, R., REZAIEAN, O., MORADZADEH, A., MEHMANDOOST, N., MOAZZEN, F., MAZRAEH, A., MARMARI,

V., EBRAHIMI, M., RASHNO, M. M., ABADI, S. J. & GHARAGOUZLO, E. 2017. Molecular Mechanisms and Biological Functions of siRNA. *Int J Biomed Sci*, 13, 48-57.

DAS, D., DAS, A. & PANDA, A. C. 2021. Antisense Oligo Pulldown of Circular RNA for Downstream Analysis. *Bio Protoc*, 11, e4088.

DAWOUD, A., ELMASRI, R. A., MOHAMED, A. H., MAHMOUD, A., ROSTOM, M. M. & YOUNESS, R. A. 2024. Involvement of CircRNAs in regulating The “New Generation of Cancer Hallmarks”: A Special Depiction on Hepatocellular Carcinoma. *Critical Reviews in Oncology/Hematology*, 196, 104312.

DEMUTH, C., MADSEN, A. T., WEBER, B., WU, L., MELDGAARD, P. & SORENSEN, B. S. 2018. The T790M resistance mutation in EGFR is only found in cfDNA from erlotinib-treated NSCLC patients that harbored an activating EGFR mutation before treatment. *BMC Cancer*, 18, 191.

DENG, H., XIE, C., YE, Y. & DU, Z. 2020. MicroRNA-1296 expression is associated with prognosis and inhibits cell proliferation and invasion by Wnt signaling in non-small cell lung cancer. *Oncol Lett*, 19, 623-630.

DOLDO, E., COSTANZA, G., FERLOSIO, A., PASSERI, D., BERNARDINI, S., SCIOLI, M. G., MAZZAGLIA, D., AGOSTINELLI, S., DEL BUFALO, D., CZERNOBILSKY, B. & ORLANDI, A. 2014. CRBP-1 expression in ovarian cancer: a potential therapeutic target. *Anticancer Res*, 34, 3303-12.

DOLDO, E., COSTANZA, G., FERLOSIO, A., POMPEO, E., AGOSTINELLI, S., BELLEZZA, G., MAZZAGLIA, D., GIUNTA, A., SIDONI, A. & ORLANDI, A. 2015. High expression of cellular retinol binding protein-1 in lung adenocarcinoma is associated with poor prognosis. *Genes Cancer*, 6, 490-502.

DONG, W., ZHANG, H., DAI, Y., ZHOU, Y., LUO, Y., ZHAO, C., CAO, Y., DU, Y. & CHEN, Y. 2021. circRNA circFAT1 (e2) Elevates the Development of Non-Small-Cell Lung Cancer by Regulating miR-30e-5p and USP22. *BioMed Research International*, 2021, 1-8.

DU, W. W., FANG, L., YANG, W., WU, N., AWAN, F. M., YANG, Z. & YANG, B. B. 2017. Induction of tumor apoptosis through a circular RNA enhancing Foxo3 activity. *Cell death & differentiation*, 24, 357-370.

DU, Z. & LOVLY, C. M. 2018. Mechanisms of receptor tyrosine kinase activation in cancer. *Molecular Cancer*, 17, 58.

DUAN, X., YU, X. & LI, Z. 2022. Circular RNA hsa_circ_0001658 regulates apoptosis and autophagy in gastric cancer through microRNA-

182/Ras-related protein Rab-10 signaling axis. *Bioengineered*, 13, 2387-2397.

EBBESEN, K. K., HANSEN, T. B. & KJEMS, J. 2017. Insights into circular RNA biology. *RNA Biol*, 14, 1035-1045.

EGER, N., SCHOPPE, L., SCHUSTER, S., LAUFS, U. & BOECKEL, J. N. 2018. Circular RNA Splicing. *Adv Exp Med Biol*, 1087, 41-52.

EIDY, M. & TISHKOWSKI, K. 2020. Radon Toxicity.

EMDAL, K. B., DITTMANN, A., REDDY, R. J., LESCARBEAU, R. S., MOORES, S. L., LAQUERRE, S. & WHITE, F. M. 2017. Characterization of In Vivo Resistance to Osimertinib and JNJ-61186372, an EGFR/Met Bispecific Antibody, Reveals Unique and Consensus Mechanisms of Resistance. *Mol Cancer Ther*, 16, 2572-2585.

ESHGHIFAR, N., FARROKHI, N., NAJI, T. & ZALI, M. 2017. Tumor suppressor genes in familial adenomatous polyposis. *Gastroenterology and hepatology from bed to bench*, 10, 3-13.

FALCONE, I., CONCIATORI, F., BAZZICHETTO, C., BRIA, E., CARBOGNIN, L., MALAGUTI, P., FERRETTI, G., COGNETTI, F., MILELLA, M. & CIUFFREDA, L. 2020. AXL Receptor in Breast Cancer: Molecular Involvement and Therapeutic Limitations. *Int J Mol Sci*, 21.

FAN, X., YANG, Y., CHEN, C. & WANG, Z. 2022. Pervasive translation of circular RNAs driven by short IRES-like elements. *Nat Commun*, 13, 3751.

FANG, W., HUANG, Y., HONG, S., ZHANG, Z., WANG, M., GAN, J., WANG, W., GUO, H., WANG, K. & ZHANG, L. 2019. EGFR exon 20 insertion mutations and response to osimertinib in non-small-cell lung cancer. *BMC Cancer*, 19, 595.

FENG, X.-Y., ZHU, S.-X., PU, K.-J., HUANG, H.-J., CHEN, Y.-Q. & WANG, W.-T. 2023. New insight into circRNAs: characterization, strategies, and biomedical applications. *Experimental Hematology & Oncology*, 12, 91.

FENG, Y., YANG, Y., ZHAO, X., FAN, Y., ZHOU, L., RONG, J. & YU, Y. 2019. Circular RNA circ0005276 promotes the proliferation and migration of prostate cancer cells by interacting with FUS to transcriptionally activate XIAP. *Cell Death & Disease*, 10, 792.

FERLOSIO, A., DOLDO, E., AGOSTINELLI, S., COSTANZA, G., CENTOFANTI, F., SIDONI, A. & ORLANDI, A. 2020. Cellular retinol binding protein 1 transfection reduces proliferation and AKT-related gene expression in H460 non-small lung cancer cells. *Mol Biol Rep*, 47, 6879-6886.

FERREIRA, R., SCHNEEKLOTH, J. S., PANOV, K. I., HANNAN, K. M. & HANNAN, R. D. 2020. Targeting the RNA Polymerase I Transcription for Cancer Therapy Comes of Age. *Cells*, 9, 266.

FERRO, A., MARINATO, G. M., MULARGIU, C., MARINO, M., PASELLO, G., GUARNERI, V. & BONANNO, L. 2024. The study of primary and acquired resistance to first-line osimertinib to improve the outcome of EGFR-mutated advanced Non-small cell lung cancer patients: the challenge is open for new therapeutic strategies. *Critical Reviews in Oncology/Hematology*, 196, 104295.

FONTEMAGGI, G., TURCO, C., ESPOSITO, G. & DI AGOSTINO, S. 2021. New Molecular Mechanisms and Clinical Impact of circRNAs in Human Cancer. *Cancers (Basel)*, 13.

FREITAS, C., SOUSA, C., MACHADO, F., SERINO, M., SANTOS, V., CRUZ-MARTINS, N., TEIXEIRA, A., CUNHA, A., PEREIRA, T., OLIVEIRA, H. P., COSTA, J. L. & HESPANHOL, V. 2021. The Role of Liquid Biopsy in Early Diagnosis of Lung Cancer. *Front Oncol*, 11, 634316.

FU, K., XIE, F., WANG, F. & FU, L. 2022. Therapeutic strategies for EGFR-mutated non-small cell lung cancer patients with osimertinib resistance. *J Hematol Oncol*, 15, 173.

GALINDO, I., GÓMEZ-MORALES, M., DÍAZ-CANO, I., ANDRADES, Á., CABA-MOLINA, M., MIRANDA-LEÓN, M. T., MEDINA, P. P., MARTÍN-PADRON, J. & FÁREZ-VIDAL, M. E. 2020. The value of desmosomal plaque-related markers to distinguish squamous cell carcinoma and adenocarcinoma of the lung. *Upsala Journal of Medical Sciences*, 125, 19-29.

GAO, X., LE, X. & COSTA, D. B. 2016. The safety and efficacy of osimertinib for the treatment of EGFR T790M mutation positive non-small-cell lung cancer. *Expert Rev Anticancer Ther*, 16, 383-90.

GAO, Y., WANG, J. & ZHAO, F. 2015. CIRI: an efficient and unbiased algorithm for de novo circular RNA identification. *Genome Biol*, 16, 4.

GAUT, D., SIM, M. S., YUE, Y., WOLF, B. R., ABARCA, P. A., CARROLL, J. M., GOLDMAN, J. W. & GARON, E. B. 2018. Clinical Implications of the T790M Mutation in Disease Characteristics and Treatment Response in Patients With Epidermal Growth Factor Receptor (EGFR)-Mutated Non-Small-Cell Lung Cancer (NSCLC). *Clin Lung Cancer*, 19, e19-e28.

GLINGE, C., CLAUSS, S., BODDUM, K., JABBARI, R., JABBARI, J., RISGAARD, B., TOMSITS, P., HILDEBRAND, B., KÄÄB, S., WAKILI, R., JESPERSEN, T. & Tfelt-Hansen, J. 2017. Stability of Circulating Blood-Based MicroRNAs - Pre-Analytic Methodological Considerations. *PLoS One*, 12, e0167969.

GOHL, D. M., MAGLI, A., GARBE, J., BECKER, A., JOHNSON, D. M., ANDERSON, S., AUCH, B., BILLSTEIN, B., FROEHLING, E., MCDEVITT, S. L. & BECKMAN, K. B. 2019. Measuring sequencer size bias using REcount: a novel method for highly accurate Illumina sequencing-based quantification. *Genome Biology*, 20, 85.

GOINA, C. A., GOINA, D. M., FARCAS, S. S. & ANDREESCU, N. I. 2024. The Role of Circular RNA for Early Diagnosis and Improved Management of Patients with Cardiovascular Diseases. *International Journal of Molecular Sciences*, 25, 2986.

GOMATOU, G., SYRIGOS, N. & KOTTEAS, E. 2023. Osimertinib Resistance: Molecular Mechanisms and Emerging Treatment Options. *Cancers (Basel)*, 15.

GONG, K., GUO, G., BECKLEY, N. A., YANG, X., ZHANG, Y., GERBER, D. E., MINNA, J. D., BURMA, S., ZHAO, D., AKBAY, E. A. & HABIB, A. A. 2021. Comprehensive targeting of resistance to inhibition of RTK signaling pathways by using glucocorticoids. *Nature Communications*, 12, 7014.

GONG, X., LIU, Y., WU, G., XU, Z., ZENG, L., TIAN, M., ZHANG, R., ZENG, C. & CHEN, Y. 2024. An updated resource for the detection of protein-coding circRNA with CircProPlus. *Scientific Reports*, 14, 19040.

GOU, Q., GOU, Q., GAN, X. & XIE, Y. 2024. Novel therapeutic strategies for rare mutations in non-small cell lung cancer. *Scientific Reports*, 14, 10317.

GREENE, J., BAIRD, A.-M., BRADY, L., LIM, M., GRAY, S. G., MCDERMOTT, R. & FINN, S. P. 2017. Circular RNAs: biogenesis, function and role in human diseases. *Frontiers in molecular biosciences*, 4, 38.

GREGORC, V., LAZZARI, C., MANDALÁ, M., IPPATI, S., BULOTTA, A., CANGI, M. G., KHATER, A., VIGANÒ, M. G., MIRABILE, A., PECCIARINI, L., OGLIARI, F. R., ARRIGONI, G., GRASSINI, G., VERONESI, G. & DOGLIONI, C. 2021. Intratumoral Cellular Heterogeneity: Implications for Drug Resistance in Patients with Non-Small Cell Lung Cancer. *Cancers*, 13, 2023.

GRIDELLI, C. & ROSSI, A. 2012. EURTAC first-line phase III randomized study in advanced non-small cell lung cancer: Erlotinib works also in European population. *J Thorac Dis*, 4, 219-20.

GRIESINGER, F., KOROL, E. E., KAYANIYIL, S., VAROL, N., EBNER, T. & GORING, S. M. 2019. Efficacy and safety of first-line carboplatin-versus cisplatin-based chemotherapy for non-small cell lung cancer: A meta-analysis. *Lung Cancer*, 135, 196-204.

GUAN, S., LI, L., CHEN, W. S., JIANG, W. Y., DING, Y., ZHAO, L. L., SHI, Y. F., WANG, J., GUI, Q. & XU, C. C. 2021. Circular RNA WHSC1 exerts oncogenic properties by regulating miR-7/TAB2 in lung cancer. *Journal of Cellular and Molecular Medicine*, 25, 9784-9795.

GUMUSAY, O., VITIELLO, P. P., WABL, C., CORCORAN, R. B., BARDELLI, A. & RUGO, H. S. 2020. Strategic Combinations to Prevent and Overcome Resistance to Targeted Therapies in Oncology. *American Society of Clinical Oncology Educational Book*, e292-e308.

GUO, X., ZHOU, Q., SU, D., LUO, Y., FU, Z., HUANG, L., LI, Z., JIANG, D., KONG, Y. & LI, Z. J. M. C. 2020. Circular RNA circBFAR promotes the progression of pancreatic ductal adenocarcinoma via the miR-34b-5p/MET/Akt axis. 19, 1-18.

GUO, Y., HU, Z. & WANG, Z. 2021. Recent Advances in the Application Peptide and Peptoid in Diagnosis Biomarkers of Alzheimer's Disease in Blood. *Frontiers in Molecular Neuroscience*, 14, 778955.

GURIA, A., VELAYUDHA VIMALA KUMAR, K., SRIKAKULAM, N., KRISHNAMMA, A., CHANDA, S., SHARMA, S., FAN, X. & PANDI, G. 2019. Circular RNA Profiling by Illumina Sequencing via Template-Dependent Multiple Displacement Amplification. *Biomed Res Int*, 2019, 2756516.

HAABETH, O. A. W., BLAKE, T. R., MCKINLAY, C. J., WAYMOUTH, R. M., WENDER, P. A. & LEVY, R. 2018. mRNA vaccination with charge-altering releasable transporters elicits human T cell responses and cures established tumors in mice. *Proceedings of the National Academy of Sciences*, 115, E9153-E9161.

HAMA FARAJ, G. S., HUSSEN, B. M., ABDULLAH, S. R., FATIH RASUL, M., HAJIESMAEILI, Y., BANIAHMAD, A. & TAHERI, M. 2024. Advanced approaches of the use of circRNAs as a replacement for cancer therapy. *Noncoding RNA Res*, 9, 811-830.

HAN, L., YANG, H., WEI, W., HU, F. & YUAN, L. 2022. Hsa_circ_0000520 Promotes Non-Small Cell Lung Cancer Progression through the miR-1258/AKT3 Axis. *J Oncol*, 2022, 3676685.

HANNA, N. H., ROBINSON, A. G., TEMIN, S., JR, S. B., BRAHMER, J. R., ELLIS, P. M., GASPAR, L. E., HADDAD, R. Y., HESKETH, P. J., JAIN, D., JAIYESIMI, I., JOHNSON, D. H., LEIGHL, N. B., MOFFITT, P. R., PHILLIPS, T., RIELY, G. J., ROSELL, R., SCHILLER, J. H., SCHNEIDER, B. J., SINGH, N., SPIGEL, D. R., TASHBAR, J. & MASTERS, G. 2021. Therapy for Stage IV Non-Small-Cell Lung Cancer With Driver Alterations: ASCO and OH (CCO) Joint Guideline Update. *Journal of Clinical Oncology*, 39, 1040-1091.

HANSEN, T. B., JENSEN, T. I., CLAUSEN, B. H., BRAMSEN, J. B., FINSEN, B., DAMGAARD, C. K. & KJEMS, J. 2013. Natural RNA circles function as efficient microRNA sponges. *Nature*, 495, 384-388.

HAO, Y., BAKER, D. & TEN DIJKE, P. 2019. TGF- β -Mediated Epithelial-Mesenchymal Transition and Cancer Metastasis. *International Journal of Molecular Sciences*, 20, 2767.

HARTMAIER, R. J., MARKOVETS, A. A., AHN, M. J., SEQUIST, L. V., HAN, J. Y., CHO, B. C., YU, H. A., KIM, S. W., YANG, J. C., LEE, J. S., SU, W. C., KOWALSKI, D. M., ORLOV, S., REN, S., FREWER, P., OU, X., CROSS, D. A. E., KURIAN, N., CANTARINI, M. & JÄNNE, P. A. 2023. Osimertinib + Savolitinib to Overcome Acquired MET-Mediated Resistance in Epidermal Growth Factor Receptor-Mutated, MET-Amplified Non-Small Cell Lung Cancer: TATTON. *Cancer Discov*, 13, 98-113.

HATA, A., KATAKAMI, N., YOSHIOKA, H., KAJI, R., MASAGO, K., FUJITA, S., IMAI, Y., NISHIYAMA, A., ISHIDA, T., NISHIMURA, Y. & YATABE, Y. 2015. Spatiotemporal T790M Heterogeneity in Individual Patients with EGFR-Mutant Non-Small-Cell Lung Cancer after Acquired Resistance to EGFR-TKI. *Journal of Thoracic Oncology*, 10, 1553-1559.

HE, A. T., LIU, J., LI, F. & YANG, B. B. 2021a. Targeting circular RNAs as a therapeutic approach: current strategies and challenges. *Signal Transduction and Targeted Therapy*, 6, 185.

HE, J., HUANG, Z., HE, M., LIAO, J., ZHANG, Q., WANG, S., XIE, L., OUYANG, L., KOEFFLER, H. P., YIN, D. & LIU, A. 2020. Circular RNA MAPK4 (circ-MAPK4) inhibits cell apoptosis via MAPK signaling pathway by sponging miR-125a-3p in gliomas. *Mol Cancer*, 19, 17.

HE, J., MAHMOUDI, A., YAO, J., YUAN, Q., FU, J. & LIU, W. 2024. N6-methyladenosine methylation analysis of circRNAs in acquired middle ear cholesteatoma. *Frontiers in Genetics*, 15.

HE, J., REN, M., LI, H., YANG, L., WANG, X. & YANG, Q. 2019. Exosomal circular RNA as a biomarker platform for the early diagnosis of immune-mediated demyelinating disease. *Frontiers in Genetics*, 10, 860.

HE, J., ZHOU, Z., SUN, X., YANG, Z., ZHENG, P., XU, S. & ZHU, W. 2021b. The new opportunities in medicinal chemistry of fourth-generation EGFR inhibitors to overcome C797S mutation. *European Journal of Medicinal Chemistry*, 210, 112995.

HE, L., MAN, C., XIANG, S., YAO, L., WANG, X. & FAN, Y. 2021. Circular RNAs' cap-independent translation protein and its roles in carcinomas. *Mol Cancer*, 20, 119.

HEAD, S. R., KOMORI, H. K., LAMERE, S. A., WHISENANT, T., VAN NIEUWERBURGH, F., SALOMON, D. R. & ORDOUKHANIAN, P. 2014. Library construction for next-generation sequencing: overviews and challenges. *Biotechniques*, 56, 61-4, 66, 68, passim.

HEERY, R., FINN, S. P., CUFFE, S. & GRAY, S. G. 2017. Long Non-Coding RNAs: Key Regulators of Epithelial-Mesenchymal Transition, Tumour Drug Resistance and Cancer Stem Cells. *Cancers*, 9, 38.

HERBST, R. S. & SANDLER, A. 2008. Bevacizumab and erlotinib: a promising new approach to the treatment of advanced NSCLC. *The Oncologist*, 13, 1166-1176.

HERBST, R. S., MORGENSZTERN, D. & BOSHOFF, C. 2018. The biology and management of non-small cell lung cancer. *Nature*, 553, 446.

HO-XUAN, H., GLAŽAR, P., LATINI, C., HEIZLER, K., HAASE, J., HETT, R., ANDERS, M., WEICHMANN, F., BRUCKMANN, A., VAN DEN BERG, D., HÜTTELMAIER, S., RAJEWSKY, N., HACKL, C. & MEISTER, G. 2020. Comprehensive analysis of translation from overexpressed circular RNAs reveals pervasive translation from linear transcripts. *Nucleic Acids Res*, 48, 10368-10382.

HOLLOWKA, D. & BAIRD, B. 2017. Mechanisms of epidermal growth factor receptor signaling as characterized by patterned ligand activation and mutational analysis. *Biochimica et Biophysica Acta (BBA) - Biomembranes*, 1859, 1430-1435.

HONG, W., XUE, M., JIANG, J., ZHANG, Y. & GAO, X. 2020. Circular RNA circ-CPA4/let-7 miRNA/PD-L1 axis regulates cell growth, stemness, drug resistance and immune evasion in non-small cell lung cancer (NSCLC). *Journal of Experimental & Clinical Cancer Research*, 39, 1-19.

HONG, Y., PARK, S. & LEE, M. K. 2022. The prognosis of non-small cell lung cancer patients according to endobronchial metastatic lesion. *Scientific Reports*, 12, 13588.

HOPSTAKEN, J. S., DE RUITER, J. C., DAMHUIS, R. A. M., DE LANGEN, A. J., VAN DIESEN, J. N. A., KLOMP, H. M., KLOMPENHOUWER, E. G. & HARTEMINK, K. J. 2021. Stage I non-small cell lung cancer: Treatment modalities, Dutch daily practice and future perspectives. *Cancer Treatment and Research Communications*, 28, 100404.

HOSSAIN, M. T., ZHANG, J., REZA, M. S., PENG, Y., FENG, S. & WEI, Y. 2022. Reconstruction of Full-Length circRNA Sequences Using Chimeric Alignment Information. *Int J Mol Sci*, 23.

HOSSEINI, B., OLSSON, A., BOUAOUN, L., HALL, A., HADJI, M., RASHIDIAN, H., NAGHIBZADEH-TAHAMI, A., MARZBAN, M., NAJAFI, F., HAGHDOOST, A. A., BOFFETTA, P., KAMANGAR, F., PUKKALA, E., ETEMADI, A., WEIDERPASS, E., SCHÜZ, J. & ZENDEHDEL, K. 2022. Lung cancer risk in relation to jobs held in a nationwide case-control study in Iran. *Occup Environ Med*, 79, 831-838.

HSU, M.-T. & COCA-PRADOS, M. 1979. Electron microscopic evidence for the circular form of RNA in the cytoplasm of eukaryotic cells. *Nature*, 280, 339-340.

HU, J., CAO, J., TOPATANA, W., JUENGPANICH, S., LI, S., ZHANG, B., SHEN, J., CAI, L., CAI, X. & CHEN, M. 2021. Targeting mutant p53 for cancer therapy: direct and indirect strategies. *Journal of Hematology & Oncology*, 14, 157.

HUANG, C., YUE, W., LI, L., LI, S., GAO, C., SI, L., QI, L., CHENG, C., LU, M., CHEN, G., CUI, J., ZHAO, R., LI, Y. & TIAN, H. 2021. Circular RNA hsa-circ-000881 suppresses the progression of lung adenocarcinoma in vitro via a miR-665/PRICKLE2 axis. *Ann Transl Med*, 9, 498.

HUANG, J., LAN, X., WANG, T., LU, H., CAO, M., YAN, S., CUI, Y., JIA, D., CAI, L. & XING, Y. 2020. Targeting the IL-1 β /EHD1/TUBB3 axis overcomes resistance to EGFR-TKI in NSCLC. *Oncogene*, 39, 1739-1755.

HUANG, Q., GUO, H., WANG, S., MA, Y., CHEN, H., LI, H., LI, J., LI, X., YANG, F., QIU, M., ZHAO, S. & WANG, J. 2020a. A novel circular RNA, circXPO1, promotes lung adenocarcinoma progression by interacting with IGF2BP1. *Cell Death & Disease*, 11, 1031.

HUANG, Q., WANG, S., LI, X., YANG, F., FENG, C., ZHONG, K., QIU, M. & WANG, J. 2019. Circular RNA ATXN7 is upregulated in non-small cell lung cancer and promotes disease progression. *Oncol Lett*, 17, 4803-4810.

HUANG, Y., DAI, Y., WEN, C., HE, S., SHI, J., ZHAO, D., WU, L. & ZHOU, H. 2020b. circSETD3 Contributes to Acquired Resistance to Gefitinib in Non-Small-Cell Lung Cancer by Targeting the miR-520h/ABCG2 Pathway. *Molecular Therapy - Nucleic Acids*, 21, 885-899.

HWANG, H. J. & KIM, Y. K. 2024. Molecular mechanisms of circular RNA translation. *Experimental & Molecular Medicine*, 56, 1272-1280.

HWANG, J. Y., KOOK, T. L., PAULUS, S. M. & PARK, J. W. 2024. Translation of Circular RNAs: Functions of Translated Products and Related Bioinformatics Approaches. *Curr Bioinform*, 19, 3-13.

INOUE, A., KOBAYASHI, K., MAEMONDO, M., SUGAWARA, S., OIZUMI, S., ISOBE, H., GEMMA, A., SAIJO, Y., YOSHIZAWA, H., MORITA, S., HAGIWARA, K., NUKIWA, T. & GROUP, N.-E. J. S. 2011. Final overall survival results of NEJ002, a phase III trial comparing gefitinib to carboplatin (CBDCA) plus paclitaxel (TXL) as the first-line treatment for advanced non-small cell lung cancer (NSCLC) with EGFR mutations. *Journal of Clinical Oncology*, 29, 7519-7519.

ISHOLA, A. A., CHIEN, C.-S., YANG, Y.-P., CHIEN, Y., YARMISHYN, A. A., TSAI, P.-H., CHEN, J. C.-Y., HSU, P.-K., LUO, Y.-H., CHEN, Y.-M., LIANG, K.-H., LAN, Y.-T., HUO, T.-I., MA, H.-I., CHEN, M.-T., WANG, M.-L. & CHIOU, S.-H. 2022. Oncogenic circRNA C190 Promotes Non-Small Cell Lung Cancer via Modulation of the EGFR/ERK Pathway. *Cancer Research*, 82, 75-89.

ITO, K. & HATAJI, O. 2018. Osimertinib therapy as first-line treatment before acquiring T790M mutation: from AURA1 trial. *J Thorac Dis*, 10, S3071-s3077.

JACOBSEN, K., BERTRAN-ALAMILLO, J., MOLINA, M. A., TEIXIDÓ, C., KARACHALIOU, N., PEDERSEN, M. H., CASTELLVÍ, J., GARZÓN, M., CODONY-SERVAT, C., CODONY-SERVAT, J., GIMÉNEZ-CAPITÁN, A., DROZDOWSKYJ, A., VITERI, S., LARSEN, M. R., LASSEN, U., FELIP, E., BIVONA, T. G., DITZEL, H. J. & ROSELL, R. 2017. Convergent Akt activation drives acquired EGFR inhibitor resistance in lung cancer. *Nat Commun*, 8, 410.

JAFARNEJAD, M., SOVÉ, R. J., DANILOVA, L., MIRANDO, A. C., ZHANG, Y., YARCHOAN, M., TRAN, P. T., PANDEY, N. B., FERTIG, E. J. & POPEL, A. S. 2019. Mechanistically detailed systems biology modeling of the HGF/Met pathway in hepatocellular carcinoma. *npj Systems Biology and Applications*, 5, 29.

JAKOBSEN, J. N., SANTONI-RUGIU, E., GRAUSLUND, M., MELCHIOR, L. & SØRENSEN, J. B. 2018. Concomitant driver mutations in advanced EGFR-mutated non-small-cell lung cancer and their impact on erlotinib treatment. *Oncotarget*, 9, 26195-26208.

JECK, W. R., SORRENTINO, J. A., WANG, K., SLEVIN, M. K., BURD, C. E., LIU, J., MARZLUFF, W. F. & SHARPLESS, N. E. 2013. Circular RNAs are abundant, conserved, and associated with ALU repeats. *Rna*, 19, 141-157.

JERÓNIMO, C., HENRIQUE, R., OLIVEIRA, J., LOBO, F., PAIS, I., TEIXEIRA, M. R. & LOPES, C. 2004. Aberrant cellular retinol binding protein 1 (CRBP1) gene expression and promoter methylation in prostate cancer. *J Clin Pathol*, 57, 872-6.

JI, Y., ZHAO, Q., FENG, W., PENG, Y., HU, B. & CHEN, Q. 2022. N6-Methyladenosine Modification of CIRCKRT17 Initiated by METTL3

Promotes Osimertinib Resistance of Lung Adenocarcinoma by EIF4A3 to Enhance YAP1 Stability. *Cancers*, 14, 5582.

JIA, Y., LIU, M. & WANG, S. 2020. CircRNA hsa_circRNA_0001776 inhibits proliferation and promotes apoptosis in endometrial cancer via downregulating LRIG2 by sponging miR-182. *Cancer Cell Int*, 20, 412.

JIANG, D., SUI, M., ZHONG, W., HUANG, Y. & FAN, W. 2013. Different administration strategies with paclitaxel induce distinct phenotypes of multidrug resistance in breast cancer cells. *Cancer letters*, 335, 404-411.

JIANG, M.-P., XU, W.-X., HOU, J.-C., XU, Q., WANG, D.-D. & TANG, J.-H. 2021a. The Emerging Role of the Interactions between Circular RNAs and RNA-binding Proteins in Common Human Cancers. *Journal of Cancer*, 12, 5206-5219.

JIANG, S., FU, R., SHI, J., WU, H., MAI, J., HUA, X., CHEN, H., LIU, J., LU, M. & LI, N. 2021b. CircRNA-Mediated Regulation of Angiogenesis: A New Chapter in Cancer Biology. *Front Oncol*, 11, 553706.

JIANG, X., XING, L., CHEN, Y., QIN, R., SONG, S., LU, Y., XIE, S., WANG, L., PU, H., GUI, X., LI, T., XU, J., LI, J., JIA, S. & LU, D. 2021c. CircMEG3 inhibits telomerase activity by reducing Cbf5 in human liver cancer stem cells. *Mol Ther Nucleic Acids*, 23, 310-323.

JIN, C. B. & YANG, L. 2021. Histological transformation of non-small cell lung cancer: Clinical analysis of nine cases. *World J Clin Cases*, 9, 4617-4626.

JOHNSON, M., GARASSINO, M. C., MOK, T. & MITSUDOMI, T. 2022. Treatment strategies and outcomes for patients with EGFR-mutant non-small cell lung cancer resistant to EGFR tyrosine kinase inhibitors: Focus on novel therapies. *Lung Cancer*, 170, 41-51.

KAKUMANI, P. K. 2022. AGO-RBP crosstalk on target mRNAs: Implications in miRNA-guided gene silencing and cancer. *Translational Oncology*, 21, 101434.

KAPP, J. D., GREEN, R. E. & SHAPIRO, B. 2021. A Fast and Efficient Single-stranded Genomic Library Preparation Method Optimized for Ancient DNA. *Journal of Heredity*, 112, 241-249.

KARACHALIOU, N., BARRON, E. B., VITERI, S., MOLINA, M. A. & ROSELL, R. 2017. Osimertinib: a breakthrough for the treatment of epidermal growth factor receptor mutant lung adenocarcinoma. *Translational Cancer Research*, S117-S121.

KARACHALIOU, N., FERNANDEZ-BRUNO, M., BRACHT, J. W. P. & ROSELL, R. 2019. EGFR first- and second-generation TKIs-there is

still place for them in EGFR-mutant NSCLC patients. *Transl Cancer Res*, 8, S23-s47.

KARL-FRÉDÉRIC, V., KATHERINE, P., LEANNE, H. K., ELEANOR, M. M., ISANA, V.-L. & KATHERINE, M. 2021. Screening by deep sequencing reveals mediators of microRNA tailing in *C. elegans*. *bioRxiv*, 2021.01.11.426275.

KATTI, A., DIAZ, B. J., CARAGINE, C. M., SANJANA, N. E. & DOW, L. E. 2022. CRISPR in cancer biology and therapy. *Nature Reviews Cancer*, 22, 259-279.

KELLY, D., BICKER, S., WINTERER, J., NANDA, P., GERMAIN, P.-L., DIETERICH, C. & SCHRATT, G. 2024. A functional screen uncovers circular RNAs regulating excitatory synaptogenesis in hippocampal neurons. *bioRxiv*, 2024.04.09.588686.

KELLY, W. J., SHAH, N. J. & SUBRAMANIAM, D. S. 2018. Management of Brain Metastases in Epidermal Growth Factor Receptor Mutant Non-Small-Cell Lung Cancer. *Front Oncol*, 8, 208.

KERR, K. M., BIBEAU, F., THUNNISSEN, E., BOTLING, J., RYŠKA, A., WOLF, J., ÖHRLING, K., BURDON, P., MALAPELLE, U. & BÜTTNER, R. 2021. The evolving landscape of biomarker testing for non-small cell lung cancer in Europe. *Lung Cancer*, 154, 161-175.

KHOZIN, S., BLUMENTHAL, G. M., JIANG, X., HE, K., BOYD, K., MURGO, A., JUSTICE, R., KEEGAN, P. & PAZDUR, R. 2014. U.S. Food and Drug Administration approval summary: Erlotinib for the first-line treatment of metastatic non-small cell lung cancer with epidermal growth factor receptor exon 19 deletions or exon 21 (L858R) substitution mutations. *Oncologist*, 19, 774-9.

KHOZIN, S., WEINSTOCK, C., BLUMENTHAL, G. M., CHENG, J., HE, K., ZHUANG, L., ZHAO, H., CHARLAB, R., FAN, I., KEEGAN, P. & PAZDUR, R. 2017. Osimertinib for the Treatment of Metastatic EGFR T790M Mutation-Positive Non-Small Cell Lung Cancer. *Clin Cancer Res*, 23, 2131-2135.

KIEGLE, E. A., GARDEN, A., LACCHINI, E. & KATER, M. M. 2018. A genomic view of alternative splicing of long non-coding RNAs during rice seed development reveals extensive splicing and lncRNA gene families. *Frontiers in plant science*, 9, 115.

KILMISTER, E. J., KOH, S. P., WETH, F. R., GRAY, C. & TAN, S. T. 2022. Cancer Metastasis and Treatment Resistance: Mechanistic Insights and Therapeutic Targeting of Cancer Stem Cells and the Tumor Microenvironment. *Biomedicines*, 10.

KIM, D., BACH, D. H., FAN, Y. H., LUU, T. T., HONG, J. Y., PARK, H. J. & LEE, S. K. 2019. AXL degradation in combination with EGFR-

TKI can delay and overcome acquired resistance in human non-small cell lung cancer cells. *Cell Death Dis*, 10, 361.

KO, B., PAUCAR, D. & HALMOS, B. 2017. EGFR T790M: revealing the secrets of a gatekeeper. *Lung Cancer (Auckl)*, 8, 147-159.

KOBAYASHI, K. 2023. Primary Resistance to EGFR Tyrosine Kinase Inhibitors (TKIs): Contexts and Comparisons in EGFR-Mutated Lung Cancer. *Journal of Respiration*, 3, 223-236.

KOPPULA, A., ABDELGAWAD, A., GUARNERIO, J., BATISH, M. & PARASHAR, V. 2022. CircFISH: A Novel Method for the Simultaneous Imaging of Linear and Circular RNAs. *Cancers (Basel)*, 14.

KUDO, K., KAWAKADO, K., KAWAJIRI, T., NISHI, T., MAKIMOTO, G., TAMURA, T., KUYAMA, S. & TANIMOTO, M. 2020. Dramatic Response of Brain Metastasis from EGFR-mutation-positive NSCLC to Dacomitinib. *Intern Med*, 59, 1739-1740.

KUO, M.-H., LEE, A.-C., HSIAO, S.-H., LIN, S.-E., CHIU, Y.-F., YANG, L.-H., YU, C.-C., CHIOU, S.-H., HUANG, H.-N., KO, J.-C. & CHOU, Y.-T. 2020. Cross-talk between SOX2 and TGF β Signaling Regulates EGFR-TKI Tolerance and Lung Cancer Dissemination. *Cancer Research*, 80, 4426-4438.

LA MONICA, S., MINARI, R., CRETELLA, D., FLAMMINI, L., FUMAROLA, C., BONELLI, M., CAVAZZONI, A., DIGIACOMO, G., GALETTI, M., MADEDDU, D., FALCO, A., LAGRASTA, C. A., SQUADRILLI, A., BAROCELLI, E., ROMANEL, A., QUAINI, F., PETRONINI, P. G., TISEO, M. & ALFIERI, R. 2019. Third generation EGFR inhibitor osimertinib combined with pemetrexed or cisplatin exerts long-lasting anti-tumor effect in EGFR-mutated pre-clinical models of NSCLC. *Journal of Experimental & Clinical Cancer Research*, 38, 222.

LAFACE, C., MASELLI, F. M., SANTORO, A. N., IAIA, M. L., AMBROGIO, F., LATERZA, M., GUARINI, C., DE SANTIS, P., PERRONE, M. & FEDELE, P. 2023. The Resistance to EGFR-TKIs in Non-Small Cell Lung Cancer: From Molecular Mechanisms to Clinical Application of New Therapeutic Strategies. *Pharmaceutics*, 15, 1604.

LANDERAS-BUENO, S., WASSERMAN, H., OLIVEIRA, G., VANAERNUM, Z. L., BUSCH, F., SALIE, Z. L., WYSOCKI, V. H., ANDERSEN, K. & SAPHIRE, E. O. 2021. Cellular mRNA triggers structural transformation of Ebola virus matrix protein VP40 to its essential regulatory form. *Cell Rep*, 35, 108986.

LAO, T. D. & LE, T. A. H. 2020. MicroRNAs: Biogenesis, Functions and Potential Biomarkers for Early Screening, Prognosis and

Therapeutic Molecular Monitoring of Nasopharyngeal Carcinoma. *Processes*, 8, 966.

LARSON, M. H., GILBERT, L. A., WANG, X., LIM, W. A., WEISSMAN, J. S. & QI, L. S. 2013. CRISPR interference (CRISPRi) for sequence-specific control of gene expression. *Nat Protoc*, 8, 2180-96.

LEÃO, R., APOLÓNIO, J. D., LEE, D., FIGUEIREDO, A., TABORI, U. & CASTELO-BRANCO, P. 2018. Mechanisms of human telomerase reverse transcriptase (hTERT) regulation: clinical impacts in cancer. *Journal of Biomedical Science*, 25, 22.

LEE, H., HONG, R. & JIN, Y. 2024. Altered circular RNA expressions in extracellular vesicles from bronchoalveolar lavage fluids in mice after bacterial infections. *Front Immunol*, 15, 1354676.

LEE, J., HAN, Y. B., KWON, H. J., LEE, S. K., KIM, H. & CHUNG, J. H. 2022. Landscape of EGFR mutations in lung adenocarcinoma: a single institute experience with comparison of PANAMutyper testing and targeted next-generation sequencing. *J Pathol Transl Med*, 56, 249-259.

LEE, P. H., HUANG, Y. H., LIN, H., HSU, K. H., CHEN, K. C., TSENG, J. S., CHANG, G. C. & YANG, T. Y. 2022. Histological Transformation after Acquired Resistance to the Third-Generation EGFR-TKI in Patients with Advanced EGFR-Mutant Lung Adenocarcinoma. *Medicina (Kaunas)*, 58.

LEONETTI, A., MINARI, R., MAZZASCHI, G., GNETTI, L., LA MONICA, S., ALFIERI, R., CAMPANINI, N., VERZÈ, M., OLIVANI, A., VENTURA, L. & TISEO, M. 2021. Small Cell Lung Cancer Transformation as a Resistance Mechanism to Osimertinib in Epidermal Growth Factor Receptor-Mutated Lung Adenocarcinoma: Case Report and Literature Review. *Front Oncol*, 11, 642190.

LI, C., NIE, W., GUO, J., XIONG, A., ZHONG, H., CHU, T., ZHONG, R., XU, J., LU, J., ZHENG, X., ZHANG, B., SHEN, Y., PAN, F., HAN, B. & ZHANG, X. 2021. Osimertinib alone as second-line treatment for brain metastases (BM) control may be more limited than for non-BM in advanced NSCLC patients with an acquired EGFR T790M mutation. *Respiratory Research*, 22, 145.

LI, D., LIU, C., LI, Y., TENCHOV, R., SASSO, J. M., ZHANG, D., LI, D., ZOU, L., WANG, X. & ZHOU, Q. 2023a. Messenger RNA-Based Therapeutics and Vaccines: What's beyond COVID-19? *ACS Pharmacology & Translational Science*, 6, 943-969.

LI, F., WU, H., DU, X., SUN, Y., RAUSSEO, B. N., TALUKDER, A., KATAILHA, A., ELZOHARY, L., WANG, Y., WANG, Z. & LIZÉE, G. 2023b. Epidermal Growth Factor Receptor-Targeted Neoantigen

Peptide Vaccination for the Treatment of Non-Small Cell Lung Cancer and Glioblastoma. *Vaccines*, 11, 1460.

LI, H., HU, H., WANG, R., PAN, Y., WANG, L., LI, Y., ZHANG, Y., YE, T., ZHANG, Y., LI, B., SHEN, L., SUN, Y. & CHEN, H. 2014a. Primary concomitant EGFR T790M mutation predicted worse prognosis in non-small cell lung cancer patients. *Onco Targets Ther*, 7, 513-24.

LI, J. & LIU, C. 2019. Coding or noncoding, the converging concepts of RNAs. *Frontiers in genetics*, 10, 496.

LI, J., LI, P., SHAO, J., LIANG, S., WAN, Y., ZHANG, Q., LI, C., LI, Y. & WANG, C. 2022. Emerging Role of Noncoding RNAs in EGFR TKI-Resistant Lung Cancer. *Cancers*, 14(18), p.4423.

LI, J., WEI, B., FENG, J., WU, X., CHANG, Y., WANG, Y., YANG, X., ZHANG, H., HAN, S., ZHANG, C., ZHENG, J., GROEN, H. J. M., VAN DEN BERG, A., MA, J., LI, H. & GUO, Y. 2022a. Case report: TP53 and RB1 loss may facilitate the transformation from lung adenocarcinoma to small cell lung cancer by expressing neuroendocrine markers. *Front Endocrinol (Lausanne)*, 13, 1006480.

LI, J., ZHANG, Q., JIANG, D., SHAO, J., LI, W. & WANG, C. 2022b. CircRNAs in lung cancer- role and clinical application. *Cancer Letters*, 544, 215810.

LI, S., LI, L., ZHU, Y., HUANG, C., QIN, Y., LIU, H., REN-HEIDENREICH, L., SHI, B., REN, H., CHU, X., KANG, J., WANG, W., XU, J., TANG, K., YANG, H., ZHENG, Y., HE, J., YU, G. & LIANG, N. 2014b. Coexistence of EGFR with KRAS, or BRAF, or PIK3CA somatic mutations in lung cancer: a comprehensive mutation profiling from 5125 Chinese cohorts. *British Journal of Cancer*, 110, 2812-2820.

LI, X. W., YANG, W. H. & XU, J. 2020. Circular RNA in gastric cancer. *Chin Med J (Engl)*, 133, 1868-1877.

LI, X.-F., SHEN, W.-Z., JIN, X., REN, P. & ZHANG, J. 2020. Let-7c regulated epithelial-mesenchymal transition leads to osimertinib resistance in NSCLC cells with EGFR T790M mutations. *Scientific reports*, 10, 11236.

LI, X., YANG, L. & CHEN, L.-L. 2018. The biogenesis, functions, and challenges of circular RNAs. *Molecular cell*, 71, 428-442.

LI, Y., HONG, X., ZHAI, J., LIU, Y., LI, R., WANG, X., ZHANG, Y. & LV, Q. 2023c. Novel circular RNA circ-0002727 regulates miR-144-3p/KIF14 pathway to promote lung adenocarcinoma progression. *Frontiers in Cell and Developmental Biology*, 11.

LI, Y., MAO, T., WANG, J., ZHENG, H., HU, Z., CAO, P., YANG, S., ZHU, L., GUO, S., ZHAO, X., TIAN, Y., SHEN, H. & LIN, F. 2023d. Toward the next generation EGFR inhibitors: an overview of osimertinib resistance mediated by EGFR mutations in non-small cell lung cancer. *Cell Communication and Signaling*, 21, 71.

LI, Y., ZHENG, Q., BAO, C., LI, S., GUO, W., ZHAO, J., CHEN, D., GU, J., HE, X. & HUANG, S. 2015. Circular RNA is enriched and stable in exosomes: a promising biomarker for cancer diagnosis. *Cell research*, 25, 981-984.

LI, Z., HUANG, C., BAO, C., CHEN, L., LIN, M., WANG, X., ZHONG, G., YU, B., HU, W. & DAI, L. 2015. Exon-intron circular RNAs regulate transcription in the nucleus. *Nature structural & molecular biology*, 22, 256-264.

LI, Z., ZHANG, R., LI, D. & GUO, R. 2024. Molecular mechanisms of circular RNA in breast cancer: a narrative review. *Transl Cancer Res*, 13, 1139-1149.

LIAM, C. K., STONE, E., ANDARINI, S., LIAM, Y. S., LAM, D. C. L. & LEE, P. 2020. Molecular testing of metastatic non-small cell lung cancer in the Asia-Pacific region. *Respirology*, 25, 685-687.

LIANG, D. & WILUSZ, J. E. 2014. Short intronic repeat sequences facilitate circular RNA production. *Genes & development*, 28, 2233-2247.

LIANG, Z., WANG, W., HU, Q., ZHOU, P., ZHANG, Y., TANG, Y., WU, Q., FU, Y., LI, X., SHAO, Y. & JIANG, L. 2022. Pulmonary large cell carcinoma with neuroendocrine morphology shows genetic similarity to large cell neuroendocrine carcinoma. *Diagnostic Pathology*, 17, 26.

LIAO, B.-C., GRIESING, S. & YANG, J. C.-H. 2019. Second-line treatment of EGFR T790M-negative non-small cell lung cancer patients. *Therapeutic advances in medical oncology*, 11, 1758835919890286-1758835919890286.

LIM, Z.-F. & MA, P. C. 2019. Emerging insights of tumor heterogeneity and drug resistance mechanisms in lung cancer targeted therapy. *Journal of Hematology & Oncology*, 12, 134.

LIN, C.-C., SHIH, J.-Y., YU, C.-J., HO, C.-C., LIAO, W.-Y., LEE, J.-H., TSAI, T.-H., SU, K.-Y., HSIEH, M.-S. & CHANG, Y.-L. 2018. Outcomes in patients with non-small-cell lung cancer and acquired Thr790Met mutation treated with osimertinib: a genomic study. *The Lancet Respiratory medicine*, 6, 107-116.

LINDA, M. O. K., GEMMA, T., RACHEL, R. H., PAUL, M., MARK, W. & SANNE, A. E. P. 2018. Smoking as a risk factor for lung cancer

in women and men: a systematic review and meta-analysis. *BMJ Open*, 8, e021611.

LIU, C.-X. & CHEN, L.-L. 2022. Circular RNAs: Characterization, cellular roles, and applications. *Cell*, 185, 2016-2034.

LIU, D., CONN, V., GOODALL, G. J. & CONN, S. J. 2018. A highly efficient strategy for overexpressing circRNAs. *Circular RNAs: Methods and Protocols*, 97-105.

LIU, D., MEISTER, M., ZHANG, S., VONG, C.-I., WANG, S., FANG, R., LI, L., WANG, P. G., MASSION, P. & JI, X. 2020. Identification of lipid biomarker from serum in patients with chronic obstructive pulmonary disease. *Respiratory Research*, 21, 242.

LIU, F., COX, C. D., CHOWDHURY, R., DOVEK, L., NGUYEN, H., LI, T., LI, S., OZER, B., CHOU, A., NGUYEN, N., WEI, B., ANTONIOS, J., SOTO, H., KORNBLUM, H., LIAU, L., PRINS, R., NGHIEMPHU, P. L., YONG, W., CLOUGHESY, T. & LAI, A. 2019. SPINT2 is hypermethylated in both IDH1 mutated and wild-type glioblastomas, and exerts tumor suppression via reduction of c-Met activation. *J Neurooncol*, 142, 423-434.

LIU, J., LIU, T., WANG, X. & HE, A. 2017. Circles reshaping the RNA world: from waste to treasure. *Molecular Cancer*, 16, 58.

LIU, J., ZHU, H., FU, L. & XU, T. 2021a. Investigating the underlying mechanisms of circular RNAs and their application in clinical research of cervical cancer. *Frontiers in Genetics*, 12, 653051.

LIU, Q., YU, S., ZHAO, W., QIN, S., CHU, Q. & WU, K. 2018b. EGFR-TKIs resistance via EGFR-independent signaling pathways. *Molecular Cancer*, 17, 53.

LIU, S., JIANG, Z., XIAO, P., LI, X., CHEN, Y., TANG, H., CHAI, Y., LIU, Y., ZHU, Z., XIE, Q., HE, W., MA, Y., JIN, L. & FENG, W. 2022a. Hsa_circ_0005576 promotes osimertinib resistance through the miR-512-5p/IGF1R axis in lung adenocarcinoma cells. *Cancer Sci*, 113, 79-90.

LIU, X. Y., ZHANG, Q., GUO, J., ZHANG, P., LIU, H., TIAN, Z. B., ZHANG, C. P. & LI, X. Y. 2021b. The Role of Circular RNAs in the Drug Resistance of Cancers. *Front Oncol*, 11, 790589.

LIU, X., SHAN, W., LI, T., GAO, X., KONG, F., YOU, H., KONG, D., QIAO, S. & TANG, R. 2021. Cellular retinol binding protein-1 inhibits cancer stemness via upregulating WIF1 to suppress Wnt/ β -catenin pathway in hepatocellular carcinoma. *BMC Cancer*, 21, 1224.

LIU, Y., LAI, M., LI, S., WANG, Y., FENG, F., ZHANG, T., TONG, L., ZHANG, M., CHEN, H., CHEN, Y., SONG, P., LI, Y., BAI, G.,

NING, Y., TANG, H., FANG, Y., CHEN, Y., LU, X., GENG, M., DING, K., YU, K., XIE, H. & DING, J. 2022b. LS-106, a novel EGFR inhibitor targeting C797S, exhibits antitumor activities both in vitro and in vivo. *Cancer Sci*, 113, 709-720.

LONE, S. N., NISAR, S., MASOODI, T., SINGH, M., RIZWAN, A., HASHEM, S., EL-RIFAI, W., BEDOGNETTI, D., BATRA, S. K., HARIS, M., BHAT, A. A. & MACHA, M. A. 2022. Liquid biopsy: a step closer to transform diagnosis, prognosis and future of cancer treatments. *Molecular Cancer*, 21, 79.

LOU, J., HAO, Y., LIN, K., LYU, Y., CHEN, M., WANG, H., ZOU, D., JIANG, X., WANG, R. & JIN, D. 2020. Circular RNA CDR1as disrupts the p53/MDM2 complex to inhibit Gliomagenesis. *Molecular cancer*, 19, 1-19.

LU, W. & KANG, Y. 2019. Epithelial-Mesenchymal Plasticity in Cancer Progression and Metastasis. *Developmental Cell*, 49, 361-374.

LUO, J., OSTREM, J., PELLINI, B., IMBODY, D., STERN, Y., SOLANKI, H. S., HAURA, E. B. & VILLARUZ, L. C. 2022. Overcoming KRAS-Mutant Lung Cancer. *American Society of Clinical Oncology Educational Book*, 700-710.

LUO, Y. H., YANG, Y. P., CHIEN, C. S., YARMISHYN, A. A., ISHOLA, A. A., CHIEN, Y., CHEN, Y. M., HUANG, T. W., LEE, K. Y., HUANG, W. C., TSAI, P. H., LIN, T. W., CHIOU, S. H., LIU, C. Y., CHANG, C. C., CHEN, M. T. & WANG, M. L. 2020. Plasma Level of Circular RNA hsa_circ_0000190 Correlates with Tumor Progression and Poor Treatment Response in Advanced Lung Cancers. *Cancers*, 12(7), p.1740.

LUSARDI, T. A., PHILLIPS, J. I., WIEDRICK, J. T., HARRINGTON, C. A., LIND, B., LAPIDUS, J. A., QUINN, J. F. & SAUGSTAD, J. A. 2017. MicroRNAs in Human Cerebrospinal Fluid as Biomarkers for Alzheimer's Disease. *J Alzheimers Dis*, 55, 1223-1233.

LUSHNIAK, B.D., SAMET, J.M., PECHACEK, T.F., NORMAN, L.A. and TAYLOR, P.A., 2014. The health consequences of smoking—50 years of progress: A report of the surgeon general.

MA, D., LIU, H., QIN, Y., LI, D., CUI, Y., LI, L., HE, J., CHEN, Y. & ZHOU, X. 2020a. Circ_0007142/miR-186/FOXK1 axis promoted lung adenocarcinoma progression. *American Journal of Translational Research*, 12, 4728.

MA, J., QI, G. & LI, L. 2020. A Novel Serum Exosomes-Based Biomarker hsa_circ_0002130 Facilitates Osimertinib-Resistance in Non-Small Cell Lung Cancer by Sponging miR-498. *OncoTargets and therapy*, 13, 5293-5307.

MA, S., KONG, S., WANG, F. & JU, S. 2020b. CircRNAs: biogenesis, functions, and role in drug-resistant Tumours. *Mol Cancer*, 19, 119.

MA, X. K., WANG, M. R., LIU, C. X., DONG, R., CARMICHAEL, G. G., CHEN, L. L. & YANG, L. 2019. CIRCexplorer3: A CLEAR Pipeline for Direct Comparison of Circular and Linear RNA Expression. *Genomics Proteomics Bioinformatics*, 17, 511-521.

MA, Z., LIU, D., LI, W., DI, S., ZHANG, Z., ZHANG, J., XU, L., GUO, K., ZHU, Y., HAN, J., LI, X. & YAN, X. 2019. STYK1 promotes tumor growth and metastasis by reducing SPINT2/HAI-2 expression in non-small cell lung cancer. *Cell Death & Disease*, 10, 435.

MALKA-MAHIEU, H., NEWMAN, M., DÉSAUBRY, L., ROBERT, C. & VAGNER, S. 2017. Molecular Pathways: The eIF4F Translation Initiation Complex—New Opportunities for Cancer Treatment. *Clinical Cancer Research*, 23, 21-25.

MARINELLI, D., SIRINGO, M., METRO, G., RICCIUTI, B. & GELIBTER, A. J. 2022. Non-small-cell lung cancer: how to manage ALK-, ROS1- and NTRK-rearranged disease. *Drugs Context*, 11.

MARTIN, T. A., YE, L., SANDERS, A. J., LANE, J. & JIANG, W. G. 2013. Cancer invasion and metastasis: molecular and cellular perspective. *Madame Curie Bioscience Database [Internet]*. Landes Bioscience.

MARTINEZ-DOMINGUEZ, M. V., ZOTTEL, A., ŠAMEC, N., JOVČEVSKA, I., DINCER, C., KAHLERT, U. D. & NICKEL, A.-C. 2021. Current Technologies for RNA-Directed Liquid Diagnostics. *Cancers*, 13, 5060.

MATTICK, J. S., AMARAL, P. P., CARNINCI, P., CARPENTER, S., CHANG, H. Y., CHEN, L.-L., CHEN, R., DEAN, C., DINGER, M. E., FITZGERALD, K. A., GINGERAS, T. R., GUTTMAN, M., HIROSE, T., HUARTE, M., JOHNSON, R., KANDURI, C., KAPRANOV, P., LAWRENCE, J. B., LEE, J. T., MENDELL, J. T., MERCER, T. R., MOORE, K. J., NAKAGAWA, S., RINN, J. L., SPECTOR, D. L., ULITSKY, I., WAN, Y., WILUSZ, J. E. & WU, M. 2023. Long non-coding RNAs: definitions, functions, challenges and recommendations. *Nature Reviews Molecular Cell Biology*, 24, 430-447.

MCCUNNEY, R. J. & YONG, M. 2022. Coal Miners and Lung Cancer: Can Mortality Studies Offer a Perspective on Rat Inhalation Studies of Poorly Soluble Low Toxicity Particles? *Front Public Health*, 10, 907157.

MECOZZI, N., NENCI, A., VERA, O., BOK, I., FALZONE, A., DENICOLA, G. M. & KARRETH, F. A. 2022. Genetic tools for the stable overexpression of circular RNAs. *RNA Biol*, 19, 353-363.

MENG, Q., LI, Y., SUN, Z. & YANG, X. 2022. CircRNA hsa_circ_0070659 predicts poor prognosis and promotes non-small cell lung cancer (NSCLC) progression via microRNA-377 (miR-377) / Ras-Associated Binding Protein 3C (RAB3C) pathway. *Bioengineered*, 13, 14578-14594.

MENG, S., ZHOU, H., FENG, Z., XU, Z., TANG, Y., LI, P. & WU, M. 2017. CircRNA: functions and properties of a novel potential biomarker for cancer. *Mol Cancer*, 16, 94.

MENG, S., ZHOU, H., FENG, Z., XU, Z., TANG, Y., LI, P. & WU, M. 2017. CircRNA: functions and properties of a novel potential biomarker for cancer. *Mol Cancer*, 16, 94.

METIBEMU, D. S., AKINLOYE, O. A., AKAMO, A. J., OJO, D. A., OKEOWO, O. T. & OMOTUYI, I. O. 2019. Exploring receptor tyrosine kinases-inhibitors in Cancer treatments. *Egyptian Journal of Medical Human Genetics*, 20, 35.

MEYER, K. D. 2019. m(6)A-mediated translation regulation. *Biochim Biophys Acta Gene Regul Mech*, 1862, 301-309.

MINARI, R., BORDI, P. & TISEO, M. 2016. Third-generation epidermal growth factor receptor-tyrosine kinase inhibitors in T790M-positive non-small cell lung cancer: review on emerged mechanisms of resistance. *Translational Lung Cancer Research*, 5, 695-708.

MISIR, S., WU, N. & YANG, B. B. 2022. Specific expression and functions of circular RNAs. *Cell Death Differ*, 29, 481-491.

MITSDOMI, T., MORITA, S., YATABE, Y., NEGORO, S., OKAMOTO, I., TSURUTANI, J., SETO, T., SATOUCHI, M., TADA, H., HIRASHIMA, T., ASAMI, K., KATAKAMI, N., TAKADA, M., YOSHIOKA, H., SHIBATA, K., KUDOH, S., SHIMIZU, E., SAITO, H., TOYOOKA, S., NAKAGAWA, K. & FUKUOKA, M. 2010. Gefitinib versus cisplatin plus docetaxel in patients with non-small-cell lung cancer harbouring mutations of the epidermal growth factor receptor (WJTOG3405): an open label, randomised phase 3 trial. *Lancet Oncol*, 11, 121-8.

MODRZEJEWSKI, D., HARTUNG, F., LEHNERT, H., SPRINK, T., KOHL, C., KEILWAGEN, J. & WILHELM, R. 2020. Which Factors Affect the Occurrence of Off-Target Effects Caused by the Use of CRISPR/Cas: A Systematic Review in Plants. *Front Plant Sci*, 11, 574959.

MOOSAVI, L. & POLINENI, R. 2022. Afatinib. *StatPearls [Internet]*. StatPearls Publishing.

MOREIRA, A.L., OCAMPO, P.S., XIA, Y., ZHONG, H., RUSSELL, P.A., MINAMI, Y., COOPER, W.A., YOSHIDA, A., BUBENDORF,

- L., PAPOTTI, M. and PELOSI, G., 2020. A grading system for invasive pulmonary adenocarcinoma: a proposal from the International Association for the Study of Lung Cancer Pathology Committee. *Journal of Thoracic Oncology*, 15(10), pp.1599-1610.
- MOTAZEDI, E., FINKERS, R., MALIEPAARD, C. & DE RIDDER, D. 2017. Exploiting next-generation sequencing to solve the haplotyping puzzle in polyploids: a simulation study. *Briefings in Bioinformatics*, 19, 387-403.
- MÜLLER, S., WEDLER, A., BREUER, J., GLAS, M., BLEY, N., LEDERER, M., HAASE, J., MISIAK, C., FUCHS, T. & OTTMANN, A. 2020. Synthetic circular miR-21 RNA decoys enhance tumor suppressor expression and impair tumor growth in mice. *NAR cancer*, 2, zcaa014.
- MUNIZ, L., NICOLAS, E. & TROUCHE, D. 2021. RNA polymerase II speed: a key player in controlling and adapting transcriptome composition. *Embo j*, 40, e105740.
- MURPHREY, M. B., QUAIM, L. & VARACALLO, M. 2018. *Biochemistry, Epidermal Growth Factor Receptor*.
- MYERS, D. J. & WALLEN, J. M. 2023. Lung adenocarcinoma. *StatPearls [Internet]*. StatPearls Publishing.
- NACCACHE, J. M., GIBIOT, Q., MONNET, I., ANTOINE, M., WISLEZ, M., CHOUAID, C. & CADRANEL, J. 2018. Lung cancer and interstitial lung disease: a literature review. *J Thorac Dis*, 10, 3829-3844.
- NAGANO, T., TACHIHARA, M. & NISHIMURA, Y. 2019. Dacomitinib, a second-generation irreversible epidermal growth factor receptor tyrosine kinase inhibitor (EGFR-TKI) to treat non-small cell lung cancer. *Drugs Today (Barc)*, 55, 231-236.
- NAGASAKA, M., UDDIN, M. H., AL-HALLAK, M. N., RAHMAN, S., BALASUBRAMANIAN, S., SUKARI, A. & AZMI, A. S. 2021. Liquid biopsy for therapy monitoring in early-stage non-small cell lung cancer. *Molecular Cancer*, 20, 82.
- NAN, A., CHEN, L., ZHANG, N., JIA, Y., LI, X., ZHOU, H., LING, Y., WANG, Z., YANG, C., LIU, S. & JIANG, Y. 2019. Circular RNA circNOL10 Inhibits Lung Cancer Development by Promoting SCLM1-Mediated Transcriptional Regulation of the Humanin Polypeptide Family. *Adv Sci (Weinh)*, 6, 1800654.
- NEDOLUZHKO, A., SHARKO, F., RBBANI, M. G., TESLYUK, A., KONSTANTINIDIS, I. & FERNANDES, J. M. O. 2020. CircParser: a novel streamlined pipeline for circular RNA structure and host gene prediction in non-model organisms. *PeerJ*, 8, e8757.

NELSON, J., SORENSEN, E. W., MINTRI, S., RABIDEAU, A. E., ZHENG, W., BESIN, G., KHATWANI, N., SU, S. V., MIRACCO, E. J., ISSA, W. J., HOGE, S., STANTON, M. G. & JOYAL, J. L. 2020. Impact of mRNA chemistry and manufacturing process on innate immune activation. *Sci Adv*, 6, eaaz6893.

NG, W. L., MARINOV, G. K., LIAU, E. S., LAM, Y. L., LIM, Y.-Y. & EA, C.-K. 2016. Inducible RasGEF1B circular RNA is a positive regulator of ICAM-1 in the TLR4/LPS pathway. *RNA Biology*, 13, 861-871.

NGUYEN, K. S., KOBAYASHI, S. & COSTA, D. B. 2009. Acquired resistance to epidermal growth factor receptor tyrosine kinase inhibitors in non-small-cell lung cancers dependent on the epidermal growth factor receptor pathway. *Clin Lung Cancer*, 10, 281-9.

NICHOLSON, A. G., TSAO, M. S., BEASLEY, M. B., BORCZUK, A. C., BRAMBILLA, E., COOPER, W. A., DACIC, S., JAIN, D., KERR, K. M. & LANTUEJOUL, S. 2022. The 2021 WHO classification of lung tumors: impact of advances since 2015. *Journal of Thoracic Oncology*, 17, 362-387.

NIELSEN, A. F., BINDEREIF, A., BOZZONI, I., HANAN, M., HANSEN, T. B., IRIMIA, M., KADENER, S., KRISTENSEN, L. S., LEGNINI, I., MORLANDO, M., JARLSTAD OLESEN, M. T., PASTERKAMP, R. J., PREIBISCH, S., RAJEWSKY, N., SUENKEL, C. & KJEMS, J. 2022. Best practice standards for circular RNA research. *Nat Methods*, 19, 1208-1220.

NILSSON, F. O., GAL, P., HOUISSE, I., IVANOVA, J. I. & ASANIN, S. T. 2021. The cost-effectiveness of dacomitinib in first-line treatment of advanced/metastatic epidermal growth factor receptor mutation-positive non-small-cell lung cancer (EGFR m NSCLC) in Sweden. *Journal of Medical Economics*, 24, 447-457.

NING, J., GE, T., JIANG, M., JIA, K., WANG, L., LI, W., CHEN, B., LIU, Y., WANG, H., ZHAO, S. & HE, Y. 2021. Early diagnosis of lung cancer: which is the optimal choice? *Aging (Albany NY)*, 13, 6214-6227.

NOORELDEEN, R. & BACH, H. 2021. Current and Future Development in Lung Cancer Diagnosis. *Int J Mol Sci*, 22.

OBI, P. & CHEN, Y. G. 2021. The design and synthesis of circular RNAs. *Methods*, 196, 85-103.

OH, S. & KIM, T. M. 2024. Histological transformation to small-cell carcinoma. *Nature Reviews Cancer*, 24, 447-447.

OLSSON, A. & KROMHOUT, H. 2021. Occupational cancer burden: the contribution of exposure to process-generated substances at the workplace. *Molecular Oncology*, 15, 753-763.

OU, S.-H. I., HONG, J.-L., CHRISTOPOULOS, P., LIN, H. M., VINCENT, S., CHURCHILL, E. N., SOEDA, J., KAZDAL, D., STENZINGER, A. & THOMAS, M. 2023. Distribution and detectability of EGFR exon 20 insertion variants in NSCLC. *Journal of Thoracic Oncology*, 18, 744-754.

PAIK, P. K., PILLAI, R. N., LATHAN, C. S., VELASCO, S. A. & PAPADIMITRAKOPOULOU, V. 2019. New Treatment Options in Advanced Squamous Cell Lung Cancer. *American Society of Clinical Oncology Educational Book*, e198-e206.

PALAZ, F., KALKAN, A. K., CAN, Ö., DEMIR, A. N., TOZLUYURT, A., ÖZCAN, A. & OZSOZ, M. 2021. CRISPR-Cas13 System as a Promising and Versatile Tool for Cancer Diagnosis, Therapy, and Research. *ACS Synthetic Biology*, 10, 1245-1267.

PAN, J., XING, J., YU, H., WANG, Z., WANG, W. & PAN, Y. 2023. CircRBM33 promotes migration, invasion and mediates osimertinib resistance in non-small cell lung cancer cell line. *Annals of Translational Medicine*, 11, 252.

PAN, M., SCHINKE, H., LUXENBURGER, E., KRANZ, G., SHAKHTOUR, J., LIBL, D., HUANG, Y., GABER, A., PAVŠIČ, M., LENARČIČ, B., KITZ, J., JAKOB, M., SCHWENK-ZIEGER, S., CANIS, M., HESS, J., UNGER, K., BAUMEISTER, P. & GIRES, O. 2018. EpCAM ectodomain EpEX is a ligand of EGFR that counteracts EGF-mediated epithelial-mesenchymal transition through modulation of phospho-ERK1/2 in head and neck cancers. *PLoS biology*, 16, e2006624-e2006624.

PANDA, A. C. & GOROSPE, M. 2018. Detection and Analysis of Circular RNAs by RT-PCR. *Bio-protocol*, 8(6), pp.e2775-e2775.

PANDEY, P. R., MUNK, R., KUNDU, G., DE, S., ABDELMOHSEN, K. & GOROSPE, M. 2020. Methods for analysis of circular RNAs. *Wiley Interdiscip Rev RNA*, 11(1), p.e1566.

PANDEY, P. R., ROUT, P. K., DAS, A., GOROSPE, M. & PANDA, A. C. 2019. RPAD (RNase R treatment, polyadenylation, and poly(A)+ RNA depletion) method to isolate highly pure circular RNA. *Methods*, 155, 41-48.

PAPADIMITRAKOPOULOU, V., MOK, T., HAN, J.-Y., AHN, M.-J., DELMONTE, A., RAMALINGAM, S., KIM, S., SHEPHERD, F., LASKIN, J. & HE, Y. 2020. Osimertinib versus platinum–pemetrexed for patients with EGFR T790M advanced NSCLC and progression on a prior EGFR-tyrosine kinase inhibitor: AURA3 overall survival analysis. *Annals of Oncology*, 31, 1536-1544.

PAPATSIROU, M., ARTEMAKI, P. I., KAROUSI, P., SCORILAS, A. & KONTOS, C. K. 2021. Circular RNAs: Emerging Regulators of the

Major Signaling Pathways Involved in Cancer Progression. *Cancers (Basel)*, 13.

PAPINI, F., SUNDARESAN, J., LEONETTI, A., TISEO, M., ROLFO, C., PETERS, G. J. & GIOVANNETTI, E. 2021. Hype or hope – Can combination therapies with third-generation EGFR-TKIs help overcome acquired resistance and improve outcomes in EGFR-mutant advanced/metastatic NSCLC? *Critical Reviews in Oncology/Hematology*, 166, 103454.

PARK, E.-H., WALKER, S. E., ZHOU, F., LEE, J. M., RAJAGOPAL, V., LORSCH, J. R. & HINNEBUSCH, A. G. 2013. Yeast Eukaryotic Initiation Factor 4B (eIF4B) Enhances Complex Assembly between eIF4A and eIF4G in Vivo*. *Journal of Biological Chemistry*, 288, 2340-2354.

PARK, J. Y., JANG, S. H., KIM, H. I., KIM, J.-H., PARK, S., HWANG, Y. I., JUNG, K.-S., SEO, J., LEE, C. Y., KO, Y. & PARK, Y.-B. 2019. Thyroid transcription factor-1 as a prognostic indicator for stage IV lung adenocarcinoma with and without EGFR-sensitizing mutations. *BMC Cancer*, 19, 574.

PASSARO, A., LEIGHL, N., BLACKHALL, F., POPAT, S., KERR, K., AHN, M., ARCILA, M., ARRIETA, O., PLANCHARD, D. & DE MARINIS, F. 2022. ESMO expert consensus statements on the management of EGFR mutant non-small-cell lung cancer. *Annals of Oncology*, 33, 466-487.

PATOP, I. L., WÜST, S. & KADENER, S. 2019. Past, present, and future of circRNAs. *Embo j*, 38, e100836.

PEI, X., CHEN, S.-W., LONG, X., ZHU, S.-Q., QIU, B.-Q., LIN, K., LU, F., XU, J.-J., ZHANG, P.-F. & WU, Y.-B. J. A. 2020. circMET promotes NSCLC cell proliferation, metastasis, and immune evasion by regulating the miR-145-5p/CXCL3 axis. 12, 13038.

PENG, J. F., ZHUANG, Y. Y., HUANG, F. T. & ZHANG, S. N. 2016. Noncoding RNAs and pancreatic cancer. *World J Gastroenterol*, 22, 801-14.

PENG, Z., HU, Q., FANG, S., ZHANG, X., HONG, X., TAO, L., PAN, J., JIANG, M., BAI, H., WU, Y., ZHAO, X., ZHOU, C., CHEN, J., HAN, Y. & GONG, Z. 2021. Circulating circTOLLIP serves as a diagnostic biomarker for liquid biopsy in non-small cell lung cancer. *Clinica Chimica Acta*, 523, 415-422.

PETRELLA, F., RIZZO, S., ATTILI, I., PASSARO, A., ZILLI, T., MARTUCCI, F., BONOMO, L., DEL GRANDE, F., CASIRAGHI, M., DE MARINIS, F. & SPAGGIARI, L. 2023. Stage III Non-Small-Cell Lung Cancer: An Overview of Treatment Options. *Curr Oncol*, 30, 3160-3175.

PIOTROWSKA, Z., ISOZAKI, H., LENNERZ, J. K., GAINOR, J. F., LENNES, I. T., ZHU, V. W., MARCOUX, N., BANWAIT, M. K., DIGUMARTHY, S. R., SU, W., YODA, S. 2018. Landscape of Acquired Resistance to Osimertinib in EGFR-Mutant NSCLC and Clinical Validation of Combined EGFR and RET Inhibition with Osimertinib and BLU-667 for Acquired RET Fusion. *Cancer Discovery*, 8, 1529-1539.

PISIGNANO, G., MICHAEL, D. C., VISAL, T. H., PIRLOG, R., LADOMERY, M. & CALIN, G. A. 2023. Going circular: history, present, and future of circRNAs in cancer. *Oncogene*, 42, 2783-2800.

PLANCHARD, D., POPAT, S., KERR, K., NOVELLO, S., SMIT, E., FAIVRE-FINN, C., MOK, T., RECK, M., VAN SCHIL, P. & HELLMANN, M. 2018. Metastatic non-small cell lung cancer: ESMO Clinical Practice Guidelines for diagnosis, treatment and follow-up. *Annals of Oncology*, 29, iv192-iv237.

POH, M.-E., LIAM, C.-K., RAJADURAI, P. & CHAI, C.-S. 2018. Epithelial-to-mesenchymal transition (EMT) causing acquired resistance to afatinib in a patient with epidermal growth factor receptor (EGFR)-mutant lung adenocarcinoma. *Journal of thoracic disease*, 10, E560-E563.

PRATS, A. C., DAVID, F., DIALLO, L. H., ROUSSEL, E., TATIN, F., GARMY-SUSINI, B. & LACAZETTE, E. 2020. Circular RNA, the Key for Translation. *Int J Mol Sci*, 21.

PRETELLI, G., SPAGNOLO, C. C., CIAPPINA, G., SANTARPIA, M. & PASELLO, G. 2023. Overview on Therapeutic Options in Uncommon EGFR Mutant Non-Small Cell Lung Cancer (NSCLC): New Lights for an Unmet Medical Need. *Int J Mol Sci*, 24.

PURBA, E. R., SAITA, E. I. & MARUYAMA, I. N. 2017. Activation of the EGF receptor by ligand binding and oncogenic mutations: the “rotation model”. *Cells*, 6(2), p.13.

QIN, Y., JIAN, H., TONG, X., WU, X., WANG, F., SHAO, Y. W. & ZHAO, X. 2020. Variability of EGFR exon 20 insertions in 24 468 Chinese lung cancer patients and their divergent responses to EGFR inhibitors. *Mol Oncol*, 14, 1695-1704.

QIU, M., XIA, W., CHEN, R., WANG, S., XU, Y., MA, Z., XU, W., ZHANG, E., WANG, J. & FANG, T. J. C. R. 2018. The circular RNA circPRKCI promotes tumor growth in lung adenocarcinoma. 78, 2839-2851.

QUAN, G. & LI, J. 2018. Circular RNAs: biogenesis, expression and their potential roles in reproduction. *Journal of ovarian research*, 11, pp.1-12.

RADANOVA, M., MIHAYLOVA, G., NAZIFOVA-TASINOVA, N., LEVKOVA, M., TASINOV, O., IVANOVA, D., MIHAYLOVA, Z. & DONEV, I. 2021. Oncogenic Functions and Clinical Significance of Circular RNAs in Colorectal Cancer. *Cancers (Basel)*, 13.

RAGAN, C., GOODALL, G. J., SHIROKIKH, N. E. & PREISS, T. 2019. Insights into the biogenesis and potential functions of exonic circular RNA. *Sci Rep*, 9, 2048.

RAJADURAI, P., YAP, N. Y., MOHAMED YOUSOOF, S. B. & CHEAH, Y. K. 2023. Mutational Profiling of Lung Cancer Using Next Generation Sequencing: A Malaysian Real-World Clinical Diagnostic Experience. *Journal of Molecular Pathology*, 4, 31-43.

RAJDEV, K., SIDDIQUI, A. H., IBRAHIM, U., PATIBANDLA, P., KHAN, T. & EL-SAYEGH, D. 2018. An Unusually Aggressive Large Cell Carcinoma of the Lung: Undiagnosed until Autopsy. *Cureus*, 10, e2202.

RAO, G., PIEROBON, M., KIM, I.-K., HSU, W.-H., DENG, J., MOON, Y.-W., PETRICOIN, E. F., ZHANG, Y.-W., WANG, Y. & GIACCONE, G. 2017. Inhibition of AKT1 signaling promotes invasion and metastasis of non-small cell lung cancer cells with K-RAS or EGFR mutations. *Scientific Reports*, 7, 7066.

REGUART, N., CARDONA, A. F. & ROSELL, R. 2010. Role of erlotinib in first-line and maintenance treatment of advanced non-small-cell lung cancer. *Cancer management and research*, 143-156.

REITA, D., PABST, L., PENCREACH, E., GUÉRIN, E., DANO, L., RIMELEN, V., VOEGELI, A. C., VALLAT, L., MASCAUX, C. & BEAU-FALLER, M. 2021. Molecular Mechanism of EGFR-TKI Resistance in EGFR-Mutated Non-Small Cell Lung Cancer: Application to Biological Diagnostic and Monitoring. *Cancers (Basel)*, 13.

REMON, J., STEUER, C. E., RAMALINGAM, S. S. & FELIP, E. 2018. Osimertinib and other third-generation EGFR TKI in EGFR-mutant NSCLC patients. *Ann Oncol*, 29, i20-i27.

REN, G., ZHAO, Q., YAN, C., XUE, Q. & ZHANG, L. 2020. Circular RNA circZFR promotes tumorigenic capacity of lung cancer via CCND1. *Translational Cancer Research*, 9, 3303.

REN, X.-D., SU, N., SUN, X.-G., LI, W.-M., LI, J., LI, B.-W., LI, R.-X., LV, J., XU, Q.-Y., KONG, W.-L. & HUANG, Q. 2023. Chapter Four - Advances in liquid biopsy-based markers in NSCLC. *In: MAKOWSKI, G. S. (ed.) Advances in Clinical Chemistry*. (Vol. 114, pp. 109-150). Elsevier.

REN, Y., MANOHARAN, T., LIU, B., CHENG, C. Z. M., EN SIEW, B., CHEONG, W. K., LEE, K. Y., TAN, I. J., LIESKE, B., TAN, K. K.

& CHIA, G. 2024. Circular RNA as a source of neoantigens for cancer vaccines. *J Immunother Cancer*, 12 (3).

REPLOGLE, J. M., BONNAR, J. L., POGSON, A. N., LIEM, C. R., MAIER, N. K., DING, Y., RUSSELL, B. J., WANG, X., LENG, K., GUNA, A., NORMAN, T. M., PAK, R. A., RAMOS, D. M., WARD, M. E., GILBERT, L. A., KAMPMANN, M., WEISSMAN, J. S. & JOST, M. 2022. Maximizing CRISPRi efficacy and accessibility with dual-sgRNA libraries and optimal effectors. *eLife*, 11, e81856.

RIBATTI, D., TAMMA, R. & ANNESE, T. 2020. Epithelial-Mesenchymal Transition in Cancer: A Historical Overview. *Transl Oncol*, 13, 100773.

RICCIUTI, B. & CHIARI, R. 2018. First line osimertinib for the treatment of patients with advanced EGFR-mutant NSCLC. *Transl Lung Cancer Res*, 7, S127-s130.

RICCIUTI, B., BAGLIVO, S., DE GIGLIO, A. & CHIARI, R. 2018. Afatinib in the first-line treatment of patients with non-small cell lung cancer: clinical evidence and experience. *Ther Adv Respir Dis*, 12, 1753466618808659.

RICHARDSON, A. M., HAVEL, L. S., KOYEN, A. E., KONEN, J. M., SHUPE, J., WILES, W. G. T., MARTIN, W. D., GROSSNIKLAUS, H. E., SICA, G., GILBERT-ROSS, M. & MARCUS, A. I. 2018. Vimentin Is Required for Lung Adenocarcinoma Metastasis via Heterotypic Tumor Cell-Cancer-Associated Fibroblast Interactions during Collective Invasion. *Clinical cancer research : an official journal of the American Association for Cancer Research*, 24, 420-432.

RIUDAVETS, M., GARCIA DE HERREROS, M., BESSE, B. & MEZQUITA, L. 2022. Radon and Lung Cancer: Current Trends and Future Perspectives. *Cancers (Basel)*, 14.

RIVLIN, N., BROSH, R., OREN, M. & ROTTER, V. 2011. Mutations in the p53 Tumor Suppressor Gene: Important Milestones at the Various Steps of Tumorigenesis. *Genes & cancer*, 2, 466-474.

RODRÍGUEZ, M., AJONA, D., SEIJO, L. M., SANZ, J., VALENCIA, K., CORRAL, J., MESA-GUZMÁN, M., PÍO, R., CALVO, A., LOZANO, M. D., ZULUETA, J. J. & MONTUENGA, L. M. 2021. Molecular biomarkers in early stage lung cancer. *Transl Lung Cancer Res*, 10, 1165-1185.

RÖNNAU, C., VERHAEGH, G., LUNA-VELEZ, M. & SCHALKEN, J. 2014. Noncoding RNAs as novel biomarkers in prostate cancer. *BioMed research international*, 2014(1), p.591703.

ROSELL, R., CARCERENY, E., GERVAIS, R., VERGNENEGRE, A., MASSUTI, B., FELIP, E., PALMERO, R., GARCIA-GOMEZ, R.,

PALLARES, C., SANCHEZ, J. M., PORTA, R., COBO, M., GARRIDO, P., LONGO, F., MORAN, T., INSA, A., DE MARINIS, F., CORRE, R., BOVER, I., ILLIANO, A., DANSIN, E., DE CASTRO, J., MILELLA, M., REGUART, N., ALTAVILLA, G., JIMENEZ, U., PROVENCIO, M., MORENO, M. A., TERRASA, J., MUÑOZ-LANGA, J., VALDIVIA, J., ISLA, D., DOMINE, M., MOLINIER, O., MAZIERES, J., BAIZE, N., GARCIA-CAMPELO, R., ROBINET, G., RODRIGUEZ-ABREU, D., LOPEZ-VIVANCO, G., GEBBIA, V., FERRERA-DELGADO, L., BOMBARON, P., BERNABE, R., BEARZ, A., ARTAL, A., CORTESI, E., ROLFO, C., SANCHEZ-RONCO, M., DROZDOWSKYJ, A., QUERALT, C., DE AGUIRRE, I., RAMIREZ, J. L., SANCHEZ, J. J., MOLINA, M. A., TARON, M. & PAZ-ARES, L. 2012. Erlotinib versus standard chemotherapy as first-line treatment for European patients with advanced EGFR mutation-positive non-small-cell lung cancer (EURTAC): a multicentre, open-label, randomised phase 3 trial. *Lancet Oncol*, 13, 239-46.

ROTOW, J. K., LEE, J. K., MADISON, R. W., OXNARD, G. R., JÄNNE, P. A. & SCHROCK, A. B. 2024. Real-World Genomic Profile of EGFR Second-Site Mutations and Other Osimertinib Resistance Mechanisms and Clinical Landscape of NSCLC Post-Osimertinib. *J Thorac Oncol*, 19, 227-239.

RUAN, H., WANG, P.-C. & HAN, L. 2023. Characterization of circular RNAs with advanced sequencing technologies in human complex diseases. *WIREs RNA*, 14, e1759.

RUSSO, A., FRANCHINA, T., RICCIARDI, G., BATTAGLIA, A., PICCIOTTO, M. & ADAMO, V. 2019. Heterogeneous Responses to Epidermal Growth Factor Receptor (EGFR) Tyrosine Kinase Inhibitors (TKIs) in Patients with Uncommon EGFR Mutations: New Insights and Future Perspectives in this Complex Clinical Scenario. *International Journal of Molecular Sciences*, 20, 1431.

SABBULA, B. R., GASALBERTI, D. P. & ANJUM, F. 2023. Squamous cell lung cancer. *StatPearls [Internet]*. StatPearls Publishing.

SAITO, S., ESPINOZA-MERCADO, F., LIU, H., SATA, N., CUI, X. & SOUKIASIAN, H. J. 2017. Current status of research and treatment for non-small cell lung cancer in never-smoking females. *Cancer Biol Ther*, 18, 359-368.

SALIFU, I., SINGH, N., BERRAONDO, M., REMON, J., SALIFU, S., SEVERSON, E., QUINTANA, A., PEIRÓ, S., RAMKISSOON, S., VIDAL, L., CHICO, I. & SAINI, K. S. 2023. Antibody-drug conjugates, immune-checkpoint inhibitors, and their combination in advanced non-small cell lung cancer. *Cancer Treatment and Research Communications*, 36, 100713.

SALZMAN, J., GAWAD, C., WANG, P. L., LACAYO, N. & BROWN, P. O. 2012. Circular RNAs are the predominant transcript isoform from hundreds of human genes in diverse cell types. *PLoS one*, 7, e30733.

SANCHEZ RIOS, C. P., RODRÍGUEZ CID, J. R. & ALATORRE ALEXANDER, J. A. 2019. Frequency and clinical-tomographic characterization of NSCLC with T790M mutation to TKI progression. *European Respiratory Journal*, 54, PA3067.

SANGER, H. L., KLOTZ, G., RIESNER, D., GROSS, H. J. & KLEINSCHMIDT, A. K. 1976. Viroids are single-stranded covalently closed circular RNA molecules existing as highly base-paired rod-like structures. *Proc Natl Acad Sci U S A*, 73, 3852-6.

SANTARPIA, M., LIGUORI, A., KARACHALIOU, N., GONZALEZ-CAO, M., DAFFINÀ, M. G., D'AVENI, A., MARABELLO, G., ALTAVILLA, G. & ROSELL, R. 2017. Osimertinib in the treatment of non-small-cell lung cancer: design, development and place in therapy. *Lung Cancer (Auckl)*, 8, 109-125.

SANTER, L., BÄR, C. & THUM, T. 2019. Circular RNAs: A Novel Class of Functional RNA Molecules with a Therapeutic Perspective. *Molecular Therapy*, 27, 1350-1363.

SANTONI-RUGIU, E., MELCHIOR, L. C., URBANSKA, E. M., JAKOBSEN, J. N., STRICKER, K., GRAUSLUND, M. & SØRENSEN, J. B. 2019. Intrinsic resistance to EGFR-Tyrosine Kinase Inhibitors in EGFR-Mutant Non-Small Cell Lung Cancer: Differences and Similarities with Acquired Resistance. *Cancers*, 11(7), p.923.

SARHADI, V. K. & ARMENGOL, G. 2022. Molecular Biomarkers in Cancer. *Biomolecules*, 12.

SARMEY, N., KAISMAN-ELBAZ, T. & MOHAMMADI, A. M. 2022. Management Strategies for Large Brain Metastases. *Front Oncol*, 12, 827304.

SCHABATH, M. B. & COTE, M. L. 2019. Cancer Progress and Priorities: Lung Cancer. *Cancer Epidemiol Biomarkers Prev*, 28, 1563-1579.

SCHERSCHINSKI, L., PREM, M., KREMENETSKAIA, I., TINHOFER, I., VAJKOCZY, P., KARBE, A. G. & ONKEN, J. S. 2022. Regulation of the Receptor Tyrosine Kinase AXL in Response to Therapy and Its Role in Therapy Resistance in Glioblastoma. *Int J Mol Sci*, 23.

SCHNEIDER, T., SCHREINER, S., PREUSSE, C., BINDEREIF, A. & ROSSBACH, O. 2018. Northern Blot Analysis of Circular RNAs. *Methods Mol Biol*, 1724, 119-133.

SEIMIYA, T., OTSUKA, M. & FUJISHIRO, M. 2022. Roles of circular RNAs in the pathogenesis and treatment of pancreatic cancer. *Frontiers in Cell and Developmental Biology*, 10, 1023332.

SEIMIYA, T., OTSUKA, M., IWATA, T., SHIBATA, C., TANAKA, E., SUZUKI, T. & KOIKE, K. 2020. Emerging roles of exosomal circular RNAs in cancer. *Frontiers in cell and developmental biology*, 8, 568366.

SEKAR, S., GEIGER, P., ADKINS, J., TASSONE, E., SERRANO, G., BEACH, T. G. & LIANG, W. S. 2020. ACValidator: A novel assembly-based approach for in silico verification of circular RNAs. *Biol Methods Protoc*, 5, bpaa010.

SEONG, G. M., HYUN, C. L., LEE, J. & KIM, C. 2020. Large cell carcinoma of the lung presenting as diffuse pulmonary infiltrates with haemoptysis. *Respirology Case Reports*, 8, e00632.

SETO, T., KATO, T., NISHIO, M., GOTO, K., ATAGI, S., HOSOMI, Y., YAMAMOTO, N., HIDA, T., MAEMONDO, M., NAKAGAWA, K., NAGASE, S., OKAMOTO, I., YAMANAKA, T., TAJIMA, K., HARADA, R., FUKUOKA, M. & YAMAMOTO, N. 2014. Erlotinib alone or with bevacizumab as first-line therapy in patients with advanced non-squamous non-small-cell lung cancer harbouring EGFR mutations (JO25567): an open-label, randomised, multicentre, phase 2 study. *Lancet Oncol*, 15, 1236-44.

SHAABAN, L. H., ZAYET, H. H., ABOUFADDAN, H. H. & ELGHAZALLY, S. A. 2016. Respiratory hazards: clinical and functional assessment in aluminum industry workers. *Egyptian Journal of Chest Diseases and Tuberculosis*, 65, 537-543.

SHAH, M. P., AREDO, J. V., PADDA, S. K., RAMCHANDRAN, K. J., WAKELEE, H. A., DAS, M. S. & NEAL, J. W. 2022. EGFR exon 20 Insertion NSCLC and Response to Platinum-Based Chemotherapy. *Clin Lung Cancer*, 23, e148-e153.

SHAH, R. & LESTER, J. F. 2020. Tyrosine Kinase Inhibitors for the Treatment of EGFR Mutation-Positive Non-Small-Cell Lung Cancer: A Clash of the Generations. *Clin Lung Cancer*, 21, e216-e228.

SHAKOORI, A. R. 2017. Fluorescence in situ hybridization (FISH) and its applications. *Chromosome structure and aberrations*, 343-367.

SHAMSEDDINE, A., RASHID, K., GHOSON, M., KATTAN, J., SAGHIR, N., BITAR, N., NSOULI, G., MOUKADEM, W., CHAHINE, G. & SALEM, Z. 2005. A retrospective review of the efficacy of gefitinib in the treatment of NSCLC in Lebanon. *Journal of Clinical Oncology*, 23, 3217-3217.

- SHANKAR, A., DUBEY, A., SAINI, D., SINGH, M., PRASAD, C. P., ROY, S., BHARATI, S. J., RINKI, M., SINGH, N., SETH, T., KHANNA, M., SETHI, N., KUMAR, S., SIROHI, B., MOHAN, A., GULERIA, R. & RATH, G. K. 2019. Environmental and occupational determinants of lung cancer. *Transl Lung Cancer Res*, 8, S31-s49.
- SHAO, J., LI, J., SONG, L., HE, Q., WU, Y., LI, L., LIU, D., WANG, C. & LI, W. 2022. The number of brain metastases predicts the survival of non-small cell lung cancer patients with EGFR mutation status. *Cancer Reports*, 5, e1550.
- SHAUROVA, T., ZHANG, L., GOODRICH, D. W. & HERSHBERGER, P. A. 2020. Understanding lineage plasticity as a path to targeted therapy failure in EGFR-mutant non-small cell lung cancer. *Frontiers in Genetics*, 11, 281.
- SHENG, P., FLOOD, K. A. & XIE, M. 2020. Short hairpin RNAs for strand-specific small interfering RNA production. *Frontiers in Bioengineering and Biotechnology*, 8, 940.
- SHENOY, S. 2019. CDH1 (E-Cadherin) Mutation and Gastric Cancer: Genetics, Molecular Mechanisms and Guidelines for Management. *Cancer Manag Res*, 11, 10477-10486.
- SHI, F., YANG, Q., SHEN, D. & CHEN, J. 2021. CircRNA WHSC1 promotes non-small cell lung cancer progression via sponging microRNA-296-3p and up-regulating expression of AKT serine/threonine kinase 3. *J Clin Lab Anal*, 35, e23865.
- SHI, H., ZHOU, Y., JIA, E., LIU, Z., PAN, M., BAI, Y., ZHAO, X. & GE, Q. 2022a. Comparative analysis of circular RNA enrichment methods. *RNA Biol*, 19, 55-67.
- SHI, K., WANG, G., PEI, J., ZHANG, J., WANG, J., OUYANG, L., WANG, Y. & LI, W. 2022. Emerging strategies to overcome resistance to third-generation EGFR inhibitors. *Journal of Hematology & Oncology*, 15, 94.
- SHI, Q. & JU, J. G. 2022. Circ_0001998 Regulates the Proliferation, Invasion, and Apoptosis of Lung Adenocarcinoma via Sponging miR-145. *Evid Based Complement Alternat Med*, 2022, 6446150.
- SHIN, G., GREER, S. U., XIA, L. C., LEE, H., ZHOU, J., BOLES, T. C. & JI, H. P. 2019. Targeted short read sequencing and assembly of rearrangements and candidate gene loci provide megabase diplotypes. *Nucleic Acids Res*, 47, e115.
- SHIRLEY, M. 2018. Dacomitinib: First Global Approval. *Drugs*, 78, 1947-1953.

SIDDIQUI, F., VAQAR, S. & SIDDIQUI, A. 2022. Lung Cancer. 2022 Dec 5. *StatPearls [Internet]. Treasure Island (FL): StatPearls Publishing.*

SIMARRO, J., PÉREZ-SIMÓ, G., MANCHEÑO, N., ANSOTEGUI, E., MUÑOZ-NÚÑEZ, C. F., GÓMEZ-CODINA, J., JUAN, Ó. & PALANCA, S. 2023. Impact of Molecular Testing Using Next-Generation Sequencing in the Clinical Management of Patients with Non-Small Cell Lung Cancer in a Public Healthcare Hospital. *Cancers (Basel)*, 15.

SINGH, S., SHYAMAL, S., DAS, A. & PANDA, A. C. 2024. Global identification of mRNA-interacting circular RNAs by CLIPPR-Seq. *Nucleic Acids Res*, 52, e29.

SKAKODUB, A., WALCH, H., TRINGALE, K. R., EICHHOLZ, J., IMBER, B. S., VASUDEVAN, H. N., LI, B. T., MOSS, N. S., HEI YU, K. K., MUELLER, B. A., POWELL, S., RAZAVI, P., YU, H. A., REIS-FILHO, J. S., GOMEZ, D., SCHULTZ, N. & PIKE, L. R. G. 2023. Genomic analysis and clinical correlations of non-small cell lung cancer brain metastasis. *Nature Communications*, 14, 4980.

SLACK, F. J. & CHINNAIYAN, A. M. 2019. The Role of Non-coding RNAs in Oncology. *Cell*, 179, 1033-1055.

SLOBBE, P., WINDHORST, A. D., STIGTER-VAN WALSUM, M., SMIT, E. F., NIESSEN, H. G., SOLCA, F., STEHLE, G., VAN DONGEN, G. A. M. S. & POOT, A. J. 2015. A comparative PET imaging study with the reversible and irreversible EGFR tyrosine kinase inhibitors [¹¹C]erlotinib and [¹⁸F]afatinib in lung cancer-bearing mice. *EJNMMI Research*, 5, 14.

SOHEL, M. H. 2016. Extracellular/Circulating MicroRNAs: Release Mechanisms, Functions and Challenges. *Achievements in the Life Sciences*, 10, 175-186.

SON, M. S. & TAYLOR, R. K. 2011. Preparing DNA libraries for multiplexed paired-end deep sequencing for Illumina GA sequencers. *Curr Protoc Microbiol*, Chapter 1, Unit 1E.4.

SOON, Y. Y., VELLAYAPPAN, B., TEY, J. C. S., LEONG, C. N., KOH, W. Y. & THAM, I. W. K. 2017. Impact of epidermal growth factor receptor sensitizing mutations on outcomes of patients with non-small cell lung cancer treated with definitive thoracic radiation therapy: a systematic review and meta-analysis. *Oncotarget*, 8, 109712-109722.

SOSA IGLESIAS, V., GIURANNO, L., DUBOIS, L. J., THEYS, J. & VOOIJS, M. 2018. Drug Resistance in Non-Small Cell Lung Cancer: A Potential for NOTCH Targeting? *Front Oncol*, 8, 267.

SOUZA, V. G. P., FORDER, A., BROCKLEY, L. J., PEWARCHUK, M. E., TELKAR, N., DE ARAÚJO, R. P., TREJO, J., BENARD, K., SENEDA, A. L., MINUTENTAG, I. W., ERKAN, M., STEWART, G. L., HASIMOTO, E. N., GARNIS, C., LAM, W. L., MARTINEZ, V. D. & REIS, P. P. 2023. Liquid Biopsy in Lung Cancer: Biomarkers for the Management of Recurrence and Metastasis. *International Journal of Molecular Sciences*, 24, 8894.

SPAGNOLO, C. C., CIAPPINA, G., GIOVANNETTI, E., SQUERI, A., GRANATA, B., LAZZARI, C., PRETELLI, G., PASELLO, G. & SANTARPIA, M. 2023. Targeting MET in Non-Small Cell Lung Cancer (NSCLC): A New Old Story? *Int J Mol Sci*, 24.

SUDA, K. & MITSUDOMI, T. 2020. Emerging oncogenic fusions other than ALK, ROS1, RET, and NTRK in NSCLC and the role of fusions as resistance mechanisms to targeted therapy. *Transl Lung Cancer Res*, 9, 2618-2628.

SUDA, K., MURAKAMI, I., YU, H., KIM, J., TAN, A.-C., MIZUUCHI, H., ROZEBOOM, L., ELLISON, K., RIVARD, C. J., MITSUDOMI, T. & HIRSCH, F. R. 2018. CD44 Facilitates Epithelial-to-Mesenchymal Transition Phenotypic Change at Acquisition of Resistance to EGFR Kinase Inhibitors in Lung Cancer. *Molecular Cancer Therapeutics*, 17, 2257.

SUDHESH DEV, S., ZAINAL ABIDIN, S. A., FARGHADANI, R., OTHMAN, I. & NAIDU, R. 2021. Receptor Tyrosine Kinases and Their Signaling Pathways as Therapeutic Targets of Curcumin in Cancer. *Front Pharmacol*, 12, 772510.

SUN, R., HOU, Z., ZHANG, Y. & JIANG, B. 2022. Drug resistance mechanisms and progress in the treatment of EGFR-mutated lung adenocarcinoma. *Oncol Lett*, 24, 408.

SUN, W., YUAN, X., TIAN, Y., WU, H., XU, H., HU, G. & WU, K. 2015. Non-invasive approaches to monitor EGFR-TKI treatment in non-small-cell lung cancer. *Journal of Hematology & Oncology*, 8, 95.

SUNG, H., FERLAY, J., SIEGEL, R. L., LAVERSANNE, M., SOERJOMATARAM, I., JEMAL, A. & BRAY, F. 2021. Global Cancer Statistics 2020: GLOBOCAN Estimates of Incidence and Mortality Worldwide for 36 Cancers in 185 Countries. *CA: A Cancer Journal for Clinicians*, 71, 209-249.

SUREKA, B., THUKRAL, B. B., MITTAL, M. K., MITTAL, A. & SINHA, M. 2013. Radiological review of pleural tumors. *Indian J Radiol Imaging*, 23, 313-20.

SURYAVANSHI, M., JAIPURIA, J., MATTOO, S., DHANDHA, S. & KHATRI, M. 2022. Audit of Molecular Mechanisms of Primary and Secondary Resistance to Various Generations of Tyrosine Kinase

Inhibitors in Known Epidermal Growth Factor Receptor-Mutant Non-small Cell Lung Cancer Patients in a Tertiary Centre. *Clinical Oncology*, 34, e451-e462.

SZABO, L., MOREY, R., PALPANT, N. J., WANG, P. L., AFARI, N., JIANG, C., PARAST, M. M., MURRY, C. E., LAURENT, L. C. & SALZMAN, J. 2015. Statistically based splicing detection reveals neural enrichment and tissue-specific induction of circular RNA during human fetal development. *Genome biology*, 16, 1-26.

TAI, Q., ZHANG, L. & HU, X. 2020. Clinical characteristics and treatments of large cell lung carcinoma: a retrospective study using SEER data. *Transl Cancer Res*, 9, 1455-1464.

TAKAHASHI, T., BOKU, N., MURAKAMI, H., NAITO, T., TSUYA, A., NAKAMURA, Y., ONO, A., MACHIDA, N., YAMAZAKI, K., WATANABE, J., RUIZ-GARCIA, A., IMAI, K., OHKI, E. & YAMAMOTO, N. 2012. Phase I and pharmacokinetic study of dacomitinib (PF-00299804), an oral irreversible, small molecule inhibitor of human epidermal growth factor receptor-1, -2, and -4 tyrosine kinases, in Japanese patients with advanced solid tumors. *Invest New Drugs*, 30, 2352-63.

TAKEDA, M. & NAKAGAWA, K. 2019. First- and Second-Generation EGFR-TKIs Are All Replaced to Osimertinib in Chemo-Naive EGFR Mutation-Positive Non-Small Cell Lung Cancer? *Int J Mol Sci*, 20.

TAMKOVICH, S., TUTANOV, O., EFIMENKO, A., GRIGOR'EVA, A., RYABCHIKOVA, E., KIRUSHINA, N., VLASSOV, V., TKACHUK, V. & LAKTIONOV, P. 2019. Blood Circulating Exosomes Contain Distinguishable Fractions of Free and Cell-Surface-Associated Vesicles. *Curr Mol Med*, 19, 273-285.

TAMURA, K. & FUKUOKA, M. 2005. Gefitinib in non-small cell lung cancer. *Expert Opin Pharmacother*, 6, 985-93.

TAN, S., KANG, Y., LI, H., HE, H.-Q., ZHENG, L., WU, S.-Q., AI, K., ZHANG, L., XU, R., ZHANG, X.-Z. J. C. D. & DISEASE 2021. circST6GALNAC6 suppresses bladder cancer metastasis by sponging miR-200a-3p to modulate the STMN1/EMT axis. 12, 1-15.

TAN, Y., WANG, K. & KONG, Y. 2022. Circular RNA ZFR promotes cell cycle arrest and apoptosis of colorectal cancer cells via the miR-147a/CACUL1 axis. *J Gastrointest Oncol*, 13, 1793-1804.

TANG, M., KUI, L., LU, G. & CHEN, W. 2020. Disease-Associated Circular RNAs: From Biology to Computational Identification. *BioMed Research International*, 2020(1), p.6798590.

TANG, Y., ZANG, H., WEN, Q. & FAN, S. 2023. AXL in cancer: a modulator of drug resistance and therapeutic target. *Journal of Experimental & Clinical Cancer Research*, 42, 148.

TAO, Y., MA, C., FAN, Q., WANG, Y., HAN, T. & SUN, C. 2018. MicroRNA-1296 facilitates proliferation, migration and invasion of colorectal cancer cells by targeting SFPQ. *Journal of Cancer*, 9, 2317.

TIVEY, A., CHURCH, M., ROTHWELL, D., DIVE, C. & COOK, N. 2022. Circulating tumour DNA — looking beyond the blood. *Nature Reviews Clinical Oncology*, 19, 600-612.

TRIPATHI, S. K. & BISWAL, B. K. 2021. Allosteric mutant-selective fourth-generation EGFR inhibitors as an efficient combination therapeutic in the treatment of non-small cell lung carcinoma. *Drug Discovery Today*, 26, 1466-1472.

TRIPHURIDET, N., ZHANG, S. S., NAGASAKA, M., GAO, Y., ZHAO, J. J., SYN, N. L., HANAOKA, T., OU, S.-H. I. & SHUM, E. 2023. Low-Dose Computed Tomography (LDCT) Lung Cancer Screening in Asian Female Never-Smokers Is as Efficacious in Detecting Lung Cancer as in Asian Male Ever-Smokers: A Systematic Review and Meta-Analysis. *Journal of Thoracic Oncology*, 18, 698-717.

TRYBEK, T., KOWALIK, A., GÓŹDŹ, S. & KOWALSKA, A. 2020. Telomeres and telomerase in oncogenesis. *Oncol Lett*, 20, 1015-1027.

TULPULE, A. & BIVONA, T. G. 2020. Acquired Resistance in Lung Cancer. *Annual Review of Cancer Biology*, 4, 279-297. TAKÁCS, T., KUDLIK, G., KURILLA, A., SZEDER, B., BUDAY, L. & VAS, V. 2020. The effects of mutant Ras proteins on the cell signalome. *Cancer and Metastasis Reviews*.

URIBE, M. L., MARROCCO, I. & YARDEN, Y. 2021. EGFR in Cancer: Signaling Mechanisms, Drugs, and Acquired Resistance. *Cancers*, 13, 2748.

VACLOVA, T., GRAZINI, U., WARD, L., O'NEILL, D., MARKOVETS, A., HUANG, X., CHMIELECKI, J., HARTMAIER, R., THRESS, K. S., SMITH, P. D., BARRETT, J. C., DOWNWARD, J. & DE BRUIN, E. C. 2021. Clinical impact of subclonal EGFR T790M mutations in advanced-stage EGFR-mutant non-small-cell lung cancers. *Nature Communications*, 12, 1780.

VERDUCI, L., STRANO, S., YARDEN, Y. & BLANDINO, G. 2019. The circRNA-microRNA code: emerging implications for cancer diagnosis and treatment. *Mol Oncol*, 13, 669-680.

VERUSINGAM, N. D., CHEN, Y.-C., LIN, H.-F., LIU, C.-Y., LEE, M.-C., LU, K.-H., CHEONG, S.-K., ONG, A. H.-K., CHIOU, S.-H. & WANG, M.-L. 2020. Generation of Osimertinib-Resistant Cells from

EGFR L858R/T790M Mutant NSCLC Cell Line. *Journal of the Chinese Medical Association*. 84(3): p. 248-254.

VISCI, G., TOLOMEO, D., AGOSTINI, A., TRAVERSA, D., MACCHIA, G. & STORLAZZI, C. T. 2020. CircRNAs and Fusion-circRNAs in cancer: New players in an old game. *Cellular Signalling*, 75, 109747.

VU, P. & PATEL, S. P. 2019. Non-small cell lung cancer targetable mutations: present and future. *Precision Cancer Medicine*, 3.

VYSE, S. & HUANG, P. H. 2019. Targeting EGFR exon 20 insertion mutations in non-small cell lung cancer. *Signal transduction and targeted therapy*, 4(1), p.5.

WAKABAYASHI, Y., MASUDA, T., FUJITAKA, K., NAKASHIMA, T., OKUMOTO, J., SHIMOJI, K., NISHIMURA, Y., YAMAGUCHI, K., SAKAMOTO, S., HORIMASU, Y., MIYAMOTO, S., IWAMOTO, H., OHSHIMO, S., HAMADA, H. & HATTORI, N. 2021. Clinical significance of BIM deletion polymorphism in chemoradiotherapy for non-small cell lung cancer. *Cancer Science*, 112, 369-379.

WALKER, C., MOJARES, E. & DEL RÍO HERNÁNDEZ, A. 2018. Role of Extracellular Matrix in Development and Cancer Progression. *International Journal of Molecular Sciences*, 19, 3028.

WAN, J., DING, G., ZHOU, M., LING, X. & RAO, Z. 2021. Circular RNA hsa_circ_0002483 promotes growth and invasion of lung adenocarcinoma by sponging miR-125a-3p. *Cancer Cell Int*, 21, 533.

WAN, J., WANG, Z., WANG, L., WU, L., ZHANG, C., ZHOU, M., FU, Z. F. & ZHAO, L. 2023. Circular RNA vaccines with long-term lymph node-targeting delivery stability after lyophilization induce potent and persistent immune responses. *Mbio*, 15(1), pp.e01775-23.

WANG, C.-C., CHIU, L.-C., TUNG, P.-H., KUO, S. C.-H., CHU, C.-H., HUANG, A. C.-C., WANG, C.-L., CHEN, C.-H., YANG, C.-T. & HSU, P.-C. 2021a. A Real-World Analysis of Patients with Untreated Metastatic Epidermal Growth Factor Receptor (EGFR)-Mutated Lung Adenocarcinoma Receiving First-Line Erlotinib and Bevacizumab Combination Therapy. *Oncology and Therapy*, 9, 489-503.

WANG, C., ZHAO, K., HU, S., LI, M. & SONG, Y. 2021. Patterns and treatment strategies of osimertinib resistance in T790M-positive non-small cell lung cancer: a pooled analysis. *Frontiers in Oncology*, 11, 600844.

- WANG, D. & FARHANA, A. 2020. Biochemistry, RNA Structure.
- WANG, F., LI, C., WU, Q. & LU, H. 2020. EGFR exon 20 insertion mutations in non-small cell lung cancer. *Translational Cancer Research*, 9, 2982-2991.
- WANG, J., ZHAO, X., WANG, Y., REN, F., SUN, D., YAN, Y., KONG, X., BU, J., LIU, M. & XU, S. 2020a. circRNA-002178 act as a ceRNA to promote PDL1/PD1 expression in lung adenocarcinoma. *Cell Death Dis*, 11, 32.
- WANG, L. H., WU, C. F., RAJASEKARAN, N. & SHIN, Y. K. 2018. Loss of Tumor Suppressor Gene Function in Human Cancer: An Overview. *Cellular Physiology and Biochemistry*, 51, 2647-2693.
- WANG, S., SONG, Y. & LIU, D. 2017a. EAI045: The fourth-generation EGFR inhibitor overcoming T790M and C797S resistance. *Cancer Lett*, 385, 51-54.
- WANG, X. & FANG, L. 2018. Advances in circular RNAs and their roles in breast Cancer. *Journal of Experimental & Clinical Cancer Research*, 37, 206.
- WANG, X. & SHAN, G. 2018. Nonradioactive Northern Blot of circRNAs. *Methods Mol Biol*, 1724, 135-141.
- WANG, Y. & WANG, Z. 2015. Efficient backsplicing produces translatable circular mRNAs. *Rna*, 21, 172-9.
- WANG, Y.-F., KUO, Y.-C., LIN, M.-Y. & TSAI, P.-J. 2021b. Assessing Lung and Skin Cancer Risks for Steel and Iron Manufacturing Industry Workers Exposed to Polycyclic Aromatic Hydrocarbons. *Aerosol and Air Quality Research*, 21, 210160.
- WANG, Y., LI, X., WANG, H. & ZHANG, G. 2022a. CircCAMSAP1 promotes non-small cell lung cancer proliferation and inhibits cell apoptosis by sponging miR-1182 and regulating BIRC5. *Bioengineered*, 13, 2428-2439.
- WANG, Y., YANG, M., WEI, S., QIN, F., ZHAO, H. & SUO, B. 2017b. Identification of circular RNAs and their targets in leaves of *Triticum aestivum* L. under dehydration stress. *Frontiers in Plant Science*, 7, p.2024.
- WANG, Y., ZHENG, F., WANG, Z., LU, J. & ZHANG, H. 2020b. Circular RNA circ-SLC7A6 acts as a tumor suppressor in non-small cell lung cancer through abundantly sponging miR-21. *Cell cycle*, 19, 2235-2246.
- WANG, Z., YU, R., CHEN, X., BAO, H., CAO, R., LI, A.-N., OU, Q., TU, H.-Y., ZHOU, Q., WU, X., LIN, Z.-B. & WU, Y.-L. 2022b. Clinical

utility of cerebrospinal fluid-derived circular RNAs in lung adenocarcinoma patients with brain metastases. *Journal of Translational Medicine*, 20, 74.

WANG, Z., DENG, H., JIN, Y., LUO, M., HUANG, J., WANG, J., ZHANG, K., WANG, L. & ZHOU, J. 2023. Circular RNAs: biology and clinical significance of breast cancer. *RNA Biology*, 20, 859-874.

WEI, S. L., YE, J. J., SUN, L., HU, L., WEI, Y. Y., ZHANG, D. W., XU, M. M. & FEI, G. H. 2023. Exosome-derived circKIF20B suppresses gefitinib resistance and cell proliferation in non-small cell lung cancer. *Cancer Cell Int*, 23, 129.

WEI, S., ZHENG, Y., JIANG, Y., LI, X., GENG, J., SHEN, Y., LI, Q., WANG, X., ZHAO, C., CHEN, Y., QIAN, Z., ZHOU, J. & LI, W. 2019. The circRNA circPTPRA suppresses epithelial-mesenchymal transitioning and metastasis of NSCLC cells by sponging miR-96-5p. *EBioMedicine*, 44, 182-193.

WEIDEMANN, S., BÖHLE, J. L., CONTRERAS, H., LUEBKE, A. M., KLUTH, M., BÜSCHECK, F., HUBE-MAGG, C., HÖFLMAYER, D., MÖLLER, K., FRAUNE, C., BERNREUTHER, C., RINK, M., SIMON, R., MENZ, A., HINSCH, A., LEBOK, P., CLAUDITZ, T., SAUTER, G., UHLIG, R., WILCZAK, W., STEURER, S., BURANDT, E., KRECH, R., DUM, D., KRECH, T., MARX, A. & MINNER, S. 2021. Napsin A Expression in Human Tumors and Normal Tissues. *Pathol Oncol Res*, 27, 613099.

WESTOVER, D., ZUGAZAGOITIA, J., CHO, B. C., LOVLY, C. M. & PAZ-ARES, L. 2018. Mechanisms of acquired resistance to first- and second-generation EGFR tyrosine kinase inhibitors. *Annals of Oncology*, 29, i10-i19.

WILL, C. L. & LÜHRMANN, R. 2011. Spliceosome structure and function. *Cold Spring Harb Perspect Biol*. 3(7), p.a003707.

WILUSZ, J. E. 2015. Repetitive elements regulate circular RNA biogenesis. *Mob Genet Elements*, 5, 1-7.

WIND, S., SCHNELL, D., EBNER, T., FREIWALD, M. & STOPFER, P. 2017. Clinical Pharmacokinetics and Pharmacodynamics of Afatinib. *Clin Pharmacokinet*, 56, 235-250.

WINKLER, J., ABISOYE-OGUNNIYAN, A., METCALF, K. J. & WERB, Z. 2020. Concepts of extracellular matrix remodelling in tumour progression and metastasis. *Nature Communications*. 1(1), p.5120.

WIUM, M., AJAYI-SMITH, A. F., PACCEZ, J. D. & ZERBINI, L. F. 2021. The Role of the Receptor Tyrosine Kinase Axl in Carcinogenesis and Development of Therapeutic Resistance: An Overview of Molecular Mechanisms and Future Applications. *Cancers*. 13(7), p.1521.

WU, S.-G. & SHIH, J.-Y. 2018. Management of acquired resistance to EGFR TKI-targeted therapy in advanced non-small cell lung cancer. *Molecular Cancer*, 17, 38.

WU, Y. L., CHENG, Y., ZHOU, X., LEE, K. H., NAKAGAWA, K., NIHO, S., TSUJI, F., LINKE, R., ROSELL, R., CORRAL, J., MIGLIORINO, M. R., PLUZANSKI, A., SBAR, E. I., WANG, T., WHITE, J. L., NADANACIVA, S., SANDIN, R. & MOK, T. S. 2017. Dacomitinib versus gefitinib as first-line treatment for patients with EGFR-mutation-positive non-small-cell lung cancer (ARCHER 1050): a randomised, open-label, phase 3 trial. *Lancet Oncol*, 18, 1454-1466.

WU, Y., YANG, L., ZHANG, L., ZHENG, X., XU, H., WANG, K. & WENG, X. 2022. Identification of a Four-Gene Signature Associated with the Prognosis Prediction of Lung Adenocarcinoma Based on Integrated Bioinformatics Analysis. *Genes (Basel)*. 13(2), p.238.

XI, X., LI, T., HUANG, Y., SUN, J., ZHU, Y., YANG, Y. & LU, Z. J. 2017. RNA Biomarkers: Frontier of Precision Medicine for Cancer. *Noncoding RNA*, 3(1), p.9.

XI, X., LI, T., HUANG, Y., SUN, J., ZHU, Y., YANG, Y. & LU, Z. J. 2017. RNA Biomarkers: Frontier of Precision Medicine for Cancer. *Noncoding RNA*, 3.

XIA, S. & ZHANG, Z. 2022. Circular RNA hsa_circ_0000317 inhibits non-small cell lung cancer progression through regulating microRNA-494-3p/phosphatase and tensin homolog deleted on chromosome 10 axis. *Clinics (Sao Paulo)*, 77, p.100086.

XIA, X., FAN, J. & FAN, Z. 2023. Hsa_circ_0129047 sponges miR-665 to attenuate lung adenocarcinoma progression by upregulating protein tyrosine phosphatase receptor type B. *The Korean Journal of Physiology & Pharmacology: Official Journal of the Korean Physiological Society and the Korean Society of Pharmacology*, 27, 131-141.

XIAO, M. S. & WILUSZ, J. E. 2019. An improved method for circular RNA purification using RNase R that efficiently removes linear RNAs containing G-quadruplexes or structured 3' ends. *Nucleic Acids Res*, 47, 8755-8769.

XIE, J., YE, F., DENG, X., TANG, Y., LIANG, J. Y., HUANG, X., SUN, Y., TANG, H., LEI, J., ZHENG, S. & ZOU, Y. 2023. Circular RNA: A promising new star of vaccine. *J Transl Int Med*, 11, 372-381.

XIE, L., MAO, M., XIONG, K. & JIANG, B. 2017. Circular RNAs: A Novel Player in Development and Disease of the Central Nervous System. *Front Cell Neurosci*, 11, 354.

XIE, R., ZHANG, Y., ZHANG, J., LI, J. & ZHOU, X. 2020. The Role of Circular RNAs in Immune-Related Diseases. *Front Immunol*, 11, 545.

XIE, X., QIU, G., CHEN, Z., LIU, T., YANG, Y., YOU, Z., ZENG, C., LIN, X., XIE, Z., QIN, Y., WANG, Y., MA, X., ZHOU, C. & LIU, M. 2024. Characteristics and prognosis of EGFR mutations in small cell lung cancer patients in the NGS era. *Clinical and Translational Oncology*, 26, 434-445.

XU, C.-W., LEI, L., WANG, W.-X., LIN, L., ZHU, Y.-C., WANG, H., MIAO, L.-Y., WANG, L.-P., ZHUANG, W., FANG, M.-Y., LV, T.-F. & SONG, Y. 2020a. Molecular Characteristics and Clinical Outcomes of EGFR Exon 19 C-Helix Deletion in Non-Small Cell Lung Cancer and Response to EGFR TKIs. *Translational Oncology*, 13, 100791.

XU, L., MA, Y., ZHANG, H., LU, Q.-J., YANG, L., JIANG, G.-N. & LIAO, W.-L. 2020. HMGA2 regulates circular RNA ASPH to promote tumor growth in lung adenocarcinoma. *Cell Death & Disease*, 11, 593.

XU, Q., DENG, B., LI, M., CHEN, Y. & ZHUAN, L. J. J. O. O. R. 2020b. circRNA-UBAP2 promotes the proliferation and inhibits apoptosis of ovarian cancer through miR-382-5p/PRPF8 axis. 13, 1-10.

XUE, J., YANG, S. & SENG, S. 2014. Mechanisms of Cancer Induction by Tobacco-Specific NNK and NNN. *Cancers (Basel)*, 6, 1138-56.

YAMAMOTO, K., KAWAGUCHI, M., SHIMOMURA, T., IZUMI, A., KONARI, K., HONDA, A., LIN, C. Y., JOHNSON, M. D., YAMASHITA, Y., FUKUSHIMA, T. & KATAOKA, H. 2018. Hepatocyte growth factor activator inhibitor type-2 (HAI-2)/SPINT2 contributes to invasive growth of oral squamous cell carcinoma cells. *Oncotarget*, 9, 11691-11706.

YAMAOKA, T., OHBA, M., ARATA, S. & OHMORI, T. 2017. Establishing Dual Resistance to EGFR-TKI and MET-TKI in Lung Adenocarcinoma Cells In Vitro with a 2-step Dose-escalation Procedure. *Journal of visualized experiments : JoVE*, 55967.

YANG, B., TENG, F., CHANG, L., WANG, J., LIU, D. L., CUI, Y. S. & LI, G. H. 2021a. Tumor-derived exosomal circRNA_102481 contributes to EGFR-TKIs resistance via the miR-30a-5p/ROR1 axis in non-small cell lung cancer. *Aging (Albany NY)*, 13, 13264-13286.

YANG, F., RUAN, H., LI, S., HOU, W., QIU, Y., DENG, L., SU, S., CHEN, P., PANG, L. & LAI, K. 2022. Analysis of circRNAs and circRNA-associated competing endogenous RNA networks in β -thalassemia. *Scientific Reports*, 12, 8071.

YANG, J. C.-H., SCHULER, M. H., YAMAMOTO, N., O'BYRNE, K. J., HIRSH, V., MOK, T., GEATER, S. L., ORLOV, S. V., TSAI, C.-M., BOYER, M. J., SU, W.-C., BENNOUNA, J., KATO, T., GORBUNOVA, V., LEE, K. H., SHAH, R. N. H., MASSEY, D., LORENCE, R. M., SHAHIDI, M. & SEQUIST, L. V. 2012. LUX-Lung 3: A randomized, open-label, phase III study of afatinib versus

pemetrexed and cisplatin as first-line treatment for patients with advanced adenocarcinoma of the lung harboring EGFR-activating mutations. *Journal of Clinical Oncology*, 30, LBA7500-LBA7500.

YANG, J. C., AHN, M. J., KIM, D. W., RAMALINGAM, S. S., SEQUIST, L. V., SU, W. C., KIM, S. W., KIM, J. H., PLANCHARD, D., FELIP, E., BLACKHALL, F., HAGGSTROM, D., YOH, K., NOVELLO, S., GOLD, K., HIRASHIMA, T., LIN, C. C., MANN, H., CANTARINI, M., GHIORGHIU, S. & JÄNNE, P. A. 2017a. Osimertinib in Pretreated T790M-Positive Advanced Non-Small-Cell Lung Cancer: AURA Study Phase II Extension Component. *J Clin Oncol*, 35, 1288-1296.

YANG, J. C., RECKAMP, K. L., KIM, Y. C., NOVELLO, S., SMIT, E. F., LEE, J. S., SU, W. C., AKERLEY, W. L., BLAKELY, C. M., GROEN, H. J. M., BAZHENOVA, L., CARCERENY COSTA, E., CHIARI, R., HSIA, T. C., GOLSORKHI, T., DESPAIN, D., SHIH, D., POPAT, S. & WAKELEE, H. 2021b. Efficacy and Safety of Rociletinib Versus Chemotherapy in Patients With EGFR-Mutated NSCLC: The Results of TIGER-3, a Phase 3 Randomized Study. *JTO Clin Res Rep*, 2, 100114.

YANG, J. H., PANDEY, P. R. & GOROSPE, M. 2021. Identification of circRNA-Interacting Proteins by Affinity Pulldown. *Methods Mol Biol*, 2372, 193-202.

YANG, Q., LI, F., HE, A. T. & YANG, B. B. 2021d. Circular RNAs: Expression, localization, and therapeutic potentials. *Molecular Therapy*, 29, 1683-1702.

YANG, X.-W., SHEN, G.-Z., CAO, L.-Q., JIANG, X.-F., PENG, H.-P., SHEN, G., CHEN, D. & XUE, P. 2014. MicroRNA-1269 promotes proliferation in human hepatocellular carcinoma via downregulation of FOXO1. *BMC cancer*, 14, 1-10.

YANG, Y., FAN, X., MAO, M., SONG, X., WU, P., ZHANG, Y., JIN, Y., YANG, Y., CHEN, L.-L., WANG, Y., WONG, C. C. L., XIAO, X. & WANG, Z. 2017b. Extensive translation of circular RNAs driven by N6-methyladenosine. *Cell Research*, 27, 626-641.

YAO, Y., CHEN, C., WANG, J., XUAN, H., CHEN, X., LI, Z., YANG, F., WANG, B., LIN, S., LI, S., TANG, D., GONG, L. & GAO, W. 2023. Circular RNA circATP9A promotes non-small cell lung cancer progression by interacting with HuR and by promoting extracellular vesicles-mediated macrophage M2 polarization. *Journal of Experimental & Clinical Cancer Research*, 42, 330.

YAO, Y., FAREED, R., ZAFAR, A., SALEEM, K., HUANG, T., DUAN, Y. & REHMAN, M. U. 2022. State-of-the-art combination treatment strategies for advanced stage non-small cell lung cancer. *Front Oncol*, 12, 958505.

YAO, Y., HUA, Q., ZHOU, Y., SHEN, H. J. B. & PHARMACOTHERAPY 2019. CircRNA has_circ_0001946 promotes cell growth in lung adenocarcinoma by regulating miR-135a-5p/SIRT1 axis and activating Wnt/ β -catenin signaling pathway. 111, 1367-1375.

YARMISHYN, A. A., ISHOLA, A. A., CHEN, C.-Y., VERUSINGAM, N. D., RENGANATEN, V., MUSTAPHA, H. A., CHUANG, H.-K., TENG, Y.-C., PHUNG, V. L., HSU, P.-K., LIN, W.-C., MA, H.-I., CHIOU, S.-H. & WANG, M.-L. 2022. Circular RNAs Modulate Cancer Hallmark and Molecular Pathways to Support Cancer Progression and Metastasis. *Cancers*, 14, 862.

YE, Y., WU, X., LONG, F., YUE, W., WU, D. & XIE, Y. 2021. Circular RNA _0015278 inhibits the progression of non-small cell lung cancer through regulating the microRNA 1278/SOCS6 gene axis. *Ann Transl Med*, 9, 1255.

YI, X. F., SONG, J., GAO, R. L., SUN, L., WU, Z. X., ZHANG, S. L., HUANG, L. T., MA, J. T. & HAN, C. B. 2022. Efficacy of Osimertinib in EGFR-Mutated Advanced Non-small-Cell Lung Cancer With Different T790M Status Following Resistance to Prior EGFR-TKIs: A Systematic Review and Meta-analysis. *Front Oncol*, 12, 863666.

YOKOI, K., YAMASHITA, K., ISHII, S., TANAKA, T., NISHIZAWA, N., TSUTSUI, A., MIURA, H., KATOH, H., YAMANASHI, T., NAITO, M., SATO, T., NAKAMURA, T. & WATANABE, M. 2017. Comprehensive molecular exploration identified promoter DNA methylation of the CRBP1 gene as a determinant of radiation sensitivity in rectal cancer. *Br J Cancer*, 116, 1046-1056.

YOSHIMURA, A., YAMADA, T., OKURA, N., TAKEDA, T., HIROSE, K., KUBOTA, Y., SHIOTSU, S., HIRANUMA, O., CHIHARA, Y., TAMIYA, N., KANEKO, Y., UCHINO, J. & TAKAYAMA, K. 2019. Clinical Characteristics of Osimertinib Responder in Non-Small Cell Lung Cancer Patients with EGFR-T790M Mutation. *Cancers (Basel)*, 11. ABDELGHAFAR, S. H., HEGAZY, M. A. & ELTANANY, B. M. 2022. Stability assessment of FDA-approved ramucirumab monoclonal antibody; validated SE-HPLC method for degradation pattern evaluation. *Biomedical*

YOU, L., ZHENG, X., DENG, D., PAN, H. & HAN, W. 2022. The benefit of anti-angiogenic therapy in EGFR exon 21 L858R mutant non-small cell lung cancer patients: a retrospective study. *Sci Rep*, 12, 14624.

YU-CHANG, L. I. U., BO-HAN, H., JING-GUNG, C., WEI-LIN, L. I. U., FEI-TING, H. S. U. & SONG-SHEI, L. I. N. 2021. Lenvatinib Inhibits AKT/NF- κ B Signaling and Induces Apoptosis Through Extrinsic/Intrinsic Pathways in Non-small Cell Lung Cancer. *Anticancer Research*, 41, 123.

- YU, C., HUANG, X., HUANG, R., WANG, P., CAI, Z., GUO, Z., LAN, Q., CAO, H. & YU, J. 2023. Hsa_circ_0079557 Promotes the Proliferation of Colorectal Cancer Cells Through the hsa_circ_0079557/miR-502-5p/CCND1 Axis. *Cancer Genomics Proteomics*, 20, 567-581.
- YU, H. A. & PAO, W. 2013. Targeted therapies: Afatinib--new therapy option for EGFR-mutant lung cancer. *Nat Rev Clin Oncol*, 10, 551-2.
- YU, J., PERRI, M., JONES, J. W., PIERZCHALSKI, K., CEAIKOVSCAIA, N., CIONE, E. & KANE, M. A. 2022. Altered RBP1 gene expression impacts epithelial cell retinoic acid, proliferation, and microenvironment. *Cells*, 11, 792.
- YU, T., RAN, L., ZHAO, H., YIN, P., LI, W., LIN, J., MAO, H., CAI, D., MA, Q. & PAN, X. 2021. Circular RNA circ-TNPO3 suppresses metastasis of GC by acting as a protein decoy for IGF2BP3 to regulate the expression of MYC and SNAIL. *Molecular Therapy-Nucleic Acids*, 26, 649-664.
- YUAN, X., WU, H., HAN, N., XU, H., CHU, Q., YU, S., CHEN, Y. & WU, K. 2014. Notch signaling and EMT in non-small cell lung cancer: biological significance and therapeutic application. *Journal of Hematology & Oncology*, 7, 87.
- ZAPPA, C. & MOUSA, S. A. 2016. Non-small cell lung cancer: current treatment and future advances. *Translational Lung Cancer Research*, 5, 288-300.
- ZHANG, F., JIANG, J., QIAN, H., YAN, Y. & XU, W. 2023. Exosomal circRNA: emerging insights into cancer progression and clinical application potential. *Journal of Hematology & Oncology*, 16, 67.
- ZHANG, G., TANG, T., CHEN, Y., HUANG, X. & LIANG, T. 2023a. mRNA vaccines in disease prevention and treatment. *Signal Transduction and Targeted Therapy*, 8, 365.
- ZHANG, G., WANG, M., ZHAO, H. & CUI, W. 2018a. Function of Axl receptor tyrosine kinase in non-small cell lung cancer. *Oncol Lett*, 15, 2726-2734.
- ZHANG, G., XIA, M., GUO, J., HUANG, Y., HUANG, J., WEI, K., ZHANG, X., ZENG, J. & LIANG, W. 2021. microRNA-1296 Inhibits Glioma Cell Growth by Targeting ABL2. *Technology in Cancer Research & Treatment*, 20, 1533033821990009.
- ZHANG, H., YU, Z., WU, B. & SUN, F. 2021a. Circular RNA circFOXP1 promotes angiogenesis by regulating microRNA -127-5p/CDKN2AIP signaling pathway in osteosarcoma. *Bioengineered*, 12, 9991-9999.

ZHANG, J., CHEN, B., GAN, C., SUN, H., ZHANG, J. & FENG, L. 2023b. A Comprehensive Review of Small Interfering RNAs (siRNAs): Mechanism, Therapeutic Targets, and Delivery Strategies for Cancer Therapy. *Int J Nanomedicine*, 18, 7605-7635.

ZHANG, J., CHEN, S., YANG, J. & ZHAO, F. 2020a. Accurate quantification of circular RNAs identifies extensive circular isoform switching events. *Nat Commun*, 11, 90.

ZHANG, J., HOSSAIN, M. T., LIU, W., PENG, Y., PAN, Y. & WEI, Y. 2022. Evaluation of CircRNA Sequence Assembly Methods Using Long Reads. *Front Genet*, 13, 816825.

ZHANG, L.-L., ZHANG, L.-F. & SHI, Y.-B. 2018b. miR-24 inhibited the killing effect of natural killer cells to colorectal cancer cells by downregulating Paxillin. *Biomedicine & Pharmacotherapy*, 101, 257-263.

ZHANG, L., HOU, C., CHEN, C., GUO, Y., YUAN, W., YIN, D., LIU, J. & SUN, Z. 2020b. The role of N(6)-methyladenosine (m(6)A) modification in the regulation of circRNAs. *Mol Cancer*, 19, 105.

ZHANG, P.-F., PEI, X., LI, K.-S., JIN, L.-N., WANG, F., WU, J. & ZHANG, X.-M. 2019. Circular RNA circFGFR1 promotes progression and anti-PD-1 resistance by sponging miR-381-3p in non-small cell lung cancer cells. *Molecular cancer*, 18, 1-13.

ZHANG, P., ZHANG, X. O., JIANG, T., CAI, L., HUANG, X., LIU, Q., LI, D., LU, A., LIU, Y., XUE, W., ZHANG, P. & WENG, Z. 2020c. Comprehensive identification of alternative back-splicing in human tissue transcriptomes. *Nucleic Acids Res*, 48, 1779-1789.

ZHANG, R., ZHU, W., MA, C. & AI, K. 2021b. Silencing of circRNA circ_0001666 represses EMT in pancreatic cancer through upregulating miR-1251 and downregulating SOX4. *Frontiers in molecular biosciences*, 8, 684866.

ZHANG, S., MO, Q. & WANG, X. 2019. Oncological role of HMGA2 (Review). *Int J Oncol*, 55, 775-788.

ZHANG, X.-L., XU, L.-L. & WANG, F. 2017. Hsa_circ_0020397 regulates colorectal cancer cell viability, apoptosis and invasion by promoting the expression of the miR-138 targets TERT and PD-L1. *Cell Biology International*, 41, 1056-1064.

ZHANG, X., HAI, L., GAO, Y., YU, G. & SUN, Y. 2023c. Lipid nanomaterials-based RNA therapy and cancer treatment. *Acta Pharmaceutica Sinica B*, 13, 903-915.

ZHANG, Y., WANG, Y., SU, X., WANG, P. & LIN, W. 2021. The Value of Circulating Circular RNA in Cancer Diagnosis, Monitoring, Prognosis, and Guiding Treatment. *Front Oncol*, 11, 736546.

ZHANG, Y., XIA, M., JIN, K., WANG, S., WEI, H., FAN, C., WU, Y., LI, X., LI, X. & LI, G. 2018a. Function of the c-Met receptor tyrosine kinase in carcinogenesis and associated therapeutic opportunities. *Molecular cancer*, 17, 1-14.

ZHANG, Y., ZHANG, X. O., CHEN, T., XIANG, J. F., YIN, Q. F., XING, Y. H., ZHU, S., YANG, L. & CHEN, L. L. 2013. Circular intronic long noncoding RNAs. *Mol Cell*, 51, 792-806.

ZHANG, Z., XIE, Q., HE, D., LING, Y., LI, Y., LI, J. & ZHANG, H. 2018c. Circular RNA: new star, new hope in cancer. *BMC Cancer*, 18, 834.

ZHANG, Z., YANG, T. & XIAO, J. 2018b. Circular RNAs: Promising Biomarkers for Human Diseases. *EBioMedicine*, 34, 267-274.

ZHAO, C., ZHANG, Z., WANG, Z. & LIU, X. 2023. Circular RNA circRANGAP1/miR-512-5p/SOD2 Axis Regulates Cell Proliferation and Migration in Non-small Cell Lung Cancer (NSCLC). *Mol Biotechnol*.

ZHAO, H.-Y., XI, X.-X., XIN, M. & ZHANG, S.-Q. 2022a. Overcoming C797S mutation: The challenges and prospects of the fourth-generation EGFR-TKIs. *Bioorganic Chemistry*, 128, 106057.

ZHAO, J. & XIA, Y. 2020. Targeting HER2 Alterations in Non-Small-Cell Lung Cancer: A Comprehensive Review. *JCO Precision Oncology*, 411-425.

ZHAO, J., LEE, E. E., KIM, J., YANG, R., CHAMSEDDIN, B., NI, C., GUSHO, E., XIE, Y., CHIANG, C.-M., BUSZCZAK, M., ZHAN, X., LAIMINS, L. & WANG, R. C. 2019. Transforming activity of an oncoprotein-encoding circular RNA from human papillomavirus. *Nature Communications*, 10, 2300.

ZHAO, S., ZHANG, Y., GAMINI, R., ZHANG, B. & VON SCHACK, D. 2018. Evaluation of two main RNA-seq approaches for gene quantification in clinical RNA sequencing: polyA⁺ selection versus rRNA depletion. *Sci Rep*, 8, 4781.

ZHAO, Y., FANG, L. T., SHEN, T.-W., CHOUDHARI, S., TALSANIA, K., CHEN, X., SHETTY, J., KRIGA, Y., TRAN, B., ZHU, B., CHEN, Z., CHEN, W., WANG, C., JAEGER, E., MEERZAMAN, D., LU, C., IDLER, K., REN, L., ZHENG, Y., SHI, L., PETITJEAN, V., SULTAN, M., HUNG, T., PETERS, E., DRABEK, J., VOJTA, P., MAESTRO, R., GASPAROTTO, D., KÖKS, S., REIMANN, E., SCHERER, A., NORDLUND, J., LILJEDAHN, U., FOOX, J., MASON,

C. E., XIAO, C., HONG, H. & XIAO, W. 2021. Whole genome and exome sequencing reference datasets from a multi-center and cross-platform benchmark study. *Scientific Data*, 8, 296.

ZHAO, Y., ZHANG, C., TANG, H., WU, X. & QI, Q. 2022b. Mechanism of RNA circHIPK3 Involved in Resistance of Lung Cancer Cells to Gefitinib. *Biomed Res Int*, 2022, 4541918.

ZHENG, M. 2016. Classification and pathology of lung cancer. *Surgical Oncology Clinics*, 25, 447-468.

ZHONG, Y., DU, Y., YANG, X., MO, Y., FAN, C., XIONG, F., REN, D., YE, X., LI, C., WANG, Y., WEI, F., GUO, C., WU, X., LI, X., LI, Y., LI, G., ZENG, Z. & XIONG, W. 2018. Circular RNAs function as ceRNAs to regulate and control human cancer progression. *Molecular Cancer*, 17, 79.

ZHOU, C., MOLINIE, B., DANESHVAR, K., PONDICK, J. V., WANG, J., VAN WITTENBERGHE, N., XING, Y., GIALLOURAKIS, C. C. & MULLEN, A. C. 2017. Genome-Wide Maps of m6A circRNAs Identify Widespread and Cell-Type-Specific Methylation Patterns that Are Distinct from mRNAs. *Cell Rep*, 20, 2262-2276.

ZHOU, Q., JU, L. L., JI, X., CAO, Y. L., SHAO, J. G. & CHEN, L. 2021. Plasma circRNAs as Biomarkers in Cancer. *Cancer Manag Res*, 13, 7325-7337.

ZHOU, T., LI, Z., JIANG, Y., SU, K., XU, C. & YI, H. 2024. Emerging roles of circular RNAs in regulating the hallmarks of thyroid cancer. *Cancer Gene Therapy*, 31, 507-516.

ZHOU, W.-Y., CAI, Z.-R., LIU, J., WANG, D.-S., JU, H.-Q. & XU, R.-H. 2020. Circular RNA: metabolism, functions and interactions with proteins. *Molecular Cancer*, 19, 172.

ZHOU, Y., ZHENG, X., XU, B., CHEN, L., WANG, Q., DENG, H. & JIANG, J. 2019. Circular RNA hsa_circ_0004015 regulates the proliferation, invasion, and TKI drug resistance of non-small cell lung cancer by miR-1183/PDPK1 signaling pathway. *Biochemical and biophysical research communications*, 508, 527-535.

ZHUO, M., ZHENG, Q., ZHAO, J., WU, M., AN, T., WANG, Y., LI, J., WANG, S., ZHONG, J., YANG, X., CHEN, H., JIA, B., DONG, Z., GAO, E., WANG, J. & WANG, Z. 2017. Survival difference between EGFR Del19 and L858R mutant advanced non-small cell lung cancer patients receiving gefitinib: a propensity score matching analysis. *Chinese journal of cancer research = Chung-kuo yen cheng yen chiu*, 29, 553-560.

ZIRKEL, A. & PAPANTONIS, A. 2018. Detecting Circular RNAs by RNA Fluorescence In Situ Hybridization. *Methods Mol Biol*, 1724, 69-75.

ZOU, K., SUN, P., HUANG, H., ZHUO, H., QIE, R., XIE, Y., LUO, J., LI, N., LI, J., HE, J., ASCHEBROOK-KILFOY, B. & ZHANG, Y. 2022. Etiology of lung cancer: Evidence from epidemiologic studies. *Journal of the National Cancer Center*, 2, 216-225.

ZUBAIR, T. & BANDYOPADHYAY, D. 2023. Small Molecule EGFR Inhibitors as Anti-Cancer Agents: Discovery, Mechanisms of Action, and Opportunities. *Int J Mol Sci*, 24.

APPENDICES

Appendix A

Divergent Primers

Target	Primer	Sequence
hsa_circ_0050818	Forward	AAGACCACTCCAGCGATATG
	Reverse	AGCACTTGGGACAGAGGAAT
hsa_circ_0066632	Forward	CCTACCCAATATATGAAGG
	Reverse	GTGAGTTGGTGAACGTGTGA
hsa_circ_0024390	Forward	GGCAGTGACCAAGAATGATG
	Reverse	ATCAGGGTACAGGCTGTTCA
hsa_circ_0002358	Forward	GATGAAGAGTCAGTTTAGGGGC
	Reverse	CCTCTGCTTCAACAATGTGC
hsa_circ_0022178	Forward	TGTCTGTAGTCTCTGTGGAG
	Reverse	GTGTAGGTCTCCACAATCTG
hsa_circ_0024745	Forward	AACAGCGCAGGACATAGGGA
	Reverse	GGTCCCTTCGTCACTCTTCT
hsa_circ_0000652	Forward	CGCAAGCTGAAATTCAAGGC
	Reverse	AAGCTGCAAATGTGTCGGCT

hsa_circ_0006884	Forward	CATAATTGGAGCCTTGCTGG
	Reverse	AGCCAATGATGCCTGCTGTA
hsa_circ_0084927	Forward	ACAGGTGAAGATTCCTTAA
	Reverse	TGCAATATCTTGATCTGAAG
hsa_circ_0049282	Forward	TGGCCACCACATCGAAGAAT
	Reverse	CCCTTGTAGTTGCGGCTGAT
hsa_circ_0024876	Forward	AAAGCCCAGGGGACATTCAA
	Reverse	GGTGCCACACAACCTCAATG
hsa_circ_0055592	Forward	ACCTGGAGGAGCACCTGGAT
	Reverse	AGCAAGGGGTACACGGAGCT
hsa_circ_0085170	Forward	CGGACAGCACATACAGCGAG
	Reverse	CTGGGCATGGGCACTAAGGC
hsa_circ_0004968	Forward	ATGGGAGAGAGAGTTCGCAT
	Reverse	AGTGTGTCCACATCCATCAC
hsa_circ_0091880	Forward	CTGGAGAGAGCTGAAGCTGGAG
	Reverse	TTGATGTCCACCTTGCTGGG
hsa_circ_0059516	Forward	ATACCAGCCTGAGTGAGGAGGA
	Reverse	AGGTGTCGTTGAAGCCCTTG
hsa_circ_0057896	Forward	TAAGCACTGATGTCCCCTGGA
	Reverse	TTCCCTATCACTCCCTCGAA
hsa_circ_0048898	Forward	AAAAGCGGCCAGTCAGAAGA
	Reverse	TGTTGGGGGTGATGATAGAG
hsa_circ_0014220	Forward	GGGGCCTGTTATGTCAAAGTGT
	Reverse	CGTTCCAGCTGCGACATTTT
hsa_circ_0049234	Forward	CACCTCAGCCTCCTGAGTAGCT
	Reverse	GGCTGCTGGCAGTTGAGAAA

Convergent Primers

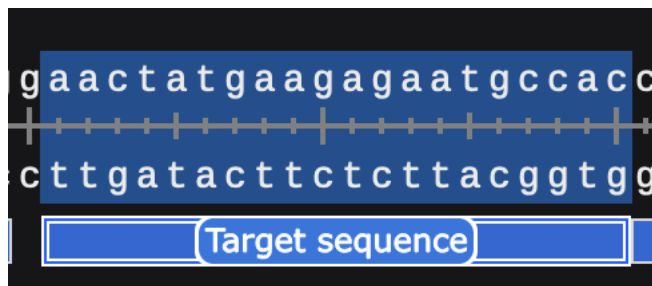
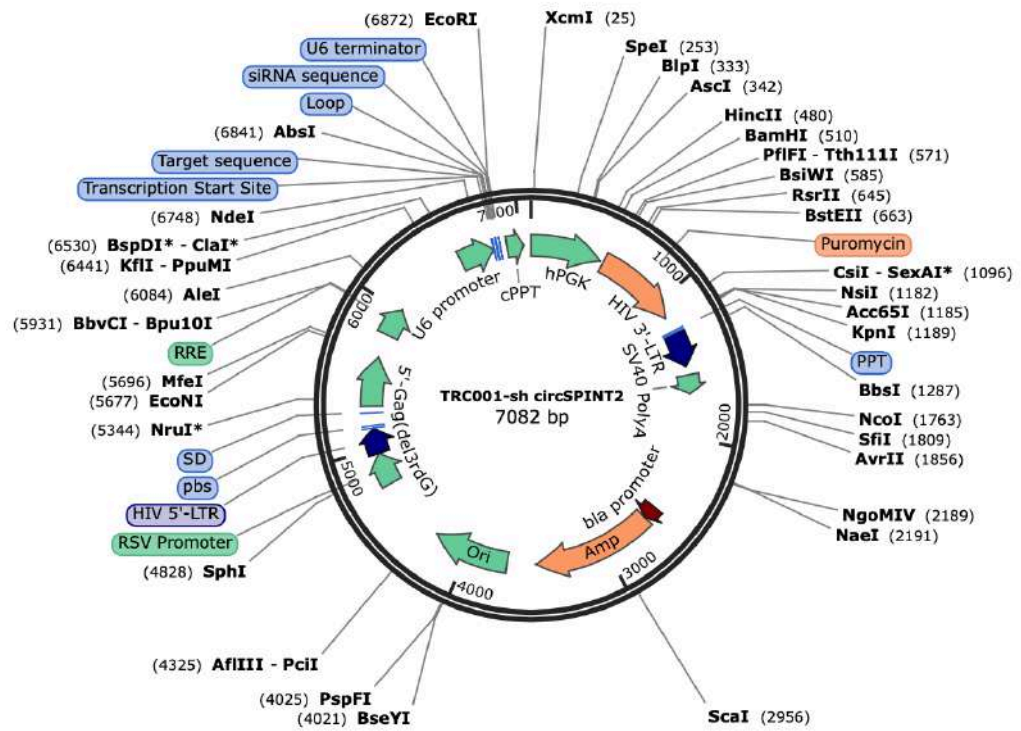
Target	Primer	Sequence
GAPDH	Forward	ATGTTTCGTCATGGGTGTGAACC
	Reverse	TGGTCATGAGTCCTTCCACGAT
SPINT2	Forward	ATGCCTAGGTGGTGGTACAATGTC
	Reverse	ACAGCCCCCATAACAAAACA
RBP1	Forward	GCACGCTGAGCACTTTTAGG
	Reverse	GCCAGTTTCACTCATGCACT

Micro RNA (miRNA) Primers

Assay Name	miRBase Accession Number (Human)	Stem Loop Sequence	Mature miRNA Sequence
hsa-mir-191-5p (Endogenous Control)	MIMAT0000440	CGGCUGGACAGCGGGCAACGGAAUCC CAAAGCAGCUGUUGUCUCCAGAGCA UCCAGCUGCGCUUGGAUUUCGUCCC CUGCUCUCCUGCCU	CAACGGAAUCCCAAAGCAGCUG
hsa-miR-101-3p	MIMAT0000099	UGCCCUGGCUCAGUUAUCACAGUGCU GAUGCUGUCUAUUCUAAAGGUACAGU ACUGUGAUAACUGAAGGAUGGCA	UACAGUACUGUGAUAACUGAA
hsa-miR-29c	MIMAT0000681	AUCUCUUACACAGGCUGACCGAUUUC UCCUGGUGUUCAGAGUCUGUUUUUGU CUAGCACCAUUUGAAAUCGGUUAUGA UGUAGGGGGA	UAGCACCAUUUGAAAUCGGUUA
hsa-miR-1296-3p	MIMAT0026637	ACCUACCUAACUGGGUUAGGGCCCUG GCUCCAUCUCCUUUAGGAAAACCUUC UGUGGGGAGUGGGGCUUCGACCCUAA CCCAGGUGGGCUGU	GAGUGGGGCUUCGACCCUAACC

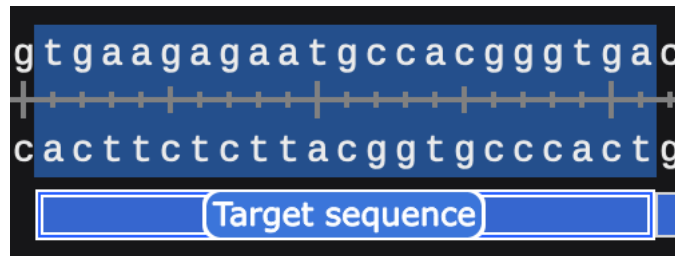
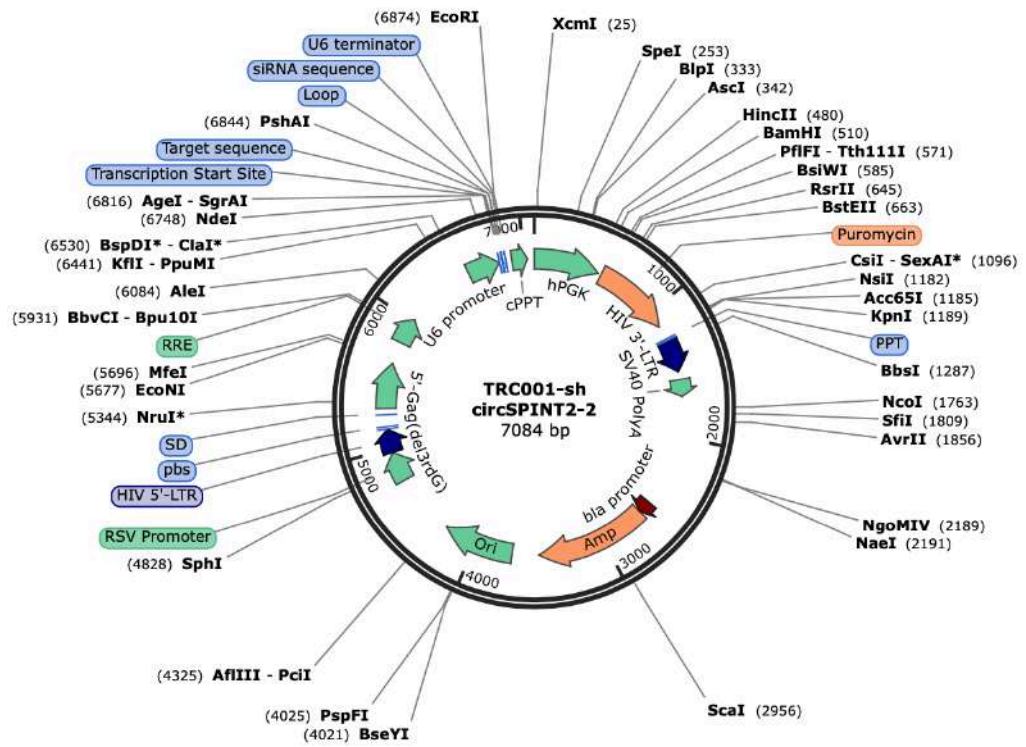
Appendix C

Knockdown Vector (PLKO.1 – 1)



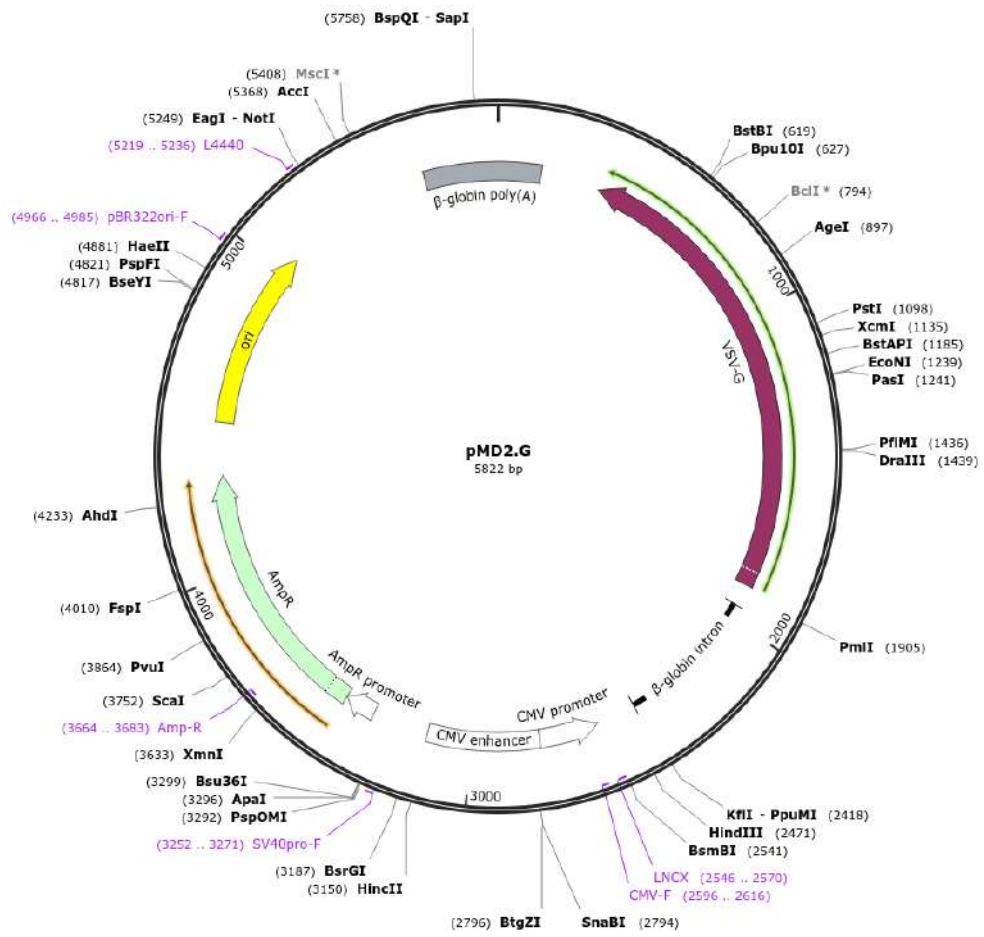
Appendix D

Knockdown Vector (PLKO.1 – 2)



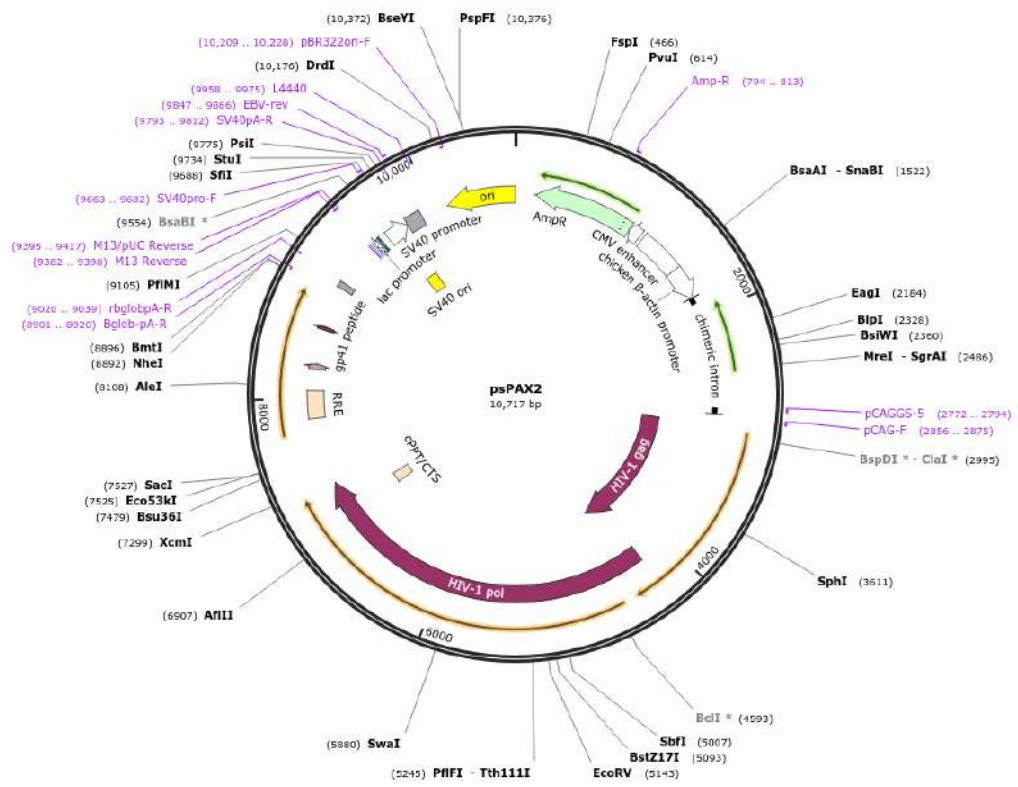
Appendix E

pMD2.G (Plasmid #12259)



Appendix F

psPAX2 (Plasmid #12260)



Appendix G

Biotinylated Labelled CircSPINT2 Probe

Target	Primer	Sequence
circSPINT2	Scramble-IP	CAGGTCACCCGTGGCATTCTTTCATAGTTGAACATATCG
	IP	CGATATGTTCAACTATGAAGAGAATGCCACGGGTGACCTG

Appendix H

Tumour Volume (Vehicle vs Osimertinib Treatment Group)

Days	Vehicle Group	Osimertinib Group
4	0.5	0.505
7	0.598333333	0.623333333
9	346.0524252	230.97207
11	427.2662657	219.0967045
14	709.2905918	334.8059317
16	688.5464143	327.7668503
17	1004.628267	297.382341
21	870.94713	607.5835202
22		715.7798242
23		723.9512087
25		858.469801
28		1271.481761
30		1180.351901

SEM Values

Days	Vehicle Group	Osimertinib Group
4	0.008164966	0.01335415
7	0.026383918	0.007149204
9	29.67156313	16.56199017
11	49.26294766	21.02082654
14	85.39091498	37.92002352
16	46.37949691	49.42658842
17	72.38809829	33.87495548
21	113.1771005	107.2393499
22		146.3852037
23		115.7631551
25		172.5858575
28		294.3918415
30		274.1640593

Appendix I

Fluorescence In Situ Hybridization Probe (circSPINT2 Probe_cy3)/IDTDNA

Target	Probe	Sequence
circSPINT2	circSPINT2_Cy3	5'-GCTATACAAGTTGATACTTCTCTTACGGTGCCCACTGGAC/3spC3/-3'

Appendix J

Antibodies

Antibody	Species	Working dilution	Size	Supplier	Cat. No.
RBP1	Rabbit-poly	(WB) 1:1,000-1:10,000 (IHC (P)) 1:100-1:1,000 (ICC/IF) 1:100-1:1,000	10~17kDa	Invitrogen	PA5-28713
GAPDH	Rabbit mAb	WB: 1:1000	37 KDa	Cell Signaling	5174S

Appendix K

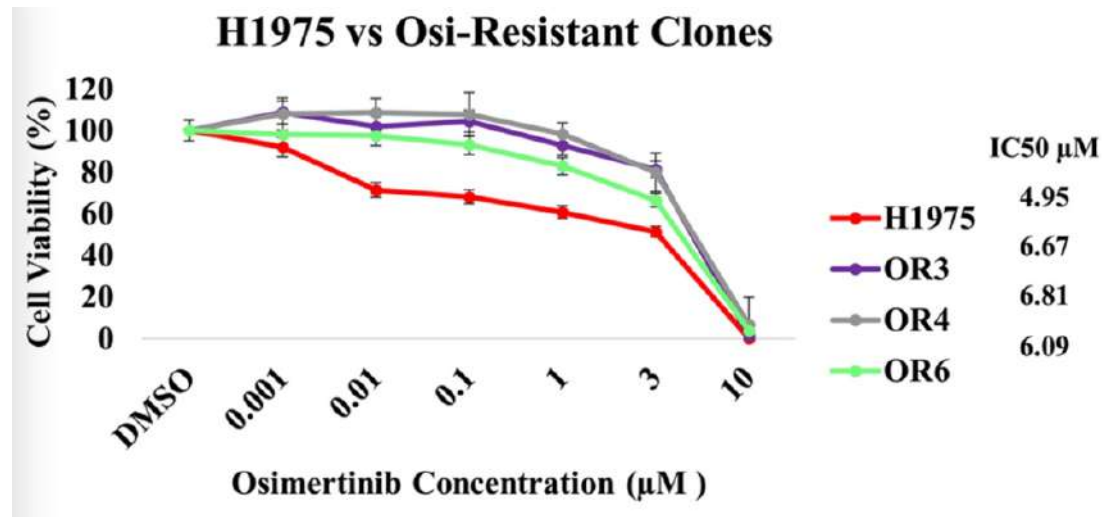


Figure 1: Osimertinib sensitivity assay. A, Alamarblue assay (colorimetric dye) were conducted in the osimertinib-resistant clones and H1975 cell lines at 48 hours. Data are presented as the mean \pm SEM (n = 3).

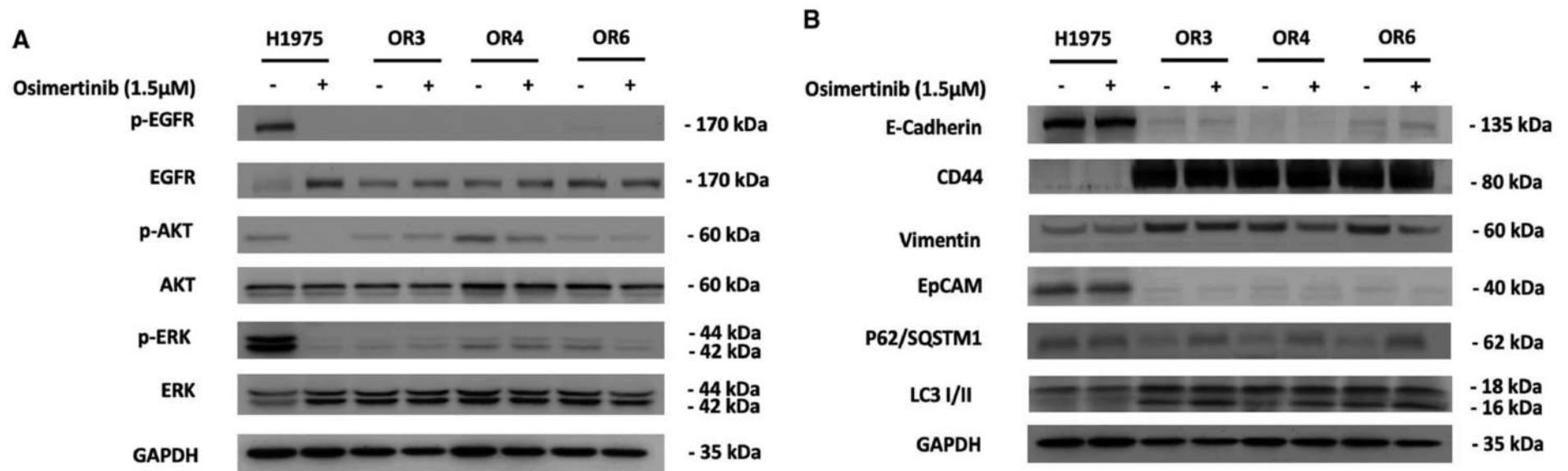


Figure 2: Western blot analysis. (A) EGFR signalling pathways, (B) EMT and autophagy related protein expressions were evaluated in both parental cell line and resistant clones prior to Osimertinib and DMSO (control) treatments for 24 h.

Appendix L

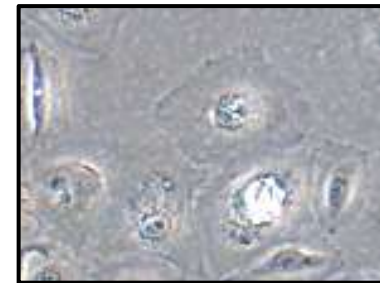
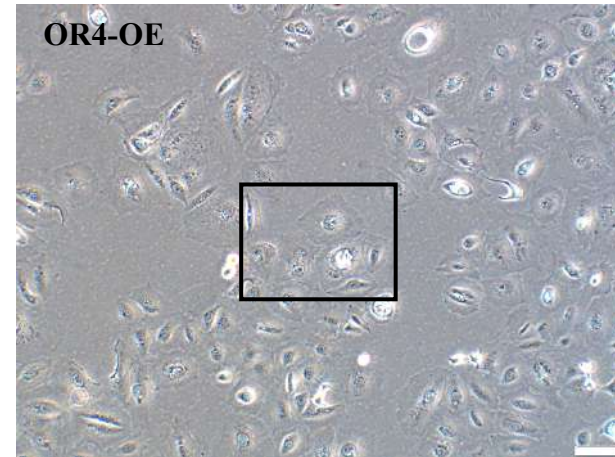
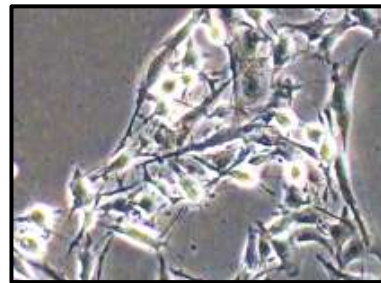
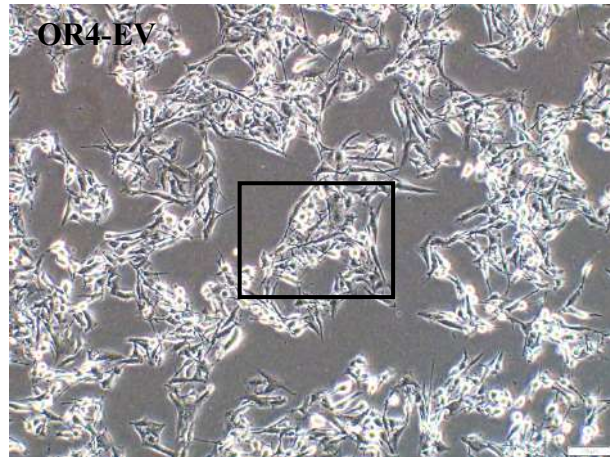
CircRNA Differential Expression (Up-regulated in Osimertinib Resistant Clones)

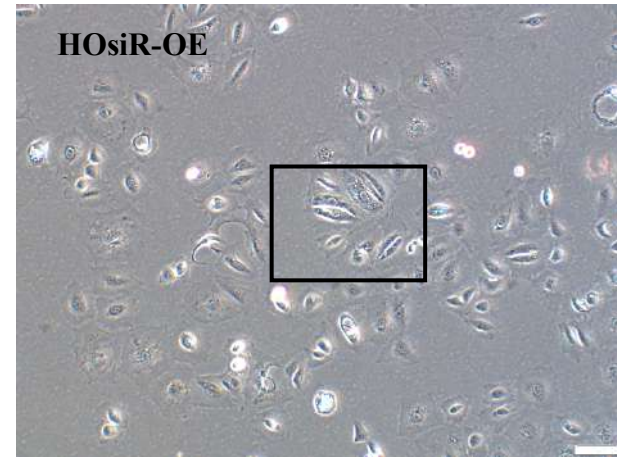
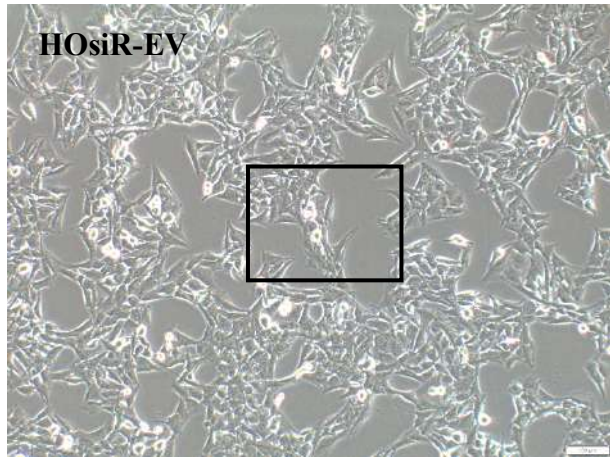
No	CircRNA	Chromosome Location	Parental Gene	Fold Change (NGS)
1	hsa_circ_0002358	chr5:170818308-170819982	NPM1	79.4
2	hsa_circ_0022178	chr11:57556508-57556627	CTNND1	67.4
3	hsa_circ_0024745	chr11:124766093-124766214	ROBO4	64.2
4	hsa_circ_0024390	chr11:117074022-117074600	TAGLN	35.9
5	hsa_circ_0000652	chr15:90984737-90986710	IQGAP1	18.9

CircRNA Differential Expression (Down-regulated in Osimertinib Resistant Clones)

No	CircRNA	Chromosome Location	Parental Gene	Fold Change (NGS)
1	hsa_circ_0059516	chr20:18022177-18037521	OVOL2	0.166
2	hsa_circ_0050818	chr19:38778515-38779831	SPINT2	0.129
3	hsa_circ_0057896	chr2:206630197-206631527	NRP2	0.059
4	hsa_circ_0024876	chr11:130064043-130064632	ST14	0.040
5	hsa_circ_0049282	chr19:10694281-10694746	APIM2	0.018

Appendix M





Appendix N

